SYNTHESES AND CHARACTERIZATION OF IRON AMINE COMPLEXES

by

CYPRIAN MUTURIA M'THIRUAINE

Submitted in fulfilment of the academic requirements for the degree of
Doctor of Philosophy in the School of Chemistry and Physics,
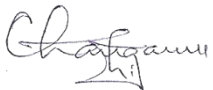University of KwaZulu-Natal, Durban.

November 2011

As the candidate's supervisor I have approved this thesis for submission.

Supervisor:

Signed: _____   Name: Prof. Holger B. Friedrich   Date: _____

Co-supervisor:

Signed: _____   Name: Dr. Evans O. Changamu   Date: _____

ABSTRACT

The organometallic Lewis acid $[(\eta^5\text{-}C_5H_5)(CO)_2Fe]BF_4$ reacts with excess dry diethyl ether at low temperatures to form the novel labile complex $[(\eta^5\text{-}C_5H_5)(CO)_2Fe(OEt_2)]BF_4$ which in turn serves as a precursor in the syntheses of various cationic dicarbonylcyclopentadienyliron complexes. The reactions of $[(\eta^5\text{-}C_5H_5)(CO)_2Fe(OEt_2)]BF_4$ with various 1-alkylamines, α,ω-diaminoalkanes, N-heterocyclics and heterofunctional amine ligands, as well as olefins, have been investigated.

 Reactions with 1-alkylamines and α,ω-diaminoalkane ligands lead to a series of novel monuclear and dinuclear complexes of the types $[(\eta^5\text{-}C_5H_5)(CO)_2FeL]BF_4$ and $[\{(\eta^5\text{-}C_5H_5)(CO)_2Fe\}_2(\mu\text{-}L)](BF_4)_2$, respectively. The reaction of $[(\eta^5\text{-}C_5H_5)(CO)_2Fe(OEt_2)]BF_4$ with N-heterocyclic ligands such as 1,3,5,7-tetraazaadamantane (HMTA) and 1,4-diazabicyclo[2.2.2]octane (DABCO) give dinuclear complexes $[\{(\eta^5\text{-}C_5H_5)(CO)_2Fe\}_2(\mu\text{-}L)](BF_4)_2$ and monuclear complexes $[(\eta^5\text{-}C_5H_5)(CO)_2FeL]BF_4$ (L = HMTA, DABCO). Its reaction with 1-methylimidazole (1-meIm) affords only the monuclear complex $[(\eta^5\text{-}C_5H_5)(CO)_2Fe(1\text{-}meIm)]BF_4$ in which the coordination of 1-methylimidazole is *via* the sp^2-N. The reaction with heterofunctional amine ligands is highly regioselective with the cation $[(\eta^5\text{-}C_5H_5)(CO)_2Fe]^+$ showing higher affinity for NH_2 than π-bonded, O or CN functionalities. Besides amines, $[(\eta^5\text{-}C_5H_5)(CO)_2Fe(OEt_2)]BF_4$ reacts with olefins and HCOOH to form complexes of the type $[(\eta^5\text{-}C_5H_5)(CO)_2Fe(\eta^2\text{-olefin})]BF_4$ and $[\{(\eta^5\text{-}C_5H_5)Fe(CO)_2\}_2(\mu\text{-OCHO})]BF_4$, respectively.

For comparison of steric and electronic effects, analogous pentamethylcyclopentadienyl amine complexes were synthesized from the THF complex $[\{\eta^5\text{-}C_5(CH_3)_5\}(CO)_2Fe(THF)]BF_4$. The reaction of 3-aminoprop-1-ene with the etherate complexes $[(\eta^5\text{-}C_5R_5)(CO)_2Fe(E)]BF_4$ (R = H: E= Et$_2$O; R = CH$_3$: E = THF) led to air stable complexes $[(\eta^5\text{-}C_5R_5)(CO)_2Fe(NH_2CH_2CHCH_2)]BF_4$ (R = H, CH$_3$), which in turn react with a mole equivalent of the etherate complexes to give dinuclear complexes of the type, $[(\eta^5\text{-}C_5R_5)(CO)_2Fe(NH_2CH_2CHCH_2)Fe(CO)_2(\eta^5\text{-}C_5R'_5)](BF_4)_2$ (R not

necessarily equal to R'). They also undergo halogenation to give the chiral dihalopropylamino complexes $[(\eta^5\text{-}C_5R_5)(CO)_2Fe(NH_2CH_2CH(X)CH_2(X))]BF_4$ (R=H, CH_3; X = Cl, Br). The reaction of the dinuclear complex $[\{(\eta^5\text{-}C_5H_5)(CO)_2Fe\}_2(NH_2CH_2CHCH_2](BF_4)_2$ with NaI in acetone gives $[(\eta^5\text{-}C_5H_5)(CO)_2Fe(NH_2CH_2CHCH_2)]I$ and $[(\eta^5\text{-}C_5H_5)Fe(CO)_2I]$. All these complexes have been fully characterized by ^1H NMR, ^{13}C NMR, IR spectroscopy and elemental analysis. The mass spectra of 1-aminoalkane and diaminoalkane complexes have also been recorded and are discussed. The structures of 16 synthesized compounds have been confirmed by single crystal X-ray crystallography. Most of the amine complexes are water-soluble and some undergo counteranion exchange with sodium tetraphenylborate in both aqueous and organic media to give BPh_4^- salts.

PREFACE

The experimental work described in this thesis was carried out in the School of Chemistry and Physics, University of KwaZulu-Natal, Durban, from September 2008 to September 2011, under the supervision of Prof. Holger B. Friedrich and Dr. Evans O. Changamu.

These studies represent original work by the author and have not otherwise been submitted in any form for any degree or diploma to any tertiary institution. Where use has been made of the work of others it is duly acknowledged in the text.

Sign _____   Date_____

Cyprian Muturia M'thiruaine

Student No. 208529737

DECLARATION 1 - PLAGIARISM

I, ………………………………………………………………….., declare that

1. The research reported in this thesis, except where otherwise indicated, is my original research.

2. This thesis has not been submitted for any degree or examination at any other university.

3. This thesis does not contain other persons' data, pictures, graphs or other information, unless specifically acknowledged as being sourced from other persons.

4. This thesis does not contain other persons' writing, unless specifically acknowledged as being sourced from other researchers. Where other written sources have been quoted, then:
   a. Their words have been re-written but the general information attributed to them has been referenced
   b. Where their exact words have been used, then their writing has been placed in italics and inside quotation marks, and referenced.

5. This thesis does not contain text, graphics or tables copied and pasted from the Internet, unless specifically acknowledged, and the source being detailed in the thesis and in the References sections.

Signed: ……………

DECLARATION 2 - PUBLICATIONS AND CONFERENCE CONTRIBUTIONS

DETAILS OF CONTRIBUTION TO PUBLICATIONS that form part and/or include research presented in this thesis (includes publications in preparation, submitted, *in press* and published and details of the contributions of each author to the experimental work and writing of each publication is given)

PUBLICATIONS

Publication 1

M'thiruaine, C. M; Friedrich, H. B; Changamu, E. O; Bala, M. D., Synthesis and characterization of amine complexes of the cyclopentadienyliron dicarbonyl complex cation, $[Cp(CO)_2Fe]^+$. *Inorg. Chim. Acta* 366 (2011) 105.
Contributions: I synthesized and characterized all compounds and wrote the paper. Dr. Bala solved the crystal structures and proof read the manuscript. Prof. Friedrich and Dr. Changamu are my supervisors.

Publication 2

M'thiruaine, C. M; Friedrich, H. B; Changamu, E. O; Omondi, B., (μ-Ethane-1,2-diamine-κ^2N:N′)bis[dicarbonyl(η^5-cyclopentadienyl)iron(II)]bis(tetrafluoridoborate). *Acta Cryst*. E67 (2011) m485.
Contributions: I synthesized the compound, grew the crystal and wrote the paper. Dr Omondi solved the crystal structure and proof read the manuscript. Prof. Friedrich and Dr. Changamu are my supervisors.

Publication 3

M'thiruaine, C. M; Friedrich, H. B; Changamu, E. O; Bala, M. D., Acetonitriledicarbonyl(η^5-pentamethylcyclopentadienyl)iron(II)tetrafluoridoborate. *Acta. Cryst*. E67 (2011) m924.
Contributions: I synthesized the compound, grew the crystal and wrote the paper. Dr. Bala soved the crystal structure and proof read the manuscript. Prof. Friedrich and Dr. Changamu are my supervisors.

Publication 4

M'thiruaine, C. M; Friedrich, H. B; Changamu, E. O; Omondi, B., (μ-formato-κ^2O:O′)bis[dicarbonyl(η^5-cyclopentadienyl)iron(II)]tetrafluoridoborate. *Acta. Cryst*. E67 (2011) m1252.
Contributions: I synthesized the compound, grew the crystal and wrote the paper, Dr Omondi soved the crystal structure and proof read the manuscript. Prof. Friedrich and Dr. Changamu are my supervisors.

Publication 5

M'thiruaine, C. M; Friedrich, H. B; Changamu, E. O; Bala, M. D., Synthesis, characterization and structural elucidation of water-soluble 1-aminoalkane and α,ω-diaminoalkane complexes of the pentamethylcyclopentadienyliron dicarbonyl cation, $[Cp*Fe(CO)_2]^+$. *Inorg. Chim. Acta 382* (2012) 27
Contributions: I synthesized and characterized all compounds and wrote the paper. Dr. Bala solved the crystal structures and proof read the manuscript. Prof. Friedrich and Dr. Changamu are my supervisors.

Publication 6

M'thiruaine, C. M; Friedrich, H. B; Changamu, E. O; Bala, M. D., Reactions of *N*-heterocyclic with substitutionally labile organometallic complexes, $[(\eta^5\text{-}C_5R_5)Fe(CO)_2E]BF_4$ (R = H,CH$_3$; E = THF, Et$_2$O). Submitted to Inorganica Chimica Acta.
Contributions: I synthesized and characterized all compounds and wrote the manuscript. Dr. Bala solved the crystal structures and proof read the manuscript. Prof. Friedrich and Dr. Changamu are my supervisors.

Publication 7

M'thiruaine, C. M; Friedrich, H. B; Changamu, E. O., Syntheses, structural elucidation and reactions of allylamino complexes of the type, $[\eta^5\text{-}C_5R_5(CO)_2Fe(NH_2CH_2CHCH_2)]BF_4$ (R = H, CH$_3$). Submitted to Polyhedron.
Contributions: I synthesized and characterized all compounds and wrote the manuscript. Prof. Friedrich and Dr. Changamu are my supervisors.

Publication 8

M'thiruaine, C. M; Friedrich, H. B; Changamu, E. O., Regioselective reactions of electrophilic iron dicarbonyl cations, $[(\eta^5\text{-}C_5R_5)(CO)_2Fe]^+$ (R = H, Me) with heterofunctional amine ligands. Manuscript.
Contributions: I synthesized and characterized all compounds and wrote the manuscript. Prof. Friedrich and Dr. Changamu are my supervisors.

CONFERENCE CONTRIBUTIONS

1. Poster presentation: Characterization and reactions of $[(\eta^5\text{-}C_5H_5)Fe(CO)_2(Et_2O)]BF_4$ with selected ligands. Annual Conference of the Catalysis Society of South Africa at Goudin Spa, Cape Town (Nov, 2009).
2. Poster presentation: Water-soluble organometallic complexes of cation $[(\eta^5\text{-}C_5R_5)(CO)_2Fe]^+$ (R = H, Me). Annual conference of the Catalysis Society of South Africa at Baines Game Lodge, Bloemfontein (Nov, 2010).

Signed: ……………..

TABLE OF CONTENTS

ACKNOWLEDGEMENT

First and foremost, I would like to thank Lord GOD almighty for his steadfast love and mercy. To him be the glory and honour.

I wish to express my deep sense of gratitude and appreciation to my supervisor Prof. Holger B. Friedrich for his enthusiastic supervision, guidance and encourangement during this study. His faith in me has served as a beacon, always summoning me to strive onwards. I will always remember his kindness and generosity.

A great debt is owed to my co-supervisor Dr. Evans O. Changamu without his aid and mentoring my goals and current level of success would never have been realized. The dark hours turned bright because of his encourangement and inspiration.

I also wish to extend my sincere gratitude to Dr. Manuel Fernandes of the University of the Witwatersrand for crystal data collection, solution and refinement.

I am indebted to Dr. Muhammad D. Bala and Dr. Bernard Omondi for their fruitfull discussion, solving the crystal structures and proof reading the manuscripts which forms a part of this thesis.

Thanks to all the former and current catalysis research group members for their generous contribution and discussion, especially during the group meetings whenever this work was presented. Indeed I am honored to have worked with such an incredible research group.

I greatefuly acknowledge the financial support by the NRF, THRIP and the University of KwaZulu-Natal without which it would have been difficult to complete this work.

During this study, many of the non-teaching staff in the School of Chemistry were of great help in the accomplishment of the task and thus they deserve an honorable mention. Charmaine, Brenda, Jayambal, Dilip, Anita, Malini, Neil, Gregory and Thulani, thank you all for your generous assistance.

I express my deepest gratitude to my parents Stanley M'thiruaine and Grace Kangai for their parental love, prayers and support. Enough thanks cannot be expressed because I cannot imagine reaching this far without their love and care.

DEDICATION

This work is dedicated to Professor Naftali T. Muriithi. A man who has an undying believe in me and acted as an inspiration towards realizing my potential. May God bless you Prof.

LIST OF ABBREVIATIONS

Abbreviation	Full meaning
ABN	4-aminobenzonitrile
ATR	Attenuated Total Reflectance
$CDCl_3$	deuterated chloroform
CD_3CN	deuterated acetonitrile
CIF	crystallographic information file
CO	carbon monoxide
COSY	correlation spectroscopy
Cp	cyclopentadienyl anion
Cp*	pentamethycyclopentadienyl anion
d	doublet
D---A	hydrogen donor-acceptor bond
DABCO	1,4-diazacyclo[2.2.2]octane
<DHA	donor-hydrogen-acceptor angle
DCM	dichloromethane
DMSO	deuterated dimethyl sulfoxide
DNA	deoxyribonucleic acid
ESI	electrospray ionisation
Et_2O	diethyl ether
FTIR	Fourier Transform Infrared
HMTA	hexamethylenetetramine
HSQC	heteronuclear single quantum coherence
Im	imidazole
IR	Infrared
m	multiplet
Me	methyl

MeCN	acetonitrile
1-meIm	1-methylimidazole
MHz	Mega hertz
M.p	melting point
MS	mass spectroscopy
NMR	Nuclear Magnetic Resonance
ORTEP	Oak Ridge Thermal Ellipsoid Plot
OTf	trifluoromethansulfonate
PDA	1,4-phenylenedimethanamine
Ph	phenyl
PTA	1, 3,5-triaza-7-phosphaadamantane
Rf	retention factor
RNA	ribonucleic acid
s	singlet
t	triplet
THF	tetrahydrofuran
TLC	thin layer chromatography
TPPMS	$P(C_6H_5)_2(C_6H_4SO_3Na)$
TPPTS	$P(C_6H_4SO_3Na)_3$

CHAPTER ONE

1. Introduction

Iron is an exceptionally ubiquitous and relatively safe transition metal. It has been at the forefront in catalyzing some important reactions such as the synthesis of ammonia and the Fischer Tropsch reactions [1] in addition to many other catalyzed organic syntheses [2-4]. In biological systems, iron is the most abundant transition metal and usually coordinated by nitrogen, oxygen or sulfur atoms belonging to amino acids in the polypeptide chain and/or a macrocyclic ligand incorporated into the protein. The presence of the iron ion allows enzymes to perform functions such as redox reactions that cannot easily be performed by the limited set of functional groups found in amino acids. Iron-containing enzymes are also essential for numerous biochemical processes, which include oxygen transportation, cellular respiration and metabolism, drug metabolism, DNA and RNA base repair and the biosynthesis of hormones and antibiotics. Cytochrome-c and hemoglobin, the iron containing parts of which are shown in Figures 1 and 2, respectively, are example of iron-containing proteins.
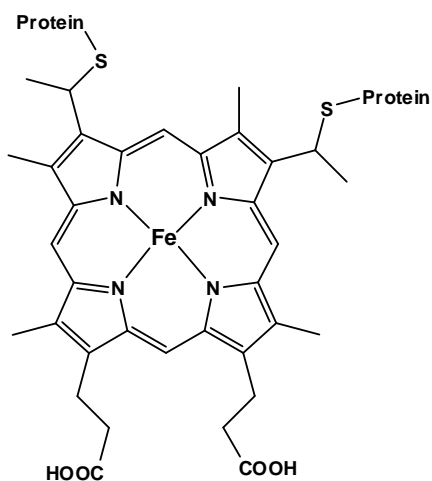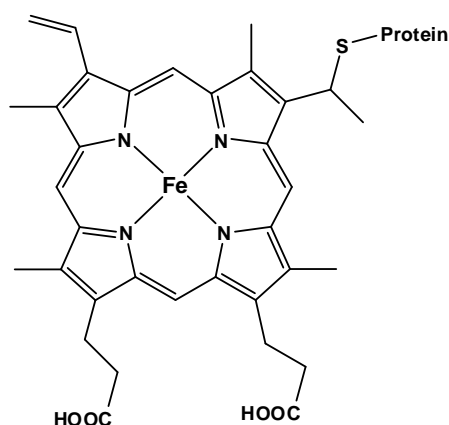
Fig. 1: Cytochrome-C   **Fig. 2:** Heme

The pivotal roles played by iron-containing enzymes have extensively attracted the attention of many chemists and a large number of models designed to mimic these enzymes in chemical transformations have been made available [5, 6]. Recently, Perera and Du *et al.* reported alkylamine ligated heme models and show that their coordination structure mimics the catalytic cycle intermediates for the nitrite bond to the heme iron centre of cytochrome *c* nitrite reductase [7]. Many other models of iron-containing proteins have been reported [8-11], the most prevalent being the iron porphyrin complexes. However, identification of discrete molecules involved in biological transformation remains a challenge. Thus, interaction of iron with simple nitrogen containing ligands is appealing, since any information obtained from their interaction would contribute to a better understanding of the chemical phenotype in iron-containing enzymes, which in turn would advance the development of catalysis, pharmacology and physiology. This thesis, therefore, reports on the synthesis of various nitrogen-containing iron complexes with the aim of improving our understanding of the interaction between iron and simple nitrogen-containing ligands.

This Thesis has been prepared according to **Format 3** as outlined in the guidelines from the Faculty of Science and Agriculture (UKZN) which states:

"This is a thesis in which the chapters are written as a set of discrete research papers, with an Overall Introduction and a Final Discussion. These research papers need not be published yet, but at least one paper would have already been submitted for publication".

Thus, this Thesis comprises of seven chapters with chapters two to six written as a set of discrete research papers. This first introductory chapter is divided into two sections. The first section presents a general introduction to the chemistry of $(\eta^5\text{-}C_5R_5)Fe(CO)_2$ complexes, giving a brief survey of compounds related to the work reported herein. The second section describes the main objectives of this thesis. Afterwards, the results obtained are presented in Chapters two to six in the form of discrete research papers (papers 1-5). Each chapter (paper) consists of an abstract, brief introduction, results and discussion, conclusion and references.

In the second chapter (**Paper I, Published**), the synthesis of a new diethyl ether complex [(η^5-C_5H_5)(CO)$_2$Fe(OEt_2)]BF_4 and its application as an excellent precursor in the syntheses of novel amine complexes of the cation [Cp(CO)$_2$ Fe]$^+$ is described. The third chapter (**paper II, in press**) presents the syntheses of novel aminoalkane and diaminoalkane complexes of pentamethylcyclopentadienyliron dicarbonyl whose water solubility and stability have been demonstrated by their counterion exchange with $NaBPh_4$ in aqueous environment. Chapter four (**paper III, submitted**) presents the reaction of *N*-heterocyclic ligands with the ethereal complexes [Cp(CO)$_2$Fe(OEt_2)]BF_4 and [{η^5-$C_5(CH_3)_5$}(CO)$_2$Fe(THF)]BF_4 leading to novel *N*-heterocyclic complexes. In chapter five (**Paper IV, submitted**), the reaction of the etherate complexes with allylamine resulting in monuclear and dinuclear allylamino complexes is described as well as the nucleophilic addition reactions of some of the complexes. Chapter six (**paper V, Manuscript**) demonstrates the regioselectivity of the cation [(η^5-C_5R_5)(CO)$_2$Fe]$^+$ towards the amine functionality when exposed to a heterobifunctional "amine" ligand. Finally, the main conclusions of this thesis are stated in chapter seven. The three papers already published in Acta Crystallographica Section E are briefly presented in Appendices 1, 2 and 3. However, the full electronic reprint of these papers is available in CD-ROM attached in the Appendix 12.

1.1. The chemistry of (η^5-C_5R_5)Fe(CO)$_2$ complexes

Compounds containing the iron fragment CpFe(CO)$_2$ (Cp = η^5-C_5H_5) have been extensively studied since the discovery of [CpFe(CO)$_2$]$_2$ [12]. The compounds can exhibit considerable stability towards air, moisture and temperature and their so-called piano-stool type structure can be characterized readily by IR and NMR spectroscopy based on simple spectroscopic features such as two strong v(C≡O) absorptions and a single Cp resonance in the ^{1}H and ^{13}C NMR spectra. The ring substituted derivatives [η^5-C_5R_5(CO)$_2$FeL] (R = Alkyl, phenyl, silyl, halides, ester, etc.) have also been studied with particular emphasis on the electronic and steric effects of such ligands on the metal centre and the auxiliary ligands. In particular, the pentamethylcyclopentadienyl derivative (Cp* = η^5-$C_5(CH_3)_5$) has been used by many researchers as a spectator ligand following the pioneering work of King and Bisnette [13]. The ligand is known to

increase solubility and stability of the compound due to its steric and electronic effect on the iron centre. Futhermore, it is known to promote formation of good crystals owing to the resolution of the disorder problem of the Cp ring.

The $[\eta^5\text{-}C_5R_5(CO)_2FeL]$ type compounds have been prepared by various methods, usually starting from the so-called iron dimer, $[\eta^5\text{-}C_5R_5Fe(CO)_2]_2$. Typical methods involve nucleophilic substitution by ferrate $[\eta^5\text{-}C_5R_5(CO)_2Fe]^-$ and functionalization of $[\eta^5\text{-}C_5R_5(CO)_2FeX]$ (X = halide) with nucleophiles as also depicted in Scheme 1.
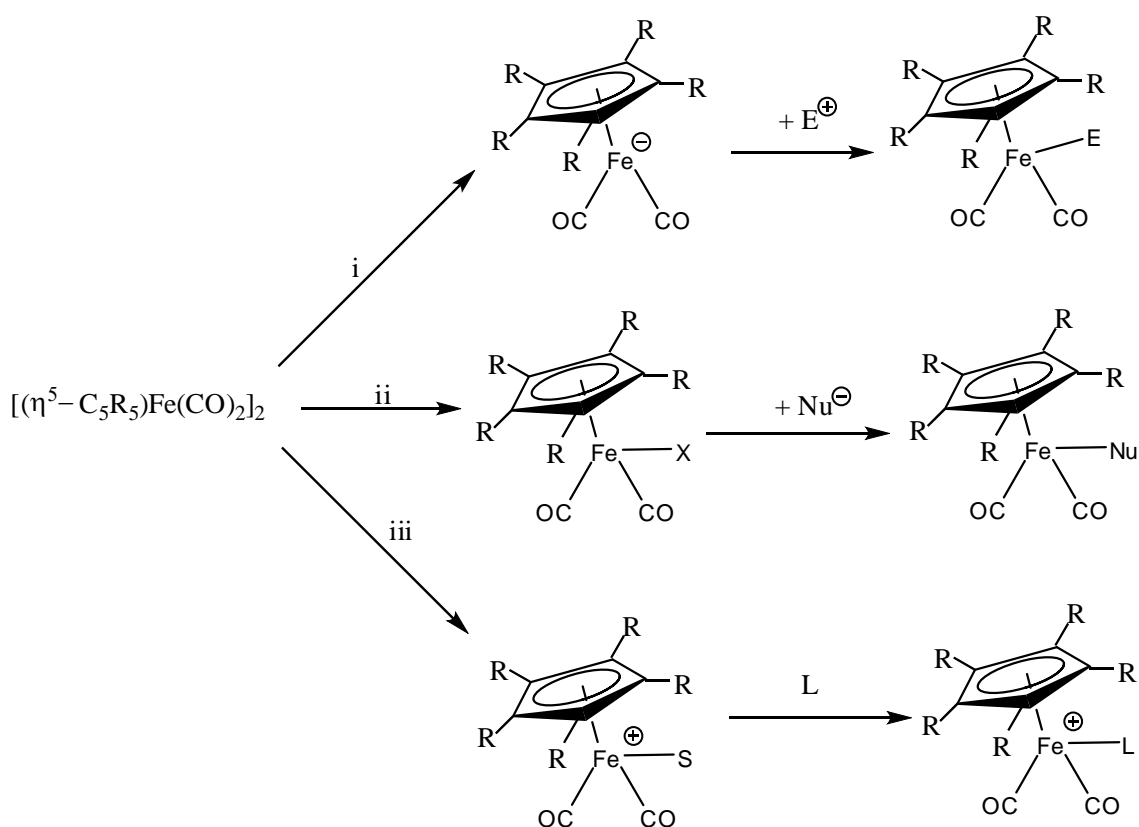
Scheme 1: Generation of complexes of the $\eta^5\text{-}C_5R_5Fe(CO)_2$ moieties

Scheme 1 presents three main routes through which complexes containing the $(\eta^5\text{-}C_5R_5)Fe(CO)_2$ moieties can be obtained. In these routes (i, ii and iii), the Fe-Fe bond of the dimer is cleaved by either reduction or oxidation processes. Reductive cleavage (path i) mainly involves monoelectronic reducing agents such as Li, Na and K in THF leading to the anionic complex $[(\eta^5\text{-}C_5R_5)(CO)_2Fe]^-$. These anionic complexes are 18-

electron species which act as strong nucleophiles and have been extensively used as starting materials or precursors in preparation of many iron dicarbonyl complexes [12, 14-24]. They are readily alkylated or acylated by reaction with the appropriate electrophiles to give neutral complexes of the type $[(\eta^5\text{-}C_5R_5)(CO)_2FeR]$ (R is an organic moiety). The complexes where R = hydrocarbon are prominent due to their application as models for the growth of hydrocarbon chains on metal catalyst surfaces in important reactions such as the Fischer-Tropsch reactions [25].

In path (ii), the Fe-Fe bond is oxidatively cleaved by halides (Cl⁻, Br⁻, I⁻). For example, the common iodo complexes $[(\eta^5\text{-}C_5R_5)(CO)_2FeI]$ are easily obtained by reacting the iron dimers $[(\eta^5\text{-}C_5R_5)Fe(CO)_2]_2$ with an excess of iodine in either $CHCl_3$ or CH_2Cl_2, followed by addition of aqueous sodium thiosulphate to remove unreacted iodine. Displacement of the halide from the compound leads to neutral or ionic complexes depending on the nature of the nucleophile (path ii).

 Oxidative cleavage of the Fe-Fe bond has also been reported to be effected by ferrocinium [26], Ag^+ [27, 28], $FeCl_3$ [29], O_2/HBF_4, H^+ [30], Ph_3C^+ or electrochemical methods [31] in solvents to generate solvento complexes of the type $[(\eta^5\text{-}C_5R_5)(CO)_2Fe(S)]BF_4$. In these complexes the solvent as ligand is weakly bound and is readily displaced by a relatively stronger ligand (path iii). This class of complexes is briefly discussed in the following section.

1.1.1 Coordinatively unsaturated organometallic compounds

Coordinatively unsaturated organometallic compounds can be regarded as coordination compounds with at least one vacant coordination site. In solution, the vacant sites are often occupied by solvent molecules which play a great role in stabilizing coordinatively unsaturated complexes. It has been reported that even the noble gases such as Xe and Kr are capable of binding to the metal centres of such complexes [32, 33]. Thus, a true vacant coordination site may not exist in solution. The term "*virtual coordination site*" was suggested by Strauss [34] to replace "*vacant site*," because what is considered a vacant coordination site in solution is actually an extremely weak or extremely labile metal-solvent bond. In this regard organometallic compounds with

weakly bound solvento ligands are also regarded as coordinatively unsaturated compounds (also known as solvento complexes).

Coordinatively unsaturated organometallic complexes have received much attention as key intermediates in catalytic cycles [35-37] and as precursors in the syntheses of other organometallic compounds. Some can be isolated, but many are used *in situ* following their generation from chemical or photochemical methods. With a few rare exceptions, the solvent that becomes a ligand on a metal centre is an intact solvent molecule that is captured by the metal during the reaction. THF is by far the most commonly encountered solvento ligand in solvated organotransition metal complexes. Particularly, THF coordinated cyclopentadienylmetal carbonyls of the type $[Cp(CO)_3M(THF)]$ are known (M = V, Nb, Ta). These are prepared by photolysis of THF solutions of $[CpM(CO)_4]$ [38, 39]. The manganese complex $[Cp(CO)_2Mn(THF)]$ was prepared by photolytic cleavage of $[CpMn(CO)_3]$ in THF solution by Fischer and Geberhold in 1964 [40] and its chemistry has since been well-developed [41, 42]. The analogous Re complex has been obtained *via* a similar route. Valyaev *et al.* reported a high yield of $[Cp(CO)_2Re(THF)]$ obtained from UV irradiation of $[CpRe(CO)_3]$ in THF using an immersed lamp at -50 to -15 ℃ [43]. The related $[Cp*(CO)_2Re(THF)]$ complex was isolated by Casey and co-workers [44] and was found to convert thermally to the unusual dimeric compound $[Cp*(CO)_2Re=Re(CO)_2Cp*]$. The cationic molybdenum complex $[Cp(CO)_3Mo(THF)]BF_4$ was synthesized by THF displacement of the weakly bound tetrafluoroborate ligand of $[Cp(CO)_3MoFBF_3]$ [45], while $[Cp(CO)_3Cr(THF)]X$ (X = halide) was obtained by Cooley and co-authors from the reaction of $[CpCr(CO)_2]_2$ in THF with alkyl halides or trialkyltin halides [46].

Compared to THF there are very few Et_2O coordinated complexes that have appeared in literature. The reported cases include $[Cp(CO)_3M(OEt_2)]^+X^-$ (M = Mo, W; X = BF_4, PF_6, AsF_6), which were obtained by reacting the Lewis acid complex $[Cp(CO)_3MY]$ (Y = FBF_3, FPF_5, $FAsF_5$) with diethyl ether and found to be stable only at temperatures below -20 ℃ [47]. The synthesis of the related pentamethylcyclopentadienyl complex $[Cp*(CO)_3W(OEt_2)]^+BAr_4^-$ was reported by Yi and co-workers and obtained through protonation of $[Cp*(CO)_3WCH_3]$ by $[H(OEt_2)_2]BAr_4^-$ (Ar = 3,5-bis(trifluoromethyl)phenyl) in diethyl ether at 0 ℃. The complex was stable enough to

be isolated and its crystal structure has also been reported [48]. $[Cp^*(CO)_3W(OEt_2)]^+BAr_4^-$ was reported to react with simple coordinating molecules through Et_2O displacement, however, its reaction with bulky ligands such as tertiary phosphines led to $[Cp^*(CO)_3WH]$ and the phosphonium salts $[EtOCH(Me)PR_3]BAr_4^-$ (R = Ph, Cy) [48].

Song *et al*. have reported ether complexes of the type, $[Cp(CO)_3W(PhCH_2OCH_3)]^+ X^-$ (X = OTf, BAr_4) which were obtained from the reaction of either HOTf or $[H(OEt_2)_2]^+BAr_4^-$ (Ar = 3, 5-bis(trifluoromethyl)phenyl] with benzaldehyde dimethyl acetal and $[Cp(CO)_3WH]$ in CH_2Cl_2 [49]. The BAr_4^- ether salt was found to be more stable than the OTf complex. The instability of $[Cp(CO)_3W(PhCH_2OCH_3)]^+ OTf^-$ has been attributed to displacement of the ether by the triflate which is a relatively stronger coordinating anion than BAr_4^-. A similar method was employed in the preparation of the vinyl ether complexes $[Cp(CO)_3W(\eta^2\text{-EtOCH=CHCH}_3)]^+ X^-$ using acrolein diethyl acetal. The $PhCH_2OCH_3$ coordinated to the metal centre *via* oxygen, while $EtOCH=CHCH_3$ coordinated *via* the vinyl carbons in a dihapto fashion [49]. In these preparations the ether ligand is formed from acetal in the course of the reaction. Another example involving the formation of an ether ligand at a metal centre comes from the synthesis of $[Cp(NO)(PPh_3)Re(OEt_2)]^+PF_6^-$, which involves transfer of an ethyl group from the oxonium salt $Et_3O^+PF_6^-$ to the alkoxide oxygen of $[Cp(NO)(PPh_3)Re(OEt)]$ [50].

A vast majority of reported oxygen-bonded complexes of the cation $[(\eta^5\text{-}C_5R_5)(CO)_2Fe]^+$ involved THF or acetone ligands. The THF complex $[Cp(CO)_2Fe(THF)]^+BF_4^-$, first reported in 1971 by Giering and Rosenblum, was prepared by treating $[Cp(CO)_2FeCl]$ with $AgBF_4$ in THF [51]. However, the focus was not the preparation of the complex, but rather the olefin complexes of the type $[Cp(CO)_2Fe(\eta^2\text{-olefin})]^+BF_4^-$ and there was no mention of any attempt to isolate the adduct until six years later when Reger and Coleman reported its synthesis, characterization and reactions [52]. They Prepared the THF complex by reacting the iodo complex $[Cp(CO)_2FeI]$ with $AgBF_4$ in THF. In 1982, Rosenblum and Scheck prepared the same complex by heating $[Cp(CO)_2Fe(isobutylene)]^+BF_4^-$ in $THF\text{-}CH_2Cl_2$

for 3.5 h [53]. About one and a half decades later, protonation of the methyl derivative $[Cp(CO)_2FeCH_3]$ using trifluoroboric acid – diethyl ether was reported to give a high yield of $[Cp(CO)_2Fe(THF)]^+BF_4^-$, which was precipitated from the solution by addition of THF [54].

The acetone complex $[Cp(CO)_2Fe(acetone)]^+$ was first reported by Johnson *et al.* from the oxidative cleavage of $[CpFe(CO)_2]_2$ by an excess of anhydrous ferric perchlorate in the presence of acetone [55], but attempts to isolate the compound were unsuccessful. Two years later Williams and Lalor prepared and isolated the hexafluorophospate salt of the acetone complex by employing $AgPF_6$ as oxidizing agent [28]. Following this isolation, various ketone cationic complexes were prepared by Foxman and co-authors by either oxidation of iron dimer using $AgPF_6$ in the presence of a ketone or by bromide abstraction from the bromo complex $[Cp(CO)_2FeBr]$ using $AgPF_6$ in the presence of a ketone [56]. In the latter route the bridging bromonium salt complex $[\{Cp(CO)_2Fe\}_2Br]PF_6$ was also formed as a competitive side reaction product, which was minimized by slow addition of $[Cp(CO)_2FeBr]$ to methylene chloride solutions of $AgPF_6$. A similar iodo bridged complex $[\{Cp(CO)_2Fe\}_2I]BF_4$ was observed by Mattson and Graham in their mechanistic study of halide abstraction using $AgBF_4$ and its formation was minimized by employing an excess of $AgBF_4$ in the reaction [57]. According to Mattson and Graham, $[Cp(CO)_2FeI]$ reacts with $AgBF_4$ to form the silver(I) adduct $[CpFe(CO)_2IAg]BF_4$, which decomposes to form AgI and $[Cp(CO)_2FeFBF_3]$. Any excess of $[Cp(CO)_2FeI]$ leads to formation of the iodo bridged complex, thus a slight excess of $AgBF_4$ was used [57]. The complex $[Cp(CO)_2Fe(FBF_3)]$ is believed to be in facile equilibrium with the 16-electron species $[Cp(CO)_2Fe]^+BF_4^-$ (Scheme 2) [58], which in turn reacts with any electron pair donor molecule to form a stable 18 electron species. When these reactions have been carried out in dichloromethane, coordination of CH_2Cl_2 has been proposed [57, 59]. However, Mattson and Graham did not observe any evidence for the formation of $[Cp(CO)_2Fe(CH_2Cl_2)]$. Despite the report by Mattson and co-authors, reports proposing the formation of the CH_2Cl_2 adduct still continue to emerge. For example the lability of the THF complex $[Cp(CO)_2Fe(THF)]^+$ is demonstrated by the equilibrium shown in Scheme 3, in which the $[Cp(CO)_2Fe(CH_2Cl_2)]^+$ intermediate is proposed [60].
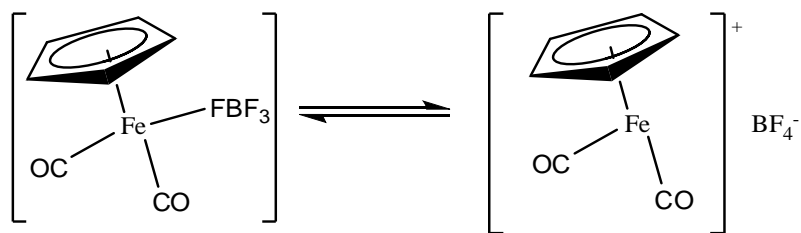
Scheme 2: A facile equilibrium between [Cp(CO)$_2$FeFBF$_3$] and [Cp(CO)$_2$Fe]BF$_4$ [58]

Solv = acetone, CH$_2$Cl$_2$, H$_2$O
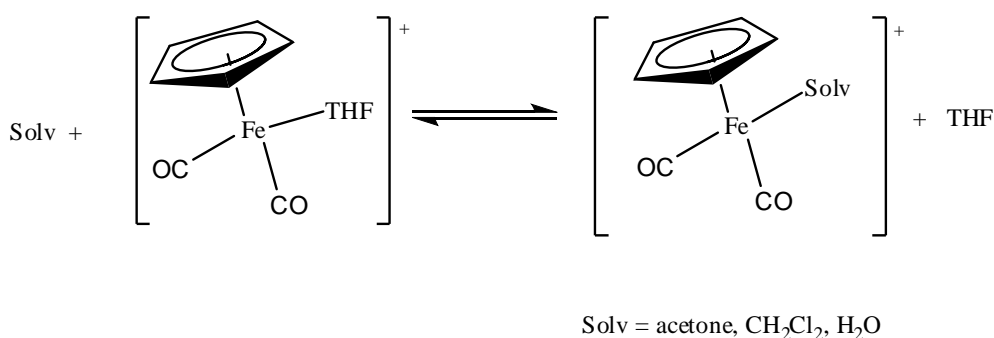
Scheme 3: Formation of the transient solvento complexes [Cp(CO)$_2$Fe(Solv)]BF$_4$ [60]

The compound [Cp(CO)$_2$Fe(FBF$_3$)] is prepared under strict anaerobic and anhydrous conditions and used *in situ* or trapped by addition of anhydrous weakly coordinating solvents such as acetone and THF. Surprisingly, whereas this appears to be a straight forward route to almost all solvento complexes of the cation [Cp(CO)$_2$Fe]$^+$, the diethyl ether complex [Cp(CO)$_2$Fe(OEt$_2$)]BF$_4$ was unknown until our recent report [61], although the Cp* analogue [Cp*(CO)$_2$Fe(OEt$_2$)]BF$_4$ [62] and the closely related dimethyl ether complex [Cp(CO)$_2$Fe(Me$_2$O)]BF$_4$ [63] were reported more than a decade ago. The Cp* analogue was obtained by protonation of the complex [Cp*(CO)$_2$Fe(CH$_2$OCH$_3$)] using HBF$_4$·OEt$_2$ at -90 °C and the mixture allowed to warm to room temperature [62]. The dimethyl ether complex was obtained at temperatures below -30 °C by protonation of [Cp(CO)$_2$FeCH$_3$] using HBF$_4$·OMe$_2$ and was found to react with acetonitrile by displacement of Me$_2$O [63]. No reaction of [Cp*(CO)$_2$Fe(OEt$_2$]BF$_4$ has been reported and its analytical data has not been reported.

Protonation of the η^3-allyl complex [Cp(CO)Fe(CH$_2$CHCH$_2$)] with HBF$_4$·OEt$_2$ or HBF$_4$·OMe$_2$ in CH$_2$Cl$_2$ has been reported, by Cutler and Todaro, to yield an extremely reactive [Cp(CO)Fe(OR$_2$)(CH$_2$CHCH$_3$)]$^+$BF$_4^-$ [63]. This complex was obtained at -75 °C and decomposed at temperatures above -65 °C. It was deprotonated by ligands such as THF back to the η^3-allyl complex, but other ligands such as acetonitrile reacted by displacing ether and η^2-propene. Ether was the first ligand to be displaced, as was demonstrated in the reaction between [Cp(CO)Fe(OR$_2$)(CH$_2$CHCH$_3$)]$^+$BF$_4^-$ and excess P(OPh)$_3$ in which the complex was first converted to the η^2-propene derivative [Cp(CO)Fe(CH$_2$=CHCH$_3$)P(OPh)$_3$]BF$_4$ and then to a disubstituted complex [Cp(CO)Fe{P(OPh)$_3$}$_2$]BF$_4$ when refluxed in CH$_2$Cl$_2$ [63].

1.1.2. Water-soluble organometallic compounds in catalysis

Catalysts can be regarded as substances that accelerate the rates of chemical transformations, facilitate establishment of equilibria and are capable of greatly enhancing product selectivities. Catalysts are broadly classified as heterogeneous and homogeneous depending on the phases of catalyst and substrate in a reaction mixture. The homogeneous catalysts are usually in the same phase with the substrates, mainly liquid – liquid, while in heterogeneous catalysis the catalyst and the substrates are in different phases (solid – liquid or solid – gas). Mostly, organometallic compounds are used as homogeneous catalysts and have many advantages over heterogeneous catalysts, which include: well defined active sites, higher activity and selectivity, lower operating temperature and pressure, as well as the possibility to tune their steric and electronic properties. The main drawback of the homogeneous catalysts is the difficulty encountered in recovery of the catalyst; a factor that lowers the catalyst's productivity. However, in recent years a great deal of effort has been put into providing a solution to this limitation by the introduction of two phase catalysis. This aspect has made the water-soluble organometallic complexes more attractive due to their utility in aqueous biphasic catalysis [64-76]. Some of these water-soluble organometallic complexes and their catalytic applications are listed in Table 1.

A catalyst in the aqueous phase can be recovered in its active form at the end of the reaction by simple separation methods such as decantation or filtration, which in turn

increases catalyst productivity. Biphasic catalysis has proven viable in both laboratory and industrial settings since 1984 when the first water-soluble rhodium catalyst was commercialized by the Ruhrchemie-Rhône Poulenc plant for the hydroformylation of olefins to aldehydes [77-79]. Since then many water soluble organometallic complexes have been reported.

The water-solubility of these organometallic complexes is usually accomplished by the introduction of polar substituents in their structures [80, 81]. The most commonly used polar substituents are hydroxyl and amino functionalities as well as ionic groups such as sulfonate, carboxylate and ammonium. Water-soluble organometallic compounds involving rhodium and ruthenium have been reported, but relatively little is known about such compounds of iron although it is an inexpensive, non-toxic metal and a biogenic element [82]. Water-soluble organometallic compounds, particularly containing a biogenic metal would be of a great interest, particularly in biomedical and biological applications.

Table 1: Some water soluble organometallic complexes and their catalyst application

Water-soluble organometallic complex	Solubilizing ligand	Application	Refs
[RuCl$_2$(TPPMS)$_2$]	TPPMS	Reduction of aldehydes	[64]
[HRh(CO)(TPPMS)$_3$]	TPPMS	Hydroformylation of 1-hexene	[65]
[*fac*-Ru(C$_2$H$_5$)(CO)$_2$(H$_2$O)$_3$]$^+$	H$_2$O	Hydrocarbonylation of alkenes	[66]
[Ru(H)(Cl)(TPPTS)$_3$]	TPPTS	Hydrogenation of α,β-unsaturated aldehydes	[67]
RhCl(PTA)$_3$	PTA	Hydrogenation of olefins, oxo-acids, allyl alcohol and 4-sulfonylstyrene	[68]
[Rh(m-Pz)(CO)(TPPTS)]$_2$	TPPTS	hydroformylation of short-chain olefins	[69]
RuCl$_2$(PTA)$_4$	PTA	Hydrogenation of aldehydes	[70]
[RuH(Cl)(CO)(TPPMS)$_3$]	TPPMS	Hydrogenation of alkenes and unsaturated aldehydes	[71]
[RuH(Cl)(NCMe)(TPPMS)$_3$]BF$_4$	TPPMS	Hydrogenation of alkenes	[72]
[Rh(PTAH)(PTA)$_2$CI]C1	PTAH, PTA	Regioselectivity reduction of unsaturated aldehydes to saturated aldehydes	[73]
CpRu(PTA)$_2$H	PTA	Hydrogenation of benzylidene acetone	[74]
[CpRu(PTA)(PTAH)H]BF$_4$	PTA, PTAH	Hydrogenation of benzylidene acetone	[74]

1.1.3. A brief survey of relevant transition metal amine complexes

The synthesis and reactions of organotransition-metal heteroatom complexes is one area of organometallic chemistry that has received relatively little attention. In particular there have been few reports on the synthesis and reactions of organometallic complexes having metal-nitrogen bonds [83]. The paucity could be due to:

(i)   A general belief that the bond between the nitrogen ligand and a late transition metal is relatively weak [84].

(ii)   Difficulty in the preparation of iron(II) complexes of aliphatic amine ligands has been ascribed to the tendency of the complexes to form hydroxo species and their tendency to oxidize to iron(III) oxo species, particularly when traces of water are present [85].

(iii)   The belief that complexes with nitrogen donors containing N–H bonds are generally unsuitable for organometallic reactions, as the H atom(s) on the coordinated nitrogen are sufficiently acidic to react with nucleophiles [86].

It is, however, well known that Fe^{2+} has a great affinity for amines such that addition of 1,10-phenonthroline to ferrous solution resulting in orange $[Fe(C_{12}H_8N_2)_3]^{2+}$ has been generally accepted as a test for the presence of Fe^{2+}. Moreover, the reduction of a colourless Fe(III) ferrozine complex to the coloured Fe(II)ferrozine amine complex is utilized in spectrophotometric determination of aromatic amines [87]. Iron(II) amine complexes incorporating pi acid ligands, such as CO in conjunction with pentadienyl ligands such as cyclopentadienyl and pentamethylcyclopentadienyl would be expected to be stable and hence isolable. This thesis reports the syntheses, reactions and characterization of various iron(II) amine complexes, of which some are stable and soluble in water. The amine complexes reported herein fall into three categories, namely: aliphatic, *N*-heterocyclic and aromatic amine complexes. Thus, only the chemistry of their related transition metal complexes is reviewed in this section.

Aliphatic amine refers to an acyclic or cyclic non aromatic organic compound bearing an amino functionality in its structure. Therefore, open chain amines, piperidine, piperazine and pyrrolidine fall under this category. Probably, the piperazine complexes

[Cp(CO)$_2$Mn(Pip)] and [{Cp(CO)$_2$Mn}$_2$(Pip)] (Pip = piperazine) were the first aliphatic amine cyclopentadienyl complexes reported in the literature. These complexes were prepared by Strohmeier and Guttenberger from the photochemical reaction between [CpMn(CO)$_3$] and piperazine in methanol [88]. One year later the same authors reported the synthesis of the manganese complex [Cp(CO)$_2$Mn(NH$_2$(CH$_2$)$_2$CH$_3$)] which was obtained from irradiation of [CpMn(CO)$_3$] and 1-aminopropane in heptane [89]. In 1977, Giordano and Wrighton, in their study of the photosubstitution behaviour of cyclopentadienyldicarbonylmanganese and related rhenium complexes, reported the compounds [Cp(CO)$_2$M(NH$_2$(CH$_2$)$_2$CH$_3$)] (M = Mn, Re), prepared from [Cp(CO)$_2$M(ether)] by substitution of the labile ether ligand by 1-propylamine [90]. The ether complex was photogenerated by irradiation of an ether solution of [CpM(CO)$_3$] and used *in situ*. Six years later, Sellmann reported that the reaction of [Cp(CO)$_2$Mn(THF)] with *p*-phenylediamine yielded only the dinuclear complex [{Cp(CO)$_2$Mn}$_2$(μ-NH$_2$C$_6$H$_4$NH$_2$)], while the reaction with *m*-NH$_2$C$_6$H$_4$CH$_3$ gave the monuclear complex [Cp(CO)$_2$Mn(*m*-NH$_2$C$_6$H$_4$CH$_3$)] which was reported to undergo deprotonation when treated with Na[N(SiMe$_3$)$_2$] to form [Cp(CO)$_2$Mn(*m*-NHC$_6$H$_4$CH$_3$)]$^-$ [91]. The pyrolidine complex [Cp(CO)$_2$Mn(pyrolidine)] was reported by Lugouskoy *et al*. from the reaction of photogenerated [Cp(CO)$_2$Mn(cyclohexane)] with pyrolidine [92]. Generally, compared to other metals, neutral amine complexes of cyclopentadienylmanganese dicarbonyl are relatively well studied.

The cyclopentadienyltungsten tricarbonyl dimer was reported to react with amines at ambient temperatures (35 ˚C in 45 min) to give [Cp$_2$W$_2$(CO)$_5$L] (L = ethylamine, isopropylamine, diethylamine, butylamine, cyclohexylamine, ethylenediamine, O-phenanthroline, 2,2′-bipyridine). Temperatures higher than 35 ˚C and longer reaction times yielded products that did not contain amines. The authors also reported that reduction of [Cp$_2$W$_2$(CO)$_5$L] with sodium amalgam and subsequent treatment with manganese pentacarbonyl bromide yielded a mixture of heterometallic complexes [CpW(CO)$_2$L]Mn(CO)$_5$ and [Cp(CO)$_3$W]Mn(CO)$_5$ [93]. Two years later Pathak showed that the dimeric tungsten complexes [Cp(CO)$_2$WL]$_2$ (L = C$_5$H$_{11}$N, C$_6$H$_{11}$NH$_2$, C$_6$H$_5$CH$_2$NH$_2$, C$_4$H$_9$NH$_2$) could be obtained by refluxing [CpW(CO)$_3$]$_2$ and an excess of the amine in benzene. When similarly treated with sodium amalgam and subsequent

addition manganese pentacarbonyl bromine, the bimetallic complexes [Cp(CO)$_2$WL]Mn(CO)$_5$ were obtained [94].

The iron dimer [CpFe(CO)$_2$]$_2$ is also known to react with amines such as ethylamine, butylamine, cyclohexylamine, piperidine and morpholine, as well as bidentate ligands such as 1,10-phenanthroline and 2,2'-bipyridyl to give monosubstituted [Cp$_2$Fe$_2$(CO)$_3$L] (L = amine), while the reaction of the iodo complex [Cp$_2$Fe$_2$(CO)$_3$I] with these amines results in the ionic complex [Cp(CO)$_2$FeL]$^+$I$^-$ [95]. The cationic complexes [Cp(CO)$_2$Fe(NHR$_2$)]PF$_6$ (R = Me, Et, SiMe$_3$) have also been synthesized by treating [Cp(CO)$_2$FeCl] with NHR$_2$. These amine complexes become less accessible as the amine becomes more bulky. Although these reactions were performed at low temperature (-20 °C), the electron transfer from the bulky amines to [Cp(CO)$_2$Fe]$^+$ competed with the formation of the amino complexes leading to low yields [96]. The compounds [Cp(CO)$_2$Fe(NH$_2$Pr^i)]BF$_4$ and [Cp(CO)$_2$Fe(NH$_2$Bu^t)]BF$_4$ were obtained along with the metallacycle complex, [Cp(CO)FeC(Et)=C(Et)CO(NHPr^i)], from the reaction between [Cp(CO)$_2$Fe(η^2-Et-C≡C-Et)]BF$_4$ and the amine ligand [97]. The same authors showed that more basic amines, such as piperidine or pyrrolidine, readily displaced the 1-hexyne giving the complexes [Cp(CO)$_2$Fe(NH(CH$_2$)$_n$)]BF$_4$ (n = 4, 5) as the only isolable organometallic species [97]. In contrast, Lennon *et al.* reported that methylamine reacted with the ethylene complex [Cp(CO)$_2$Fe(η^2-CH$_2$=CH$_2$)]BF$_4$ to form [Cp(CO)$_2$Fe(CH$_2$CH$_2$)]$_2$NHCH$_3$, thus resulting in addition of the methylamine instead of displacement of the ethylene. This was believed to proceed *via* the intermediate [Cp(CO)$_2$Fe(η^2-CH$_2$CH$_2$NH$_2$CH$_3$)]BF$_4$ [98].

Iron tetracarbonyl complexes of the type [(Me$_3$N)Fe(CO)$_4$] are well studied [99, 100] and are generally obtained *via* the reaction:

$$[Fe(CO)_5] + Me_3NO \rightarrow [(Me_3N)Fe(CO)_4] + CO_2$$
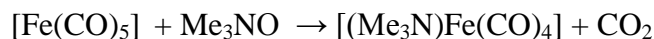
or alternatively by reaction between an aliphatic tertiary amine R$_3$N (R = Me, Et, n-Pr, n-Bu) and [Fe$_2$(CO)$_9$] in hexane or THF at ambient temperature. They are generally

unstable and their instability has been associated with the disproportionatation reaction of iron(0) in presence of the amine [101, 102].

Most of the cyclopentadienyliron dicarbonyl *N*-heterocyclic complexes reported are those of pyridine [103], pyrrole [104-107] and imidazole [108]. Cyclopentadienylirondicarbonyl complexes of 1-methylimidazole, hexamethylenetetramine (HMTA) and diazabicyclo[2.2.2]octane (DABCO) have not been reported prior to this work. There are only two cyclopentadienylmetal carbonyl compounds of DABCO that have been reported. That is the monuclear complex [CpMn(CO)$_2$(DABCO)] and the dinuclear complex [{CpMn(CO)$_2$}$_2$(μ-DABCO)] synthesized by Strohmeier and Guttenberger in 1964, by irradiation of [CpMn(CO)$_3$] and DABCO in wet methanol [89]. In the same paper, the irradiation of [CpMn(CO)$_3$] and HMTA is reported to give only the monuclear [CpMn(CO)$_2$(HMTA)]. The iron carbonyl derivatives [(CO)$_4$Fe(DABCO)] and [{(CO)$_4$Fe}$_2$DABCO] have been reported by Matos and Verkade from the irradiation of [Fe(CO)$_5$] with DABCO in THF [101]. A similar HMTA complex of chromium carbonyl, [(CO)$_5$Cr(HMTA)] has been obtained as a side product in a hydrolysis reaction of the Cr=C bond of aryl and alkenyl(ethoxy)carbene chromium complexes in the presence of hexamethylenetetramine [109]. It can also be obtained from treatment of [(CO)$_5$Cr(NH$_3$)] with HMTA at 65 °C in methanol, or by the reaction between [(CO)$_5$Cr(THF)] and HMTA at 20 °C in THF [110].

Pyrrolylcyclopentadienylirondicarbonyl is one of the *N*-hetrocyclic complexes of iron that has been well studied, probably due to its use as a starting material to a reactive azaferrocene [107, 111, 112] and in the polymerization of pyrrole [105, 106]. For instance, the treatment of [Cp(CO)$_2$Fe(NC$_4$H$_4$)] with N(Bu)$_4$S$_2$O$_8$ in the presence of dodecylbenzenesulfonic acid has been reported to form the soluble, electrically conducting polymer shown in Fig. 3, which on heating forms a polyazaferrocene polymer (Fig. 4) [105].
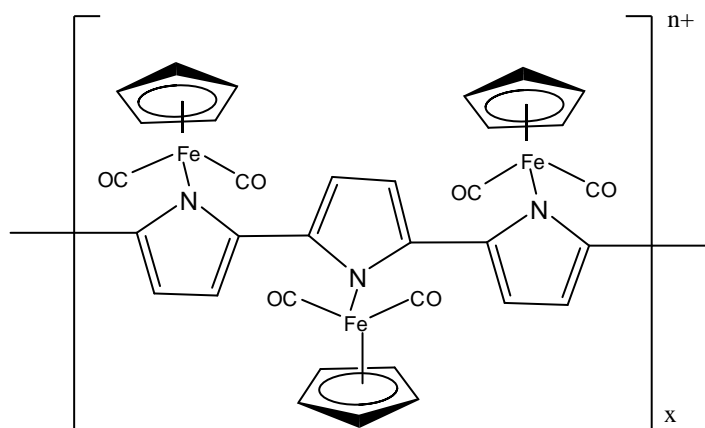
Fig. 3: Polypyrrolylcyclopentadienylirondicarbonyl
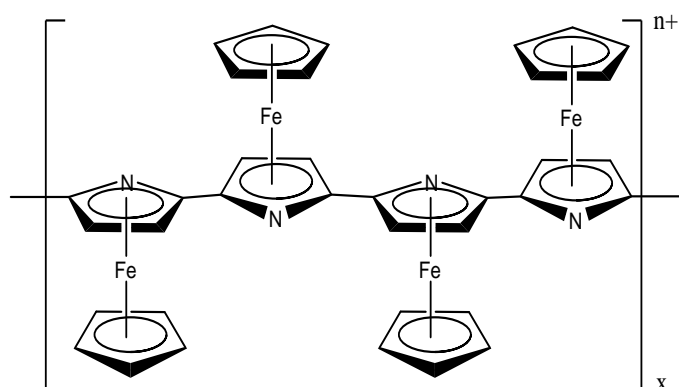
Fig. 4: Polyazaferrocene

Interactions of the cation $[Cp(CO)_2Fe]^+$ with various nitrile and pyridine derivatives have been studied by Schumann and co-authors [103]. They found that oxidative cleavage of $[CpFe(CO)_2]_2$ by $[Cp_2Fe]BF_4$ in the presence of excess L (L = monosubstituted nitrile or pyridine) leads to the cationic complexes $[Cp(CO)_2FeL]BF_4$. However, when the oxidation was done in the presence of the strong nitrogen donor, NH_nR_{3-n} (n = 0-3; R = CH_3, C_6H_5), all CO groups and C_5H_5 were eliminated [103]. The aniline complex $[Cp(CO)_2Fe(NH_2Ph)]^+$ is also known and has been obtained from the reaction between $[Cp(CO)_2Fe(THF)]^+$ and aniline [52].

1.1.4. Rationale for the choice of ligands

Carbon-nitrogen systems are found in a majority of organic molecules, drug pharmacophores [113] and proteins in biological systems. In particular, the amine functionality is found in many biogenic molecules which are generated in the course of microbial, vegetable and animal metabolisms. Some prominent examples of biogenic amines include: histamine (**1**), tryptamine (**2**), tyramine (**3**), serotonin (**4**), putrescine (**5**), spermidine (**6**) and spermine (**7**), and catecholamine components such as epinephrine (**8**), norepinephrine (**9**) and dopamine (**10**) (Fig.5).
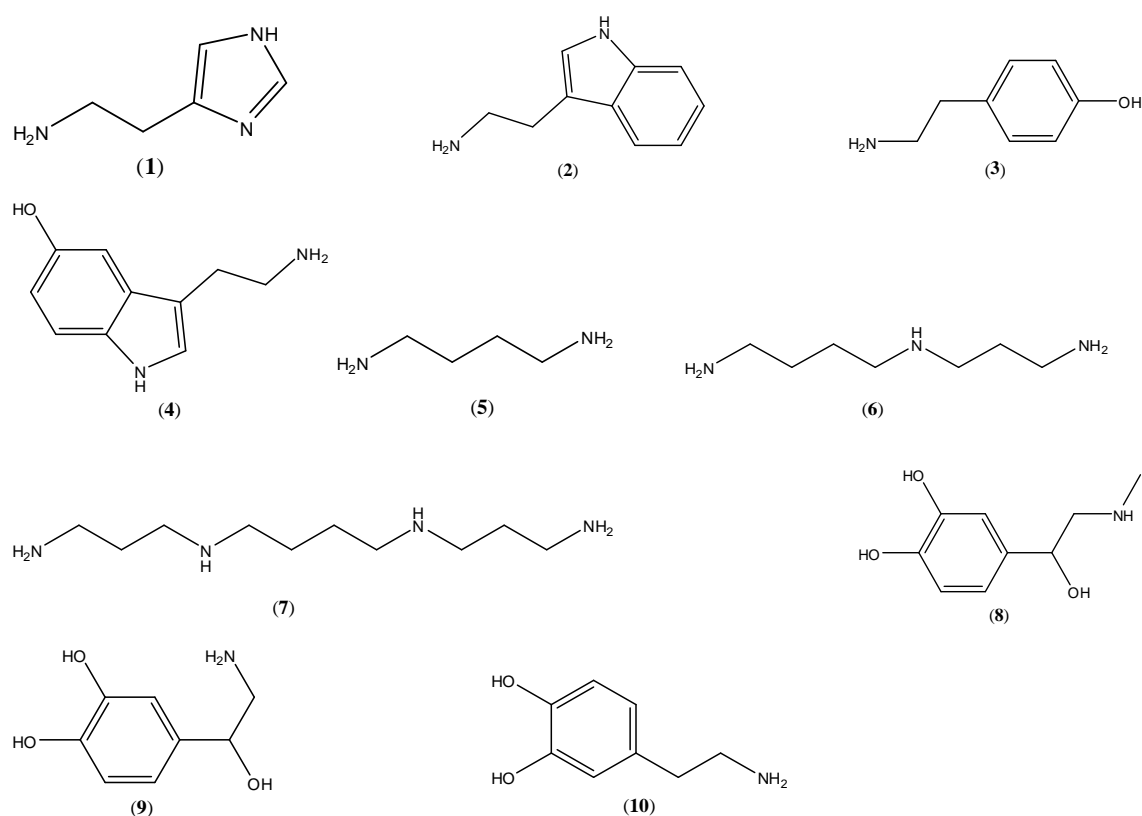
Fig 5: Some biogenic amines

Biogenic amines are a source of nitrogen and precursors for the synthesis of hormones, alkaloids, nucleic acids and proteins [114]. The polyamines **6** and **7** are important for the growth, renovation and metabolism of every organ in the body and essential for

maintaining the high metabolic activity of the normal functioning and immunological system of the gut [114, 115]. It is widely recognized that **5, 6** and **7** are involved in tumor growth and the inhibition of polyamine biosynthesis in tumor-bearing individuals is one of the major targets of cancer therapy research [115]. It has been proposed that polyamines may be part of the possible cellular defence mechanisms against the oxidative damage caused by Fe^{2+} [116]. The biogenic amines **1-4** and **8-10** are neurotransmitters and are found in many animals, including humans [117]. Nitrogen-containing molecules play a great role in pharmacology, in this regard the diaminoalkanes [118, 119], ferrocenyl diamine [120] and ferrocenyl diaminoalcohol [121] complexes have shown high activity against mycobacterium tuberculosis H37Rv. While hexamethylenetetramine has been used mainly in the treatment of urinary tract infections [122-124], some nitrogen-containing compounds such as DABCO are good catalysts in a variety of organic syntheses [125, 126].

The carbonyl, CO, on the other hand, is an interesting ligand due to its ability to accept electrons into π^*-molecular orbitals, thus stabilizing transition metal complexes in low oxidation states. In addition, the physiological effects of CO are now well documented [127-131] and in recent years metal carbonyls have attracted interest as potential CO-releasing molecules (CO-RMs). The metal carbonyls such as η^4-(4-bromo-6-methyl-2-pyrone)tricarbonyliron(0) [132], The tricarbonyldichloro ruthenium(II) dimer [130], dimanganese decacarbonyl [130] and tricarbonylchloro(glycinato)ruthenium(II) [130] have been shown to promote vasodilatory, cardioprotective and anti-inflammatory activities. CO delivered through organometallic CO-RMs has been shown to cause rapid death of pathogenic bacteria such as *Escherichia Coli* and *Staphylococcus Aureus* [133, 134]. The increased activity of CO against anaerobic bacteria has been attributed to preferential binding of CO to the ferrous iron of the heme protein [133]. Metal carbonyl compounds have also found application as tracers in carbonylmetalloimmunoassay procedures as an alternative to radioimmunoassay procedures in molecular recognition [135, 136], due to the characteristic vCO bands appearing in the 1800–2200 cm^{-1} region, where few other functional groups absorb. Based on the above information, the interaction of iron carbonyl complexes with nitrogen-containing species is warranting of

research and appropriate for the development of such organometallic chemistry, as well as its physiology and pharmacology.

1.2. Aims of the project

The broad objective of this study was to develop synthetic routes to various cationic amine complexes of Fe(II) and to study their chemistry. It was hoped that the findings would improve our understanding of the functions of iron in iron-containing enzymes and proteins. Therefore the specific objectives of this study were to:

- Synthesize and characterize the substitutionally labile ether complexes of the type $[(\eta^5-C_5R_5)Fe(CO)_2(E)]BF_4$ (R = CH$_3$; E = THF, R= H; E = Et$_2$O)

- Study the reactions of the ether complexes with various nitrogen-containing ligands and representing varying steric and electronic properties.

- Study the bonding and structures of nitrogen containing iron complexes and provide possible explanations for different behaviours observed.

References

[1]   H. Hayakawa, H. Tanaka, K. Fujimoto, Catal. Commun. 8 (2007) 1820.

[2]   B.C.G. Söderberg, Coord. Chem. Rev. 252 (2008) 57.

[3]   B.C.G. Söderberg, Coord. Chem. Rev. 248 (2004) 1085.

[4]   B.C.G. Söderberg, Coord. Chem. Rev. 250 (2006) 2411.

[5]   P. Rydberg, L. Olsen, J. Phys. Chem. A 113 (2009) 11949.

[6]   D.M.A. Smith, M. Dupuis, E.R. Vorpagel, T.P. Straatsma, J. Am. Chem. Soc. 125 (2003) 2711.

[7]   J. Du, R. Perera, J.H. Dawson, Inorg. Chem. 50 (2011) 1242.

[8]   M.A. Blank, C.C. Lee, Y. Hu, K.O. Hodgson, B. Hedman, M.W. Ribbe, Inorg. Chem. 50 (2011) 7123 and refs. therein.

[9]   J.B. Fernandes, D. Feng, A. Chang, A. Keyser, M.D. Ryan, Inorg. Chem. 25 (1986) 2606.

[10] Q.-Z. Yang, D. Khvostichenko, J.D. Atkinson, R. Boulatov, Chem. Commun. (2008) 963.

[11] L. Marboutin, A. Desbois, C. Berthomieu, J. Phys. Chem. B 113 (2009) 4492.

[12] T.S. Piper, F.A. Cotton, G. Wilkinson, J. Inorg. Nucl. Chem. 1 (1955) 165.

[13] R.B. King, M.B. Bisnette, J. Organomet. Chem. 8 (1967) 287.

[14] R.B. King, J. Am. Chem. Soc. 85 (1963) 1918.

[15] A.F. Clifford, A.K. Murkharjee, J. Inorg. Nucl. Chem. 25 (1965) 1065.

[16] R.B. King, M.B. Bisnette, J. Organomet. Chem. 2 (1964) 38.

[17] M.I. Bruce, J. Organomet. Chem. 21 (1970) 415.

[18] R.D. Theys, M.E. Dudley, M.M. Hossain, Coord. Chem. Rev. 253 (2009) 180 and refs. therein.

[19] M.I. Bruce, F.G.A. Stone, J. Chem. Soc (A). (1966) 1837.

[20] M.I. Bruce, J. Organomet. Chem. 10 (1967) 495.

[21] T.S. Piper, G. Wilkinson, J. Inorg. Nucl. Chem. 3 (1956) 10.

[22] L. Hermans, S.F. Mapolie, polyhedron 16 (1997) 869.

[23] H.B. Friedrich, J.R. Moss, Adv. Organomet. Chem. 33 (1991) 235.

[24] A. Sivaramakrishna, H.S. Clayton, C. Kaschula, J.R. Moss, Coord. Chem. Rev. 251 (2007) 1294.

[25] M.A. Gafour, A.T. Hutton, J.R. Moss, J. Organomet. Chem. 510 (1996) 233.

[26] D. Catheline, D. Astruc, J. Organomet. Chem. 266 (1984) C11.

[27] B. Callan, A.R. Manning, F.S. Stephens, J. Organomet. Chem. 331 (1987) 357.

[28] W.E. Williams, F.J. Lalor, J. Chem. Soc. Dalton Trans. (1973) 1329.

[29] T.J. Meyer, E.C. Johnson, N. Winterton, Inorg. Chem. 10 (1971) 1673.

[30] B. Callan, A.R. Manning, J.Organomet. Chem. 252 (1983) C81.

[31] J.P. Bullock, M.C. Palazotto, K.R. Mann, Inorg. Chem. 30 (1991) 1284.

[32] R.N. Perutz, J.J. Turner, J. Am. Chem. Soc. 97 (1975) 4791.

[33] B.H. Weiller, J. Am. Chem. Soc. 114 (1992) 10910.

[34] S.H. Strauss, Chem. Rev. 93 (1993) 927.

[35] R.H. Crabtree, The organometallic Chemistry of the Transition Metals, Wiley, New York, 1994, p. 206.

[36] J.P. Collman, L.S. Hegedus, J.R. Norton, R.G. Finke, Principles and Applications of Organotransition Metal chemistry, University science books, Mill valley, 1987, p. 521.

[37] M. Kawano, Y. Kobayashi, T. Ozeki, M. Fujita, J. Am. Chem. Soc. 128 (2006) 6558.

[38] W.A. Hermann, H. Biersack, J. Organomet. Chem. 191 (1980) 397.

[39] J.W. Freeman, F. Basolo, Organometallics 10 (1991) 256.

[40] E.O. Fischer, M. Gerberhold, Experienta Suppl. 9 (1964) 259.

[41] B.H.G. Swennenhuis, R. Poland, N.J. DeYonker, C.E. Webster, D.J. Darensbourg, A.A. Bengali, Organometallics 30 (2011) 3054.

[42] S.M. Mansell, R.H. Herber, I. Nowik, D.H. Ross, C.A. Russell, D.F. Wass, Inorg. Chem. 50 (2011) 2252.

[43] D.A. Valyaev, O.V. Semeikin, M.G. Peterleitner, Y.A. Borisov, V.N. Khrustalev, A.M. Mazhuga, E.V. Kremer, N.A. Ustynyuk, J. Organomet. Chem. 689 (2004) 3837.

[44] C.P. Casey, H. Sakaba, P.N. Hasin, D.R. Powell, J. Am. Chem. Soc. 113 (1991) 8165.

[45] K. Schloter, W. Beck, Z. Naturforsch 35b (1980) 985.

[46] N.A. Cooley, K.A. Watson, S. Fortier, M.C. Baird, Organometallics 5 (1986) 2563.

[47] K. Sünkel, G. Urban, W. Beck, J. Organomet. Chem. 290 (1985) 231.

[48] C. Yi, D. Wodka, A.L. Rheingold, G.P.A. Yap, Organometallics 15 (1996) 2.

[49] J.-s. Song, D.J. Szalda, R.M. Bullock, J. Am. Chem. Soc. 118 (1996) 11134.

[50] S.K. Agbossou, J.M. Fernández, J.A. Gladysz, Inorg. Chem. 29 (1990) 476.

[51] W.P. Giering, M. Rosenblum, Chem. Commun. (1971) 441.

[52] D.L. Reger, C. Coleman, J. Organomet. Chem. 131 (1977) 153.

[53] M. Rosenblum, D. Scheck, Organometallics 1 (1982) 397.

[54] S.J. Mahmood, M.M. Hossain, J. Org. Chem. 63 (1998) 3333.

[55] C.J. Eugene, J.M. Thomas, W. Neil, Chem. Commun. (1970) 934.

[56] B.M. Foxman, P.T. Klemarczyk, R.E. Liptrot, M. Rosenblum, J. Organomet. Chem. 187 (1980) 253 and refs. therein.

[57] B.M. Mattson, W.A.G. Graham, Inorg. Chem. 20 (1981) 3186.

[58]   J.M. Fernández, J.A. Gladysz, Organometallics 8 (1989) 207.

[59]   W. Beck, K. Sunkel, Chem. Rev. 88 (1988) 1405.

[60]   M. Akita, M. Tarada, M. Tanaka, Y. Morooka, J. Organomet. Chem. 510 (1996) 255.

[61]   C.M. M'thiruaine, H.B. Friedrich, E.O. Changamu, M.D. Bala, Inorg. Chim. Acta 366 (2011) 105.

[62]   V. Guerchais, A. Didier, J. Chem. Soc., Chem. Commun. (1985) 835.

[63]   A.R. Cutler, A.B. Todaro, Organometallics 7 (1988) 1782.

[64]   A. Benyei, F. Joo, J. Mol. Catal. 58 (1990) 151.

[65]   J.R. Anderson, E.M. Campi, W.R. Jackson, Catal. Lett. 9 (1991) 55.

[66]   T. Funaioli, ClaudiaCavazza, F. Marchetti, G. Fachinetti, Inorg. Chem. 38 (1999) 3361.

[67]   M. Hemandez, P. Kalck, J. Mol. Catal. A Chem. 116 (1997) 117.

[68]   F. Joó, L. Nádasdi, A.C. Bényei, D.J. Darensbourg, J. Organomet. Chem. 512 (1996) 45.

[69]   V.J. Guanipa, L.G. Melean, M.M. Alonzo, A. Gonzalez, M. Rosales, F. Lopez-Linares, P.J. Baricelli, Appl. Cat. A. General 358 (2009) 21.

[70]   D.J. Darensbourg, F. Joó, M. Kannisto, A. Kathó, J.H. Reibenspies, D.J. Daigle, Inorg. Chem. 33 (1994) 200.

[71]   A. Andriollo, J. Carrasquel, J. Marino, F.A. López, D.E. párez, I. Rojas, N. Valencia, J. Mol. Catal. A Chem. 116 (1997) 157.

[72]   P.J. Baricelli, L. Izaguirre, J. López, E. Lujano, F. López-Linares, J. Mol. Catal. A Chem. 208 (2004) 67.

[73]   D.J. Darensbourg, N.W. Stafford, F. Joó, J.H. Reibenspies, J. Organomet. Chem. 488 (1995) 99.

[74]   C.A. Mebi, B.J. Frost, Organometallics 24 (2005) 2339.

[75]   J. Canivet, G. Süss-Fink, Green Chem. 9 (2007) 391.

[76]   J. Canivet, G. Labat, H. Stoeckli-Evans, G. Süss-Fink, Eur. J. Inorg. Chem. 22 (2005) 4493.

[77]   B. Cornils, W.A. Herrrnann, R.W. Eckl, J. Mol. Catal. A Chem. 116 (1997) 27.

[78]   H. Bricout, F. Hapiot, A. Ponchel, S. Tilloy, E. Monflier, sustainability 1 (2009) 924.

[79] B. Cornils, Org. Process Res. Dev. 2 (1998) 121.

[80] K.H. Shaughnessy, Chem. Rev 109 (2009) 643.

[81] M.Y. Darensbourg (Ed.), Inorganic Syntheses, A Wiley-Interscience Publication, New York, 1998.

[82] A.D. Phillips, L. Gonsalvi, A. Romerosa, F. Vizza, M. Peruzzini, Coord. Chem. Rev. 248 (2004) 955.

[83] F.L. Joslin, M.P. Johnson, J.T. Mague, D.M. Roundhill, Organometallics 10 (1991) 2781.

[84] F. Basolo, R.G. Pearson, Mechanism of inorganic reactions, A study of metal com-plexes in solution, Wiley, New York, 1967, pp. 23.

[85] V.L. Goedken, P.H. Merrell, D.H. Busch, J. Am. Chem. Soc. 94 (1972) 3397.

[86] A. Togni, L.M. Venanzi, Angew.Chem. Int. Ed. 33 (1994) 497.

[87] N.A. Zatar, A. Abu-Zuhri, A.A. Abu-Shaweesh, Talanta 47 (1998) 883.

[88] W. Strohmeier, J.F. Guttenberger, Chem. Ber. 96 (1963) 2112.

[89] W. Strohmeier, J.F. Guttenberger, Chem. Ber. 97 (1964) 1256.

[90] P.J. Giordano, M.S. Wrighton, Inorg. Chem. 16 (1977) 160.

[91] D. Sellmann, J. Müller, J. Organomet. Chem. 281 (1985) 249.

[92] S. Lugovskoy, J. Lin, R.H. Schultz, Dalton Trans. (2003) 3103.

[93] S.C. Tripathi, S.C. Srivastava, D.N. Pathak, J. Organomet. Chem. 110 (1976) 73.

[94] D.N. Pathak, J. Inorg. Nucl. Chem. 40 (1978) 2063.

[95] S.C. Tripath, S.C. Srivastava, V.N. Pandey, Trans. Met. Chem. 1 (1976) 58.

[96] E. Román, D. Catheline, D. Astruc, J. Organomet. Chem. 236 (1982) 229.

[97] M. Akita, S. Kakuta, S. Sugimoto, M. Terada, M. Tanaka, Y. Moro-oka, Organometallics 20 (2001) 2736.

[98] P. Lennon, M. Mathavarao, A. Rosan, M. Rosenblum, J. Organomet. Chem. 108 (1976) 93.

[99] Y.Shvo, E. Hazun, Proed, 7th Int. Conf. on Organomet. Chem. (1975) 122.

[100] J. Elzinga, H. Hogeveen, J. Chem. Soc., Chem. Comm. (1977) 705.

[101] R.M. Matos, J.G. Verkade, J. Braz. Chem. Soc. 14 (2003) 71.

[102] H. Sternberg, R. Friedal, S. Shuffler, I. Wender, J. Am. Chem. Soc. 77 (1955) 2675.

[103] H. Schumann, M. Speis, W.P. Bosman, J.M.M. Smits, P.T. Beurskens, J. Organomet. Chem. 403 (1991) 165.

[104] M. Powell, R.D. Bailey, C.T. Eagle, G.L. Schimek, T.W. Hanks, W.T. Pennington, Acta Cryst. C53 (1997) 1611.

[105] K.F. Martin, T.W. Hanks, Organometallics 16 (1997) 4857.

[106] K. Martin, M. Dotson, M. Litterer, T.W. Hanks, C. Veas, Synth. Metals 78 (1996) 161.

[107] D.P. Heenan, C. Lay, V. Montiel-Palma, R.N. Perutz, M.T. Pryce, Organometallics 19 (2000) 3867.

[108] A.N. Nesmeyanov, Y.A. Belousov, V.N. Babin, O.G. Aleksandrov, Y.T. Struchkov, N.S. Kochetkova, Inorg. Chim. Acta 23 (1977) 155.

[109] R. Anmann, P. Hinterding, C. Kruger, R. Goddand, J. Organomet. Chem. 459 (1993) 145.

[110] D. Sellmann, E. Thallmair, J. Organomet. Chem. 164 (1979) 337.

[111] J. Zakrzewski, J.Organomet. Chem. 327 (1987) C41.

[112] J. Zakrzewski, C. Giannotti, J.Organomet. Chem. 388 (1990) 175.

[113] A.M. Kaufmann, J.P. Krise, J. Pharm. Sci. 96 (2007) 729.

[114] M.H. Silla-Santos, Int. J. Food Microbiol. 29 (1996) 213.

[115] A. Bardócz, Trends Food Sci. Technol. 6 (1995) 346.

[116] B. Tadolini, J. Biochem. 249 (1988) 33.

[117] J.H. Biel, L.G. Abood, Biogenic amines and physiological membrane in drug therapy Part B, (1971) 162.

[118] F.M.F. Vergara, M.d.G.M.O. Henriques, A.L.P. Candea, J.L. Wardell, M.V.N.D. Souza, Bioorg. Med. Chem. Lett. 19 (2009) 4937.

[119] R.P. Tripathi, V.K. Tiwari, N. Tewari, D. Katiyar, N. Saxena, S. Sinha, A. Gaikwad, A. Srivastava, V. Chaturvedi, Y.K. Manju, R. Srivastavac, B.S. Srivastavac, Bioorg. Med. Chem. 13 (2005) 5668.

[120] D. Razafimahefa, D.A. Ralambomanana, Lies Hammouche, L. Pélinski, S. Lauvagie, C. Bebear, J. Brocard, J. Maugeind, Bioorg. Med. Chem. Lett. 15 (2005) 2301.

[121] D.A. Ralambomanana, D. Razafimahefa-Ramilison, A.C. Rakotohova, J. Maugein, L. Pélinski, Bioorg. Med. Chem. 16 (2008) 9546.

[122] J. Bango, J. Joseph, L. Browman, Drug delivery system and methods of use, in: W.P.O (Ed.), PCT, vol. WO 2010/120489A2, 2010.

[123] J.G.J. Strom, H.W. Jun, J. Pharm. Sci. 75 (1986) 416.

[124] S.D. Greenwood, Infection 9 (1981) 223.

[125] B. Baghernejad, Eur. J. Chem. 1 (2010) 54.

[126] M.M. Heravi, R.H. Shoar, L. Pedram, Mol. Cat. A. Chem. 231 (2005) 89.

[127] T.R. Johnson, B.E. Mann, J.E. Clark, R. Foresti, C.J. Green, R. Motterlini, Angew. Chem. Int. Ed. 42 (2003) 3722 – 3729 and refs. therein.

[128] J. Steidle, M. Diener, Am. J. Physiol.gastrointest. Liver Physiol. 300 (2011) G207.

[129] P. Sawle, R. Foresti, B.E. Mann, T.R. Johnson, C.J. Green, R. Motterlini, Br. J. Pharmacol. 145 (2005) 800.

[130] R. Motterlini, J.E. Clark, R. Foresti, P. Sarathchandra, B.E. Mann, C.J. Green, Circ. Res 90 (2002) e17.

[131] T. Vera, J.R. Henegar, H.A. Drummond, J.M. Rimoldi, D.E. Stec, J. Am. Soc. Nephrol. 16 (2005) 950.

[132] P. Sawle, J. Hammad, I.J.S. Fairlamb, B. Moulton, C.T. O'Brien, J.M. Lynam, A.K. Duhme-Klair, R. Foresti, R. Motterlini, J. Pharmaco. Exp. Ther. 318 (2006) 403.

[133] L.S. Nobre, J.D. Seixas, C.C. Romão, L.M. Saraiva, Antimicrob. Agents Chemother. 51 (2007) 4303.

[134] K.S. Davidge, G. Sanguinetti, C.H. Yee, A.G. Cox, C.W. McLeod, C.E. Monk, B.E. Mann, R. Motterlini, R.K. Poole, J. Biol. Chem. 284 (2009) 4516.

[135] G. Jaouen, A. Vessieres, Acc. Chem. Res. 26 (1993) 361.

[136] M. Salmain, A. Vessières, A. Varenne, P. Brossier, G. Jaouen, J. Organomet. Chem. 589 (1999) 92.

CHAPTER TWO

Synthesis and characterization of amine complexes of the cyclopentadienyliron dicarbonyl complex cation, $[Cp(CO)_2Fe]^+$

Cyprian M. M'thiruaine[a], Holger B. Friedrich[a*], Evans O. Changamu[b], Muhammad D. Bala[a]

[a] **School of Chemistry, University of KwaZulu-Natal, Private Bag X54001, Durban 4000, South Africa** [b] **Chemistry Department, Kenyatta University, P.O Box 43844, Nairobi, Kenya**

* Corresponding author

Abstract

The organometallic Lewis acid, $[Cp(CO)_2Fe]^+BF_4^-$ ($Cp = \eta^5\text{-}C_5H_5$) reacts with excess dry diethyl ether at low temperatures to form the labile complex $[Cp(CO)_2Fe(OEt_2)]^+[BF_4]^-$ (**1**) which is stable at low temperatures and has been fully characterized. Complex **1** in turn reacts with 1-aminoalkanes and α,ω-diaminoalkanes to form new complexes of the type $[Cp(CO)_2Fe\{NH_2(CH_2)_nCH_3\}]BF_4$ (n = 2-6) (**2**) and $[\{Cp(CO)_2Fe\}_2\{\mu\text{-}NH_2(CH_2)_nNH_2\}](BF_4)_2$ (n = 2-4, 6) (**3**), respectively. These complexes have been fully characterized and the mass spectra of complexes **2** are reported. The structures of compounds **2a** (n = 2) and **2b** (n = 3) have been confirmed by single crystal X-ray crystallography. The single crystal X-ray diffraction data show that complex **2a**, $[Cp(CO)_2Fe\{NH_2(CH_2)_2CH_3\}]BF_4$, crystallizes in a triclinic $P\bar{1}$ space group while **2b**, $[Cp(CO)_2Fe\{NH_2(CH_2)_3CH_3\}]BF_4$, crystallizes in an orthorhombic $P\text{ca}2_1$ space group with two crystallographically independent molecular cations in the asymmetric unit. Furthermore, the reaction of **1** with 1-alkenes gives the η^2-alkene complexes in high yield.

Keywords: α,ω-Diaminoalkanes, Diethyl ether complex, 1-Aminoalkanes, Cyclopentadienyliron dicarbonyl

1. Introduction

The cationic complexes of type, $[Cp(CO)_2FeL]^+$ (L = labile ligand) [1-4] are an important class of transition metal compounds that have been extensively utilized in synthesis [2, 4-21] and catalysis [3, 14, 22-33]. A particular example is the ethereal complex, $[Cp(CO)_2Fe(THF)]BF_4$ [34] in which the labile tetrahydrofuran (THF) is coordinated to the metal centre through the oxygen atom. This complex has been proven to be an essential precursor in the synthesis of various cyclopentadienyliron complexes [4, 10-13, 15-20, 35], as well as catalyst in various organic syntheses such as the [2+2] cycloaddition of alkenes [36], Diels-Alder reactions [37, 38], cyclopropanation [27, 31-33], epoxidation [29, 30] and aziridination [25-28], among others [3, 22-24, 27, 29, 39]. In all these reactions THF is easily displaced by the desired substrate to form either the desired intermediate or desired end product. $[Cp(CO)_2Fe(acetone)]^+$ is another complex with an oxygen-bonded ligand which has also been extensively used in the synthesis of both neutral and cationic complexes based on the $CpFe(CO)_2$ moiety [2, 5-9, 21, 40, 41].

Although diethyl ether has a higher donor number (0.49) than acetone (0.44) [42, 43], the analogous diethyl ether complex, $[Cp(CO)_2Fe(OEt_2)]^+$ has not been previously reported. However, the phosphine complex, $[CpFe(CO)(PPh_3)(OEt_2)][BAr_4]$ (Ar = 3,5-$(CF_3)_2C_6H_3$) has been synthesized by protonation of $[CpFe(CO)(PPh_3)CH_3]$ using $H(OEt_2)BAr_4$ at −80 °C [44]. The dimethyl ether complex, $[Cp(CO)_2Fe(OMe_2)]BF_4$, and its reaction with acetonitrile to give $[Cp(CO)_2Fe(NCCH_3)]BF_4$ has also been reported [1]. $[Cp(CO)_2Fe(OMe_2)]BF_4$ decomposed within a few hours even when stored under vacuum at -20 °C. This thermal instability made the complex difficult to handle, leading to its limited application as a starting material for $CpFe(CO)_2$ complexes. Diethyl ether complexes of other cyclopentadienylmetal carbonyls such as Mn [45], Re [45], Mo [46], and W [46] are known.

There have been very few reports on aminoalkane complexes of cyclopentadienyliron dicarbonyl in which the aminoalkane is coordinated to the metal *via* the nitrogen atom. Reported cases include a reaction between $[Cp(CO)_2Fe(\eta^2-Et-C\equiv C-Et)]BF_4$ and 2-aminopropane, (NH_2Pr^i), to yield the black solid $[Cp(CO)_2Fe(NH_2Pr^i)]^+$ [47]. This is in

sharp contrast to the yellow solid complex $[Cp(CO)_2Fe(NH_2Pr^n)]^+$ reported herein. The reaction between $[Cp(CO)_2Fe(\eta^2\text{-Ph-C}\equiv\text{C-Ph})]BF_4$ and 2-amino-2-methylpropane to give $[Cp(CO)_2Fe(NH_2Bu^t)]^+$ was also reported [47] but no physical or analytical details were given.

Cyclopentadienyliron dicarbonyl complexes of secondary [48], tertiary [35] and cyclic [49] amines are established. Reaction of the acetone complex $[Cp(CO)_2Fe(acetone)]^+$ with half a molar equivalent of either di(tertiary phosphine) [9, 50], 2,5-dithiahexane or pyrazine [9] have been reported to yield dinuclear complexes in which the ligand acts as a bridge between two metal centres. However, to our knowledge, there are no reports on diaminoalkane complexes of iron in which the diaminoalkane links two iron centres.

Hence, in this paper we report the synthesis and characterization of $[Cp(CO)_2Fe(OEt_2)]^+[BF_4]^-$ **1** and its reactions with a series of 1-aminoalkanes, and α,ω-diaminoalkanes to form new complexes, $[Cp(CO)_2Fe\{NH_2(CH_2)_nCH_3\}]BF_4$ (n = 2-6) **(2)** and $[\{Cp(CO)_2Fe\}_2\{\mu\text{-}NH_2(CH_2)_nNH_2\}](BF_4)_2$ (n = 2-4) **(3),** respectively.

2. Results and discussion

2.1. Synthesis of $[Cp(CO)_2Fe(OEt_2)]BF_4$ (**1**)

Reaction of the $[Cp(CO)_2Fe]BF_4$ with a large excess of diethyl ether at low temperatures results in the immediate formation of the diethyl ether complex **1** in excellent yield. The product precipitates and is easily isolated by filtration under inert atmosphere. Reaction of $[Cp(CO)_2Fe]BF_4$ with two equivalents of diethyl ether in CH_2Cl_2 gave low yields (20%) of **1** and was difficult to isolate in pure form. It thus appears that the rate of reaction is partially dictated by the amount of diethyl ether present.

Compound **1** is a moisture sensitive red powder, insoluble in hexane, sparingly soluble in chloroform, but very soluble in acetone and dichloromethane. The complex can be stored in anhydrous atmosphere at -6 ˚C for at least three months without any decomposition.

2.1.1. Characterization

The IR spectrum of the complex **1** shows two carbonyl absorption peaks at 2063 and 2010 cm^{-1}. These suggest a weak synergic interaction between the iron centre and the carbonyl due to lower electron density on the metal centre which is as a result of the coordination of the ethereal group relative to the starting materials, $[Cp(CO)_2FeI]$ and $[Cp(CO)_2FeCH_3]$. A medium and two weak intensity bands due to the symmetrical and asymmetrical C-H stretching modes were observed in the region between 2990 - 2850 cm^{-1}. Two other medium intensity bands due to C-H rocking and C-O stretching were observed at 1392 and 1286 cm^{-1}, respectively.

The ^1H NMR spectrum of **1** recorded in CD_2Cl_2 at -26 ˚C exhibited a Cp peak at 5.42 ppm and a characteristic quartet at 3.47 ppm and a triplet at 1.09 ppm assignable to CH_2 and CH_3, respectively, of the two identical ethyl groups in coordinated diethyl ether. The distinct quartet at 3.43 ppm and a triplet at 1.15 ppm assignable to the CH_2 and CH_3 protons, respectively, of the two identical ethyl group in uncoordinated diethyl ether were also observed. The free diethyl ether was displaced from **1** by water molecules in the CD_2Cl_2 leading to the more stable aqua complex, $[Cp(CO)_2Fe(OH_2)]^+$ [51]. The aqua complex is responsible for a Cp resonance peak observed at 5.28 ppm and a peak due to coordinated water observed at 2.33 ppm.

^{13}C NMR (CD_2Cl_2 at -26 ˚C) spectra also showed separate resonance peaks corresponding to coordinated and uncoordinated diethyl ether. The carbons of the coordinated diethyl ether methylene and methyl groups appear at 78.9 and 13.4 ppm, respectively, while resonance peaks corresponding to uncoordinated diethyl ether were observed at 66.0 and 15.2 ppm, respectively. The spectrum exhibited two Cp peaks at 86.0 and 85.3 ppm corresponding to the Cp carbons of the etherate and aqua complexes, respectively. The carbonyl peak of the etherate complex was observed at 209.6 ppm while that of the aqua complex appeared at 209.1 ppm. The assignment was done by comparing the spectrum with that of the isolated aqua complex.

Similarly, the proton NMR spectrum of compound **1** recorded in acetone-d_6 at -30 ˚C gave a quartet at 3.67 and a triplet at 1.16 ppm assignable to the CH_2 and CH_3 protons of the identical ethyl groups in coordinated diethyl ether, respectively. Separate

resonance peaks corresponding to the protons of the methylene and methyl groups of uncoordinated diethyl ether were observed at 3.39 and 1.10 ppm, respectively. The uncoordinated diethyl ether in this case had been displaced from the coordination centre by acetone, leading to the known acetone complex, $[Cp(CO)_2Fe(OCMe_2)]^+$ [52]. The chemical shift due to the Cp protons of the etherate complex was observed at 5.78 ppm, while a separate resonance peak assignable to the Cp protons of the acetone complex was observed at 5.71 ppm. When wet acetone-d_6 was used, a peak due to the Cp protons of the aqua complex, $[Cp(CO)_2Fe(OH_2)]^+$, was observed at 5.23 ppm.

The intensity of the peaks at 5.78, 3.67 and 1.16 ppm corresponding to the etherate complex diminished as the temperature was raised from -30 to -10 ˚C and eventually disappeared at higher temperature. Conversely, the intensity of the resonance peaks at 5.71, 3.39 and 1.10 corresponding to the acetone complex increased and dominated at -5 ˚C. In general, the proton NMR spectrum of compound **1** shows that diethyl ether is coordinated to the metal centre in the coordination sphere and is not just a solvent molecule trapped within the crystal lattice.

2.2. Reaction studies

The poor electron donating nature of diethyl ether makes complex **1** very electrophilic and thus it reacts with a wide range of nucleophiles.

2.2.1. Reactions of **1** with n-aminoalkanes

Equimolar quantities of **1** and 1-aminoalkanes react smoothly at room temperature in CH_2Cl_2 to give a series of the new complexes, **2**, *via* displacement of diethyl ether according to Scheme 1.

The reaction time of **1** with 1-aminoalkanes at room temperature is chain length dependent. The longer aminoalkanes, though stronger Lewis bases than the shorter ones, required longer reaction times, probably due to steric effects. For example, while the reactions of **1** with 1-aminopropane and 1-aminobutane took less than 2 h, its reaction with longer aminoalkanes took 3 − 6 h. All these complexes were obtained in good yields as yellow crystalline solids after purification by recrystallization. However, the yield diminished as the aminoalkane chain became longer with concomitant increase in

[CpFe(CO)₂]₂ as side product. The complexes are soluble in chlorinated solvents, methanol, acetone, acetonitrile and water, but sparingly soluble in hexane and diethyl ether. Thus they were easily purified by recrystallization from either hexane or diethyl ether without a significant change in yield. They are moderately air stable, both in solid state and solution for short periods of time. Their melting points were sharp and generally decreased with increase in alkyl chain length.

$$NH_2(CH_2)_nCH_3 \quad + \quad \underset{OC}{\overset{}{}}\!\!\!\!\!\!\!\!\!+\!Fe-OEt_2 \quad \xrightarrow[CH_2Cl_2]{24\ ^oC} \quad \underset{OC}{\overset{}{}}\!\!\!\!\!\!\!\!\!+\!Fe-NH_2(CH_2)_nCH_3 \quad + \quad OEt_2$$

2a, n = 2

2b, n = 3

2c, n = 4

2d, n = 5

2e, n = 6
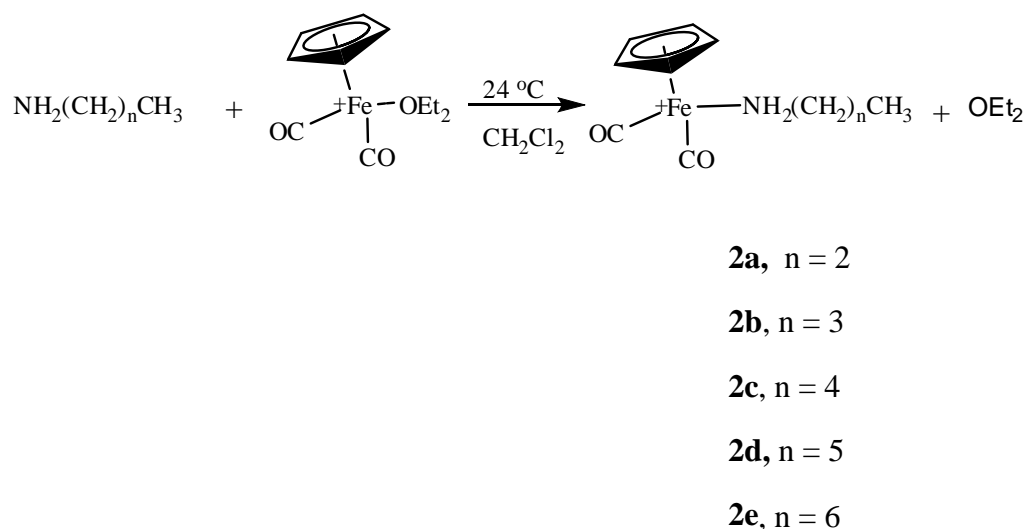
Scheme 1. Preparation of aminoalkane complexes

2.2.1.1. Characterization

The aminoalkane complexes have been fully characterized by elemental analysis, IR spectroscopy, ^{1}H NMR and ^{13}C NMR spectroscopy (Sections 4.3 – 4.7), as well as mass spectroscopy. The crystal structures of **2a** and **2b** have also been determined by single crystal X-ray crystallography.

The IR spectra of the aminoalkane complexes show two very strong absorption bands in the ν(CO) region in the range 1993 - 2061 cm^{-1}, which are assignable to the two terminal carbonyls. The positions of the ν(CO) absorption bands are at lower

wavenumbers relative to those of **1**. This is consistent with the increase in electron density on the iron centre (caused by the coordinated aminoalkane group), which results in increased back-bonding to the carbonyl groups, and hence a lower $\nu(CO)$ absorption frequency. A slight shift towards lower wavenumbers is observed as the carbon chain becomes longer because the nucleophilicity of aminoalkanes increases with increase in chain length [53, 54]. The complexes also show a medium split absorption band in the $\nu(N–H)$ region in the range $3278 – 3313$ cm^{-1} assignable to the N–H stretching mode. A single absorption band due to the N–H bending mode is observed in the range 1605 - 1620 cm^{-1}.
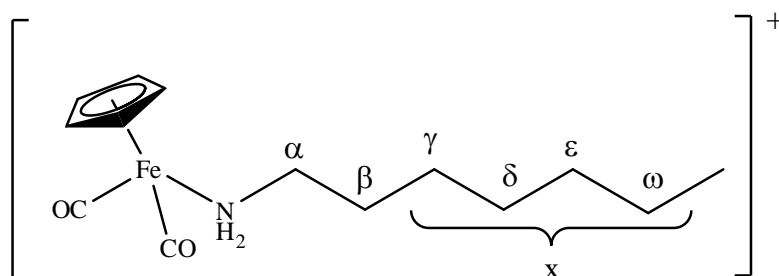
Fig. 1. General structure of the aminoalkane complexes (n = 6 in this instance)

The ^{1}H NMR data for the aminoalkane complexes were recorded in CDCl$_3$ and the assignments made by help of 2D NMR spectra (COSY, HSQC and HMBC). The proton spectrum of each complex shows a characteristic singlet assignable to the two amine protons at ca. 2.90 ppm, which is a down-field shift by ca. 1.80 ppm relative to free aminoalkane (1.10 ppm). This shift can be attributed to the deshielding of the amine proton as nitrogen donates its lone pair to the metal and partially to the presence of a hydrogen bond as found in the structure determinations of compounds **2a** and **2b**. The spectra also exhibited a sharp singlet at ca. 5.27 ppm due to the five equivalent cyclopentadienyl protons. As the chain becomes longer the resonance peaks due to the γ, δ, ε and ω carbon protons (Fig.1) overlapped at ca. 1.20 ppm suggesting that the

influence of the amine group attached to the metal on the chain end is minimal or absent.

The ^{13}C NMR spectra for these complexes were recorded in $CDCl_3$ and assignments made by comparison with the data reported for the cationic complexes, $[Cp(CO)_2M(\eta^2\text{-}CH_2=CHR)]^+$ [13] and $[\{Cp(CO)_2M\}_2\{CH_2=CH(CH_2)_n\}]^+$ (M = Fe, Ru) [55] as well as HSQC and HMBC experiments. The Cp singlets of these complexes at ca. 86 ppm are not affected by the increase of the polymethylene chain length of the aminoalkane. Similarly, chain length does not appear to affect the position of the CO peaks. However, there is a slight down-field shift of the methylene and methyl resonances as the chain grows longer. This is probably due to a deshielding effect caused by increased charge transfer by the alkyl group to the amine group.

The electrospray mass spectra of the series **2a** – **2e** were recorded and are summarized in Table 1. All these complexes show a similar fragmentation pattern (see Appendix 5). Thus loss of BF_4 leads to the base peak of each aminoalkane complex ion, $[\eta^5\text{-}Cp(CO)_2Fe\{NH_2(CH_2)_nCH_3\}]^+$ (parental molecular ion without counteranion), followed by successive loss of the carbonyl groups to give $[CpFe\{NH_2(CH_2)_nCH_3\}]^+$. Peaks due to $[CpFe(CO)_2)]^+$ (m/e 177) or $[CpFe]^+$ (m/e 121) were not observed. However, peaks due to the protonated aminoalkane were observed and their intensity increased with hydrocarbon chain length. This is not unexpected since aminoalkanes are strong Lewis bases due to inductive and polarization stabilization effects of the alkyl group directly bonded to the nitrogen atom [53, 54].

Table 1: Mass spectral data for aminoalkane complexes $[Cp(CO)_2Fe\{NH_2(CH_2)_nCH_3\}]BF_4$ (n = 2 - 6)

Ion	Relative intensity (%)				
	2a (m/e)	**2b** (m/e)	**2c** (m/e)	**2d** (m/e)	**2e** (m/e)
M^+	100 (235.7)	100 (249.7)	100 (263.8)	57.5 (277.7)	13.7 (291.7)
$[M-CO]^+$	15.4 (207.7)	16.2 (221.7)	19.4 (235.8)	6.8 (249.7)	0.0
$[M-2CO]^+$	23.1 (179.7)	23.0 (193.7)	37.0 (207.8)	37.0 (221.7)	5.5 (235.6)
$[\{M-Fp\}+H]^+$	0.0	2.7 (73.8)	19.4 (87.8)	100 (101.7)	100 115.7)

2.2.1.2. Structural analysis of 1-aminoalkane complexes

Single crystal X-ray diffraction data were obtained for complexes **2a** and **2b**. Crystals of both complexes were grown from $CHCl_3$ solutions layered with hexane. Complex **2a** crystallized in a triclinic *P-1* space group, with one molecular cation and a counterion in each asymmetric unit, while **2b** crystallized as orange needles in the orthorhombic *Pca2₁* space group, with two independent molecular cations and two anions in each asymmetric unit. The molecular structures of **2a** and **2b** are shown in Figs. 2 and 3, respectively. In both structures the Fe atom is coordinated in pseudo-octahedral 3-legged piano-stool fashions, with the η^5-coordinated cyclopentadienyl ligand occupying three apical positions while the two carbonyl groups and the alkylamine ligand occupy basal positions. Crystal data and structure refinement information for compounds **2a** and **2b** are summarized in Table 2.
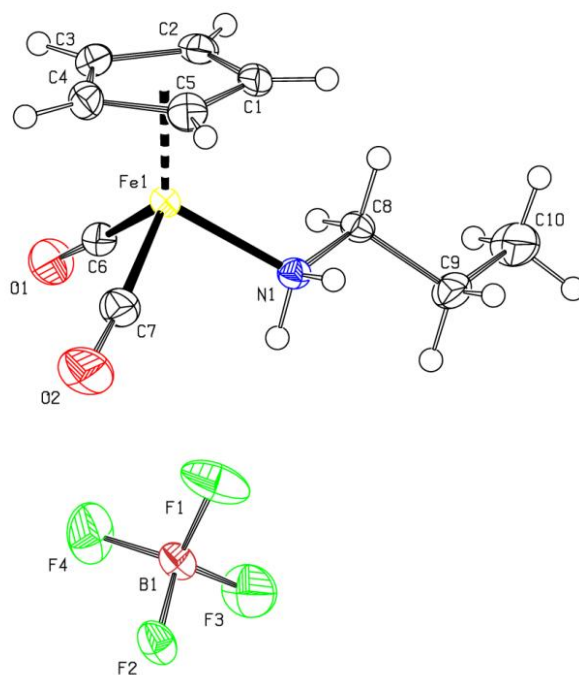
Fig. 2. The molecular structure of **2a** showing atomic numbering scheme. Displacement ellipsoids are drawn at the 50% probability level and H atoms are shown as small spheres

The coordination by alkylamine occurs *via* a single σ-bond through donation of the electron pair on the sp^3-hybridized orbital of nitrogen to the metal. In the crystal, both **2a** and **2b** adopt energetically favoured gauche type conformation (Fig. 4a and 4b) in

which the α-carbon of the alkylamine lies in a conformation between a CO ligand and the cyclopentadienyl ring. This is in agreement with the IR data that shows two peaks for the symmetric and anti-symmetric stretches of the two nominally *cis*-CO ligands. Figs. 5a and 5b show crystal packing and hydrogen bonds in the crystals of **2a** and **2b,** in which molecules are arranged in layers. Alkyl chains of molecules of **2a** are oriented in the same direction within each layer, while those of **2b** are oriented in opposite direction within the same layer as well as in alternating layers. This mode of packing is observed in related structures [47, 56] which aims to minimize steric repulsion. Hence, a set of molecules in a layer of **2a** are related to the subsequent layer *via* a screw axis, while **2b** favored a packing arrangement in which the bulky Cp ligands of subsequent layers occupy the spaces created due to the mutual repulsion of the flexible alkyl chains of adjacent neighbouring molecules.

Molecule A   **Molecule B**
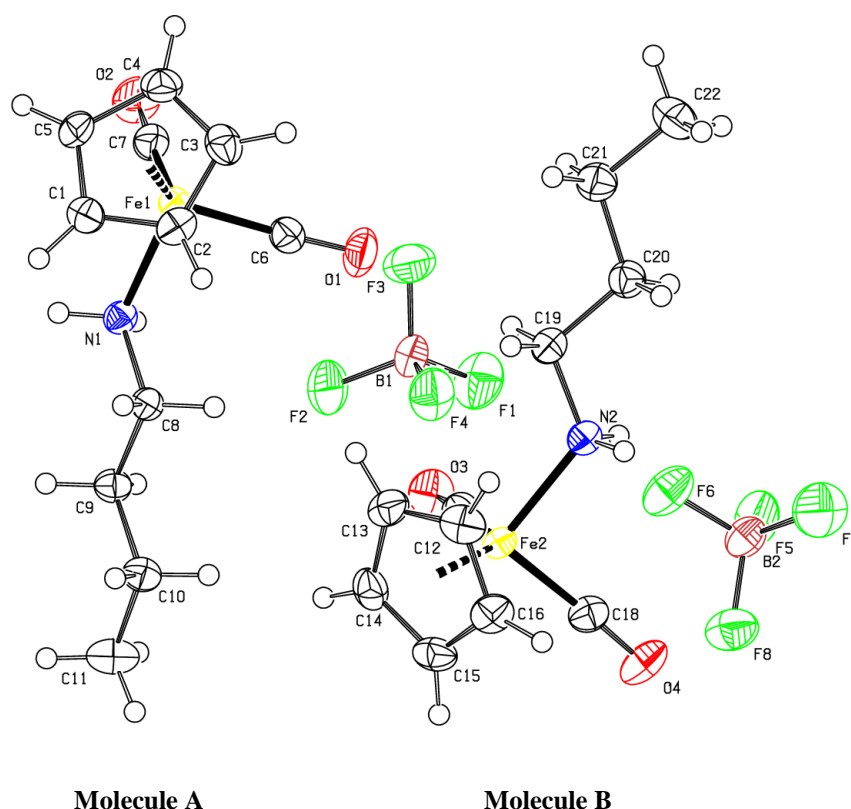
Fig. 3. The molecular structures of the crystallographically independent molecules (A and B) in the asymmetric unit of **2b** showing atom-numbering scheme. Displacement ellipsoids are drawn at 50% probability level and H atoms are shown as small spheres

Fig. 4a
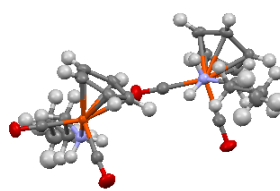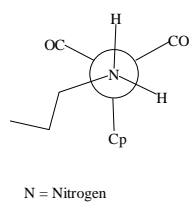
Fig. 4b
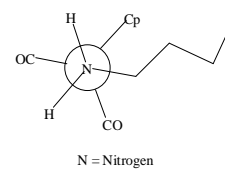
Fig. 4. Molecular structure of **2a** (Fig. 4a) and **2b** (Fig. 4b) showing staggered gauche type conformation
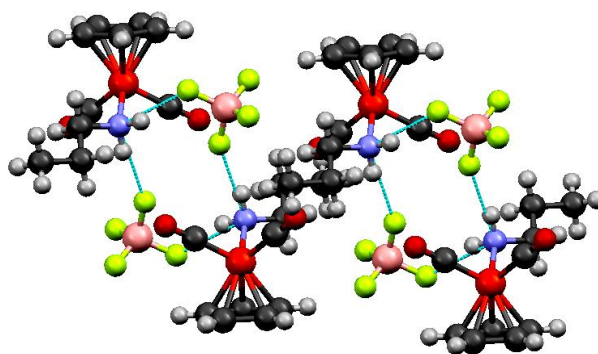
Fig. 5a
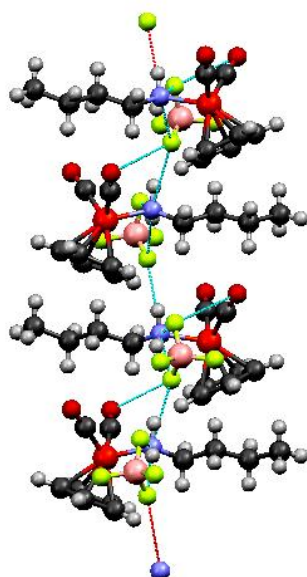
Fig. 5b

Fig. 5. Crystal structures of compound **2a** (Fig. 6a) and **2b** (Fig. 6b) showing hydrogen bonds

Table 2: Crystal data and structure refinement information for **2a** and **2b**

Compound	2a	2b
Empirical formula	$C_{10}H_{14}BF_4FeNO_2$	$C_{11}H_{16}BF_4FeNO_2$
Formula weight	322.88	336.91
Temperature (K)	173(2)	173(2)
Wavelength (Å)	0.71073	0.71073
Crystal system	Triclinic	Orthorombic
Space group	*P-1*	*Pca2₁*
Unit cell dimension (Å, °)		
a	8.8559(12) , α = 108.727(3)	18.4242(3), α = 90
b	8.9932(12), β = 92.219(3)	8.88960(10), β = 90
c	8.9932(12), γ = 92.219(3)	17.4545(3), γ = 90
Volume (Å³)	676.83(16)	2858.76(7)
Z	2	8
Density (calculated)(Mg/m³)	1.584	1.566
Absorption coefficient (mm⁻¹)	1.156	1.098
F(000)	328	1376
Crystal size (mm)	0.43 x 0.30 x 0.25	0.45 x 0.17 x 0.05
Theta range for data collection	2.30 - 28.00°.	2.21 – 27.99
Index ranges		
h	-11 → 11	-24 → 24
k	-10 → 10	-11 → 11
l	-11 → 11	-23 → 20
Reflections collected	8250	31377
Independent reflections	3252	6794
Internal fit	R(int) = 0.0394	0.0499
Absorption correction	Integration	Integration
Transmission factor (T_{Min};T_{Max})	0.7610; 0.6363	0.9471; 0.6378
Refinement method	Full-matrix least-squares on F^2	Full-matrix least-squares on F^2
parameters	173	364
Goodness-of-fit on F^2	1.179	1.026
Final R indices [I>2sigma(I)]	R1 = 0.0377, wR2 = 0.0967	R1 = 0.0306, wR2 = 0.0635
R indices (all data)	R1 = 0.0413, wR2 = 0.1031	R1 = 0.0401, wR2 = 0.0658
Largest diff. peak and hole(e.Å⁻³)	0.423 and -1.178	0.342 and -0.518

The Fe–N bonds were found to be 2.018, 2.013 and 2.006 Å which is in close agreement with 2.015Å observed for the same bond in the complex [Cp(CO)₂Fe{NH₂ CH(CH₃)₂}]⁺ [47]. The N–C bond length was found to fall in the range 1.479 - 1.491 Å, slightly longer than the C–N bond (1.47 Å) observed for free methylamine [57] and shorter than the N–C bond length (1.502 Å) observed for [Cp(CO)₂Fe{NH₂CH(CH₃)₂}]⁺ [47]. The C–C bond lengths in the alkyl chain of the alkylamine fall within the range 1.511-1.527 Å which is in close agreement with that of typical C–C bond lengths (1.53 Å) of alkane chains, indicating that the alkylamine suffered no distortion. Selected bond lengths and angles in molecules of compounds **2a** and **2b** are given in Table 3.

In both crystals the molecules are held together by strong intermolecular hydrogen bonds and charge-assisted van der Waals forces of attraction. The hydrogen bonding occurs between the hydrogen and the fluoride of the counter anion, BF_4^-, as well as the carbonyl oxygen of the complex cation. Formation of the hydrogen-bond results in an electron density shift from the hydrogen atoms to the more electronegative nitrogen [58], leaving the hydrogen atom with a significant positive charge which leads to a coulombic interaction with the fluorine atoms. The down-field shift of the resonance peak due to the coordinated amine proton relative to uncoordinated amine observed in the ^{1}H NMR spectra of complexes **2** may partially be as a result of this electron density transfer. The N–H---F bonds are in the range between 2.07 and 2.53 Å, shorter than N–H---F (2.62 Å) in hydrazinium difluoride [59], while the N–H---O bond lengths fall in the range between 3.02 and 3.08 Å which is significantly shorter than simple van der Waals (3.50 Å) interactions. Tables 4 and 5 show the hydrogen bonding data for compounds **2a** and **2b,** respectively.

Table 3: Selected bond lengths and angles for compound **2a** and **2b**

Bond length(Å)				Bond Angle (°)			
	2a	**2b**			**2a**	**2b**	
		A	B			A	B
Cent - Fe1* (Cent - Fe2)	1.721(7)	1.717(4)	1.714(1)	Cent-Fe1-C6 (Cent-Fe2-C17)	123.7(6)	122.9(4)	123.5(2)
C6 – Fe1 (C17 - Fe2)	1.776	1.795(2)	1.790(2)	Cent-F1-C7 (cent-Fe2-C18)	121.8(8)	122.1(1)	121.0(6)
C7 – Fe1 (C18 - Fe2)	1.793(2)	1.791(3)	1.789(3)	Cent-Fe1-N1 (Cent-Fe2-N2)	122.5(8)	122.4(6)	123.0
N1 – Fe1 (N2 - Fe2)	2.017(8)	2.013(2)	2.006(2)	C6-Fe1-C7 (C17-Fe2-C18)	93.4(10)	96.2(11)	95.8(11)
C6 – O1 (C17 - O3)	1.139(3)	1.132(3)	1.138(3)	C6-Fe1-N1 (C17-Fe2-N2)	93.9(8)	93.0(11)	94.1(10)
C7 – O2 (C18 - O4)	1.142(3)	1.134(3)	1.133(3)	C7-Fe1-N1 (C18-Fe2-N2)	93.2(8)	92.2(10)	91.4(10)
N1 – C8 (N2 - C19)	1.489(2)	1.492(3)	1.479(3)	Fe1-N1-C8 (Fe2-N2-C19)	118.0(11)	117.4(15)	120.4(17)
C8 – C9 (C19 - C20)	1.527(3)	1.514(3)	1.527(4)	N1-C8-C9 (N2-C19-C20)	111.4(16)	112.1(2)	110.3(2)

*Cent is the centroid of the atoms forming the Cp ring, (e.g. C1, C2, C3, C4 and C5)

Table 4: Hydrogen bonds and angles for compound **2a**

D-H...A	[d(D-H) Å]	[d(H...A) Å]	[d(D...A) Å]	[<(DHA) °]
N(1)-H(1A)...F(1)#1	0.92	2.62	3.319(2)	132.8
N(1)-H(1A)...F(2)#1	0.92	2.07	2.954(2)	159.4
N(1)-H(1B)...F(1)	0.92	2.08	2.973(2)	164.2
N(1)-H(1B)...O(1)	0.92	3.02	3.537(2)	117.0

Symmetry transformations used to generate equivalent atoms: #1 -x,-y+1,-z+1

Table 5: Hydrogen bonds and angles for compound **2b**

D-H...A	[d(D-H) Å]	[d(H...A) Å]	[d(D...A) Å]	[<(DHA) °]
N(1)-H(1A)...F(1)	0.92	2.53	3.178(3)	122.1
N(1)-H(1A)...F(4)	0.92	2.31	3.178(3)	156.7
N(1)-H(1B)...F(6)	0.92	2.16	3.077(2)	173.2
N(1)-H(1B)...O(3)	0.92	3.08	3.702(2)	126.3
N(2)-H(2A)...F(5)	0.92	2.23	3.003(3)	140.8
N(2)-H(2A)...F(6)	0.92	2.33	3.195(3)	157.2
N(2)-H(2B)...F(2)#1	0.92	2.45	3.363(3)	171.9
N(2)-H(2B)...F(4)#1	0.92	2.42	3.116(3)	132.5

Symmetry transformations used to generate equivalent atoms: #1 x-1/2,-y+1,z

2.2.2. Reactions of α,ω-diaminoalkanes with two equivalents of 1

Complex **1** was found to undergo facile displacement of Et$_2$O by diaminoalkanes at room temperature when reacted with half equivalents of α,ω-diaminoalkanes, affording symmetrically bridged dinuclear complexes **3a-3d** in good yields (Scheme 2).

These complexes were isolated as yellow microcrystalline solids by precipitation with diethyl ether. They are soluble in water, acetone and acetonitrile but insoluble in chlorinated solvents, hexane and diethyl ether, making them easily separated by filtration under nitrogen. In all cases [CpFe(CO)$_2$]$_2$ was obtained as a side product, the yield of which increased as the diaminoalkane chains became longer. The stability of complexes **3** in acetone varied with chain length. For example, whereas **3a** was purified by recrystallization from an acetone / diethylether mixture, the decomposition of **3c** and **3d** was rapid even in nitrogen-saturated acetone. However, **3c** and **3d** are moderately stable in air and in nitrogen-saturated acetonitrile. They decompose without melting in the range 120 – 183 ˚C, with the decomposition temperature increasing with increase in alkyl chain length.
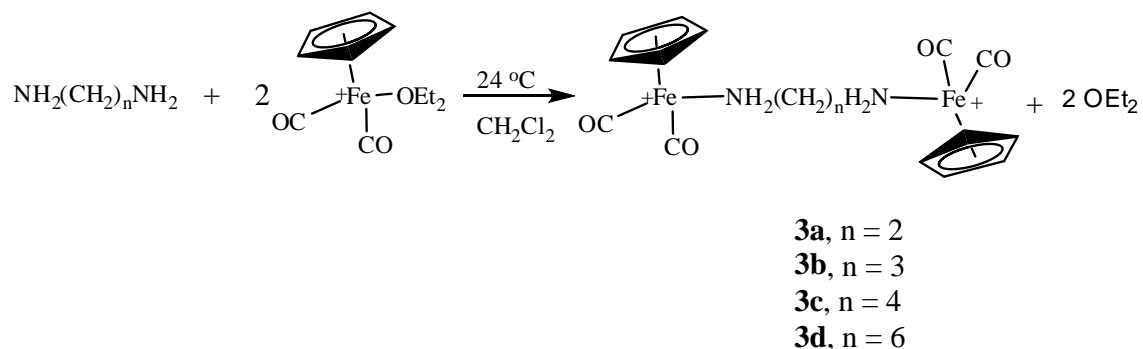
Scheme 2. Preparation of bridged diaminoalkane complexes

2.2.2.1. Characterization

The diaminoalkane complexes have been fully characterized by elemental analysis, IR, ^{1}H NMR, ^{13}C NMR and mass spectroscopy (Sections 4.8 - 4.11).

Their IR spectra exhibited two strong absorption bands in the $\nu(CO)$ region in the range 1991 - 2057 cm^{-1}, which characterize identical cationic CpFe(CO)$_2$ groups [9, 55]. Again, the positions of the $\nu(CO)$ absorption bands are at lower wavenumbers relative to those of **1** for similar reasons given in Section 2.2.1.1. The complexes also show two medium absorption bands in the $\nu(N–H)$ region in the range 3276 - 3315 cm^{-1}, assignable to the symmetric and antisymmetric N–H stretching mode.
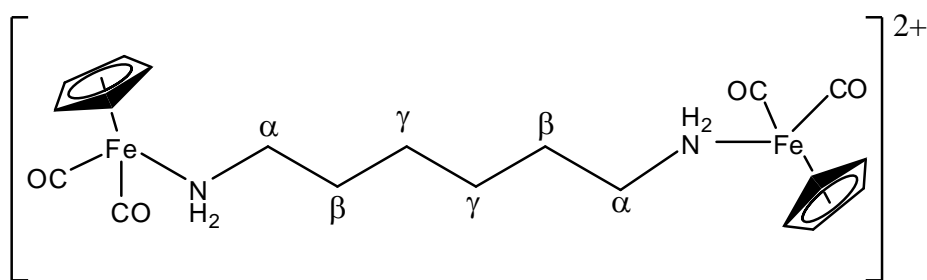
Fig. 6. General structure of the diaminoalkane complexes (n = 6, in this instance)

The ^{1}H and ^{13}C NMR data for **3a**[*] and **3b** were recorded in acetone-d$_6$, while those of **3c** and **3d** were recorded in acetonitrile-d$_3$. The assignments are made by help of 2D NMR spectra and by comparison with data reported by Peng *et al*., for the bridged diphosphine complexes, $[\{Cp(CO)_2Fe\}_2\{\mu\text{-}Ph_2P(CH_2)_nPPh_2\}]^{2+}$ (n = 1-4) [50]. The proton spectra of **3a** and **3b** exhibited a characteristic peak assignable to the Cp protons at ca. 5.50 ppm, while this resonance peak was observed at ca. 5.26 ppm for **3c** and **3d** recorded in acetonitrile-d$_3$. ^{1}H and ^{13}C NMR data suggested a symmetrical structure (Fig. 6), which is also evidence that the diaminoalkane bridges the two metal centres. For instance, the ^{1}H NMR spectrum of compound **3b** shows a triplet resonance peak at 1.74 ppm (J_{HH} = 7.20 Hz) and a quintet at 2.51 (J_{HH} = 7.12 Hz) assignable to two β-methylene protons and four α-methylene protons, respectively.

The ^{13}C NMR spectrum shows four resonance peaks at 36.4, 50.7, 87.5 and 212.2 ppm corresponding to the β-carbon, two identical α-carbons, five equivalent Cp carbons and four identical carbonyls, respectively.

The electrospray mass spectra of the four diaminoalkane complexes, **3a**-**3d** were obtained. Unlike aminoalkane complexes, the fragmentation of diaminoalkane complexes is influenced by the two metal ends and therefore is more complicated (Scheme 3). First BF$_4$ is lost leading to parental molecular ion M$^+$ (i.e $[Cp(CO)_2Fe\{NH_2(CH_2)_nNH_2\}BF_4]$) of weak intensity. Loss of the second counter anion is accompanied by loss of a Fp fragment forming M$^+$ – FPBF$_4$ which was of the strongest intensity peak for the ethylenediamine and diaminoalkane complexes, but decreased with increase in bridge length. Carbonyl ligands were lost in either of five ways as follows: M$^+$ – 2CO, M$^+$ – 4CO – 6H$_2$, M$^+$ – FpBF$_4$ – CO – xH$_2$, M$^+$ – FpBF$_4$ – 2CO or M$^+$ – FpBF$_4$ – CO – (CH$_2$)$_x$NH$_2$ (x = 1, 2, 5 for diaminoethane, diaminopropane and diaminohexane, respectively).

---

[*] Single crystal structure of **3a** was determined and published. See: M'thiruaine et al. *Acta Cryst.* E67(2011) m485. (Appendix 1)

M^+ - FpBF4 - (CO) - $(CH_2)_xNH_2$

- (CO + $(CH_2)_xNH_2$)

- 2 CO M^+ - ($FpBF_4$)

M^+ - 2CO M^+ - FpBF4

- $FpNH_2(CH_2)_nNH_2BF_4$

- 2CO - $6H_2$ - CO - xH_2

- 2 CO

M^+- 4CO - $6H_2$

M^+ - $FpBF_4$ - 2CO M^+ - $FpBF_4$ - CO - xH_2

M^+ - $FpNH_2(CH_2)_nNH_2BF_4$
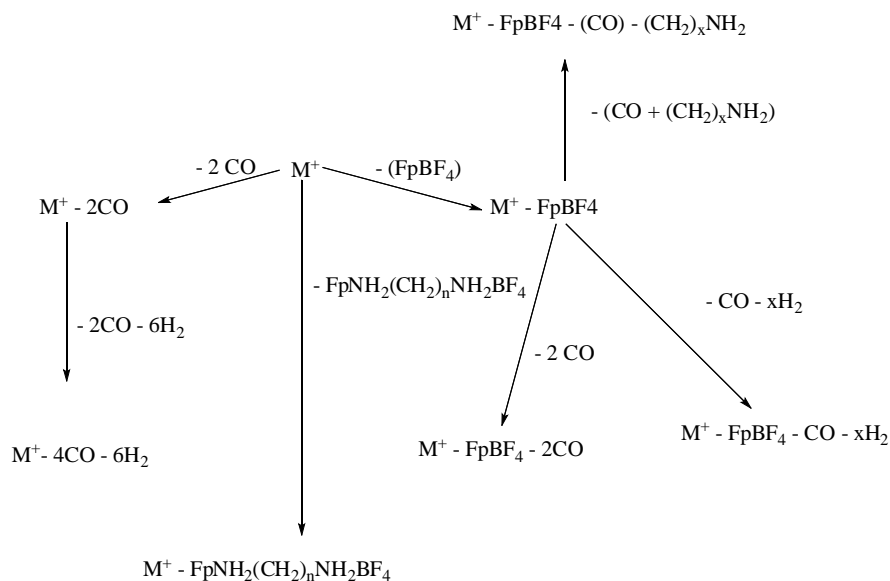
Scheme 3. Fragmentation of diaminoalkane complexes (Fp = $CpFe(CO)_2$; n = 2-4,6; x =1-3)

2.2.3. Reactions of **1** with 1-alkenes, and triphenylphosphine

The ether complex **1** reacts with terminal alkenes and triphenyl phosphine to give known complexes of the type $[Cp(CO)_2FeL]BF_4$ (L = $CH_2CH(CH_2)_2CH_3$, $CH_2CH(CH_2)_3CH_3$, PPh_3) as air stable yellow solids. The IR and NMR spectroscopy data obtained are identical to reported data [13, 60]. These alkene complexes had been previously prepared by either hydride abstraction from their respective alkyl complexes, ligand substitution reactions using Fe–THF or Fe-isobutene complexes or *in situ* reaction of alkenes with the reactive complex $[Cp(CO)_2Fe]BF_4$. In cases where isobutene has been used, low yields are reported because isobutene is not easily displaced by the incoming olefin ligand. Normally heat is used to induce the dissociation but this also leads to the formation of side products, such as the iron dimer, thus lowering the yield. In reactions where the THF complex has been used, $BF_3.Et_2O$ is added to remove THF from the system. The disadvantage of using BF_3 is that it is a highly corrosive gas and catalyses polymerization of some olefins [61], thus making the method difficult. An *in situ* reaction of the alkene with $[Cp(CO)_2Fe]BF_4$ generated by iodide abstraction from $CpFe(CO)_2I$ using $AgBF_4$ leads to low yields of alkene complexes due to formation of an iodo bridged complex, $[Cp(CO)_2Fe]_2IBF_4$ as a side product [51]. Contrary to these reactions, the diethyl ether complex **1** reacts smoothly

with alkenes and triphenylphosphine at room temperature to give excellent yields of the alkene and triphenylphosphine complexes, respectively (Sections 4.12 and 4.13).

3. Conclusion

The diethyl ether complex, $[Cp(CO)_2Fe(OEt_2)]BF_4$ has been successfully synthesized, isolated and shown to be an excellent precursor for the synthesis of a range of cationic cyclopentadienyliron dicarbonyl complexes. Its reaction with 1-aminoalkanes and α,ω-diaminoalkanes leads to formation of novel compounds of type $[Cp(CO)_2Fe\{NH_2(CH_2)_nCH_3\}]BF_4$ and $[\{Cp(CO)_2Fe\}_2\{\mu-NH_2(CH_2)_nNH_2\}](BF_4)_2$ respectively. The structures of some of these compounds have been determined by single crystal X-ray crystallography.

4. Experimental

4.1. General

All manipulations were carried out under inert atmosphere (UHP or HP nitrogen) using Schlenk line techniques. Nitrogen gas was dried over phosphorus(V) oxide. Reagent grade THF, hexane and Et_2O were distilled from sodium/benzophenone and stored over sodium wire; acetone, CH_2Cl_2 and MeCN were distilled from anhydrous $CaCl_2$. The other chemical reagents were obtained from the suppliers shown in parentheses: dicyclopentadiene, iron pentacarbonyl, aminoheptane, 1,3-diaminopropane, 1,4-diaminobutane, 1,6-diaminohexane, tetrafluoroboric acid diethyl ether, iodomethane, mercury (Aldrich), aminopropane, aminopentane, aminohexane 1,2-diaminoethane, silver tetrafluoroborate (Merck), aminobutane (BDH), sodium (Fluka) and iodine (Unilab) were used as supplied. Melting points were recorded on an Ernst Leitz Wetzlar hot-stage microscope and are uncorrected. Elemental analyses were performed on LECO CHNS-932 elemental analyzer. Infrared spectra were recorded using an ATR PerkinElmer Spectrum 100 spectrophotometer between 4000 - 400 cm^{-1}, in the solid state. Mass spectra were recorded on an Agilent 1100 series LC/MSD trap with electrospray ionization (ESI) source and quadrupole ion trap mass analyzer by direct

infusion and ESI operated in the positive mode. Acetonitrile (100%) was used as mobile phase and 10 μL of the sample injected at 0.3 ml/min flow rate. NMR spectra were recorded on Bruker topspin 400 and 600 MHz spectrometers. The deuterated solvents $CDCl_3$ (Aldrich, 99.8%), acetonitrile-d_3 (Merck, 99%) and acetone-d_6 (Aldrich, 99.5%), were used as purchased. Solutions for NMR spectroscopy were prepared under nitrogen using nitrogen-saturated solvents. The precursors $[CpFe(CO)_2]_2$ [62], $CpFe(CO)_2I$ [63], $CpFe(CO)_2CH_3$ [22] and $[Cp(CO)_2Fe]BF_4$ [51], were prepared by the literature methods. The reactions between **1** and aminoalkanes were monitored by IR spectroscopy, and stopped after all of **1** was consumed as indicated by the complete shift in the $v(CO)$ peak from 2063 to lower wavenumbers.

4.2. Preparation of [Cp(CO)₂(OEt₂)]BF₄ (**1**)

The complex was prepared from $[Cp(CO)_2Fe]BF_4$ made by either iodide abstraction using $AgBF_4$ or by methyl abstraction using $HBF_4.Et_2O$. These two routes and an *in situ* reaction of diethyl ether with $[Cp(CO)_2Fe]BF_4$ are described below.

(i)   Iodide complex route

A foil-wrapped 100 ml Schleck tube was charged with $CpFe(CO)_2I$ (0.213 g, 0.70 mmol) and $AgBF_4$ (0.196 g, 1.00 mmol). The mixture was dried under reduced pressure for at least 6 h to remove any water absorbed by $AgBF_4$ during transfer. Dichloromethane (20 ml) was then added and the mixture stirred in the dark for 45 min. The reaction mixture was cooled to -78 ˚C and stirred for 30 min. The resulting wine red-coloured solution was cannula filtered into a Schleck tube previously flushed with nitrogen and filled with ice-cooled dry nitrogen-saturated diethyl ether (30 ml, 290 mmol). Immediately a red precipitate formed and the mixture was cooled to -78 ˚C and maintained there for at least 2 h. The mother liquor was removed by the use of a cannula under nitrogen to leave a red solid residue. The solid was dried under reduced pressure at 0 ˚C for at least 6 h resulting in a red-orange moisture sensitive microcrystalline solid. It was purified further by recrystallization from a dichloromethane/diethyl ether mixture (1:1 ratio). Brief exposure to air caused conversion to the known aqua complex, $[Cp(CO)_2Fe(OH_2)]BF_4$ [51]. However, the solid product was stored at -6 ˚C under nitrogen atmosphere for three months without noticeable decomposition. The mother

liquor was evaporated and dried under similar conditions to give a thick brown oil which was found to be a decomposition product as suggested by ^{1}H NMR due to the presence of numerous Cp resonance peaks. Yield: 0.175 g, 74%. ^{1}H NMR (600 MHz, CD$_2$Cl$_2$): δ 5.42 (s, 5H, Cp), 3.47 (q, J_{HH} = 6.54 Hz, 4H), 1.09 (t, J_{HH} = 6.54 Hz, 6H). ^{13}C NMR (600 MHz, CD$_2$Cl$_2$): δ 85.95 (Cp), 78.93 (O-CH$_2$), 13.38 (CH$_3$), 209.59 (CO). IR (solid state): ν(CO) 2063, 2010 cm^{-1}.

(ii)   Methyl complex route

A pre-weighed 100 ml Schlenk tube was charged with a solution of Cp(CO)$_2$FeCH$_3$ (0.949 g, 4.94 mmol) in freshly distilled CH$_2$Cl$_2$ (20 ml) followed by HBF$_4$.Et$_2$O (1 ml, 7.29 mmol) added dropwise while stirring. The mixture was stirred for 10 min and then cooled to -78 ˚C for 10 min, after which 15 ml of diethyl ether was added, resulting in a red precipitate. This was allowed to warm up to a temperature of -6 ˚C, cooled and allowed to stand at -78 ˚C for at least 10 min. Filtration through a cannula and drying the residue at 0 ˚C for 8 h provided a red microcrystalline solid identical to the one obtained through the iodide complex route. Yield: 1.503 g, 90%.

(iii)   In situ reaction of diethyl ether with [Cp(CO)$_2$Fe]BF$_4$

A nitrogen-saturated solution of CpFe(CO)$_2$CH$_3$ (0.286 g, 1.47 mmol) in dry diethyl ether (20 ml) in a 50 ml Schleck tube was cooled to -78 ˚C and 0.4 ml of HBF$_4$ .Et$_2$O added dropwise while stirring. No reaction was observed at this temperature. On warming the mixture to ca. -6 ˚C, evolution of methane gas began and a red precipitate started to form. The mixture was then cooled further to -78 ˚C, separated and purified as explained in (i) and (ii) above. Yield: 0.343 g, 69%.

4.3. Reaction of *1* with 1-aminopropane

Aminopropane (0.12 ml, 1.46 mmol) was added dropwise to a stirred solution of the diethyl ether complex, **1** (0.460 g, 1.36 mmol) in dry dichloromethane (10 ml). This resulted in an immediate change of colour from red to brown. The mixture was stirred for 3 h and then dry diethyl ether added until a yellow precipitate formed. The mixture was allowed to stand for 10 min, after which the mother liquor was removed using a cannula. Washing the residue with diethyl ether (2 x 10 ml) and drying under reduced

pressure provided 0.383 g (87% yield) of yellow-orange solid. Anal. Calc. for $C_{10}H_{14}BF_4FeNO_2$: C, 37.15; H, 4.33; N, 4.33. Found: C, 37.13; H, 4.47; N, 4.13%. ^{1}H NMR (600 MHz, CDCl$_3$): δ 5.27 (s, 5H, Cp), 2.95 (s, 2H, -NH$_2$), 2.19 (m, J_{HH} = 7.38 Hz, 2H, αCH$_2$), 1.52 (m, J_{HH} = 7.34 Hz, 2H, βCH$_2$), 0.82 (t, J_{HH} = 7.38 Hz, 3H, CH$_3$). ^{13}C NMR (600 MHz, CDCl$_3$): δ 86.06 (Cp), 55.31 (α C), 25.74 (β C) 10.82 (CH$_3$), 210.06 (CO). IR (solid state): ν(CO) 2057, 2000 cm^{-1}; ν(NH) 3311, 3281 cm^{-1}. M.p., 102 - 103 ˚C

4.4. Reaction of *1* with 1-aminobutane

To **1** (0.960 g, 2.84 mmol) in a Schleck tube, freshly distilled dichloromethane (20 ml) was added followed by 1-aminobutane (0.30 ml, 3.05 mmol). The mixture was stirred for 3 h when the reaction was judged complete using IR (appearance of absorption band at 2055 cm^{-1} and disappearance of absorption band at 2066 cm^{-1}). On addition of diethyl ether to the mixture and allowing it to stand for 1 h, yellow flake-like crystals formed. The mixture was filtered *via* cannula and the solid washed with 2 x 20 ml diethyl ether, dried under reduced pressure and purified further by recrystalisation from a dichloromethane-diethyl ether mixture to give 0.909 g (95% yield) yellow solid. Anal. Calc. for $C_{11}H_{16}BF_4FeNO_2$: C, 39.17; H, 4.75; N, 4.15. Found: C, 39.75; H, 4.44; N, 4.35%. ^{1}H NMR (600 MHz, CDCl$_3$): δ 5.27 (s, 5H, Cp), 2.91 (S, 2H, -NH$_2$), 2.23 (m, 2H, αCH$_2$), 1.47 (m, 2H, βCH$_2$), 1.24 (m, 2H, γCH$_2$), 0.83 (t, J_{HH} = 7.35 Hz, 3H, CH$_3$). ^{13}C NMR (600 MHz, CDCl$_3$): δ 86.07 (Cp), 53.35 (α C), 34.42 (β C), 19.62 (γ C) 13.53 (CH$_3$), 210.62 (CO). IR (solid state): ν(CO) 2055, 2000 cm^{-1}; ν(NH) 3307, 3279 cm^{-1}. M.p., 58 - 60 ˚C.

4.5. Reaction of *1* with 1-aminopentane

1-aminopentane (0.16 ml, 1.39 mmol) was added dropwise, while stirring, into a solution of **1** (0.440 g, 1.30 mmol) in dichloromethane (20 ml). The solution turned from red to light brown. The mixture was stirred overnight and then hexane was added to precipitate the product as a yellow solid. The mixture was then treated similarly to that of the 1-aminobutane complex to give 0.324 g (71% yield) of yellow solid. On evaporation of the filtrate under reduced pressure, purple needle-like crystals were obtained and identified as [CpFe(CO)$_2$]$_2$ by IR, ^{1}H NMR and ^{13}C NMR spectroscopy.

Anal. Calc. for $C_{12}H_{18}BF_4FeNO_2$: C, 41.03; H, 5.13; N, 3.99. Found: C, 40.87; H, 4.95; N, 4.13%. ^{1}H NMR (600 MHz, CDCl$_3$): δ 5.27 (s, 5H, Cp), 2.90 (S, 2H, -NH$_2$), 2.22 (m, 2H, αCH$_2$), 1.50 (m, 2H, βCH$_2$), 1.18 (m, 2H, (CH$_2$)$_2$), 0.82 (t, J_{HH} = 6.96 Hz, 3H, CH$_3$). ^{13}C NMR (600 MHz, CDCl$_3$): δ 86.07 (Cp), 53.62 (α C), 32.15 (β C), 28.54 (γ C) 22.14 (δ C), 13.80 (CH$_3$), 210.60 (CO). IR (solid state): ν(CO) 2061, 1993 cm^{-1}; ν(NH) 3312, 3282 cm^{-1}. M.p., 83 - 85 °C.

4.6. Reaction of 1 with 1-aminohexane

This reaction procedure was executed as described above for aminopentane with the following quantities of reagents: **1** (1.47 g, 4.35 mmol),1-aminohexane (0.6 ml, 4.54 mmol). A yellow solid was obtained, 1.13 g (71% yield). Anal. Calc. for $C_{13}H_{20}BF_4FeNO_2$: C, 42.74; H, 5.48; N, 3.84. Found: C, 42.51; H, 5.25; N, 4.47%. ^{1}H NMR (600 MHz, CDCl$_3$): δ 5.27 (s, 5H, Cp), 2.90 (s, 2H, -NH$_2$), 2.22 (m, 2H, αCH$_2$), 1.49 (m, 2H, βCH$_2$), 1.20 (m, 2H, (CH$_2$)$_3$), 0.82 (t, J_{HH} = 10.44 Hz, 3H, CH$_3$). ^{13}C NMR (600 MHz, CDCl$_3$): δ 86.08 (Cp), 53.72 (α C), 32.58 (β C), 31.30 (γ C) 26.21 (δ C) 22.48 (ε C), 14.00 (CH$_3$), 210.68 (CO). IR (solid state): ν(CO) 2048, 1994 cm^{-1}; ν(NH) 3309, 3277 cm^{-1}. M.p., 61 - 62 °C.

4.7. Reaction of 1 with 1-aminoheptane

The reaction procedure was executed as described for aminopentane with the following quantities of reagents: **1** (0.87 g, 2.57 mmol), 1-aminoheptane (0.4 ml, 2.70 mmol). A yellow solid was obtained, 0.575 g (59% yield). Anal. Calc. for $C_{14}H_{22}BF_4FeNO_2$: C, 44.32; H, 5.80; N, 3.69. Found: C, 44.61; H, 6.29; N, 3.43%. ^{1}H NMR (600 MHz, CDCl$_3$): δ 5.27 (s, 5H, Cp), 2.88 (s, 2H, -NH$_2$), 2.23 (m, 2H, αCH$_2$), 1.49 (m, 2H, βCH$_2$), 1.19 (m, 2H, (CH$_2$)$_4$), 0.82 (t, J_{HH} = 6.84 Hz, 3H, CH$_3$). ^{13}C NMR (600 MHz, CDCl$_3$): δ 86.06 (Cp), 53.64 (α C), 32.46 (β C), 31.57 (γ C) 28.74 (δ C) 26.45 (ε C), 22.47 (ω C), 13.96 (CH$_3$), 210.55 (CO). IR (solid state): ν(CO) 2055, 2020 cm^{-1}; ν(NH) 3304, 3269 cm^{-1}. M.p., 40 - 41 °C.

4.8. Reaction of *1* with 1,2-diaminoethane

1,2-diaminoethane (0.05 ml 0.75 mmol) was added dropwise to a solution of **1** (0.500 g, 1.48 mmol) in CH_2Cl_2 (15 ml) at 0 °C and the mixture stirred rapidly for 10 min. The mixture was then allowed to stand at room temperature for 6 h during which a brown precipitate formed. The mother liquor was removed through a cannula and the residue washed with 2 x 10 ml portions of CH_2Cl_2 and dried under reduced pressure to give a yellow solid. This solid was extracted with 10 ml of dry acetone and dry diethyl ether added to the extract until yellow precipitate formed. Filtration of the precipitate, followed by drying under reduced pressure provided a yellow microcrystalline solid. This was purified further by recrystallization from an acetone-diethyl ether mixture. Yield: 0.339 g, 78%; Anal. Calc. for $C_{16}H_{18}B_2F_8Fe_2N_2O_4$: C, 32.65; H, 3.06; N, 4.76. Found: C, 32.96; H, 3.28; N, 5.02%. ^{1}H NMR (400 MHz, acetone-d_6): δ 5.48 (s, 10H, Cp), 3.33 (s, 4H, NH$_2$), 2.58 (s, 4H, CH$_2$). ^{13}C NMR (400 MHz, acetone-d_6): δ 87.43 (Cp), 54.50 (CH$_2$), 211.92 (CO). IR (solid state): ν(CO) 2054, 2001 cm^{-1}; ν(NH) 3315, 3276 cm^{-1}. Decomposes without melting at temperature >120 °C.

4.9. Reaction of *1* with 1,3-diaminopropane

To a solution of **1** (0.520 g, 1.54 mmol) in CH_2Cl_2 (20 ml), 1,3-diaminopropane (0.06 ml, 0.72 mmol) was added dropwise at room temperature and stirred for 12 h. The mixture was filtered, the residue washed with 2 x 10 ml portion of CH_2Cl_2 to give a yellow solid. The yellow solid was extracted with 10 ml of dry nitrogen-saturated acetonitrile and dry nitrogen-saturated diethyl ether added to the extract until a yellow precipitate formed. Filtration, followed by drying of the residue under reduced pressure provided a yellow microcrystalline solid. Yield: 0.310 g, 67%; Anal. Calc. for $C_{17}H_{20}B_2F_8Fe_2N_2O_4$: C, 33.89; H, 3.32; N, 4.65. Found: C, 33.95; H, 3.86 ; N, 4.80%. ^{1}H NMR (400 MHz, acetone-d_6): δ 5.50 (s, 10H, Cp), 3.43 (s, 4H, NH$_2$), 2.51 (m, J_{HH} = 7.12 Hz, 4H, αCH$_2$), 1.74 (t, J_{HH} = 7.20 Hz, 4H, βCH$_2$). ^{13}C NMR (400 MHz, acetone-d_6): δ 87.45 (Cp), 50.73 (α C), 36.41 (β C), 212.23 (CO). IR (solid state): ν(CO) 2051, 1997 cm^{-1}; ν(NH) 3307, 3280 cm^{-1}. Decomposes without melting at temperature >160 °C.

4.10. Reaction of **1** with 1,4-diaminobutane

To a solution of **1** (0.45 g, 1.33 mmol) in 15 ml of CH_2Cl_2, 1,4-diaminopropane (0.06 ml, 0.60 mmol) was added dropwise at room temperature while stirring. Stirring was continued for 5 h and then the mixture was allowed to stand at room temperature overnight. The rest of the procedure was executed as described in Section 4.9 for 1,3-diaminopropane complex to provide yellow microcrystalline solid: Yield: 0.283 g, 69%; Anal. Calc. for $C_{18}H_{22}B_2F_8Fe_2N_2O_4$: C, 35.06; H, 3.57; N, 4.55. Found: C, 35.58; H, 3.61; N, 4.27%. ^1H NMR (600 MHz, CD_3CN): δ 5.26 (s, 10H, Cp), 2.61 (s, 4H, NH_2), 2.23 (m, 4H, αCH$_2$), 1.34 (m, 4H, βCH$_2$). ^{13}C NMR (400 MHz, CD_3CN): δ 86.24 (Cp), 52.04 (α C), 29.08 (β C), 211.15 (CO). IR (solid state): ν(CO) 2057, 1991 cm^{-1}; ν(NH) 3310, 3281 cm^{-1}. Decomposes without melting at temperature >180 ˚C.

4.11. Reaction of **1** with 1,6-diaminohexane

This reaction procedure was executed as described above for the diaminobutane complex with the following quantities of reagents: **1** (0.470 g, 1.39 mmol), 1,6-diaminohexane (0.09 ml, 0.69 mmol). A yellow solid was obtained, 0.313 g (70% yield). Anal. Calc. for $C_{20}H_{26}B_2F_8Fe_2N_2O_4$: C, 37.27; H, 4.04; N, 4.35. Found: C, 37.56; H, 4.58; N, 4.23%. ^1H NMR (400 MHz, CD_3CN): δ 5.26 (s, 10H, Cp), 2.61 (s, 4H, NH_2), 2.26 (m, 4H, αCH$_2$), 1.58 (m, 4H, βCH$_2$) 1.18 (m, 4H, γCH$_2$). ^{13}C NMR (400 MHz, CD_3CN): δ 85.93 (Cp), 52.33 (α C), 31.88 (β C), 25.21 (γ C), 210.90 (CO). IR (solid state): ν(CO) 2052, 2004 cm^{-1}; ν(NH) 3327, 3285 cm^{-1}. Decomposes without melting at temperature >183 ˚C.

4.12. Reaction of **1** with 1-alkenes

The procedure for the reaction of **1** with 1-pentene is described as an illustration of the general procedure followed in the reactions with 1-alkenes. To a solution of **1** (0.246 g, 0.73 mmol) in 10 ml dichloromethane, 1-pentene (2 ml, 18.31 mmol) was added and the mixture stirred for 10 min and then allowed to stand overnight at room temperature. The resulting mixture was filtered and dry diethyl ether added to the filtrate. Although a yellow precipitate formed immediately, the mixture was allowed to stand for 5 h to allow its settling. The precipitate was then filtered off, washed with 3 x 5 ml portions of

diethyl ether and dried under reduced pressure. A yellow solid was obtained and purified by recrystallization from a dichloromethane-diethyl ether mixture (1:2 volume ratio) Yield: 0.221 g, 91%. Anal. Calc. for $C_{12}H_{15}BF_4Fe\,O_2$: C, 43.11; H, 4.49. Found: C, 42.67; H, 5.03%. ^{1}H NMR (600 MHz, CDCl$_3$): δ 5.62 (s, 5H, Cp), 5.17 (m, 1H, =CH), 4.06 (d, J_{HH} = 7.68 Hz, 1H, =CH$_2$, *cis*), 3.28 (d, J_{HH} = 14.7 Hz, 1H, =CH$_2$, *trans*), 2.43 (m, 1H, =CHCH), 1.57 (m, 3H, CHCH$_2$), 0.95 (t, J_{HH} = 12.96 Hz, 3H, -CH$_3$). ^{13}C NMR (600 MHz, CDCl$_3$): δ 88.95 (Cp), 85.62 (β C), 54.56 (α C), 38.88 (γ C), 25.63 (δ C), 13.51 (CH$_3$). 208.16, 209.23 (CO). IR (solid state): ν(CO) 2073, 2032 cm^{-1}.

[Cp(CO)$_2$Fe{CH$_2$CH(CH$_2$)$_3$CH$_3$}]BF$_4$ was synthesized in a similar way to the pentene analogue, by reacting **1** (0.368 g; 1.09 mmol) with 1-hexene (2 ml; 15.48 mmol). Yield: 0.368 g, 97%. ^{1}H NMR (400 MHz, CDCl$_3$): δ 5.62 (s, 5H, Cp), 5.17 (m, 1H, =CH), 4.05 (d, J_{HH} = 7.8 Hz, 1H, =CH$_2$, *cis*), 3.27 (d, J_{HH} = 14.9 Hz, 1H, =CH$_2$, *trans*), 2.42 (m, 1H, =CHCH) 1.56 (m, 5H, CHCH$_2$CH$_2$) 0.87 (t, J_{HH} = 12.9 Hz, 3H, -CH$_3$). IR (solid state): ν(CO) 2075, 2033 cm^{-1}.

4.13. Reaction of *1* with PPh$_3$

A solution of **1** (0.352 g, 1.041 mmol) in 20 ml of dry dichloromethane was treated with 0.620 g (2.37 mmol) of triphenylphosphine and the mixture stirred overnight at room temperature. Then the mixture was filtered and dry diethyl ether added to the filtrate until a yellow precipitate formed. The mother liquor was syringed off and the solid residue washed with 3 x 5 ml diethyl ether to yield a yellow solid. Yield: 0.520 g, 95%. *Anal.* Calc. for $C_{25}H_{20}\,BF_4FePO_2$: C, 57.03; H, 3.80. Found: C, 56.41; H, 4.03%. ^{1}H NMR (400 MHz, CD$_3$NO): δ 5.41 (s, 5H, Cp), 7.62 (m, 15H). ^{13}C NMR (400 MHz, CDCl$_3$): δ 88.97 (Cp), 132.57 (m, phenyl), 210.38 (CO). IR (solid state): ν(CO) 2048, 2013 cm^{-1}.

4.14. X-ray crystal structure determination of complexes *2a* and *2b*

Crystals of compounds **2a** and **2b** suitable for single crystal X-ray diffraction studies were grown by liquid diffusion method. Solutions of the compounds in dry chloroform were layered with ca. fourfold of excess hexane and allowed to stand undisturbed in the dark at room temperature for 6 weeks. Intensity data were collected on a Bruker *APEX*

II CCD area detector diffractometer with graphite monochromated Mo K_α radiation (50kV, 30mA) using the *APEX 2* [64] data collection software. The collection method involved ω-scans of width 0.5° and 512 x 512 bit data frames. Data reduction was carried out using the program *SAINT+* [65] and face indexed absorption corrections were made using *XPREP* [65].

The crystal structure was solved by direct methods using *SHELXTL* [66]. Non-hydrogen atoms were first refined isotropically followed by anisotropic refinement by full matrix least-squares calculations based on F^2 using *SHELXTL*. Hydrogen atoms were first located in the difference map then positioned geometrically and allowed to ride on their respective parent atoms. Diagrams and publication material were generated using *SHELXTL*, *PLATON* [67] and *ORTEP-3* [68]. Table 2 summarizes crystal data and structure refinement information while selected bond length and angles are given in Tables 3 - 5.

Acknowledgments

Supplementary material

Supplementary data associated with this article can be found, in the online version, at doi: 10.1016/j.ica.2010.10.018. Crystallographic data for compounds **2a** and **2b** are given in Appendix 4. CD-ROM containing all CIF files and spectroscopic data is provided in Appendix 12.

References

[1]   A.R. Cutler, A.B. Todaro, Organometallics 7 (1988) 1782.

[2] M.J.M. Campbell, E. Morrison, V. Rogers, P.K. Baker, D.C. Povey, G.W. Smith, Polyhedron 8 (1989) 2371.

[3] V. Artero, M. Fontecave, C. R. Chimie 11 (2008) 926.

[4] G.M. Scott, A.V. Paul, E. Arkady, J.A. Robert, Dalton. Trans. (2004) 788.

[5] T.C. Forschner, A.R. Cutler, Inorg. Synth. 26 (1989) 231.

[6] M.J.M. Campbell, E. Morrison, V. Rogers, P.K. Baker, Polyhedron 6 (1987) 1703.

[7] J.A. Armstead, D.J. Cox, R. Davis, J. Organomet. Chem. 236 (1982) 213.

[8] R.B. English, R.J. Haines, C.R. Nolte, J. Chem. Soc. Dalton Trans. (1975) 1030.

[9] M.L. Brown, J.L. Cramer, J.A. Ferguson, T.J. Meyer, N. Winterton, J. Am. Chem. Soc. 94 (1972) 8707.

[10] N.M. Amarendra, S. Brigitte, S. Biprajit, Z.l. Stanislav, F. Jan, K. Sanjib, K.L. Goutam, D. Carole, G. Matthias, G. Philipp, K. Wolfgang, Inorg. Chem. 46 (2007) 7312.

[11] A. Palazzi, S. Stagni, J. Organomet. Chem. 690 (2005) 2052.

[12] A. Palazzi, P. Sabatino, S. Stagni, S. Bordoni, V.G. Albano, C. Castellari, J. Organomet. Chem. 689 (2004) 2324.

[13] H.S. Clayton, J.R. Moss, M.E. Dry, J. Organomet. Chem. 688 (2003) 181.

[14] D.R. Mark, F.M. Michael, M.M. Hossain, Aldrichimica Acta 36 (2003) 3.

[15] I. Kovács, F. Bélanger-Gariépy, A. Shaver, Inorg. Chem. 42 (2003) 2988.

[16] D.D. Ellis, P.A. Jelliss, F.G.A. Stone, Organometallics 18 (1999) 4982.

[17] N.J. Holmes, W. Levason, M. Webster, J. Organomet. Chem. 584 (1999) 179.

[18] H.-J. Jeon, N. Prokopuk, C. Stern, D.F. Shriver, Inorg. Chim. Acta 286 (1999) 142.

[19] J. Ipakfschi, F.A. Mirzael, B.G. Mueller, J. Beck, M. Sarafin, J. Organomet. Chem. 526 (1996) 363.

[20] P.M. Treichel, E.K. Rublein, J. Organomet. Chem. 512 (1996) 157.

[21] R.D. Adams, S. Miao, J. Organomet. Chem. 665 (2003) 43.

[22] S.J. Mahmood, M.M. Hossain, J. Org. Chem. 63 (1998) 3333.

[23] D.J. Casper, A.V. Sklyarov, H. Steve, T.L. Barr, F.H. Forsterling, F.S. Kristene, M.M. Hossain, Inorg. Chim. Acta 359 (2006) 3129.

[24] M.E. Dudley, M.M. Morshed, C.L. Brennan, M. Shahidul Islam, M.S. Ahmad, M.-R. Atuu, B. Branstetter, M.M. Hossain, J. Org. Chem. 69 (2004) 7599.

[25] B.D. Heuss, M.F. Mayer, S. Dennis, M.M. Hossain, Inorg. Chim. Acta 342 (2003) 301.

[26] M.F. Mayer, Q. Wang, M.M. Hossain, J. Organomet. Chem. 630 (2001) 78.

[27] D.R. Mark, J.M. Syed, M.M. Hossain, Synth. Commun. 30 (2000) 1401.

[28] M.F. Mayer, M.M. Hossain, J. Org. Chem. 63 (1998) 6839.

[29] J. Picione, S.J. Mahmood, A. Gill, M. Hilliard, M.M. Hossain, Tetrahedron. Lett. 39 (1998) 2681.

[30] S.J. Mahmood, A.K. Saha, M.M. Hossain, Tetrahedron 54 (1998) 349.

[31] W.J. Seitz, A.K. Saha, M.M. Hossain, Organometallics 12 (1993) 2604.

[32] W.J. Seitz, M.M. Hossain, Tetrahedron. Lett. 35 (1994) 7561.

[33] W.J. Seitz, A.K. Saha, D. Casper, M.M. Hossain, Tetrahedron. Lett. 33 (1992) 7755.

[34] D.L. Reger, C. Coleman, J. Organomet. Chem. 131 (1977) 153.

[35] H. Schumann, L. Eugene, J. Organomet. Chem. 403 (1991) 183 and refs therein.

[36] M. Rosenblum, D. Scheck, Organometallics 1 (1982) 397.

[37] P.V. Bonnesen, C.L. Puckett, R.V. Honeychuck, W.H. Hersh, J. Am. Chem. Soc. 111 (1989) 6070.

[38] E.P. Kundig, B. Bourdin, G. Bernardinelli, Angew. Chem., Int. Ed. Engl 33 (1994) 1856.

[39] A.K. Saha, M.M. Hossain, Tetrahedron. Lett. 34 (1993) 3833.

[40] E.K.G. Schmidt, C.H. Thiel, J. Organomet. Chem. 209 (1981) 373.

[41] W.E. Williams, F.J. Lalor, J. Chem. Soc., Dalton Trans. 1972-1999 (1973) 1329.

[42] M. Nicolas, R. Reich, J. Phys. Chem. 85 (1981) 2843.

[43] V.D. Kiseler, E.A. Kashaeva, N.A. Luzanova, A.I. Konovalov, Thermochim. Acta. 303 (1997) 225.

[44] S. Chang, E. Scharre, M. Brookhart, J. Mol. Catal. A Chem. 130 (1998) 107.

[45] P.J. Giordano, M.S. Wrighton, Inorg. Chem. 16 (1977) 160.

[46] K. Sünkel, G. Urban, W. Beck, J. Organomet. Chem. 290 (1985) 231.

[47] M. Akita, S. Kakuta, S. Sugimoto, M. Terada, M. Tanaka, Y. Moro-oka, Organometallics 20 (2001) 2736.

[48]   E. Roman, D. Catheline, D. Astruc, J. Organomet. Chem. 236 (1982) 229.

[49]   H. Schumann, S. Martin, J. Organomet. Chem. 403 (1991) 165.

[50]   P. James, L.-K. Liu, C. R. Chimie 5 (2002) 319.

[51]   B.M. Mattson, W.A.G. Graham, Inorg. Chem. 20 (1981) 3186 and refs therein.

[52]   E.C. Johnson, T.J. Meyer, N. Winterton, Inorg. Chem. 10 (1971) 1673.

[53]   P. Janamillo, P. Parez, P. Fuentealba, J. Phys. Org. Chem. 20 (2007) 1050.

[54]   H. Umeyama, K. Morokuma, J. Am. Chem. Soc. 98 (1976) 4400.

[55]   E.O. Changamu, H.B. Friedrich, J. Organomet. Chem. 692 (2007) 1138.

[56]   E.O. Changamu, H.B. Friedrich, M. Rademeyer, J. Organomet. Chem. 693 (2008) 164.

[57]   F.A. Carey, Organic Chemistry 6th edition Mc Graw-Hill , inc. international edition (2006) 943.

[58]   B. Kojic-Prodic, Z. Stefanic, M. Zinic, Croat. Chem. Acta. 77 (2004) 415.

[59]   W, Fuller, J. Phys. Chem. 63 (1959) 1705.

[60]   A.R. Manning, J. Chem. Soc., (A) (1968) 1670.

[61]   D.L. Reger, C.J. Coleman, P.J. McElligott, J. Organomet. Chem. 171 (1979) 73.

[62]   R.B. King, F.G.A. Stone, Inorg. Synth. 7 (1963) 110.

[63]   T.S. Piper, F.A. Cotton, G. Wilkinson, J. Inorg. Nucl. Chem. 1 (1955) 165.

[64]   Bruker, *APEX2*. Version 2009.1-0. Bruker AXS Inc., Madison, Wisconsin, USA, (2005a).

[65]   Bruker, *SAINT+*. Version 7.60A. (includes *XPREP* and *SADABS*) Bruker AXS Inc., Madison, Wisconsin, USA, (2005b).

[66]   Bruker, *SHELXTL*. Version 5.1. (includes XS, XL, XP, XSHELL) Bruker AXS Inc., Madison, Wisconsin, USA, (1999).

[67]   A.L. Spek, J. Appl. Cryst. 36 (2003) 7.

[68]   L.J. Farrugia, J. Appl. Cryst. 30 (1997) 565.

CHAPTER THREE

Synthesis, characterization and structural elucidation of water-soluble 1-aminoalkane and α,ω-diaminoalkane complexes of the pentamethylcyclopentadienyliron dicarbonyl cation, [Cp*(CO)$_2$Fe]$^+$

Cyprian M. M'thiruaine[a], Holger B. Friedrich[a*], Evans O. Changamu[b], Muhammad D. Bala[a].

[a] **School of Chemistry, University of KwaZulu-Natal, Private Bag X54001, Durban 4000, South Africa** [b] **Chemistry Department, Kenyatta University, P.O Box 43844, Nairobi, Kenya**

* Corresponding author

Abstract

A series of water-soluble alkylaminopentamethylcyclopentadienyliron dicarbonyl complexes, [Cp*(CO)$_2$Fe{NH$_2$(CH$_2$)$_n$CH$_3$}]BF$_4$ (n = 2–6; Cp* = η^5-C$_5$Me$_5$) and the diaminopropane bridged complex, [{Cp*(CO)$_2$Fe}$_2${μ-NH$_2$(CH$_2$)$_3$NH$_2$}](BF$_4$)$_2$ have been synthesized and fully characterized. [Cp*(CO)$_2$Fe{NH$_2$(CH$_2$)$_5$CH$_3$}]BF$_4$ undergoes counteranion exchange with sodium tetraphenylborate in both aqueous and organic media to give water insoluble [Cp*(CO)$_2$Fe{NH$_2$(CH$_2$)$_5$CH$_3$}]BPh$_4$. The molecular structures for compounds [Cp*(CO)$_2$Fe{NH$_2$(CH$_2$)$_3$CH$_3$}]BF$_4$ and [{Cp*(CO)$_2$Fe}$_2${μ-NH$_2$(CH$_2$)$_3$NH$_2$}](BF$_4$)$_2$ have been determined by single crystal X-ray crystallography and show that they crystallize in the orthorhombic and monoclinic crystal systems, respectively.

Keywords: α,ω-Diaminoalkanes, 1-Aminoalkanes, Alkylaminopentamethylcyclopentadienyliron dicarbonyl, Water-soluble organometallic

1. Introduction

Cp*(CO)$_2$Fe complexes having a hydrocarbon chain in their coordination sphere have been known for more than three decades [1-8] . These compounds can exist as neutral complex molecules or complex salts of weakly coordinating anions such as BF$_4^-$, PF$_6^-$,

SbF_6^-, BPh_4^- and $CF_3SO_3^-$. Monuclear neutral complexes of the type $[Cp*(CO)_2FeR]$ (R = alkyl group) [7] and dinuclear complexes of the type $[\{Cp*(CO)_2Fe\}_2\{\mu-(CH_2)_n\}]$ (n = 3-6) [8] , as well as mixed ligand complexes $[Cp*(CO)_2Fe\{\mu-(CH_2)_n\}Fe(CO)_2Cp]$ (n = 6) [2] are well known. The cationic complexes are mainly prepared by hydride abstraction from these neutral complexes [2, 3, 9], or alternatively by the reaction of substitutionally unsaturated complexes such as $[Cp*(CO)_2Fe(THF)]BF_4$ [5] and $[Cp*(CO)_2Fe(OH_2)]BF_4$ [10, 11] with relatively stronger binding ligands.

Incorporating a hydrophilic functionality such as an amine group will make these organometallic species compatible with water. The compatibility of organometallic compounds with water is one of the conditions necessary for advancements in biomedicine [12], bioorganometallic chemistry and organometallic radiopharmaceuticals, since water is the main solvent in biological systems. Furthermore, the growing interest in green chemistry has prompted chemists to use aqueous phase catalysis and thus the solubility of organometallic compounds in water has become important in both laboratory and industry. We recently reported the syntheses of a series of 1-aminoalkane and α,ω-diaminoalkane complexes of cyclopentadienyliron dicarbonyl [13]. We found that the aminoalkane complexes are soluble in water and can be recovered from their aqueous solutions with minimal loss. They react with sodium salts such as $NaBPh_4$ and NaI in aqueous media to give the respective BPh_4^- and I^- salts [14]. Other cyclopentadienyliron dicarbonyl amines previously reported are $[Cp(CO)_2FeL]^+$ ($Cp = \eta^5\text{-}C_5H_5$; L = NH_2Pr^i, NH_2Bu^t [15], $NH(CH_2CH_3)_2$, $NH(CH_3)_2$, $NH(SiMe_3)_2$) [16].

Supported palladium alkylamine complexes, $[PdCl_2\{NH_2(CH_2)_{12}CH_3\}_2]$ have been reported to exhibit high catalytic activity in the hydrogenation of cyclohexene to cyclohexane [17-20]. Alkylamino complexes of rhodium and palladium, $[RhCl\{NH_2(CH_2)_{12}CH_3\}_3]$, $[RhCl\{NH_2(CH_2)_5CH_3\}_3]$, and $[PdCl_2\{NH_2(CH_2)_5CH_3\}_2]$ have also been reported to be active in catalytic semi-hydrogenation of 1-heptyne to 1-heptene. In fact all these compounds except the hexylamine compounds have been found to exhibit catalytic activity higher than that of the Lindler catalyst [21].

Diaminoalkanes constitute a very important class of compounds with potential application in pharmaceuticals. Ethambutol (diaminoethane based derivative) has been

the first class antitubercular drug on the market since the 1960's, a factor which has recently led to the syntheses of a wide range of diaminoalkane derivatives and their biological testing against mycobacterium tuberculosis H37Rv [22-26]. A series of neutral ferrocenyl diaminoalcohol and diaminoalkane complexes in which the ferrocenyl groups are bridged by a diaminoalkane bonded directly to the cyclopentadienyl moiety has been synthesized and evaluated against mycobacterium tuberculosis H37Rv [27, 28]. A comparative study revealed that the ferrocenyl diaminoalkane complexes show higher activity than their diaminoalcohol counterparts [28]. In view of this information, amine complexes are very important and, therefore, their chemistry needs to be well explored. Herein we report a fully characterized series of the 1-aminoalkane and 1,3-diaminopropane complexes of pentamethylcyclopentadienyliron dicarbonyl.

2. Results and discussion

2.1. Synthesis of [Cp*(CO)$_2$Fe{NH$_2$(CH$_2$)$_n$CH$_3$}]BF$_4$ (2a-2e)

The reactions of the cationic tetrahydrofuran complex [Cp*(CO)$_2$Fe(THF)]BF$_4$ (**1**) with 1-aminoalkanes in CH$_2$Cl$_2$ at room temperature gave yellow–brown solutions from which the analytically pure cationic aminoalkane complexes, (**2a**-**2e**) were obtained in moderate yields as yellow crystalline solids (Scheme 1).
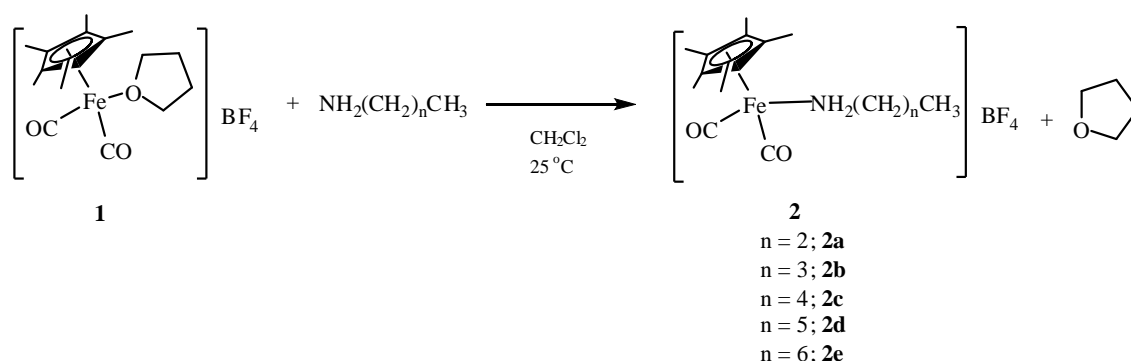
Scheme 1. Reaction of [Cp*(CO)$_2$Fe(THF)]BF$_4$ with 1-aminoalkanes

All these complexes are moderately air stable either in the solid state or in solution but decompose slowly upon exposure to light. However, when protected from light they can be stored for a long period of time at temperatures in the range of 273 - 298 K. They are soluble in halogenated solvents, acetonitrile, acetone, water, and slightly soluble in hexane and diethyl ether. For this reason they crystallized out as pure crystals from CH_2Cl_2/Et_2O (1:5) after 6 - 16 h. The complex where n = 5, exhibited high stability in an aqueous environment. Indeed, 75% of originally dissolved complex was recovered from the aqueous solution by solvent extraction.

The stability and water-solubility of these compounds probably could be attributed to the ionic nature of the complexes and the polarity of amine functionality. The stability of these complexes, particularly in an aqueous environment, may enable them to be used in studies of biphasic catalysis and in biomedicine. They melt at temperatures in the range 85 - 135 °C (Table 1) and the melting points roughly decreased with increase in hydrocarbon chain length. The melting points of these compounds are higher than their corresponding Cp analogues [13]. This is not unexpected since the electronic and steric effects imparted by the Cp* ligand increases their thermal stability.

All the compounds have been characterized by NMR and IR spectroscopy, elemental analysis and mass spectrometry. The IR and other physical data are summarized in Table 1, while NMR data are given in Section 4.2. The structure of **2b** has been confirmed by single crystal X-ray crystallography and is discussed in Section 2.1.1. IR spectra of the compounds **2a-2e** show two strong characteristic v(CO) bands at ca. 2023 and 1970 cm^{-1} and two medium peaks assignable to N–H asymmetric and symmetric stretching at ca. 3311 and 3270 cm^{-1}, respectively. As expected, the v(CO) peaks are at lower wavenumbers than those of recently reported Cp analogues [13] by ca. 32 cm^{-1}. This is due to the increase in electron density on the iron centre from the Cp* ligand leading to increased backdonation to the carbonyl carbon and subsequent weakening of the C=O bond [4], an observation which is reflected in C=O bond length differences observed in crystal structures of the compound **2b** (Table 3) and its Cp analogue, $[Cp(CO)_2Fe\{NH_2(CH_2)_3CH_3\}]BF_4$ [13]. The C=O bonds of compound **2b** are on average marginally longer than those of the compound $[Cp(CO)_2Fe\{NH_2(CH_2)_3CH_3\}]BF_4$ by ca. 0.007(3) Å, indicating that due to increased

back donation from the electron-rich iron centre, the C=O bond in Cp* alkylamine compounds is weaker than that in unsubstituted Cp alkylamines.

A slight trend towards lower wavenumbers as the carbon chain length increased from 3 to 5 was observed in the v(CO) and v(NH) absorption bands. Generally v(CO) stretching frequencies in this series of compounds are higher than those reported for $[Cp*(CO)_2FeCH_2R]$ [7], but lower than the cationic complexes, $[Cp*(CO)_2FeCH_2CHR]^+$ [5] by ca. 32 - 45 cm^{-1}. Unlike alkenes, amines are good sigma donors but poor pi acceptors and hence they increase electron density on the metal centre which results in increased synergistic interactions between the metal and the carbonyl groups. IR spectra of all alkylamine complexes also show a characteristic absorption band that corresponds to the N–H bending mode at ca. 1600 cm^{-1} and an overtone at ca. 3180 cm^{-1}.
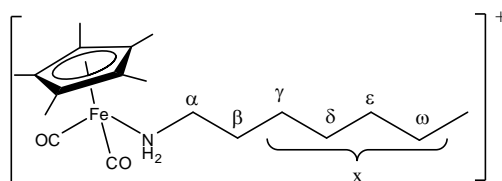
Fig. 4: General structure of the complexes, $[Cp*(CO)_2Fe\{NH_2(CH_2)_nCH_3\}]BF_4$

The NMR data of **2a–2e** were recorded in CDCl$_3$ and the assignments made by comparison with the data reported for analogous Cp complexes [13], as well as by use of 2D NMR experiments which included ^{15}N, ^{1}H HSQC. The ^{1}H NMR spectrum of each of these compounds exhibited a separate singlet at ca. 1.83 ppm assignable to the methyl protons of the Cp* ring and a triplet at ca. 0.85 ppm assignable to the aminoalkane methyl, while the resonance peaks due to the amine protons appeared to overlap with those of the αCH$_2$ at ca. 2.30 ppm, representing a 0.6 ppm upfield shift relative to the Cp complexes [13]. This shift can be attributed to the increase in electron density on the iron centre leading to reduced electrophilicity and consequent shielding of the N–H protons. This corresponds to the slightly longer Fe–N bond length of 2.022 Å observed in **2b** (Table 3) relative to 2.006 Å observed in the reported complex

$[Cp(CO)_2Fe\{NH_2(CH_2)_3CH_3\}]BF_4$ [13]. A separate multiplet assignable to the β-methylene protons is observed at ca. 1.50 ppm, and as the alkyl chain became longer the resonance peaks due to the γ, δ, ε and ω carbon protons (Fig. 1) overlap at ca. 1.20 ppm. However, the ^{13}C NMR spectra show separate peaks corresponding to each of the methylene carbons. The peaks assignable to the methyl groups of the Cp*, the Cp* ring carbons, and CO were observed at ca. 9.21, 97.37 and 212.45, respectively. The positions of the Cp* and CO carbons are independent of the hydrocarbon chain length. However, there is a clear downfield shift trend of the signals for the γ–ω methylenes as the chain grows longer. A similar trend was observed in the ^{13}C NMR spectra of the Cp analogues which can be attributed to increased charge transfer by the alkyl group to the amine group.

Table 1: Yields, M.p., IR and elemental analyses data of compounds $[Cp*(CO)_2Fe\{NH_2(CH_2)_nCH_3\}]BF_4$

Compound	n	V(CO) cm^{-1}#	V(NH) cm^{-1}#	M.p. (˚C)	Yield (%)	Elemental Analysis‡ (%) C	H	N
2a	2	2025, 1970	3313, 3274	134 - 135	27	45.61(45.80)	5.80(6.10)	3.69(3.56)
2b	3	2021, 1969	3311, 3266	104 - 105	47	47.47(47.17)	6.27(6.39)	3.11(3.44)
2c	4	2019, 1968	3308, 3266	121 - 122	33	48.80(48.46)	6.15(6.65)	2.96(3.32)
2d	5	2022, 1970	3311, 3265	118 - 119	54	50.19(49.66)	6.55(6.90)	2.81(3.22)
2e	6	2028, 1973	3313, 3280	84 – 85	40	56.81(57.08)	7.13(7.11)	3.44(3.12)

‡ Calculated values in parenthesis. # IR data collected in solid state

Electrospray mass spectra were obtained for compounds **2a-2e** and the results are shown in Table 2. The molecular ion peaks are observed in the mass spectra of all these compounds (see Appendix 7). Except for **2a,** the molecular ion peaks are of the strongest intensity due to the enhanced stability caused by the Cp* ligand [7]. Loss of the counter anion, BF_4^-, leads to the base peak corresponding to $[Cp*(CO)_2Fe\{NH_2(CH_2)_nCH_3\}]^+$, followed by successive loss of carbonyl groups leading to the daughter ions $M^+ - CO$ and $M^+ - 2CO$, respectively.

Table 2: Mass spectroscopy data of compounds [Cp*(CO)$_2$Fe{NH$_2$(CH$_2$)$_n$CH$_3$}]BF$_4$

Fragment	Relative Intensity (%)				
	n = 2	n = 3	n = 4	n = 5	n = 6
[Cp*(CO)$_2$Fe(NH$_2$(CH$_2$)$_n$CH$_3$)]$^+$,	41.9	100	100	100	100
[Cp*(CO)Fe(NH$_2$(CH$_2$)$_n$CH$_3$)]$^+$,	100	33.9	31.3	22.6	27.0
[Cp*Fe(NH$_2$(CH$_2$)$_n$CH$_3$)]$^+$,	83.9	38.7	43.8	38.7	37.8
[Cp*(CO)$_2$Fe]$^+$	0.0	0.0	0.0	3.2	0.0
[Cp*(CO)$_2$FeH]$^+$	0.0	0.0	0.0	0.0	8.1

2.1.1. Structural analysis of [Cp*(CO)$_2$Fe{NH$_2$(CH$_2$)$_3$CH$_3$}]BF$_4$ (2b)

X-ray quality crystals of complex **2b** were grown from CH$_2$Cl$_2$ solution layered with diethyl ether. When subjected to single crystal X-ray diffraction studies, it was found to crystallize in a rhombic *Pn$_a$2$_1$* space group, with four molecular cations and four counterions per unit cell. An anion-cation pair occupy the asymmetric unit of **2b** which is presented in Fig. 2, while Fig. 3 shows the packing diagram of the cationic moiety with the anion eliminated for clarity. The packing in **2b** is such that the molecules are arranged in layers with neighbouring units alternating in orientation along the *b*-axis. If the Cp* region of **2b** is described as the 'head' of the compound and the alkylamine chain as the 'tail', then the packing in the complex as shown in Fig. 3 can be described as a head-to-tail configuration that alternates between layers in order to keep steric repulsion to a minimum. The heads of one layer neatly fit into spaces created by the flexible tails of the adjacent layers. This mode of packing is common in many Cp and Cp* piano stool and related complexes [7, 29, 30]

The iron atom in **2b** is coordinated by Cp*, two carbonyls and the aminoalkane in a pseudo-octahedral 3-legged piano-stool fashion in which the α-carbon of the aminoalkane lies in the energetically favored conformation between two carbonyl ligands. This kind of conformation is similar to that found in other related Cp* systems [2, 7, 29] and arises because it leads to reduced steric interaction as observed in the packing diagram (Fig. 3).

The Fe–N bond was found to be 2.022 Å which is slightly longer than Fe–N observed for the related complexes [Cp(CO)$_2$Fe{NH$_2$CH(CH$_3$)$_2$}]$^+$ [15] and [Cp(CO)$_2$Fe{NH$_2$(CH$_2$)$_n$CH$_3$}]$^+$ (*n* = 2, 3) [13], but within the reported range for these compounds [31, 32]. The N–C bond length was found to be 1.482 Å, which is slightly

shorter than the C-N bond observed for $[Cp(CO)_2Fe\{NH_2(CH_2)_2CH_3\}]^+$ (1.489 Å) and $[Cp(CO)_2Fe\{NH_2(CH_2)_3CH_3\}]^+$ (ca. 1.486 Å). Changing Cp to Cp* has an effect of increasing electron density on the metal centre which in turn strengthens the Fe–CO bond as a result of increased back-donation but lowers the interaction between the metal centre and N leading to a relatively stronger N–C bond. This is also reflected in upfield and downfield shifts observed for NH_2 and α-CH_2 proton resonance peaks, respectively, in the NMR spectra.

Hydrogen bonding is observed between the fluoride of the counter anion, BF_4^-, and the amine hydrogen (Table 4). This is very similar to those of $[Cp(CO)_2Fe\{NH_2(CH_2)_nCH_3\}]^+$ (n = 2, 3) [13] in terms of the interaction, which is still longer than the 2.15 and 2.27Å reported by Xu *et al.* [33] for NH---F---HN.

Table 3: Selected bond lengths [Å] and angles [°] for $[Cp*(CO)_2Fe(NH_2(CH_2)_3CH_3)]BF_4$ (**2b**)

Bond	Length (Å)	Bond	Angle (°)
*Cent –Fe1	1.725	Cent-Fe1-C11	120.16
N1-Fe1	2.022(15)	Cent-Fe1-C12	122.61
C11-Fe1	1.787(2)	Cent-Fe1-N1	123.08
C11-O1	1.143(3)	C11-Fe1-C12	95.79(11)
C12-Fe1	1.777(2)	C11-Fe1-N1	94.82(8)
C12-O2	1.143(3)	C12-Fe1-N1	93.17(8)
C13-N1	1.482(3)	Fe1-N1-C13	119.16(12)
C13-C14	1.517(2)	N1-C13-C14	112.61(17)

*Cent is the centroid of C1-C5 atoms

Table 4: Hydrogen bonding for $[Cp*(CO)_2Fe\{NH_2(CH_2)_3CH_3\}]BF_4$ [Å and °].

D-H...A	d(D-H)	d(H...A)	d(D...A)	<(DHA)
N1-H1A...F2#1	0.92	2.12	2.999(2)	160
N1-H1B...F1	0.92	2.08	2.963(2)	162

Symmetry transformations used to generate equivalent atoms: #1 -x+2,-y+1, z+1/2
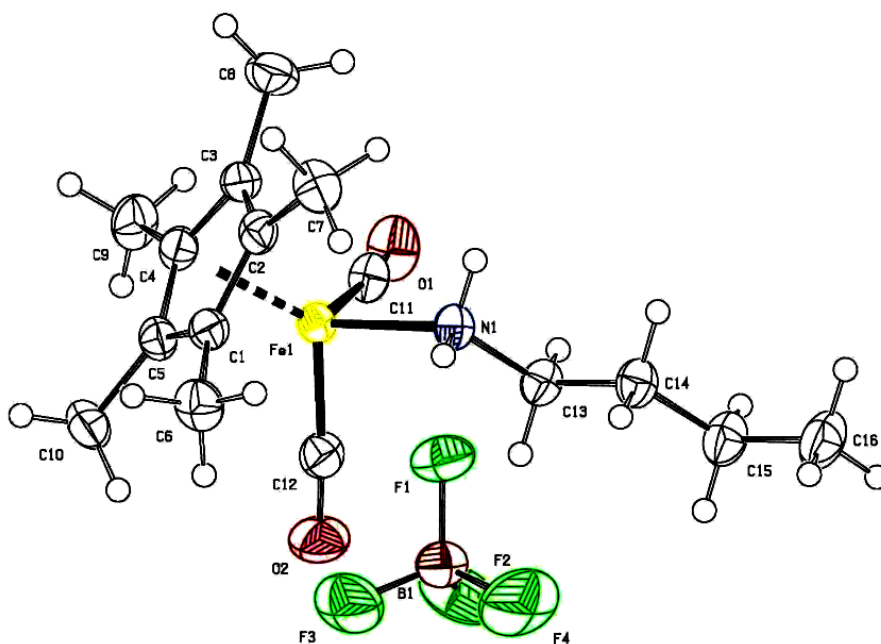
Fig. 2: The molecular structure of **2b** showing the atomic numbering scheme, displacement ellipsoids are drawn at the 50% probability level and H atoms are shown as small spheres
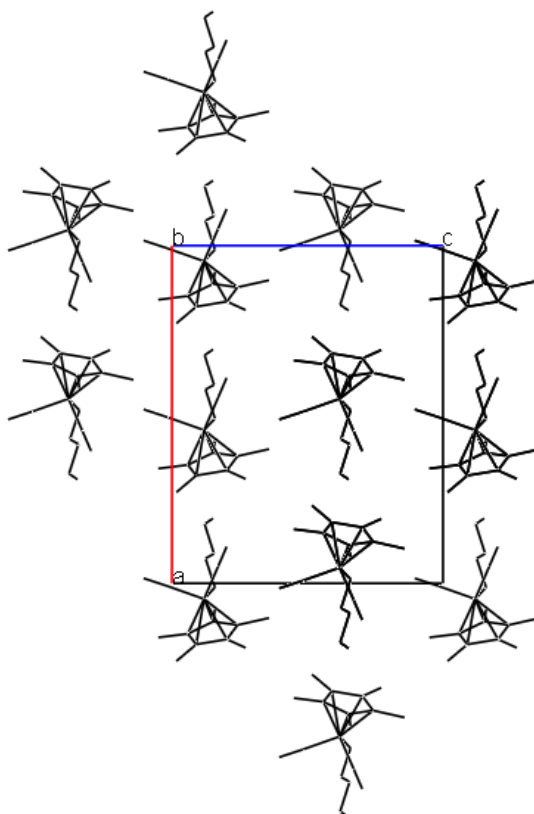
Fig 3: Packing diagram for $[Cp^*(CO)_2Fe\{NH_2(CH_2)_3CH_3\}]BF_4$ **2b** viewed along the *b*-axis with hydrogen atoms and counter anions omitted for clearity

2.2. Synthesis of [{Cp*(CO)$_2$Fe}$_2${μ-NH$_2$(CH$_2$)$_3$NH$_2$}](BF$_4$)$_2$ (**3**)

Reaction of diaminopropane with two equivalents of [Cp*(CO)$_2$Fe(THF)]BF$_4$ in dichloromethane gave the diaminoalkane-bridged dinuclear complex [{Cp*(CO)$_2$Fe}$_2${μ-NH$_2$(CH$_2$)$_3$NH$_2$}](BF$_4$)$_2$ (**3**) in 73 % yield (Scheme 2). It was characterized by IR, NMR spectroscopy, elemental analysis and single crystal X-ray diffraction. The solid state IR spectrum shows two strong ν(CO) stretching bands at 2033 and 1979 cm^{-1} which as expected are observed at wavenumbers lower than the reported Cp analogue [13].

The proton NMR spectrum of **3** recorded at room temperature in acetone-d$_6$ shows that the diaminopropane spans between the two iron centres. This was indicated by a singlet integrating for 30H of the two identical Cp* group at 1.88 ppm and a quintet at 2.40 ppm corresponding to four identical α-CH$_2$ protons in the neighborhood of the amine and the β-CH$_2$ protons. A triplet assignable to the two identical β-CH$_2$ groups was observed at 1.81 ppm. The ^{13}C NMR spectrum shows the signals due to the α and β-carbons at 49.8 and 35.7 ppm, respectively.
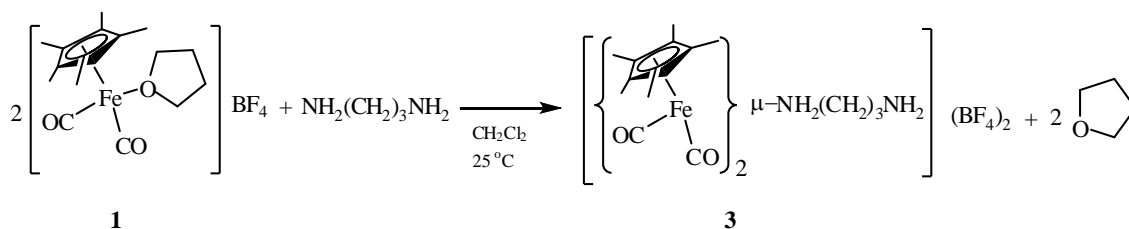
Scheme 2. Reaction of [Cp*(CO)$_2$Fe(THF)]BF$_4$ with diaminopropane

2.2.1. Structural analysis of [{Cp*(CO)$_2$Fe}$_2${μ-NH$_2$(CH$_2$)$_3$NH$_2$}](BF$_4$)$_2$ (**3**)

Crystals of **3** suitable for X-ray diffraction were obtained by vapour diffusion of diethyl ether into a concentrated solution of **3** in acetone at 5 °C which was kept in the dark for a period of one week. The molecular structure (Fig. 4) shows that the two metal centres are connected by the bridging diaminopropane ligand with a kink in the alkyl chain. This strained gauche conformation has been observed in other organometallic complexes [2, 30, 34-36]. The torsion angles N1–C13–C14–C15 = 171.02(15), C13–C14–C15–N2 = -73.23(19), C14–C13–N1–Fe1 = 177.50(12) and C14–C15–N2–Fe2 = -

160.66(12) confirm that diaminopropane is σ-bonded to two iron centres *via* the N atoms. The significantly reduced angle C13–C14–C15–N2 = -73.23(19) reflects the unusual kink in the alkyl chain. The structure is disordered on one set of pentamethylcyclopentadienyl carbons. The disorder was modeled with site occupancy factors of 66.4 and 33.6% for the A and B Me-Cp positions, respectively.

The C13–C14 and C14–C15 bond distances within the alkyl chain of the diaminopropane are 1.521(2) and 1.527(2)Å, respectively, which are within the range of reported values [2, 7, 13]. The bond lengths Fe1–N1 = 2.0182(16) and Fe2–N2 = 2.0202(14)Å are slightly shorter than those observed in the unbridged compound **2b**, but within the reported range [13, 15, 31, 32]. The C=O bond lengths of the carbonyl ligands fall within the range 1.136(2) – 1.137(2) Å which are shorter than similar bonds in **2b** by ca. 0.0065 Å. This difference is also reflected by v(CO) peaks which may be attributed to steric effects. This steric effect may be due to constraints imposed on the bridging alkylamino group in **3** which are absent in **2b**, accounting for shorter bonds. Selected bond angles and lengths are given in Table 5. The geometry at the iron atom is that of a distorted pyramid in which the base is made up of the two carbonyl ligands and the diaminopropane nitrogen atom and the apex is the iron metal capped with the pentamethylcyclopentadienyl ligand. Fig. 4 shows an Ortep diagram of compound **3** with the disordered components omitted.

Fig. 5 shows the packing of the molecules within a crystal of **3** in which alternate pairs of neighbouring molecules are related by a screw axis along the *a*-axis. The bond length between the amine hydrogen and fluorine of the counteranion falls in the range 2.048 – 2.228 Å which is shorter than the sum of their van der Waals radii (2.67 Å) [37]. Hence, the packing in a crystal of **3** is assisted by these weak intermolecular interactions. The details of the crystallographic data, as well as data collection and reduction information, are summarized in Table 6.
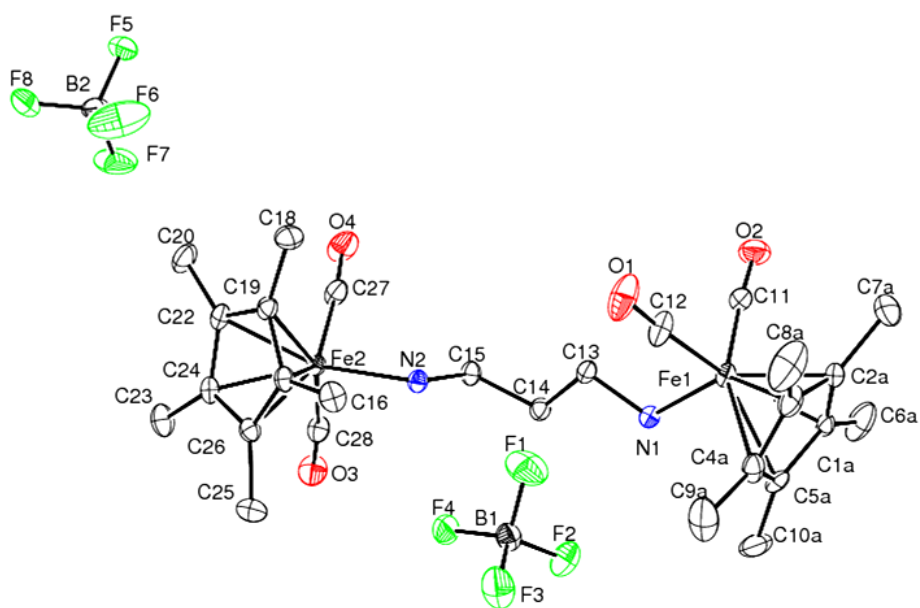
Fig. 4: The molecular structure of **3** with disorder components and H atoms omitted for clarity. Displacement ellipsoids are drawn at the 50% probability level
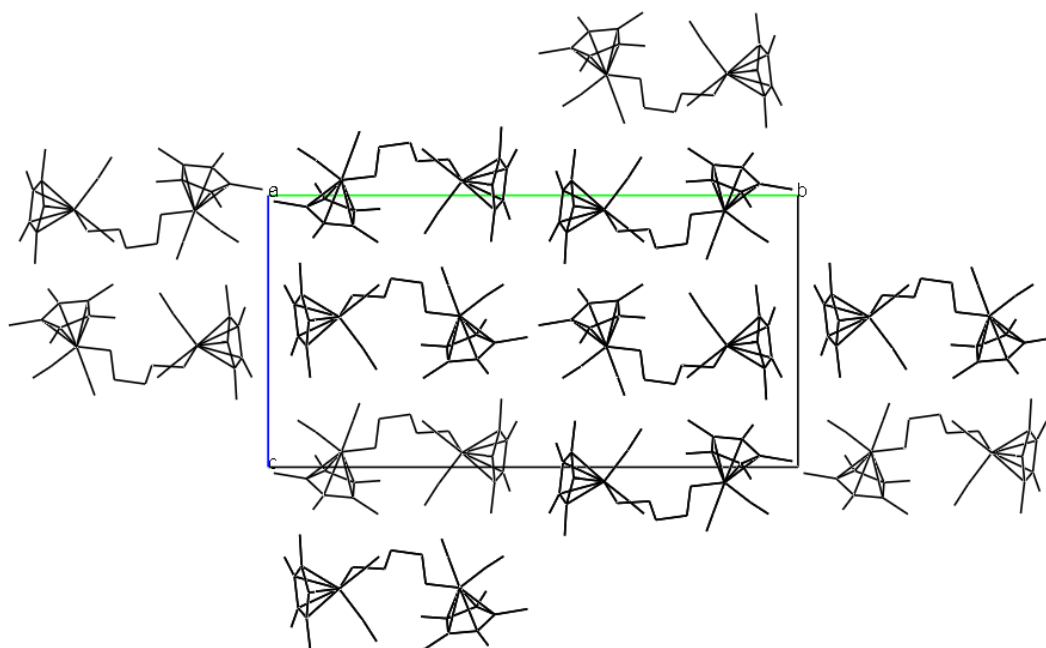
Fig. 5: Packing diagram for **3** viewed along the *a*-axis with hydrogen atoms and counter anions hidden to improve the clarity

Table 5: Selected bond lengths [Å] and angles [°] for [{Cp*(CO)$_2$Fe}$_2${μ-NH$_2$(CH$_2$)$_3$NH$_2$}](BF$_4$)$_2$ (**3**)

Bond	Length (Å)	Bond	Angle (°)
Fe1- Cent 1*	1.719	Cent1 -Fe1-C11	122.86
Fe2 - Cent 2*	1.718	Cent1 -Fe1-C12	122.92
C11-O2	1.136(2)	Cent2 -Fe2-C27	122.38
C12-O1	1.137(2)	Cent2 -Fe2-C28	119.33
C11-Fe1	1.7839(19)	Cent1 -Fe1-N1	120.07
C12-Fe1	1.7893(19)	Cent2 -Fe2-N2	122.99
C13-N1	1.489(2)	C11-Fe1-C12	95.41(9)
C13-C14	1.521(2)	C27-Fe2-C28	97.00(9)
C27-O4	1.137(2)	C11-Fe1-N1	93.32(8)
C28-O3	1.136(2)	C12-Fe1-N1	94.91(8)
C27-Fe2	1.7864(19)	C27-Fe2-N2	94.14(8)
C28-Fe2	1.7932(19)	C28-Fe2-N2	94.16(7)
N1-Fe1	2.0182(16)	Fe1-N1-C13	117.68(11)
N2-Fe2	2.0202(14)	Fe2-N2-C15	117.61(11)

Cent 1* = Centroid: C1A C2A C3A C4A C5A; Cent 2* = Centroid: C17 C19 C22 C24 C26

2.3. Reaction of **2d** with sodium tetraphenylborate in aqueous and organic media

Compounds **2a**-**2e** were recovered in 60 − 75 % yields from their aqueous solutions by extraction with dichloromethane. No noticeable signs of decomposition were observed in the recovered samples. This observation motivated us to investigate the reaction of **2d** with NaBPh$_4$ in deionized water and hence compare the product with that obtained when the same reaction was carried out in an anaerobic and anhydrous environment. The two different environments gave identical compounds, which according to ^{1}H NMR, ^{13}C NMR, IR and elemental analysis was pure [Cp*(CO)$_2$Fe{NH$_2$(CH$_2$)$_5$CH$_3$}]BPh$_4$ (**4**). The IR spectrum of compound **4** exhibited two strong ν(CO) peaks assignable to the two carbonyls, at 2015 and 1956 cm^{-1}, which are significantly lower than those observed for **2d**. A similar shift was observed for [Cp(CO)$_2$Fe{NH$_2$(CH$_2$)$_3$CH$_3$}]BPh$_4$ which was prepared following a similar procedure. The shift of ν(CO) to a lower wavenumber could be attributed to a tight ion pairing effect of BPh$_4^-$ [38-40]. The BPh$_4^-$ prefers the position that maximizes the lyophilic interaction with the organic moiety of the organometallic cation [41], in this case the amine, which consequently increases electron density around the metal centre. The success of the reaction was further marked by the disappearance of the strong broad IR absorption band due to BF$_4^-$ between 1083 − 1015 cm^{-1} and a concurrent appearance of two strong absorption bands at 738 and 707 cm^{-1} assignable to the C–H bending of the phenyl groups. A characteristic absorption band corresponding to C–H stretching of the

phenyl ring was also observed at 3055 cm^{-1}. A sharp medium absorption band assignable to N–H bending was observed at 1597 cm^{-1}, as opposed to a relatively broad band observed at 1581 cm^{-1} corresponding to the same vibration mode in the IR spectrum of **2d** indicating a reduction in hydrogen bonding on replacement of BF_4^- with BPh_4^-.

The NMR data of compound **4** were recorded in $CDCl_3$ and assignment made by comparison with that of compound **2d**, as well as with the help of 2D NMR experiments. The ^{1}H NMR spectrum shows separate resonances corresponding to β, γ, δ and ε methylene protons in the region 0.81 – 1.23, while the α-CH_2 peak was observed at 1.52 ppm and the Cp* methyl protons at 1.59 ppm. A triplet corresponding to the methyl of the hexylamine group appeared at 0.86 ppm. Generally all resonance peaks significantly shifted upfield relative to those of the starting material (**2d**), indicating a greater extent of shielding exerted by the π-electrons on the phenyl rings of the BPh_4^- [40, 42, 43]. This effect is experienced more on the amine group protons whose resonance peak is observed upfield at -0.17 ppm. This further indicates the proximity of BPh_4^- to the amine group which result from the accumulation of positive charges at the junction of the moieties containing the N-donor atoms [43]. The position of the α-CH_2 chemical shift can be explained in terms of a σ type of interaction between the nitrogen atom and the iron centre which results in a drift of electron density from the adjacent α-CH_2 to nitrogen, hence dishielding the α-CH_2 protons to a greater extent than the other methylene protons in the chain. This effect is expected to diminish along the hydrocarbon chain, but appears to be complicated by the shielding effect of BPh_4^-. Thus the resonance peak corresponding to the CH_3 group of the chain appears at a slightly higher resonance than that of the ε methylene protons. As expected, two triplets and a broad singlet corresponding to *para*, *meta* and *ortho* protons of BPh_4^- are observed at 6.91, 7.07 and 7.49 ppm, respectively. The ^{19}F NMR spectrum of **4** further confirmed that BF_4^- was displaced by BPh_4^- as the peak observed for **2d** at -152 ppm corresponding to F was not observed in the ^{19}F NMR spectrum of compound **4.** The ^{13}C NMR spectrum of compound **4** shows slight variation in the position of the alkylamine carbons relative to **2d**. The resonance peaks appeared slightly upfield and resonance peaks due to γ and ε carbons overlapped at the same position owing to the same explanation given above.

3. Conclusion

[Cp*(CO)$_2$Fe(THF)]BF$_4$ reacts with 1-aminoalkanes and α,ω-diaminoalkanes to give novel water-soluble complexes of the types [Cp*(CO)$_2$Fe{NH$_2$(CH$_2$)$_n$CH$_3$}]BF$_4$ and [{Cp*(CO)$_2$Fe}$_2${μ-NH$_2$(CH$_2$)$_n$NH$_2$}](BF$_4$)$_2$, respectively. The molecular structures of [Cp*(CO)$_2$Fe{NH$_2$(CH$_2$)$_3$CH$_3$}]BF$_4$ and [{Cp*(CO)$_2$Fe}$_2${μ-NH$_2$(CH$_2$)$_3$NH$_2$}](BF$_4$)$_2$ show that the amine group utilizes the lone pair of electrons on the nitrogen atom to coordinate to the metal, and the molecules in the crystal are held together by N–H---F hydrogen bonds which enhances their stability and solubility in water.

4. Experimental

4.1. General

Preparation of the alkylamino complexes **2a** − **2e** and the diaminopropane complex **3** were carried out under inert atmosphere (UHP or HP nitrogen) using Schlenk line techniques. Nitrogen gas was obtained from Afrox and dried over phosphorus(V) oxide. Reagent grade THF and Et$_2$O were distilled from sodium/benzophenone and stored over sodium wire; CH$_2$Cl$_2$ was distilled from phosphorus(V) oxide and used immediately. Acetone and MeCN were distilled from anhydrous CaCl$_2$ and stored over type 4A molecular sieves. The other chemical reagents were obtained from the suppliers shown in parentheses: 1,2,3,4,5-pentamethylcyclopentadiene, iron pentacarbonyl, aminoheptane, iodomethane, mercury (Aldrich), aminopropane, aminopentane, aminohexane, silver terafluoroborate (Merck), aminobutane (BDH), sodium (Fluka) and iodine (Unilab) were used as supplied. Melting points were recorded on an Ernst Leitz Wetzlar hot-stage microscope and are uncorrected. Elemental analyses were performed on a LECO CHNS-932 elemental analyzer. Infrared spectra were recorded using an ATR PerkinElmer Spectrum 100 spectrophotometer between 4000 - 400 cm^{-1}, in the solid state. Mass spectra were recorded on an Agilent 1100 series LC/MSD trap with an electrospray ionization (ESI) source and quadrupole ion trap mass analyzer by direct infussion and ESI operated in the positive mode. Acetonitrile (100%) was used as mobile phase and 10 μL of the sample injected at a 0.3 ml/min flow rate. NMR spectra were recorded on Bruker topspin 400 MHz and 600 MHz spectrometers. The deuterated

solvents, CDCl$_3$ (Aldrich, 99.8%), acetone-d$_6$ (Aldrich, 99.5%), and acetonitrile-d$_3$ (Aldrich, 99.8%) were used as purchased. The precursors [Cp*Fe(CO)$_2$]$_2$ [44], Cp*Fe(CO)$_2$I [45], and [Cp*(CO)$_2$Fe(THF)]BF$_4$ [46] were prepared by the literature methods.

4.2. Synthesis of [Cp*(CO)$_2$Fe{NH$_2$(CH$_2$)$_n$CH$_3$}]BF$_4$ (2a-2e)

The procedure for the synthesis of the compound [Cp*(CO)$_2$Fe(NH$_2$(CH$_2$)$_5$CH$_3$)]BF$_4$, **2d,** will be described to illustrate the general procedure that was followed. 1-aminohexane (0.07 ml, 0.530 mmol) was added to a solution of [Cp*(CO)$_2$Fe(THF)]BF$_4$ (0.18 g, 0.443 mmol) in CH$_2$Cl$_2$ (10 ml) at room temperature with stirring. The solution was then stirred under nitrogen atmosphere, while monitoring the progress of the reaction using IR and the reaction was stopped after 7 hours when judged complete as was indicated by a shift of the CO absorption bands from 2035 and 1983 cm^{-1} to 2020 and 1970 cm^{-1}, respectively, as well as the immergence of a band due to the dimer, [Cp*Fe(CO)$_2$]$_2$ at 1751 cm^{-1}. The mixture was filtered through a cannula into a pre-weighed Schlenk tube and dry diethyl ether (50 ml) was added to the filtrate. The mixture was allowed to stand in the dark for 16 hours after which a yellow crystalline solid collected on the walls of the Schlenk tube. Washing the residue with two portions of diethyl ether (2 x 5 ml) and drying under reduced pressure gave 0.10 g of yellow crystalline solid of [Cp*(CO)$_2$Fe{NH$_2$(CH$_2$)$_5$CH$_3$}]BF$_4$. The percentage yields, IR and other physical data are summarized in Tables 1, together with those of **2a, 2b, 2c** and **2e**. ^{1}H NMR (600 MHz, CDCl$_3$ δ(ppm)): 2.28 (m, 4H, αCH$_2$ overlapped with NH$_2$), 1.81 (s, 15H, C$_5$(CH$_3$)$_5$)**,** 1.52 (m, 2H, βCH$_2$), 1.15 (m, 6H, (CH$_2$)$_3$), 0.80 (t, J_{HH} = 6.84 Hz, 3H, CH$_3$). ^{13}C NMR (600 MHz, CDCl$_3$): δ 9.41 (C$_5$(CH$_3$)$_5$), 14.37 (CH$_3$), 22.85 (εCH$_2$) 26.69 (δCH$_2$), 31.47 (γCH$_2$), 32.61 (βCH$_2$), 53.88 (αCH$_2$), 97.35 (C$_5$(CH$_3$)$_5$), 212.77 (CO). ^{15}N NMR (400 MHz, CDCl$_3$): δ -35.58 (NH$_2$).

[Cp*(CO)$_2$Fe{NH$_2$(CH$_2$)$_3$CH$_3$}]BF$_4$ (2b): ^{1}H NMR (600 MHz, CDCl$_3$): δ 2.30 (m, 4H, αCH$_2$ overlapped with NH$_2$) 1.82 (s, 15H, C$_5$(CH$_3$)$_5$), 1.54 (m, 2H, βCH$_2$) 1.24 (m, 2H, γCH$_2$) 0.86 (t, J_{HH} = 7.38 Hz, 3H, CH$_3$). ^{13}C NMR (600 MHz, CDCl$_3$): δ 9.12 (C$_5$(CH$_3$)$_5$), 13.55 (CH$_3$), 19.82 (γCH$_2$), 34.04 (βCH$_2$), 53.06 (αCH$_2$), 97.37 (C$_5$(CH$_3$)$_5$), 212.46 (CO). ^{15}N NMR (400 MHz, CDCl$_3$): δ -35.63 (NH$_2$).

[Cp*(CO)₂Fe{NH₂(CH₂)₄CH₃}]BF₄ (2c): ¹H NMR (400 MHz, CDCl₃): δ 2.30 (m, 4H, αCH₂ overlapped with NH₂) 1.83 (s, 15H, C₅(CH₃)₅), 1.52 (m, 2H, βCH₂) 1.24 (m, 2H, γCH₂), 1.21 (m, 2H, εCH₂), 0.85 (t, J_{HH} = 7.12 Hz, 3H, CH₃). ¹³C NMR (400 MHz, CDCl₃): δ 9.19 (C₅(CH₃)₅), 13.88 (CH₃), 22.16 (εCH₂) 28.74 (γCH₂), 31.93 (βCH₂), 53.35 (αCH₂), 97.38 (C₅(CH₃)₅), 212.35 (CO). ¹⁵N NMR (400 MHz, CDCl₃): δ -35.60 (NH₂).

[Cp*(CO)₂Fe{NH₂(CH₂)₆CH₃}]BF₄ (2e): ¹H NMR (400 MHz, CDCl₃): δ 2.29 (m, 4H, αCH₂ overlapped with NH₂) 1.82 (s, 15H, C₅(CH₃)₅), 1.54 (m, 2H, βCH₂) 1.22 (m, 8H, (CH₂)₄), 0.84 (t, J_{HH} = 6.99 Hz, 3H, CH₃). ¹³C NMR (400 MHz, CDCl₃): δ 9.17 (C₅(CH₃)₅), 14.02 (CH₃), 22.51 (εCH₂) 26.62 (ωCH₂) 28.76 (δCH₂) 31.65 (γCH₂), 32.22 (βCH₂), 53.34 (αCH₂), 97.37 (C₅(CH₃)₅), 212.38 (CO). ¹⁵N NMR (400 MHz, CDCl₃): δ -35.60 (NH₂).

4.3. Synthesis of [{Cp(CO)₂Fe }₂{μ-NH₂(CH₂)₃NH₂}](BF₄)₂ (3)*

A 100 ml-Schlenk tube was charged with a solution of [Cp*(CO)₂Fe(THF)]BF₄ (0.57 g, 1.404 mmol) in CH₂Cl₂ (10 ml) in the dark. While stirring, diaminopropane (0.06 ml, 0.711 mmol) was added and the mixture stirred at room temperature for 10 h after which the solution changed from red to brown-yellow. The mixture was filtered into a pre-weighed Schlenk tube through a cannula and diethyl ether added to the filtrate until a yellow precipitate formed. This was allowed to settle for 5 min and then the mother liquor was syringed off. The yellow residue was washed with 2 x 5 ml diethyl ether and dried under reduced pressure giving analytically pure [{Cp*(CO)₂Fe}₂{μ-NH₂(CH₂)₃NH₂}](BF₄)₂. Yield: 0.325 g, 73%; Anal. Calc. for C₂₇H₄₀B₂F₈Fe₂N₂O₄: C, 43.67; H, 5.39; N, 3.77. Found: C, 44.07; H, 5.25; N, 4.09%. ¹H NMR (600 MHz, acetone-d₆): δ 1.88 (s, 30 H, C₅(CH₃)₅), 2.90 (s, 4H, NH₂), 2.40 (m, 4H, αCH₂), 1.81 (t, J_{HH} = 6.84 Hz, 2H, βCH₂). ¹³C NMR (600 MHz, acetone-d₆): δ 97.71 (C₅(CH₃)₅), 8.24 (C₅(CH₃)₅), 49.79 (αCH₂), 35.69 (βCH₂), 213.32 (CO). IR (solid state): ν(CO) 2033, 1979 cm⁻¹; ν(NH) 3312, 3269 cm⁻¹. Decomposes without melting at temperature > 170 °C.

4.4. Reaction of [Cp(CO)₂Fe{NH₂(CH₂)₅CH₃}]BF₄ (**2d**) with sodium tetraphenylborate in water and acetone*

In water: A filtered solution of $NaBPh_4$ (0.175 g, 0.526 mmol) in deionised water (10 ml) was added to a solution of **2d** (0.092 g, 0.212 mmol) in deionised water (7 ml). Although the light yellow precipitate formed immediately, the mixture was stirred for 5 min to ensure proper mixing of the reagent and hence complete reaction. The mixture was filtered by suction and the residue was washed with three portions of water (3 x 10 ml) to remove any unreacted $NaBPh_4$. Then the residue was washed further with ice cooled methanol (3 ml), followed by diethyl ether (10 ml). The residue was transferred into a Schlenk tube and dried under reduced pressure for 5 h. The product was recrystallized from dichloromethane/diethyl ether (1:4 v/v) to give a yellow microcrystalline solid. Yield: 0.09 g, 64 %; Anal. Calc. for $C_{42}H_{50}BFeNO_2$: C, 75.56; H, 7.50; N, 2.10. Found: C, 75.62; H, 7.67; N, 2.43%. ^1H NMR (400 MHz, $CDCl_3$): δ 1.59 (s, 15 H ($C_5(CH_3)_5$), -0.17 (s, 2H, NH_2), 1.52 (m, 2H, αCH_2), 1.23 (m, 2H, βCH_2), 1.13 (m, 2H, γCH_2), 0.98 (m, 2H, δCH_2), 0.81 (m, 2H, ϵCH_2) 0.86 (t, J_{HH} = 6.64 Hz, 3H, CH_3), 6.91 (t, J_{HH} = 6.96, 4H, *para*-phenyl), 7.07 (t, J_{HH} = 7.28 , 8H, *meta*-phenyl), 7.49 (s br, 8H, *ortho*-phenyl), ^{13}C NMR (400 MHz, $CDCl_3$): δ 9.28 ($C_5(\underline{C}H_3)_5$), 13.94 (CH_3), 22.49 (ϵCH_2) 26.33 (δCH_2), 31.17 (γCH_2 + βCH_2), 51.74 (αCH_2), 96.99 ($\underline{C}_5(CH_3)_5$), 211.94 (CO), 121.93 (*para*-C), 125.89 (*meta*-C), 136.07 (*ortho*-C), 163.44 – 164.90 (C-B).

In acetone: A Schlenk tube equipped with a bar magnet was charged with a solution of compound **2d** (0.075 g, 0.172 mmol) in acetone (8 ml) and a filtered solution of $NaBPh_4$ (0.123 g, 0.370 mmol) in acetone (7 ml) was added. The mixture was stirred at room temperature for 3 h under nitrogen atmosphere after which the solvent was removed under reduced pressure. The residue was extracted with CH_2Cl_2 (10 ml) and the extract filtered into a pre-weighed Schlenk tube. Diethyl ether was added into the filtrate until the yellow precipitate formed and the mixture was allowed to settle for 10 minutes. The mother liquor was syringed off and the residue dried under reduced pressure for 4 h to give 0.089 g (78% yield) of yellow microcrystalline solid whose analytical data was identical to those of the product obtained in the aqueous environment described above.

4.5. Crystal structure determination and refinement

The crystal evaluation and data collection were performed on a Bruker *APEX II* diffractometer with Mo Kα (λ = 0.71073 Å) radiation and diffractometer to crystal distance of 4.00 cm. The initial cell matrix was obtained from three series of scans at different starting angles. Each series consisted of 12 frames collected at intervals of 0.5º in a 6º range with the exposure time of 10 seconds per frame. The reflections were successfully indexed by an automated indexing routine built in the *APEX II* program suite [47] . The final cell constants were calculated from a set of 6460 strong reflections from the actual data collection.

The crystal structures were solved by direct methods using *SHELXTL* [48]. Non-hydrogen atoms were first refined isotropically followed by anisotropic refinement by full matrix least-squares calculations based on F^2 using *SHELXTL*. Hydrogen atoms were first located in the difference map then positioned geometrically and allowed to ride on their respective parent atoms. Diagrams and publication material were generated using *SHELXTL*, *PLATON* [49] and *ORTEP-3* [50].

Table 6: Crystal data and structure refinement for $[Cp^*(CO)_2Fe\{NH_2(CH_2)_3CH_3\}]BF_4$ (**2b**) and $[\{Cp^*(CO)_2Fe\}_2\{\mu\text{-}NH_2(CH_2)_3NH_2\}](BF_4)_2$ (**3**)

Compound	2b	3
Empirical formula	$C_{16}H_{26}BF_4FeNO_2$	$C_{27}H_{40}B_2F_8Fe_2N_2O_4$
Formula weight	407.04	741.93
Temperature (K)	173(2)	100
Wavelength (Å)	0.71073	0.71073
Crystal system	Orthorhombic	Monoclinic
Space group	$Pna2_1$	$P2_1/c$
Unit cell dimension (Å)		
a	15.3998(2) , $\alpha = 90$	11.1061(11), $\alpha = 90$
b	10.34100(10), $\beta = 90$	23.832(2), $\beta = 97.813(2)$
c	12.3468(2), $\gamma = 90$	12.2952(12), $\gamma = 90$
Volume ($Å^3$)	1966.22(5)	3224.1(6)
Z	4	4
Density (calculated)(Mg/m^3)	1.375	1.528
Absorption coefficient (mm^{-1})	0.811	0.981
F(000)	848	1528
Crystal size (mm)	0.39 x 0.24 x 0.18	0.29 x 0.16 x 0.09
Crystal description	prism	Block
Crystal colour	orange	Yellow
Theta range for data collection	2.37 - 28.00°.	1.71 – 28.41
Index ranges		
h	$-20 \rightarrow 20$	$-14 \rightarrow 14$
k	$-13 \rightarrow 13$	$-31 \rightarrow 31$
l	$-16 \rightarrow 16$	$-16 \rightarrow 16$
Reflections collected	30935	104728
Independent reflections	4706	8072
Internal fit	R(int) = 0.0513	0.0627
Absorption correction	Integration	Semi-empirical from equivalents
Transmission factor (T_{Min};T_{Max})	0.7426; 0.8677	0.7639; 0.9169
Refinement method	Full-matrix least-squares on F^2	Full-matrix least-squares on F^2
parameters	232	528
Goodness-of-fit on F^2	0.953	1.031
Final R indices [I>2sigma(I)]	R1 = 0.0299, wR2 = 0.0639	R1 = 0.0321, wR2 = 0.0733
R indices (all data)	R1 = 0.0381, wR2 = 0.0664	R1 = 0.0459, wR2 = 0.0815
Largest diff. peak and hole(e.$Å^{-3}$)	0.220 and -0.254	0.092 and -0.518

Acknowledgments

Supplementary material

Supplementary data associated with this article can be found, in the online version, at doi: 10.1016/j.ica.2011.09.058. Crystallographic data for compounds **2b** and **3** are given in Appendix 6. CD-ROM containing all CIF file and spectroscopic data is provided in Appendix 12.

References

[1]   A. Sivaramakrishna, H.S. Clayton, C. Kaschula, J.R. Moss, Coord. Chem. Rev. 251 (2007) 1294.

[2]   E.O. Changamu, H.B. Friedrich, M. Rademeyer, J. Organomet. Chem. 692 (2007) 2456.

[3]   E.O. Changamu, H.B. Friedrich, J. Organomet. Chem. 692 (2007) 1138.

[4]   H.B. Friedrich, P.A. Makhesha, J.R. Moss, B.K. Williamson, J. Organomet. Chem. 384 (1990) 325.

[5]   H.S. Clayton, J.R. Moss, M.E. Dry, J. Organomet. Chem. 688 (2003) 181.

[6]   H.B. Friedrich, R.A. Howie, M. Laing, M.O. Onani, J. Organomet. Chem. 689 (2004) 181.

[7]   R.O. Hill, C.F. Marais, J.R. Moss, K.J. Naidoo, J. Organomet. Chem. 587 (1999) 28.

[8]   S.F. Mapolie, J.R. Moss, S. Afr. J. Chem. 40 (1987) 12.

[9]   E.O. Changamu, H.B. Friedrich, R.A. Howie, M. Rademeyer, J. Organomet. Chem. 692 (2007) 5091.

[10]   A. Tahiri, T.L. Guerchais, C. Lapinte, J. Organomet. Chem. 381 (1990) C47.

[11]   V. Guerchais, S. Lévéque, A. Hornfeck, C. Lapinte, Organometallics 11 (1992) 3926.

[12]   A. Conde, R. Fandos, A. Otero, A. Rodríguez, Organometallics 26 (2007) 1568.

[13]   C.M. M'thiruaine, H.B. Friedrich, E.O. Changamu, M.D. Bala, Inorg.Chim. Acta 366 (2011) 105.

[14]   C.M. M'thiruaine, H. B.Friedrich, E.O. Changamu, (Unpublished results).

[15] M. Akita, S. Kakuta, S. Sugimoto, M. Terada, M. Tanaka, Y. Moro-oka, Organometallics 20 (2001) 2736.

[16] E. Roman, D. Catheline, D. Astruc, J. Organomet. Chem. 236 (1982) 229.

[17] C.S.-M.d. Lecea, A. Linares-Solano, J.A. Díaz-Auñón, P.C. L'Argentière, Carbon 38 (2000) 157.

[18] P.C. L'Argentière, E.A. Cagnola, D.A. Liprandi, M.C. Román-Martnez, C.S.-M.d. Lecea, Appl. Catal. A. General 172 (1998) 41.

[19] M.C. Román-Martínez, J.A. Díaz-Auñón, P.C.L. Argentière, C.S.-M.d. Lecea, Catal. Lett. 77 (2001) 41.

[20] J.A. Díaz-Auñón, M.C. Román-Martínez, C.S.-M.d. Lecea, P.C. L'Argentière, E.A. Cagnola, D.A. Liprandi, M.E. Quiroga, J. Mol. Catal. A Chem. 153 (2000) 243.

[21] M.E. Quiroga, D.A. Liprandi, E.A. Cagnola, P.C. L'Argentière, Appl. Cat. A. General 326 (2007) 121.

[22] F.M.F. Vergara, M.d.G.M.O. Henriques, A.L.P. Candea, J.L. Wardell, M.V.N.D. Souza, Bioorg. Med. Chem. Lett. 19 (2009) 4937.

[23] R. Yendapally, R.E. Lee, Bioorg. Med. Chem. Lett. 18 (2008) 1607.

[24] X. Zhang, Y. Hu, S. Chen, R. Luo, J. Yue, Y. Zhang, W. Duan, H. Wanga, Bioorg. Med. Chem. Lett. 19 (2009) 6074.

[25] R.P. Tripathi, V.K. Tiwari, N. Tewari, D. Katiyar, N. Saxena, S. Sinha, A. Gaikwad, A. Srivastava, V. Chaturvedi, Y.K. Manju, R. Srivastavac, B.S. Srivastavac, Bioorg. Med. Chem. 13 (2005) 5668.

[26] P. Chen, J. Gearhart, M. Protopopova, L. Einck, C.A. Nacy, J. Antimicrob. Chemoth. 58 (2006) 332 and references therein.

[27] D. Razafimahefa, D.A. Ralambomanana, Lies Hammouche, L. Pélinski, S. Lauvagie, C. Bebear, J. Brocard, J. Maugeind, Bioorg. Med. Chem. Lett. 15 (2005) 2301.

[28] D.A. Ralambomanana, D. Razafimahefa-Ramilison, A.C. Rakotohova, J. Maugein, L. Pélinski, Bioorg. Med. Chem. 16 (2008) 9546.

[29] H.B. Friedrich, M.O. Onani, M. Rademeyer, Acta Cryst. E60 (2004) m551.

[30] E.O. Changamu, H.B. Friedrich, M.O. Onani, M. Rademeyer, J. Organomet. Chem. 691 (2006) 4615.

[31]   J.D. Oliver, D.F. Mullica, B.B. Hutchinson, W.O. Milligan, Inorg. Chem. 19 (1980) 165.

[32]   S. Mahapatra, R.J. Butcher, R. Mukherjee, J. Chem. Soc. Dalton Trans. (1993) 3723.

[33]   W. Xu, A.J. Lough, R.H. Morris, Inorg. Chem. 35 (1996) 1549.

[34]   B.D. Gupta, R. Yamuna, D. Mandal, Organometallics 25 (2006) 706.

[35]   X. Zhang, Y. Li, H. Chen, J. Organomet. Chem. 691 (2006) 659.

[36]   J.D. Holbrey, A.E. Visser, S.K. Spear, W.M. Reichert, R.P. Swatoski, G.A. Broker, R.D. Rogers, Green Chem. 5 (2003) 129.

[37]   A. Bondi, J. Phys. Chem. 68 (1964) 441.

[38]   K. Gruet, E. Clot, O. Eisenstein, D.H. Lee, B. Patel, A. Macchioni, R.H. Crabtree, New J. Chem. 27 (2003) 80.

[39]   A. Macchioni, Eur. J. Inorg. Chem. 2003 (2003) 195.

[40]   L. Rocchigiani, G. Bellachioma, G. Ciancaleoni, S. Crocchianti, A. Laganà, C. Zuccaccia, D. Zuccaccia, A. Macchioni, ChemPhysChem. 11 (2010) 3243.

[41]   G. Bellachioma, G. Cardaci, A. Macchioni, G. Reichenbach, S. Terenzi, Organometallics 21 (1996) 4349.

[42]   A. Macchioni, C. Zuccaccia, E. Clot, K. Gruet, R.H. Crabtree, Organometallics 20 (2001) 2367.

[43]   G. Bellachioma, G. Cardaci, A. Macchioni, G. Reichenbach, S. Terenzi, Organometallics. 15 (1996) 4349.

[44]   R.B. King, F.G.A. Stone, Inorg. Synth. 7 (1963) 110.

[45]   T.S. Piper, F.A. Cotton, G. Wilkinson, J. Inorg. Nucl. Chem. 1 (1955) 165.

[46]   M. Akita, M. Tarada, M. Tanaka, Y. Morooka, J. Organomet. Chem. 510 (1996) 255.

[47]   Bruker, AXS. *APEX2*, *SADABS*, and *SAIN*T Software Reference Manuals. Bruker-AXS, Madison, Wisconsin, USA, (2009).

[48]   Bruker, *SHELXTL*. Version 5.1. (includes XS, XL, XP, XSHELL) Bruker AXS Inc., Madison, Wisconsin, USA, (1999).

[49]   A.L. Spek, J. Appl. Cryst. 36 (2003) 7.

[50]   L.J. Farrugia, J. Appl. Cryst. 30 (1997) 565.

CHAPTER FOUR

Reactions of *N*-heterocyclic ligands with substitutionally labile organometallic complexes, [η^5-C$_5$R$_5$)Fe(CO)$_2$E]BF$_4$ (E = Et$_2$O, THF)

Cyprian M. M'thiruaine[a], Holger B. Friedrich[a*], Evans O. Changamu[b], Muhammad D. Bala[a]

[a] School of Chemistry, University of KwaZulu-Natal, Private Bag X54001, Durban 4000, South Africa [b] Chemistry Department, Kenyatta University, P.O Box 43844, Nairobi, Kenya

* Corresponding author

Abstract

The ether complexes [Cp(CO)$_2$Fe(OEt$_2$)]BF$_4$ (Cp = η^5-C$_5$H$_5$) (**1**) and [Cp*(CO)$_2$Fe(THF)]BF$_4$ (Cp* = η^5-C$_5$(CH$_3$)$_5$) (**2**) react with 1,3,5,7-tetraazaadamantane (HMTA) to give stable water-soluble dinuclear complexes [{(η^5-C$_5$R$_5$)(CO)$_2$Fe}$_2$(μ-HMTA)](BF$_4$)$_2$ (R = H; R = CH$_3$) and monuclear complexes [(η^5-C$_5$R$_5$)(CO)$_2$Fe(HMTA)]BF$_4$ (R = H; R = CH$_3$). The reaction of **1** with 1,4-diazabicyclo[2.2.2]octane (DABCO) gave good yields of the dinuclear and monuclear complexes, [{Cp(CO)$_2$Fe}$_2$(μ-DABCO)](BF$_4$)$_2$ (**6a**) and [Cp(CO)$_2$Fe(DABCO)]BF$_4$ (**6b**), respectively, depending on reagent ratios. Similar reactions with **2** gave very low yields of the monuclear complex [Cp*(CO)$_2$Fe(DABCO)]BF$_4$ (**6c**) as the only product. The reactions of [Cp(CO)$_2$Fe(HMTA)]BF$_4$ (**3b**) and [Cp*(CO)$_2$Fe(HMTA)]BF$_4$ (**4b**) with NaBPh$_4$ in acetone proceeded smoothly at room temperature to give the corresponding BPh$_4^-$ salts. Reaction of **4b** with **1** at room temperature gave the dinuclear complex [{Cp(CO)$_2$Fe}$_2$(μ-HMTA)](BF$_4$)$_2$ (**3a**) as the major product, while the same reaction conducted at 0 ˚C led to the unstable mixed ligand complex [{Cp(CO)$_2$Fe}(μ-HMTA){Fe(CO)$_2$Cp*}](BF$_4$)$_2$. The reactions of **1** and **2** with 1-methylimidazole (1-meIm) gave high yields of [(η^5-C$_5$R$_5$)(CO)$_2$Fe(1-meIm)]BF$_4$ (R = H (**7**); R = CH$_3$ (**8**)), of which the NMR, IR and single crystal X-ray studies reveal the coordination of 1-methylimidazole to be *via* the sp^2-N of the imidazole ring. Single-crystal X-ray diffraction studies reveal that compounds **3a** and **8** crystallize in the orthorhombic *P2$_1$2$_1$2$_1$* and *Pna2$_1$* space groups, respectively. Compound **7** however, crystallized in the

monoclinic $P2_1/c$ space group with three independent molecular cations and anions each in the asymmetric unit.

1. Introduction

In recent years, there has been a great deal of interest in complexes bearing cage-like 1,3,5-triaza-7-phosphaadamantane (PTA) [1-6] due to its ability to solubilize metal complexes in the aqueous phase [7]. Some of these complexes have found application in aqueous phase and biphasic catalytic systems [8-10] as well as in pharmaceuticals [5, 7]. The synthesis of water-soluble organometallic derivatives has been widely achieved by the design of water-soluble ligands that, when incorporated into the coordination sphere of the metal, impart water-solubility to the complexes. The solubilizing ability of the PTA complexes for instance is imparted by the nitrogen atoms which form hydrogen bonds with water molecules.

PTA and other N-based aromatic heterocycles have also been widely used as metal coordination spacers owing to their good donor ability and rigidity [11-13]. HMTA and its derivatives, in particular, have been used as antibacterial agents in the treatment of urinary tract infections since 1932 [14-16], and their anti-bacterial activity has been the subject of many patents in recent years. For example, methenamine (HMTA), methenamine anhydromethylene-citrate, methenamine hippurate, methenamine mandelate and methenamine sulfosalicylate have all been reported as synthetic antibacterials [17] and as anti-infectives [18]. HMTA has also been applied in the treatment of ear canal infections in combination with anti-inflammatory and antiseptic agents [19], and as an adjuvant to radiation and cisplatin in the treatment of solid tumors [20]. In recent years HMTA has been used as base catalyst in the synthesis of phenolic gel and most recently García *et al.* published a report on the use of HMTA as a base catalyst to control the porosity and pore size of resorcinol furaldehyde cryogels synthesized in *t*-butanol [21].

DABCO is known mainly as an organic catalyst in a large variety of organic syntheses [22-24]. For example it has displayed high catalytic activity in the methylation of indole in conjunction with dimethyl carbonate [25]. Gordon *et al.* have demonstrated that DABCO derivatives can also be used as Voltage-Gated potassium channel blockers [26]. To the best of our knowledge, the DABCO iron complexes of the type $[(CO)_4Fe(DABCO)]$ and $[\{(CO)_4Fe\}_2(\mu\text{-}DABCO)]$ are the only reported iron carbonyl complexes incorporating the DABCO ligand in the coordination sphere [27].

1-methylimidazole (1-meIm) is a derivative of imidazole (Im) which also finds application in drug design [28, 29] and catalysis [29, 30]. This has instigated interest in coordination of imidazole–based ligands to transition metals [31] leading to the reporting of a wide variety of imidazole transition metal complexes [32, 33]. This includes the complexes $[Cp(CO)_2FeL\text{-}BPh_3]$ (L = imidazole, benzimidazole) reported by Nesmayanov *et al.*, as a product of the decomposition reaction of the salts $[Cp(CO)_2FeLH]^+ BPh_4^-$ [32]. A ligand substitution reaction could be an alternative route to the cationic complex $[Cp(CO)_2FeL]^+$, whereby labile ligands such as THF, Et_2O or acetone are replaced by the imidazole ligand. However, such reactions have not been previously reported.

The importance of *N*-heterocyclic ligands in physiology, pharmaceuticals and catalysis, as well as interest in exploration of the coordination chemistry of amine ligands, aroused our interest in the coordination of such ligands to transition metal centres of varying electronic and steric environments. This may enhance an understanding of their interactions with a metal ion and, hence, provide models for active anti-bacterials or catalysts. For this report, iron was the metal of choice since it is relatively non-toxic, inexpensive and easy to handle due to the high stability exhibited by its complexes. Moreover, iron complexes with bidentate *N,N*-ligands and tridentate *N,N,N*-ligands have been shown to catalyse ethylene oligomerization and polymerization reactions [34-37]. Iron is also found in the blood of both vertebrates and invertebrates in which it forms Fe-N bonds in the *heme* group of hemoglobin or myoglobin. To the best of our knowledge HMTA, DABCO and 1-meIm complexes with the $(\eta^5\text{-}C_5R_5)(CO)_2Fe$ moiety are unknown. Herein we report the syntheses and characterization of the novel complexes of the types, $[\{(\eta^5\text{-}C_5R_5)(CO)_2Fe\}_2L)](BF_4)_2$ and $[(\eta^5\text{-}C_5R_5)(CO)_2FeL]BF_4$

(R = H, CH$_3$; L = HMTA, DABCO) as well as [(η^5-C$_5$R$_5$)(CO)$_2$Fe(1-meIm)]BF$_4$ (R = H, CH$_3$; 1-meIm = 1-methylimidazole), which is a part of an on-going study on functionalized transition metal alkyl complexes [38-45].

2. Results and discussion

The three *N*-heterocyclic ligands employed in this investigation react with the ether complexes [Cp(CO)$_2$Fe(OEt$_2$)]BF$_4$ (**1**) and [Cp*(CO)$_2$Fe(THF)]BF$_4$ (**2**) at room temperature in dichloromethane to afford complexes **3**-**8** as shown in Scheme 1. The *N*-heterocyclic ligands are generally good electron donors and therefore readily displace weakly bound Et$_2$O and THF molecules. All the complexes were obtained in moderate to excellent yields as yellow to orange solids, except for compound **6c** which was obtained in a low yield. They are fairly stable in air but slowly decompose when in solution and particularly when exposed to light. For this reason, manipulations of the compounds in solution were done in the dark under strictly anaerobic conditions. The complexes have been fully characterized by elemental analysis, NMR and IR spectroscopy (Sections 4.2 - 4.12) as well as single crystal X-ray diffraction.

Mononuclear complexes			Dinuclear complexes			Ether complexes			Mononuclear complexes		
R	**L**		**R**	**L**		**R**	**E**		**R**	**L**	
3b H	HMTA		**3a** H	HMTA		**1** H	Et$_2$O		**7** H	1-meIm	
4b CH$_3$	HMTA		**4a** CH$_3$	HMTA		**2** CH$_3$	THF		**8** CH$_3$	1-meIm	
6b H	DABCO		**6a** H	DABCO							
6c CH$_3$	DABCO										
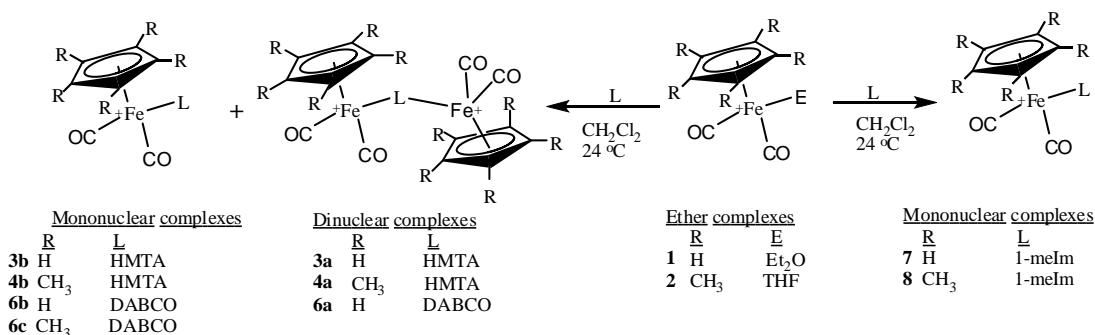
Scheme 1: Reaction of etherate complexes **1** and **2** with *N*-heterocyclic ligands

*2.1. Reaction of hexamethylenetetramine (HMTA) with the ether complexes [(η⁵-C₅R₅)(CO)₂Fe(E)]BF₄ (R = H, E = Et₂O (**1**), R = CH₃, E = THF(**2**))*

1,3,5,7-Tetraazaadamantane (commonly known as hexamethylenetetramine and abbreviated HMTA), readily reacts with **1** at room temperature to give the dinuclear complex **3a** and the monuclear complex **3b**. Similarly, the reaction of HMTA with **2** yields the dinuclear complex **4a** and the monuclear complex **4b** whether the dinuclear or the monuclear complex is isolated depends on the stoichiometric ratio of the reagents employed. Thus, the reaction of the etherate complexes with a slight excess of HMTA furnished only the monuclear product, while 1:1 or 2:1 mole ratios (etherate complex to HMTA) gave mixtures of dinuclear [{(η⁵-C₅R₅)(CO)₂Fe}₂(μ-HMTA)](BF₄)₂ and monuclear [(η⁵-C₅R₅)(CO)₂Fe(HMTA)]BF₄ (R = H, CH₃) complexes as products with the relative amount of the monuclear product decreasing with increase in etherate reactant used in the reaction. When the mole ratio of the reaction is raised to 4:1, only the dinuclear complex [{(η⁵-C₅R₅)(CO)₂Fe}₂(μ-HMTA)](BF₄)₂ was isolated. No evidence for the formation of the tetranuclear complex [{(η⁵-C₅R₅)(CO)₂Fe}₄(μ₄-HMTA)](BF₄)₄ was obtained, even when large excesses of the etherate complexes were employed. This is probably due to the steric hindrance induced by the two (η⁵-C₅R₅)(CO)₂Fe groups occupying two of the four binding sites of the HMTA ligand.

The monuclear complexes were obtained as yellow, while the dinuclear complexes were obtained as orange solids. All the complexes were soluble in water, acetone and acetonitrile. The complexes **4a** and **4b** were also soluble in dichloromethane and were easily isolated from solution by precipitation using diethyl ether. It was difficult to separate the dinuclear from the monuclear compounds, thus pure samples of the dinuclear and monuclear compounds were obtained by using the appropriate mole ratios of the reactants.

The IR spectra of compounds **3a-4b** show two strong absorption bands in the range 2058 – 1982 cm⁻¹ assignable to the two terminal carbonyls as expected for cationic amine complexes [41, 45-47]. The IR spectra of **4a** and **4b** exhibited characteristic *v*(CO) stretching vibrations at wavenumbers lower than those of **3a** and **3b** by *ca.* 21 cm⁻¹, which is due to the enhanced back-donation of metal to carbon as a result of the electron rich C₅(CH₃)₅ ligand. A characteristic band due to CN stretching of HMTA was

observed at 1227-1244 cm^{-1} as expected [48]. The v(CO) vibrations of the monuclear complexes were not significantly different from those of the dinuclear complexes and therefore it was not possible to distinguish the monuclear from the dinuclear complexes based solely on carbonyl vibration frequency. However, the IR spectra of the monuclear complexes exhibited bands in the fingerprint region which were significantly different from those of the dinuclear complexes. For example, the IR spectrum of dinuclear complex **3a** show peaks at 918, 847, 712, 646 and 473 cm^{-1} which were absent in the IR spectrum of monuclear complex **3b**. On the other hand **3b** exhibited peaks at 824, 655, 530 and 390 cm^{-1} which were missing in the IR spectrum of **3a.**

Coordination of HMTA to the metal decreases molecular symmetry resulting in a highly complex ^{1}H NMR spectrum with a multiple spin system making the assignment of the methylene protons difficult. Hence, the literature NMR data for the coordinated HMTA or its derivative 1,3,5-triaza-7-phosphaadamantane (PTA) are often reported as a range [1, 4, 7, 49], and a similar strategy is adopted for this study. The proton NMR spectrum of **3a** in acetonitrile-d$_3$ consists of a sharp singlet at 5.42 ppm integrating to 10 protons, assignable to two identical cyclopentadienyl ligands, while the Cp* analogue, compound **4a** exhibited a resonance peak due to the two identical pentamethylcyclopentadienyl protons at 1.86 ppm, integrating to 30 protons. Multiple resonance peaks assignable to the 12 protons of the 1,3,5,7-tetraazaadamantane methylenes bridging the nitrogen atoms of HMTA ligand in the dinuclear complexes **3a** and **4a** are observed in the range 4.16 - 4.50 ppm.

The ^{1}H NMR spectra of the monuclear complexes **3b** and **4b** show three resonance peaks each; a singlet peak integrating for 6 protons, assignable to methylene protons adjacent to coordinated nitrogen, and a set of two broad resonance peaks, integrating for 3 protons, each assignable to axial and equatorial protons of methylenes bridging the uncoordinated nitrogen. Similar observations were made by Darensbourg and Daigle in the ^{1}H NMR spectrum of Mo(CO)$_5$(HMTA) recorded in acetone [50].

In the ^{13}C NMR spectra of the dinuclear complexes **3a** and **4a** (Fig. 1a), a peak corresponding to C2 is observed at ca. 86.6 ppm, shifted downfield as a result of the deshielding effect of the two metal centres. The peak assignable to the less deshielded C6 is observed upfield relative to other methylene carbons at ca. 73 ppm, while the peak

corresponding to the four identical methylene carbons C4, C8, C9 and C10 appears at ca. 81.0 ppm. Unlike the dinuclear complexes, the ^{13}C NMR spectra of the monuclear complexes **3b** and **4b** gave two peaks for the bridging methylene carbons of the coordinated HMTA ligand; one peak corresponding to the three equivalent methylene carbons closer to the coordinated nitrogen and the other peak corresponding to the three equivalent methylenes bridging the uncoordinated nitrogen atoms. The ^{13}C NMR spectrum of **3b** shows a singlet at 83.5 ppm corresponding to the methylene carbons C2, C8 and C9 (Fig. 1b), while a singlet corresponding to the equivalent methylene carbons was observed at 81.8 ppm in the ^{13}C NMR spectrum of compound **4b** indicating a decrease in σ acidity of the metal fragment upon changing from Cp to Cp* which conforms with the expected enhanced π-back donation in Cp* complexes. The peak corresponding to less deshielded methylene carbons C4, C6, and C10 bridging the uncoordinated nitrogen atoms were observed at 71.1 and 71.2 ppm for compounds **3b** and **4b**, respectively, implying that the effect of changing the Cp to Cp* was insignificant on these methylene groups.

3a R = H
4a R = CH$_3$

3b R = H
4b R = CH$_3$
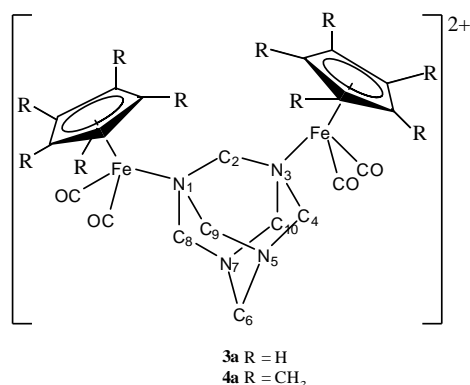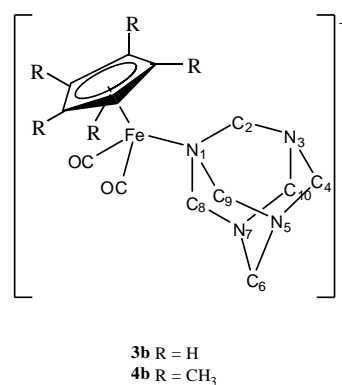
Fig. 1a   **Fig. 1b**

Fig 1: Atomic numbering scheme of HMTA in dinuclear (Fig 1a) and monuclear (Fig 1b)

Complex **4b** reacted with **1** at room temperature by displacing the Cp*(CO)$_2$Fe fragment to give a mixture of compounds **3a**, **3b** and [Cp*(CO)$_2$Fe]$_2$ rather than the expected mixed ligand complex [{Cp(CO)$_2$Fe}(μ-HMTA){Fe(CO)$_2$Cp*}](BF$_4$)$_2$. There was no

evidence indicating formation of the mixed ligand complex at room temperature. This was probably due to the highly electrophilic nature of the Cp(CO)$_2$Fe group which rapidly reacted by displacing the relatively less electrophilic Cp*(CO)$_2$Fe group at room temperature. However, when the reaction was repeated and maintained at 0 °C for 1 h the compound [{Cp(CO)$_2$Fe}(μ-HMTA){Fe(CO)$_2$Cp*}](BF$_4$)$_2$ was obtained as an air-sensitive orange solid which was characterized by ^{1}H and ^{13}C NMR spectroscopy.

In another attempt to prepare the mixed ligand complexes, a mixture of a solution of **3b** in acetonitrile and compound **2** in dichloromethane were stirred at room temperature for 3 h after which the starting material **3b** precipitated out as a yellow residue. The acetonitrile complex [Cp*(CO)$_2$Fe(NCMe)]BF$_4$ was obtained in 98% yield (based on compound **2**) from the filtrate by precipitation using diethyl ether. The molecular structure, physical and spectroscopic data of [Cp*(CO)$_2$Fe(NCMe)]BF$_4$ are reported elsewhere [51]. Thus, the Cp*(CO)$_2$Fe group has preferential binding affinity for NCMe when compared to the coordinated HMTA. It should be noted that based on Pearson's rule on hard and soft acids and bases the preferential binding of the Cp*(CO)$_2$Fe group to acetonitrile does not in any way contradict the formation of the bridged complex **4b,** since the soft acid will interact more strongly with a soft base than a hard base. Generally, metal centres that are electron rich will interact weakly with strong electron-donating ligands. This leads to weak M–L bonding and ease of ligand dissociation. The strong interaction of iron-acetonitrile in [Cp*(CO)$_2$Fe(NCCH$_3$)]BF$_4$ is confirmed by a shorter Fe-N bond (1.924 Å) [51].

2.1.1. Structural analysis of [{Cp(CO)$_2$Fe}$_2$(μ-HMTA)](BF$_4$)$_2$

The single-crystal X-ray diffraction study reveals that [{Cp(CO)$_2$Fe}$_2$(μ-HMTA)](BF$_4$)$_2$ crystallizes in the orthorhombic $P2_12_12_1$ space group with one dicationic molecule and two counter-anions in the asymmetric unit. The two Cp(CO)$_2$Fe units are linked by the HMTA ligand through the nitrogen atoms in which the coordination geometry around Fe can be described as distorted octahedral with three sites occupied by a cyclopentadienyl ligand, while the two carbonyls and the HMTA ligand occupy the remaining three sites. The Fe–N bond distances were found to be 2.0817(17) and 2.0858(18) Å, which are comparable to the 2.092(4) Å in [(CO)$_4$Fe(DABCO) [27], but longer than the Fe–N bond lengths previously reported for

cyclopentadienylirondicarbonyl amine complexes [41, 45, 47]. The three carbon atoms adjacent to the iron centre form a base with a distorted tetragonal geometry about nitrogen with N–C bonds in the range 1.514 ± 0.010 Å. Valence angles are: Fe–N–C, $111.89 \pm 1.51°$ and C–N–C, $106.94 \pm 0.84°$. The length of the remaining C–N bonds in the molecule fall in the range 1.458 ± 0.017 Å, unlike the equivalent C–N bonds (1.476 Å) reported for the uncoordinated HMTA structure [52]. The difference in bond lengths can be attributed to loss of symmetry upon coordination to the electrophilic iron centre. Similar observations were reported by Hanic and Šubrtová in the structural study of $C_6H_{12}N_4 \cdot BH_3$ [53]. Other selected bond distances and angles are listed in Table 1. The *ORTEP* diagrams showing the atomic numbering scheme and the packing of the molecules in the crystal are shown in Figs. 2 and 3, respectively. Crystallographic and refinement data are given in Table 2.
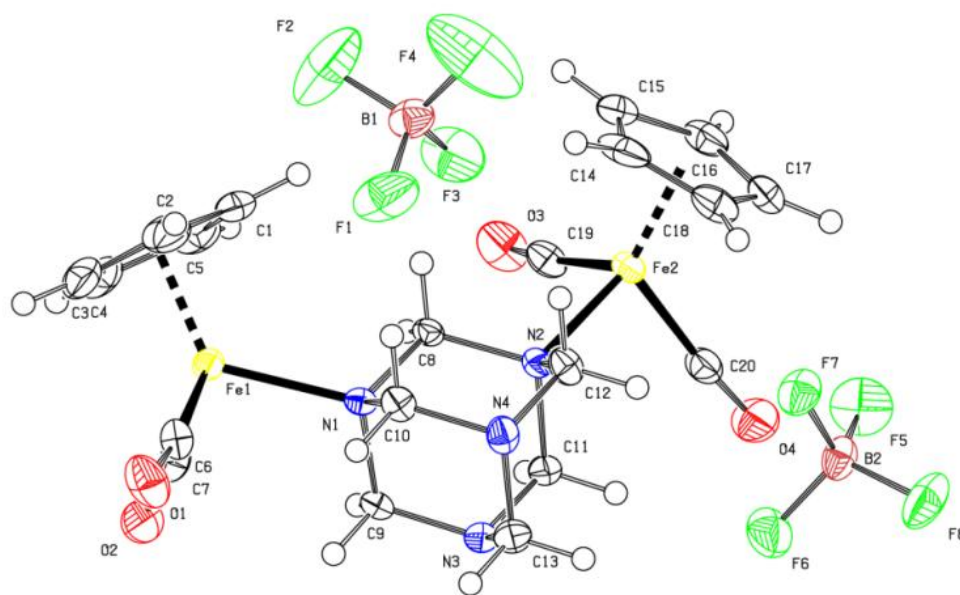
Fig. 2: The molecular structure of **3a** showing atomic numbering scheme. Displacement ellipsoids are drawn at the 50% probability level with H atoms presented as small spheres

Table 1: Selected bond lengths [Å] and angles [°] for [{Cp(CO)$_2$Fe}$_2$(μ-HMTA)](BF$_4$)$_2$ (**3a**)

Bond	Length (Å)	Bonds	Angle (°)
C(8)-N(2)	1.506(3)	N(2)-C(8)-N(1)	112.77(16)
C(8)-N(1)	1.506(3)	N(4)-C(10)-N(1)	112.35(17)
C(9)-N(3)	1.456(3)	C(10)-N(1)-C(9)	107.11(16)
C(9)-N(1)	1.516(3)	C(12)-N(2)-C(11)	106.38(16)
C(10)-N(4)	1.451(3)	C(12)-N(4)-C(10)	110.07(17)
C(10)-N(1)	1.510(3)	C(12)-N(4)-C(13)	109.46(19)
C(13)-N(4)	1.469(3)	C(10)-N(4)-C(13)	109.06(17)
C(13)-N(3)	1.475(3)	C(6)-Fe(1)-C(7)	93.01(11)
N(1)-Fe(1)	2.0858(18)	C(6)-Fe(1)-N(1)	94.48(9)
N(2)-Fe(2)	2.0817(17)	C(7)-Fe(1)-N(1)	95.27(9)
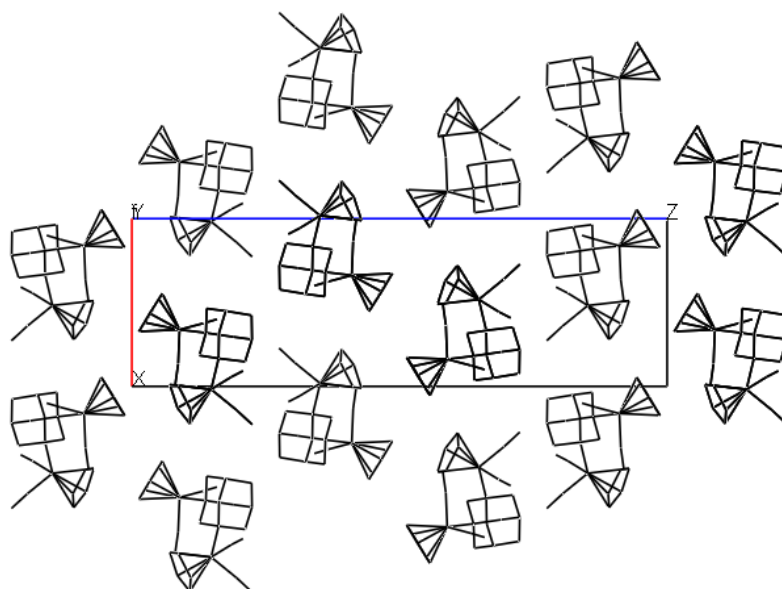
Fig. 3: Crystal packing of compound **3a** viewed down the *b*-axis

Table 2: Crystal data and structure refinement data for [{Cp(CO)$_2$Fe}$_2$(μ-HMTA)](BF$_4$)$_2$ (**3a**), [Cp(CO)$_2$Fe(1-meIm)]BF$_4$ (**7**) and [Cp*(CO)$_2$Fe(1-meIm)]BF$_4$ (**8**).

Compound	3a	7	8
Empirical formula	C$_{20}$ H$_{22}$ B$_2$ F$_8$ Fe$_2$ N$_4$ O$_4$	C$_{11}$H$_{11}$BF$_4$FeN$_2$O$_2$	C$_{16}$H$_{21}$BF$_4$FeN$_2$O$_2$
Formula weight	667.74	345.88	416.01
Temperature (K)	173(2)	173(2)	173(2)
Wavelength (Å)	0.71073	0.71073	0.71073
Crystal system	Orthorhombic	Monoclinic	Orthorhombic
Space group	P2$_1$2$_1$2$_1$	P2$_1$/c	Pna2$_1$
Unit cell dimension			
a (Å)	8.60250(10), α = 90	17.8135(6), α = 90	17.0840(4), α = 90
b	10.2951(2), β = 90	9.9651(4), β = 95.3860(10)	13.9877(4), β = 90
c	27.5041(4), γ = 90	23.9093(10), γ = 90	7.6884(2), γ = 90
Volume (Å^3)	2435.86(7)	4225.5	1839.65(8)
Z	4	12	4
Density (calculated)(Mg/m^3)	1.821	1.631	1.502
Absorption coefficient (mm^{-1})	1.290	1.119	0.871
F(000)	1344	2088	856
Crystal size (mm)	0.47 x 0.46 x 0.16	0.44 x 0.41 x 0.13	0.44 x 0.40 x 0.01
Crystal description	plate	Plate	Prism
Crystal colour	brown	yellow	yellow
Theta range for data collection	1.48 - 27.99°.	1.15 – 28.00	1.88 – 28.00
Index ranges			
h	-11 → 11	-23 → 15	-22 → 21
k	-13 → 13	-13 → 9	-18 → 18
l	-36 → 36	-31 → 31	-10 → 10
Reflections collected	33919	28785	20793
Independent reflections	5902	10195	4441
Internal fit	R(int) = 0.0418	R(int) = 0.0355	R(int) = 0.0465
Absorption correction	Integration	Integration	Integration
Transmission factor (T$_{Min}$;T$_{Max}$)	0.5823; 0.8202	0.6388; 0.8682	0.7006; 0.9913
Refinement method	Full-matrix least-squares on F^2	Full-matrix least-squares on F^2	Full-matrix least-squares on F^2
parameters	361	571	241
Goodness-of-fit on F^2	1.051	1.046	1.038
Final R indices [I>2sigma(I)]	R1 = 0.0284, wR2 = 0.0705	R1 = 0.0535, wR2 = 0.1456	R1 = 0.0342, wR2 = 0.0836
R indices (all data)	R1 = 0.0314, wR2 = 0.0715	R1 = 0.0787, wR2 = 0.1663	R1 = 0.0418, wR2 = 0.0870
Largest diff. peak and hole(e.Å^{-3})	0.683 and -0.473	1.604 and -0.943	0.400 and -0.312

2.2. Reaction of 3b and 4b with NaBPh₄

The reaction of monuclear complexes **3b** and **4b** with NaBPh$_4$ in acetone proceeds smoothly at room temperature with counter-anion exchange to provide complexes [Cp(CO)$_2$Fe(HMTA)]BPh$_4$ (**5a**) and [Cp*(CO)$_2$Fe(HMTA)]BPh$_4$ (**5b**), respectively. These complexes were obtained in high yields as yellow microcrystalline solids by precipitation using diethyl ether from their CH$_2$Cl$_2$ solutions. The bulky BPh$_4^-$ anion renders the cationic complexes soluble in dichloromethane and relatively more soluble in acetone and acetonitrile. It also stabilizes the cations in solution and consequently improves the resolution of their NMR spectrum. For example, the ^{1}H NMR spectra of **5a** and **5b** exhibited two doublets corresponding to the axial and equatorial protons of the methylene groups bridging the uncoordinated nitrogen atoms which were observed as broad peaks in the ^{1}H NMR spectra of **3b** and **4b**. Unfortunately, the dinuclear complexes of BPh$_4^-$ were insoluble in dichloromethane and they could not be obtained in pure form.

2.3. Reaction of 1 and 2 with DABCO

1,4-diazabicyclo[2.2.2]octane (DABCO) reacts with one equivalent of the ether complex (**1**) at room temperature to give a mixture of the dinuclear complex [{Cp(CO)$_2$Fe}$_2$(μ-DABCO)](BF$_4$)$_2$ (**6a**) and monuclear complex [Cp(CO)$_2$Fe(DABCO)]BF$_4$ (**6b**) in a 9:10 ratio. The reaction of DABCO with two equivalents of compound **1** also gave a mixture of **6a** and **6b**, however, the amount of **6a** in the mixture increased as the amount of compound **1** used in the reaction is increased. The dinuclear complex **6a** formed as an orange precipitate after six hours of reaction and was easily separated by filtration under nitrogen. The monuclear complex remained in solution and was obtained as a yellow solid by precipitation using diethyl ether. The reaction of DABCO with three equivalents of **1** afforded only the dinuclear complex **6a**. In contrast, the reaction of DABCO with one to three equivalents of the THF complex (**2**) gave only the monuclear complex [Cp*(CO)$_2$Fe(DABCO)]BF$_4$ (**6c**), which was obtained as a yellow solid in low yield by addition of diethyl ether into its solution in CH$_2$Cl$_2$. The failure to form the dinuclear complex by [Cp*(CO)$_2$Fe(THF)]BF$_4$ can be attributed to the high steric demand of both the

Cp*(CO)$_2$Fe moiety and the ligand itself. Unlike HMTA, which has a Tolman's cone angle of 118° [54], DABCO has a Tolman's cone angle of *ca.*132° [55] implying that, once one of its nitrogens is bound to the metal centre, the other nitrogen becomes sterically crowded thus preventing the coordination of the second Cp*(CO)$_2$Fe moiety.

Complex **6a** is an air stable orange solid which decomposes without melting at temperatures above 174 °C. It is insoluble in chlorinated solvents and hexane but soluble in water, acetone and acetonitrile. The infrared spectrum of complex **6a** exhibited two bands at 2053 and 2000 cm^{-1} assigned to the v(CO) of the two equivalent [Cp(CO)$_2$Fe]$^+$ fragments. Moreover, the ^{1}H NMR spectrum of compound **6a** in CD$_3$CN exhibited a singlet at 3.00 ppm assignable to the 12 protons of six equivalent N–CH$_2$–N groups and presenting a slight downfield shift relative to the N–CH$_2$–N of free uncoordinated DABCO by 0.33 ppm. A singlet attributed to 10 protons of the two identical η^5-cyclopentadienyl groups appeared at 5.33 ppm. Its ^{13}C NMR spectrum shows three singlets at 58.2, 86.7 and 209.8 ppm assignable to the six identical carbons of the methylene groups, 10 identical carbons of the two η^5-cyclopentadienyl ligands and 4 identical carbons of the carbonyl groups, respectively, confirming the molecular symmetry of the DABCO bridging the two [Cp(CO)$_2$Fe]$^+$ fragments. The peak corresponding to methylene carbons of the ligated DABCO also appears downfield relative to the non complexed DABCO ligand (46.7 ppm). This downfield shift can be attributed to the deshielding effect upon the coordination of the DABCO to the electrophilic metal centre. These NMR data are in agreement with those reported by Matos and Verkade in their NMR elucidation of the complex [{(CO)$_4$Fe}$_2$(μ-DABCO)] [27].

The monuclear complexes **6b** and **6c** are moderately air stable and are soluble in water, dichloromethane, acetone and acetonitrile. Each show two strong v(CO) stretching bands, with those of **6c** appearing at lower wavenumbers due to the high electron density at the metal centre. The ^{1}H NMR spectra of **6b** and **6c** exhibit two broad peaks assigned to the two sets of non methylene protons. The ^{1}H NMR spectrum of **6b** obtained in D$_2$O shows a peak corresponding to the six protons of the methylene closer to the coordinated nitrogen at 3.21 ppm, while the peak due to the six protons of the methylenes in the neighbourhood of the uncoordinated nitrogen appeared at 2.84 ppm.

Its ^{13}C NMR spectrum shows two peaks at 58.3 and 46.0 ppm corresponding to carbons bonded to the coordinated nitrogen and those bonded to uncoordinated nitrogen, respectively. The assignment of these peaks was done with the aid of heteronuclear NMR experiments and with comparison of NMR data of the free DABCO ligand.

Similarly, the ^{1}H NMR spectrum of **6c** obtained in CD$_3$CN shows peaks corresponding to the two sets of methylene protons at 3.33 and 3.18 ppm. The ^{13}C NMR spectrum shows two peaks at 56.4 and 44.2 ppm corresponding to carbons bonded to the coordinated nitrogen and those bonded to the uncoordinated nitrogen, respectively.

2.4. Reaction of 1-methylimidazole (1-meIm) with *1* and *2*

Treatment of the etherate complexes **1** and **2** with a slight excess of 1-methylimidazole (1-meIm) in dichloromethane at room temperature furnished the novel iron 1-methylimidazole complexes [(η^5-C$_5$R$_5$)(CO)$_2$Fe(1-meIm)]BF$_4$ (R = H, **7;** and R = CH$_3$, **8**) in high yields. These complexes and the dimeric iron complexes [(η^5-C$_5$R$_5$)(CO)$_2$Fe]$_2$ were the only products detected in the reaction mixture. The 1-methylimidazole complexes **7** and **8** were obtained as yellow microcrystalline solids by precipitation from their solutions using diethyl ether. Compound **8** exhibited higher stability relative to **7** towards light, air and heat. For instance, the melting point of **8** is significantly higher than that of **7** by *ca.* 100 ˚C and it was stable in air and exposure to light for several hours in the solid state with minimal decomposition. In contrast, compound **7** decomposed within 2 h when it was subjected to similar conditions. However, these complexes can be preserved for long periods of time when sealed under nitrogen and kept in the dark at temperatures below 0 ˚C. The stability of Cp* complexes is generally enhanced by the more electron-releasing Cp* ligand. The infrared spectra of compounds **7** and **8** show two strong CO stretching bands as expected. The *v*(CO) of **8** were as expected lower by *ca.* 13 cm^{-1} as compared to those of **7**.

Two medium absorption bands corresponding to C=C and C=N stretching were observed at *ca.* 1531 and 1515 cm^{-1}, respectively, indicating that the π-electrons of the ring were not involved in coordination. The ^{1}H NMR spectra of compounds **7** and **8** show three peaks corresponding to the protons attached to the three different sp^2 hybridized carbons C2, C4 and C5 (Fig. 4) in the range between 6.89 – 7.90 ppm, which

is the typical region for uncoordinated olefins. This supports the IR data and is supported by the single crystal X-ray diffraction data presented in Table 3. Peaks corresponding to the protons attached to C5 and C2 appear at *ca.* 7.23 and 7.88 ppm, respectively, which is a downfield shift of *ca.* 0.16 and 0.31 ppm relative to the uncoordinated 1-methylimidazole ligand. The coordination of the 1-methylimidazole is *via* the sp²-N and this has the effect of deshielding the neighbouring carbons C5 and C2. The effect appears to diminish across the ring, implying that the delocalized π-electrons are not evenly distributed within the ring of the coordinated 1-methylimidazole and hence the geometry of the imidazole ring is slightly affected. This is clearly reflected in the single crystal X-ray diffraction data presented in Table 3. ^{13}C NMR spectra of compound **7** and **8** show a slight downfield shift of all peaks relative to the free 1-methyimidazole ligand with a larger downfield shift observed for **7** than for **8**.

$N_1 = sp^2$ nitrogen
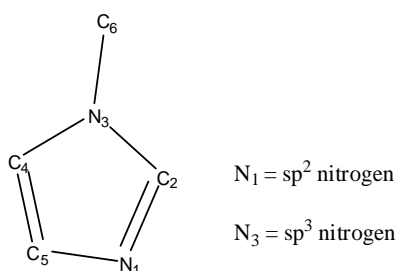
$N_3 = sp^3$ nitrogen

Fig. 4: Diagram of 1-methylimidazole showing the sp² and sp³ nitrogens

2.4.1. Structural analysis of [(η⁵-C₅R₅)(CO)₂Fe(1-meIm)]BF₄ (R = H, CH₃) (7, 8)

For a more detailed understanding of the bonding of the 1-methylimidazole (1-meIm) ligand, the molecular structures of [Cp(CO)$_2$Fe(1-meIm)]BF$_4$ (**7**) and [Cp*(CO)$_2$Fe(1-meIm)]BF$_4$ (**8**) were studied by single crystal X-ray crystallography. Selected bond distances and angles are given in Tables 3 and 4, respectively. Crystals of compound **7** were obtained as yellow plates that crystallized in the monoclinic *P2₁/c* space group, with three independent molecular cations and anions each in the asymmetric unit, while compound **8** crystallized in the orthorhombic *Pna21* space group as yellow prisms, with one cation and a counterion in the asymmetric unit. Crystal data and structure

refinement information for compounds **3a**, **7** and **8**, are summarized in Table 2. The 1-methylimidazole ligand is σ-bonded to iron *via* the sp^2-N through the lone pair of electrons in the hybrid orbital. This mode of bonding is thermodynamically favoured in order to retain the aromaticity within the imidazole ring [56]. The coordination about the iron is the familiar 3-legged piano-stool geometry adopted by the $[(\eta^5\text{-}C_5R_5)(CO)_2Fe(1\text{-}meIm]^+$ (Figs. 5a and 5b) with mean bond angles around Fe involving the basal carbonyl and imidazole ligands of about 90˚.

Table 3: Selected bond lengths [Å] for compounds **7** and **8**

7(a)		7 (b)		7 (c)		8	
Bond	Length (Å)	Bond	Length (Å)	Bond	Length (Å)	Bond	Length (Å)
C(6)-O(1)	1.136(4)	C(17)-O(3)	1.129(5)	C(28)-O(5)	1.136(5)	C(11)-O(1)	1.142(3)
C(6)-Fe(1)	1.787(4)	C(17)-Fe(2)	1.787(4)	C(28)-Fe(3)	1.788(4)	C(11)-Fe(1)	1.778(3)
C(7)-O(2)	1.136(5)	C(18)-O(4)	1.139(5)	C(29)-O(6)	1.133(4)	C(12)-O(2)	1.133(3)
C(7)-Fe(1)	1.789(4)	C(18)-Fe(2)	1.788(4)	C(29)-Fe(3)	1.789(4)	C(12)-Fe(1)	1.787(3)
C(8)-C(9)	1.357(5)	C(19)-C(20)	1.352(6)	C(30)-C(31)	1.354(5)	C(13)-N(1)	1.330(3)
C(8)-N(1)	1.385(5)	C(19)-N(3)	1.376(5)	C(30)-N(5)	1.380(4)	C(13)-N(2)	1.347(3)
C(9)-N(2)	1.372(5)	C(20)-N(4)	1.365(5)	C(31)-N(6)	1.367(5)	C(14)-C(15)	1.362(3)
C(10)-N(1)	1.326(4)	C(21)-N(3)	1.318(4)	C(32)-N(5)	1.328(4)	C(14)-N(1)	1.385(3)
C(10)-N(2)	1.339(4)	C(21)-N(4)	1.336(4)	C(32)-N(6)	1.341(4)	C(15)-N(2)	1.362(3)
N(1)-Fe(1)	1.973(3)	N(3)-Fe(2)	1.977(3)	N(5)-Fe(3)	1.980(3)	N(1)-Fe(1)	1.9781(18)

Table 4: Selected bond angles [˚] for compounds **7** and **8**

7(a)		7 (b)		7 (c)		8	
Bonds	Angle (˚)	Bonds	Angle (˚)	Bonds	Angle (˚)	Bonds	Angle (˚)
N(1)C(10)N(2)	111.0(3)	N(3)C(21)N(4)	110.7(3)	N(5)C(32)N(6)	110.2(3)	N(1)C(13)N(2)	110.6(2)
C(9)C(8)N(1)	108.8(3)	C(20)C(19)N(3)	108.6(4)	C(31)C(30)N(5)	108.3(3)	C(15)C(14)N(1)	108.9(2)
C(8)C(9)N(2)	106.6(3)	C(19)C(20)N(4)	106.7(3)	C(30)C(31)N(6)	107.0(3)	C(14)C(15)N(2)	106.71(19)
C(10)N(1)C(8)	106.0(3)	C(21)N(3)C(19)	106.3(3)	C(32)N(5)C(30)	106.7(3)	C(13)N(1)C(14)	105.91(19)
C(10)N(2)C(9)	107.6(3)	C(21)N(4)C(20)	107.6(3)	C(32)N(6)C(31)	107.7(3)	C(13)N(2)C(15)	107.88(19)
C(6)Fe(1)C(7)	93.00(17)	C(17)Fe(2)C(18)	92.31(18)	C(28)Fe(3)C(29)	95.72(18)	C(11)Fe(1)C(12)	93.55(13)
C(6)Fe(1)N(1)	93.27(14)	C(17)Fe(2)N(3)	93.09(14)	C(28)Fe(3)N(5)	91.11(14)	C(11)Fe(1)N(1)	94.72(10)
C(7)Fe(1)N(1)	93.73(14)	C(18)Fe(2)N(3)	95.92(15)	C(29)Fe(3)N(5)	92.79(14)	C(12)Fe(1)N(1)	93.04(10)

The Fe–N bond lengths are between 1.973(3) and 1.9781(18) Å as expected for iron-cyclic amine complexes [57-59]. These values are close to Fe–N = 1.970(7) Å in the iron benzimidazole complex $[Cp(CO)_2Fe(C_7H_6N_2)]BPh_4$ [32], Fe–N = 1.983(28), 1.973(31) Å observed in the two independent molecules of $[Cp(CO)_2Fe(C_5H_5N)]SbF_6$ [59] and falls within the range (1.958(5) – 1.999(2) Å) reported for iron imidazole

complexes [33, 60, 61]. The Fe-N bond (1.977 Å) in **7** is marginally shorter than the average Fe–N bond (1.978 Å) in **8** (Table 3). This was expected because the Cp* ligand is known to increase electron density on the metal centre which in this case leads to a weaker Fe–N bond in **8** relative to that observed in the Cp analogue**.** 1-methylimidazole is planar and lies on the same plane with Fe, with angles about the sp^2-N adding up to *ca.* 360 ˚C. The 1-methylimidazole geometry is similar to that of the coordinated 1-methylimidazole in [Fe(TPP)(1-meIm)N_3] [61] and bis(1-methylimidazole) complexes of manganese [62].

Figures 6a and 6b show the packing of **7** and **8**, respectively, in the crystal lattice. The packing of **7** is characterized by an inversion centre resulting in a head to head and tail to tail orientation of the molecules in alternating layers. On the other hand in **8** discrete cationic moieties are separated by alternating BF_4^- anions arranged in layers forming a zigzag pattern that are related by glide planes perpendicular to the (0, 1, 0) and (1, 0, 0) axes and a 2-fold screw axis along the *z*-axis.
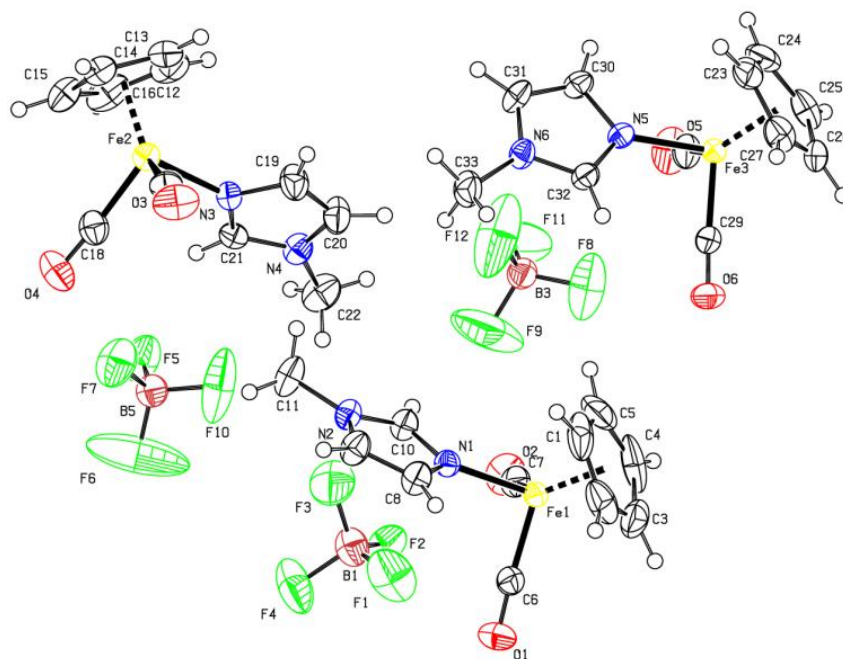
Fig.5a
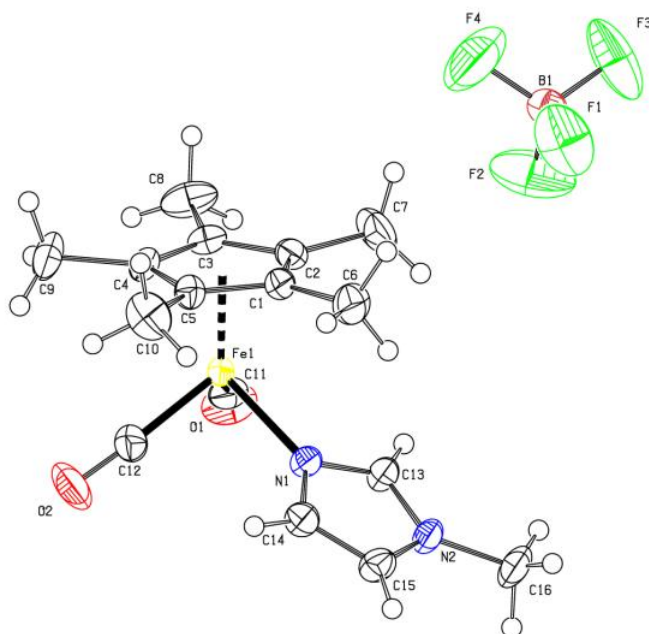
Fig.5b

Fig 5: The molecular structures of **7** (Fig. 5a) and **8** (Fig. 5b) showing atomic numbering scheme. Displacement ellipsoids are drawn at the 50% probability level with H atoms presented as small spheres
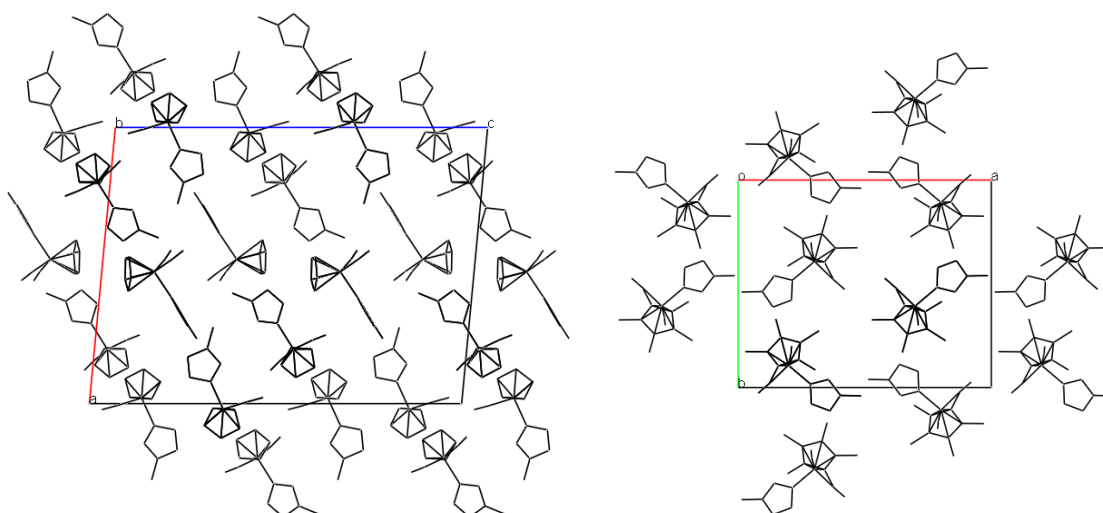
Fig. 6a: Crystal packing of **7** viewed down the *b*-axis.   **Fig. 6b**: Crystal packing of **8** viewed down the *c*-axis

3. Conclusion

The ether complexes, $[(\eta^5\text{-}C_5R_5)(CO)_2Fe(E)]BF_4$ (R = H; E = Et_2O and R = CH_3, E = THF) have been shown to undergo nucleophilic substitution with *N*-heterocyclic ligands such as hexamethylenetetramine (HMTA), 1,4-diazabicyclo[2.2.2]octane (DABCO) and 1-methylimidazole (1-meIm) to form dinuclear and mononuclear complexes of the types $[\{(\eta^5\text{-}C_5R_5)(CO)_2Fe\}_2L](BF_4)_2$ (R = H; L = HMTA, DABCO; R = CH_3; L = HMTA) and $[(\eta^5\text{-}C_5R_5)(CO)_2FeL]BF_4$ (L = HMTA, DABCO, 1-meIm), respectively. The more electrophilic Cp containing metal fragment $[Cp(CO)_2Fe]^+$ displaced the Cp* analogue $[Cp*(CO)_2Fe]^+$ from its complex with HMTA when the reaction was carried out at room temperature, but not when the reaction was conducted at 0 ^{o}C. The reaction of the ethereal complexes with 1-methylimidazole gave complexes of the type $[(\eta^5\text{-}C_5R_5)(CO)_2Fe(1\text{-}meIm)]BF_4$ (R = H, CH_3). The NMR, IR and single crystal X-ray diffraction data of the compounds $[Cp*(CO)_2Fe(1\text{-}meIm)]BF_4$ and $[Cp(CO)_2Fe(1\text{-}meIm)]BF_4$ show that the iron centre has preferential binding affinity towards the sp^2-N of the 1-methylimidazole ring resulting in a positive inductive effect that makes the Fe–N bond in 1-methylimidazole complexes significantly shorter than the Fe–N bond in the dinuclear HMTA complex.

4. Experimental

4.1. General

All manipulations were carried out under nitrogen atmosphere using Schlenk line techniques. Nitrogen (Afrox) was dried over phosphorus(V) oxide. Reagent grade THF, hexane and Et_2O were distilled from sodium/benzophenone and stored over sodium wire; CH_2Cl_2 was distilled from phosphorus(V) oxide and used immediately. Acetone and MeCN were distilled from anhydrous $CaCl_2$ and stored over type 4A molecular sieves. The other chemical reagents were obtained from the suppliers shown in parentheses: dicyclopentadiene, 1,2,3,4,5-pentamethylcyclopentadiene, iron pentacarbonyl, tetrafluoroboric acid diethyl ether, iodomethane, mercury (Aldrich), silver tetrafluoroborate and DABCO (Merck), HMTA (BDH), sodium (Fluka) and iodine (Unilab) were used as supplied. Melting points were recorded on an Ernst Leitz Wetzlar hot-stage microscope and are uncorrected. Elemental analyses were performed on a LECO CHNS-932 elemental analyzer. Infrared spectra were recorded using an ATR PerkinElmer Spectrum 100 spectrophotometer between 4000 - 400 cm^{-1}, in the solid state. NMR spectra were recorded on Bruker topspin 400 MHz and 600 MHz spectrometers and the chemical shifts are reported in ppm. The deuterated solvents, D_2O (Aldrich, 99.9%), $CDCl_3$ (Aldrich, 99.8%), acetone-d_6 (Aldrich, 99.5%), and acetonitrile-d_3 (Aldrich, 99.8%), were used as purchased. The precursors $[CpFe(CO)_2(OEt_2)]BF_4$ [41] and $[Cp*(CO)_2Fe(THF)]BF_4$ [63] were prepared as previously reported.

4.2. Reactions of $[Cp(CO)_2Fe(OEt_2)]BF_4$ with a slight excess of HMTA

A Schlenk tube equipped with a magnetic stirrer was charged with a solution of compound **1** (0.580 g, 1.72 mmol) in CH_2Cl_2 (10 ml) in the dark and a solution of HMTA (0.300 g, 2.14 mmol) in CH_2Cl_2 (20 ml) added. The mixture was stirred at room temperature for 16 h after which a yellow precipitate formed. The mixture was then filtered through a cannula and the residue washed with portions of CH_2Cl_2 (3 x 10 ml) and the residue dried under reduced pressure to give a yellow solid of **3b**. Yield: 0.65 g, 94%. Anal. Calc. for $C_{13}H_{17}BF_4FeN_4O_2$: C, 38.61; H, 4.21; N, 13.86. Found: C, 38.60;

H, 4.15; N, 13.76%. ^{1}H NMR (600 MHz, CD$_3$CN): δ 5.39 (s, 5H, C$_5$H$_5$), 4.83 (br. s, 3H, axial), 4.46 (br s, 3H, equitorial), 4.60 (br, s 6H, CH$_2$). ^{13}C NMR (600 MHz, CD$_3$CN): δ 86.37 (C$_5$H$_5$), 83.49 (C2, C8, C9), 71.06 (C4, C6, C10), 209.79 (CO). IR (solid state): ν(CO) 2054, 2003 cm^{-1}. Decomposes without melting at temperature >183 ºC.

4.3. Reactions of HMTA with four equivalents of [Cp(CO)$_2$Fe(OEt$_2$)]BF$_4$

A solution of HMTA (0.219 g, 1.56 mmol) in CH$_2$Cl$_2$ (20 ml) was added to a solution of the ether complex **1** (2.200 g, 6.51 mmol) in CH$_2$Cl$_2$ (20 ml) in a Schlenk tube and the mixture was stirred for 10 h under nitrogen at room temperature after which an orange precipitate formed. The red mother liquor was syringed off and the precipitate washed with portions of CH$_2$Cl$_2$ (5 x 10 ml), and dried under reduced pressure resulting in an orange powdery solid of **3a**. Yield: 1.012 g, 97%. Anal. Calc. for C$_{20}$H$_{22}$B$_2$F$_8$Fe$_2$N$_4$O$_4$: C, 35.93; H, 3.29; N, 8.38. Found: C, 36.03; H, 3.27; N, 8.22%. ^{1}H NMR (400 MHz, CD$_3$CN): δ 5.42 (s, 10H, C$_5$H$_5$), 4.16 (s, 2H, CH$_2$), 4.38 – 4.47 (m, 8H, CH$_2$), 4.50(s, 2H, CH$_2$). ^{13}C NMR (400 MHz, CD$_3$CN): δ 86.37 (C$_5$H$_5$), 86.77 (C2), 80.17 (C4, C8, C9, C10), 68.47 (C6), 208.63 (CO). IR (solid state): ν(CO) 2058, 2009 cm^{-1}. Decomposes without melting at temperature > 196 ºC.

4.4. Reaction of [Cp(CO)$_2$Fe(HMTA)]BF$_4$ with NaBPh$_4$

Into a solution of [Cp(CO)$_2$Fe(HMTA)]BF$_4$ (0.120 g, 0.30 mmol) in acetone (10 ml), a solution of NaBPh$_4$ (0.180 g, 0.53 mmol) in acetone (15 ml) was added and the mixture stirred for 4 h. the solvent was removed under reduced pressure and the residue extracted with CH$_2$Cl$_2$ (15 ml). Diethyl ether was added to the extract until the yellow precipitate had formed. The mixture was allowed to stand for 20 min after which the mother liquor was syringed off. The residue was washed with diethyl ether (2 x 5 ml) and then dried under reduced pressure to give 0.17 g (90 % yield) of a yellow solid (**5a**). Anal. Calc. for C$_{37}$H$_{37}$BFeN$_4$O$_2$: C, 69.81; H, 5.82; N, 8.81. Found: C, 70.24; H, 5.26; N, 8.95%. ^{1}H NMR (400 MHz, acetone-d$_6$): δ 5.69 (s, 5H, C$_5$H$_5$), 4.87 (s, 6H, (CH$_2$)$_3$), 4.74 (d, J_{HH} = 12.29, 3H, axial CH), 4.56(d, J_{HH} = 12.13, 3H, equatorial CH). ^{13}C NMR (400 MHz, acetone-d$_6$): δ 87.89 (C$_5$H$_5$), 86.89 (C2, C8, C9), 72.47 (C4, C6, C10). IR (solid state): ν(CO) 2052, 2004 cm^{-1}. M.p., 138 - 139 ˚C.

4.5. Reaction of DABCO with one equivalent of [Cp(CO)$_2$Fe(OEt$_2$)]BF$_4$

A solution of complex **1** (0.940 g, 2.78 mmol) in CH$_2$Cl$_2$ (15 ml) and DABCO (0.300g, 2.68 mmol) in CH$_2$Cl$_2$ (10 ml) was stirred at room temperature overnight after which a yellow precipitate formed. This was filtered *via* a cannula and the residue washed with CH$_2$Cl$_2$ (5 x 10 ml) to give 0.77 g (45% yield) of a yellow solid (**6a**). Anal. Calc. for C$_{20}$H$_{22}$B$_2$F$_8$Fe$_2$N$_2$O$_4$: C, 37.50; H, 3.44; N, 4.38. Found: C, 37.29; H, 3.60; N, 4.67%. ^{1}H NMR (400 MHz, CD$_3$CN): δ 5.33 (s, 5H, C5H5), 3.00 (s, 12H, CH$_2$), ^{13}C NMR (400 MHz, CD$_3$CN): δ 86.70 (C5H5), 58.21 (CH$_2$), 209.79 (CO). IR (solid state): ν(CO) 2053, 2000 cm^{-1}. Decomposes without melting at temperature > 174 ˚C.

The filtrate was treated as follows: diethyl ether was added and the mixture allowed to stand for 2 h when a yellow precipitate formed. The mother liquor was syringed off and the precipitate washed with 3 x 10 ml of diethyl ether to give 0.54 g (52 % yield) of a yellow solid (**6b**). Anal. Calc. for C$_{13}$H$_{17}$BF$_4$FeN$_2$O$_2$: C, 41.49; H, 4.52; N, 7.45. Found: C, 41.98; H, 4.77; N, 7.37%. ^{1}H NMR (600 MHz, D$_2$O): δ 5.39 (s, 5H, C$_5$H$_5$), 3.14 (CH$_2$), 2.84 (CH$_2$). ^{13}C NMR (600 MHz, D$_2$O); δ 86.75 (C$_5$H$_5$), 58.31 (CH$_2$) 46.00 (CH$_2$) 210.60 (CO) IR (solid state): ν(CO) 2050, 1996 cm^{-1}.

4.6. Reaction of DABCO with three equivalent of [Cp(CO)$_2$Fe(OEt$_2$)]BF$_4$

A Schlenk tube was charged with a solution of complex **1** (1.921g, 5.68 mmol) in CH$_2$Cl$_2$ (15 ml) and a solution of DABCO (0.212 g, 1.89 mmol) in CH$_2$Cl$_2$ (10 ml) added. The mixture was stirred for 6 h at room temperature after which an orange precipitate formed. The mother liquor was removed by filtration using a cannula and the residue washed with CH$_2$Cl$_2$ (3 x 5 ml) and dried under reduced pressure, resulting in an orange solid. The residue was purified further by washing with acetone (2 x 10 ml) and dried under reduced pressure to give a yellow solid of **6a**. Yield: 0.860 g, 71%. Anal. Calc. for C$_{20}$H$_{22}$B$_2$F$_8$Fe$_2$N$_2$O$_4$: C, 37.50; H, 3.44; N, 4.38. Found: C, 37.20; H, 3.23; N, 4.12%. ^{1}H NMR (400 MHz, CD$_3$CN): δ 5.33 (s, 5H, C$_5$H$_5$), 3.00 (s, 12H, CH$_2$), ^{13}C NMR (400 MHz, CD$_3$CN): δ 86.70 (C$_5$H$_5$), 58.21 (CH$_2$), 209.79 (CO). IR (solid state): ν(CO) 2053, 2000 cm^{-1}. Decomposes without melting at temperature > 174 ˚C.

4.7. Reactions of [Cp*(CO)₂Fe(THF)]BF₄ with a slight excess of HMTA

A Schlenk tube was charged with a solution of compound **2** (0.633 g, 1.55 mmol) in CH_2Cl_2 (15 ml) and a solution of HMTA (0.250 g, 1.79 mmol) in CH_2Cl_2 (20 ml) was added. The mixture was stirred at room temperature under nitrogen for 18 h. The mixture was then filtered through a cannula into a pre-weighed Schlenk tube and diethyl ether was then added until a yellow precipitate formed. This was allowed to stand for 10 min after which the mother liquor was removed by filtration and the yellow residue washed with portions of CH_2Cl_2 (4 x 10 ml) and dried under reduced pressure. Yield: 0.45 g, 61%. Anal. Calc. for $C_{18}H_{27}BF_4FeN_4O_2$: C, 45.57; H, 5.70; N, 11.81. Found: C, 46.01; H, 5.86; N, 11.74%. ^{1}H NMR (400 MHz, CD_3CN): δ 1.83 (s, 15H, $C_5(CH_3)_5$), 4.84 (br. s, 6H,$(CH_2)_3$), 4.49 (br, s, 6H, $(CH_2)_3$). ^{13}C NMR (400 MHz, CD_3CN): δ 8.39 ($C_5(\underline{C}H_3)_5$), 71.25 (C4, C6, C10), 81.84 (C2, C8, C9), 98.98 ($\underline{C}_5(CH_3)_5$). 210.51 (CO). IR (solid state): ν(CO) 2031, 1982 cm^{-1}. M.p., 159 – 161 ˚C.

4.8. Reactions of HMTA with four equivalents of [Cp*(CO)₂Fe(THF)]BF₄

A solution of HMTA (0.142 g, 1.01mmol) in CH_2CH_2 (10 ml) was added dropwise into a stirred solution of compound **2** (1.650 g, 4.06 mmol) in CH_2Cl_2 (10 ml) within 60 seconds. The mixture was stirred under nitrogen at room temperature overnight and then filtered into a pre-weighed Schlenk tube. Diethyl ether was added until an orange precipitate formed and the mixture was allowed to stand for 30 min, after which the mother liquor was syringed off. The residue was washed with portions of diethyl ether (3 x 10 ml) and dried under reduced pressure to give the orange solid of **4a**. Yield: 0.275 g, 34%. Anal. Calc. for $C_{30}H_{42}B_2F_8Fe_2N_4O_4$: C, 44.55; H, 5.20; N, 6.93. Found: C, 44.34; H, 5.35; N, 6.88%. ^{1}H NMR (400 MHz, CD_3CN): δ 1.86 (s, 30H, $C_5(CH_3)_5$), 4.32 – 4.50 (m, 12H, $(CH_2)_6$), ^{13}C NMR (400 MHz, CD_3CN): δ 8.93 ($C_5(\underline{C}H_3)_5$), 86.43 (C2), 81.90 (C4,C8, C9,C10), 78.42(C6), 98.45 ($\underline{C}_5(CH_3)_5$), 211.76 (CO). IR (solid state): ν(CO) 2035, 1991 cm^{-1}.

4.9. Reaction of [Cp*(CO)₂Fe(HMTA)]BF₄ with NaBPh₄

The solution of **4b** (0.090 g, 0.19 mmol) in acetone was treated with a solution of NaBPh₄ (0.100 g, 0.29 mmol) in acetone (15 ml) and the rest of the procedure was

executed as described in Section 4.4 to give 0.11 g (82%) of compound **5b**. Anal. Calc. for $C_{42}H_{47}BFeN_4O_2$: C, 71.39; H, 6.66; N, 7.93. Found: C, 70.72; H, 6.70; N, 8.17%. ^{1}H NMR (400 MHz, acetone-d_6): δ 2.01 (s, 15H, $C_5(CH_3)_5$), 4.68 (s, 6H, CH_2), 4.60 (s, 3H, axial, CH), 4.57 (s, 3H, equatorial CH), 6.77 (br, 4H, *p*-CH), 6.92 (br, 8H, *o*-CH), 7.33 (br, 8H, *m*-CH). ^{13}C NMR (400 MHz, acetone-d_6): δ 10.02 ($C_5(CH_3)_5$), 72.67 (C4, C6, C10), 83.29 (C2, C8, C9), 99.50 ($\underline{C}_5(CH_3)_5$), 122.22 (*para*-C, Ph), 125.97 (*meta*-C, Ph), 130.90 (B-C)137.05 (*ortho*-C, Ph). IR (solid state): ν(CO) 2029, 1986 cm^{-1}. M.p., 149 – 150 ˚C.

4.10. Reaction of DABCO with [Cp*(CO)$_2$Fe(THF)]BF$_4$

A solution mixture of complex **2** (0.300 g, 0.74 mmol) in CH_2Cl_2 (15 ml) and DABCO (0.030 g, 0.27 mmol) in CH_2Cl_2 (10 ml) was stirred at room temperature overnight. Diethyl ether (30 ml) was added to the mixture and the mixture then allowed to stand undisturbed for 16 h at room temperature. A yellow microcrystalline solid collected on the walls of Schlenk tube. The mother liquor was syringed off, the crystals were washed with diethyl ether (2 x 5 ml) and dried under reduced pressure to give 0.03 g (25% yield) of yellow solid, **6c**. Anal. Calc. for $C_{18}H_{27}BF_4FeN_2O_2$: C, 48.43; H, 6.05; N, 6.28. Found: C, 48.87; H, 6.14; N, 5.77 %. ^{1}H NMR (400 MHz, CD_3CN): δ 2.01 (s, 15H, $C_5(CH_3)_5$), 3.17 (t, J_{HH} = 6.68 Hz, 6H, CH_2),3.34 (t, J_{HH} = 6.74, 6H, $(CH_2)_3$).^{13}C NMR (400 MHz, CD_3CN): δ 8.75 ($C_5(CH_3)_5$), 44.17 (CH_2), 51. 11 (CH2) 97.88 ($\underline{C}_5(CH_3)_5$) 212.41 (CO). IR (solid state): ν(CO) 2021, 1969 cm^{-1}.

4.11. Reaction of [Cp(CO)$_2$Fe(OEt$_2$)]BF$_4$ with excess 1-methylimidazole (1-meIm)

1-methylimidazole (0.40 ml, 5.04 mmol) was added to a solution of compound **1** (0.532 g, 1.57 mmol) in CH_2Cl_2 (10 ml) in a Schlenk tube and the mixture stirred under nitrogen at room temperature for 6 h. Into the resultant yellow-brown solution diethyl ether was added until a yellow precipitate was formed. The precipitate was allowed to stand for 5 min after which the mother liquor was syringed off and the yellow residue was washed with diethyl ether (3 x 5 ml). Drying of the residue under reduced pressure for 5 h gave 0.489 g (90 %) of [Cp(CO)$_2$Fe(1-meIm)]BF$_4$. Anal. Calc. for

$C_{11}H_{11}BF_4FeN_2O_2$: C, 38.15; H, 3.18; N, 8.09. Found: C, 37.90; H, 3.25; N, 8.16%. ^{1}H NMR (400 MHz, MeOD): δ 7.85 (s, 1H, CH), 7.19 (s, 1H, CH), 6.93 (s, 1H, CH), 5.38 (s, 5H, C_5H_5), 3.71 (s, 3H, CH_3), ^{13}C NMR (400 MHz, MeOD): δ 87.90 (C_5H_5), 36.08 (CH_3), 125.19 (CH), 136.08 (CH), 209.79 (CO). IR (solid state): ν(CO) 2052, 2000 cm$^-$^{1}. M.p., 48 - 50 ˚C.

4.12. Reaction of [Cp*(CO)$_2$Fe(THF)]BF$_4$ with excess 1-methylimidazole (1-meIm)

Into a solution of [Cp*(CO)$_2$Fe(THF)]BF$_4$ (0.370 g, 0.91 mmol) in CH_2Cl_2 (15 ml) 1-methylimidazole (0.30 ml, 3.78 mmol) was added and the mixture stirred in the dark for 8 h at room temperature. After this period the reaction mixture changed colour from red to yellow. It was then filtered into a pre-weighed Schlenk tube and diethyl ether (30 ml) was added into the filtrate. The mixture was allowed to stand for 10 min after which a bright yellow crystalline solid formed. The mother liquor was syringed off and the residue was washed with portions of diethyl ether (2 x10 ml), and then dried under reduced pressure. Yield: 0.364 g, 96%. Anal. Calc. for $C_{16}H_{21}BF_4FeN_2O_2$: C, 46.15; H, 5.04; N, 6.73. Found: C, 46.11; H, 5.20; N, 6.65%. ^{1}H NMR (400 MHz, CD$_3$OD): δ 1.78 (s, 15H, $C_5(CH_3)_5$), 3.76 (s, 3H, N-CH_3), 6.89 (s, 1H, =CH), 7.25 (s, 1H, =CH), 7.90 (s, 1H, =CH), ^{13}C NMR (400 MHz, CDCl$_3$): δ 9.32 ($C_5(\underline{C}H_3)_5$), 35.12 (N-CH_3), 98.36 ($\underline{C}_5(CH_3)_5$), 123.60 (=CH), 132.55 (=CH), 212.42 (CO). IR (solid state): ν(CO) 2041, 1986 cm^{-1}. M .p., 145 -148 ˚C.

4.13. Reaction of [Cp*(CO)$_2$Fe(HMTA)]BF$_4$ with [Cp(CO)$_2$Fe(OEt$_2$)]BF$_4$ in dichloromethane at room temperature

Into a stirred solution of [Cp*(CO)$_2$Fe(HMTA)]BF$_4$ (0.147 g, 0.31 mmol) in CH_2Cl_2 (10 ml), a solution of (**1**) (0.117 g, 0.35 mmol) in CH_2Cl_2 (10 ml) was added within 3 min using a cannula. The mixture was stirred overnight at room temperature after which an orange solid stuck to the walls of the Schlenk tube. The mixture was filtered into a clean and dry Schlenk tube and the residue washed with CH_2Cl_2 (4 x 5 ml) to give 0.087 g of orange solid, which by NMR and IR was found to be a mixture of [Cp(CO)$_2$Fe(HMTA)]BF$_4$ and [{Cp(CO)$_2$Fe}$_2$μ-(HMTA)](BF$_4$)$_2$. Into the filtrate, diethyl ether 30 ml was added and the mixture was allowed to stand overnight. After

this period no precipitate formed and therefore the solvent was removed under reduced pressure to give a deep red oil which was found to be a mixture of decomposed Cp* and Cp compounds as was suggested by the ^{1}H NMR spectrum which show numerous peaks in the Cp* and Cp regions.

4.14. Reaction of [Cp*(CO)$_2$Fe(HMTA)]BF$_4$ with [Cp(CO)$_2$Fe(OEt$_2$)]BF$_4$ in dichloromethane at 0 ˚C

To a pre-cooled solution of [Cp*(CO)$_2$Fe(HMTA)]BF$_4$ (0.138 g, 0.29 mmol) in CH$_2$Cl$_2$ (10 ml) at -78 ˚C, a solution of [Cp(CO)$_2$Fe(OEt$_2$)]BF$_4$ (0.102 g, 0.30 mmol) in CH$_2$Cl$_2$ (10 ml) was added and the mixture allowed to warm to 0 ˚C. It was then stirred at this temperature for 1h after which an orange solid stuck on the wall of Schlenk tube. The mixture was filtered and the residue washed with CH$_2$Cl$_2$ portions until the washings were almost colourless. The residue was then dried under reduced pressure to give 0.034 g of an air sensitive orange spongy solid. ^{1}H NMR (400MHz, CD$_3$CN): 5.46 (s, 5H, C$_5$H$_5$), 4.63-4.4.23 (m, 12H, HMTA), 1.81 (s,15H, C$_5$(CH$_3$)$_5$). ^{13}C NMR (400 MHz, CD$_3$CN): δ 86.38 (C$_5$H$_5$), 86.73 (C2), 83.43 (C4, C9), 80.17 (C8, C10), 68.48 (C6), 8.38 (C$_5$(CH$_3$)$_5$), 99.00 (C$_5$(CH$_3$)$_5$).209.78, 208.62 (CO).

4.15. Single-crystal X-ray data

Crystals of [Cp*(CO)$_2$Fe(1-meIm)]BF$_4$, [Cp(CO)$_2$Fe(1-meIm)]BF$_4$ and [{Cp*(CO)$_2$Fe}$_2$(μ-HMTA)](BF$_4$)$_2$ suitable for X-ray diffraction studies were obtained by different methods of crystal growth as described below:

Crystallization of [Cp(CO)$_2$Fe(1-meIm)]BF$_4$.* A filtered and nitrogen-saturated solution of [Cp*(CO)$_2$Fe(1-meIm)]BF$_4$ in dry CH$_2$Cl$_2$ was layered with dry and degassed diethyl ether. The mixture was kept undisturbed in the dark at room temperature. Yellow crystals were obtained over 3 days of liquid diffusion under strict anaerobic conditions.

Crystallization of [Cp(CO)$_2$Fe(1-meIm)]BF$_4$. Vapours of dry diethyl ether were allowed to diffuse into a filtered solution of [Cp(CO)$_2$Fe(1-meIm)]BF$_4$ in dry CH$_2$Cl$_2$ and the mixture allowed to stand undisturbed and under strict anaerobic conditions for a period of one month in the dark at 5 ˚C. This gave yellow crystals suitable for X-ray diffraction.

Crystallization of [{Cp*(CO)₂Fe}₂(μ-HMTA)](BF₄)₂. Crystals of [{Cp*(CO)₂Fe}₂{μ-HMTA)](BF₄)₂ suitable for the X-ray diffraction study were grown by slow evaporation of acetonitrile solution at 279 K over a period of 4 weeks.

Intensity data were collected on a Bruker *APEX II CCD* area detector diffractometer with graphite monochromated Mo Ka radiation (50 kV, 30 mA) using the *APEX II* [64] data collection software. The collection method involved x-scans of width 0.5° and 512 x 512 bit data frames. Data reduction was carried out using the program *SAINT+* [65] and face indexed absorption corrections were made using *XPREP* [65]. The crystal structure was solved by direct methods using *SHELXTL* [66]. Non-hydrogen atoms were first refined isotropically followed by anisotropic refinement by full matrix least-squares calculations based on F^2 using *SHELXTL*. Hydrogen atoms were first located in the difference map then positioned geometrically and allowed to ride on their respective parent atoms. Diagrams and publication material were generated using *SHELXTL*, platon [67] and *ORTEP-3* [68]. Table 2 summarizes crystal data and structure refinement information while selected bond length and angles are given in Tables 1, 3 and 4.

Acknowledgments

Supplementary material

CCDC 844986, 844987 and 844988 contains the supplementary crystallographic data for compounds **3a**, **7** and **8**. These data can be obtained free of charge *via* http://www.ccdc.cam.ac.uk/conts/retrieving.html, or from the Cambridge Crystallographic Data Centre, 12 Union Road, Cambridge CB2 1EZ, UK; fax: (+44) 1223-336-033; ore-mail: deposit@ccdc.cam.ac.uk. Crystallographic data for compounds

3a, **7** and **8** are given in Appendix 8. CD-ROM containing all CIF file and spectroscopic data is provided in Appendix 12.

References

[1]   R.P. Nair, T.H. Kim, B.J. Frost, Organometallics 28 (2009) 4681.

[2]   A. Rossin, L. Gonsalvi, A.D. Phillips, O. Maresca, A. Lledós, M. Peruzzini, Organometallics 26 (2007) 3289.

[3]   E.M. Peña-Méndez, B. González, P. Lorenzo, A. Romerosa, J. Havel, Rapid Commun. Mass Spectrom. 23 (2009) 3831.

[4]   C.A. Mebi, B.J. Frost, Organometallics 24 (2005) 2339.

[5]   W.H. Ang, A. Casini, G. Sava, P.J. Dyson, J. Organomet. Chem. 696 (2011) 989.

[6]   M. Xue, G. Zhu, H. Ding, L. Wu, X. Zhao, Z. Jin, S. Qiu, Cryst. Growth Des. 9 (2009) 1481.

[7]   A.D. Phillips, L. Gonsalvi, A. Romerosa, F. Vizza, M. Peruzzini, Coord. Chem. Rev. 248 (2004) 955.

[8]   G. Kovács, L. Nádasdi, G. Laurenczy, F. Joó, Green Chem. 5 (2003) 213.

[9]   A. Mentes, M.E. Hanhan, Trans. Met. Chem. 33 (2008) 91.

[10]   D.J. Darensbourg, F. Joó, M. Kannisto, A. Kathó, J.H. Reibenspies, D.J. Daigle, Inorg. Chem. 33 (1994) 200.

[11]   C. Lidrissi, A. Romerosa, Mustapha Saoud, M. Serrano-Ruiz, a. Luca Gonsalvi, M. Peruzzini, Angew. Chem. Int. Ed. 44 (2005) 2568.

[12]   M.S. Ruiz, A. Romerosa, B. Sierra-Martin, A. Fernandez-Barbero, Angew. Chem. Int. Ed. 47 (2008) 8665.

[13]   H.V. Huynh, Y.X. Chew, Inorg. Chim. Acta 363 (2010) 1979.

[14]   J.G.J. Strom, H.W. Jun, J. Pharm. Sci. 75 (1986) 416.

[15]   S.D. Greenwood, Infection 9 (1981) 223.

[16]   A. Duthod, C.R. Seances Soc. Bio. Fil. 111 (1932) 721.

[17]   J. Bango, J. Joseph, L. Browman, PCT (2010) WO 2010/120489A120482.

[18]   V.G. Wong, L.L. Wood, P. Nixon, U S. Patent (2008) Pub No. 20080038316A2.

[19]   J.A. Giordano, U S. Patent (2009) Pub. No. 2009/0111780 A1.

[20] S. Masunaga, K. Tano, J. Nakamura, M. Watanabe, G. Kashino, A. Takahashi, H. Tanaka, M. Suzuki, K. Ohnishi, Y. Kinashi, Y. Liu, T. Ohnishi, K. Ono, J. Radiat. Res. 51 (2010) 27.

[21] B.B. García, D. Liu, S. Sepehri, S. Candelaria, D.M. Beckham, L.W. Savage, G. Cao, J. Non-Cryst. Solids 356 (2010) 1620 and refs. therein.

[22] B. Baghernejad, Eur. J. Chem. 1 (2010) 54.

[23] Y. Hon, C. Kao, Tetrahedron Lett. 50 (2009) 748 and refs. therein. .

[24] F. Zhang, X. Wang, C. Cai, J. Liu, Tetrahedron 65 (2009) 83.

[25] W. Shieh, S. Dell, A. Bach, O. Repíc, T.J. Blacklock, J. Org. Chem. 68 (2003) 1954.

[26] E. Gordon, J. Cohen, R. Engel, G.W. Abbott, Mol. Pharmacol. 69 (2006) 718.

[27] R.M. Matos, J.G. Verkade, J. Braz. Chem. Soc. 14 (2003) 71.

[28] L.E. Kapinos, B. Song, H. Sigel, J. Eur. Chem. 5 (1999) 1794.

[29] M.S. Szulmanowicz, W. Zawartka, A. Gniewek, A.M. Trzeciak, Inorg. Chim. Acta 363 (2010) 4346.

[30] H. Nakamura, M. Fujii, Y. Sunatsuki, M. Kojima, N. Matsumoto, Eur. J. Inorg. Chem. (2008) 1258.

[31] R. Sívek, F. Burěs, O. Pytela, J. Kulhānek, Molecules 13 (2008) 2326.

[32] A.N. Nasmeyanov, Y.A. Belousov, V.N. Babin, G.G. Aleksandrov, Y.T. Struchkov, N.S. Kochetkova, Inorg. Chim. Acta 23 (1977) 155.

[33] H. Tchouka, A. Meetsma, W.R. Browne, Inorg. Chem. 49 (2010) 10557.

[34] S. Wen-Hua, X. Tang, T. Gao, B. Wu, W. Zhang, H. Ma, Organometallics 23 (2004) 5037.

[35] S. Wen-Hua, S. Jie, S. Zhang, W. Zhang, Y. Song, H. Ma, J. Chen, K. Wedeking, R. Fröhlich, Organometallics 25 (2006) 666.

[36] S. Wen-Hua, P. Hao, S. Zhang, Q. Shi, W. Zuo, X. Tang, X. Lu, Organometallics 26 (2007) 2720.

[37] S. Zhang, S. Wen-Hua, T. Xiao, X. Hao, Organometallics 29 (2010) 1168.

[38] E.O. Changamu, H.B. Friedrich, M. Rademeyer, J. Organomet. Chem. 693 (2008) 164.

[39] E.O. Changamu, H.B. Friedrich, M. Rademeyer, J. Organomet. Chem. 692 (2007) 2456.

[40] E.O. Changamu, H.B. Friedrich, J. Organomet. Chem. 692 (2007) 1138.

[41] C.M. M'thiruaine, H.B. Friedrich, E.O. Changamu, M.D. Bala, Inorg. Chim. Acta 366 (2011) 105.

[42] E.O. Changamu, H.B. Friedrich, M. Rademeyer, Acta Cryst. E62 (2006) m442.

[43] E.O. Changamu, H.B. Friedrich, M.O. Onani, M. Rademeyer, J. Organomet. Chem. 691 (2006) 4615.

[44] E.O. Changamu, H.B. Friedrich, J. Organomet. Chem. 693 (2008) 3351.

[45] C.M. M'thiruaine, H.B. Friedrich, E.O. Changamu, B. Omondi, Acta Cryst. E67 (2011) m485.

[46] M. Akita, S. Kakuta, S. Sugimoto, M. Terada, M. Tanaka, Y. Moro-oka, Organometallics 20 (2001) 2736.

[47] C.M. M'thiruaine, H.B. Friedrich, E.O. Changamu, M.D. Bala, Inorg. Chim. Acta (2011) in press. doi:10.1016/j.ica.2011.09.058.

[48] A. Banerjee, P. Maiti, T. Chattopadhyay, K.S. Banu, M. Ghosh, E. Sureh, E. Zangrando, D. Das, Polyhedron 29 (2010) 951.

[49] A. Romerosa, T. Campos-Malpartida, C. Lidrissi, M. Saoud, M. Serrano-Ruiz, M. Peruzzini, J.A. Gárrido-cardenas, F. Garciá-Maroto, Inorg. Chem. 45 (2006) 1289.

[50] M.Y. Darensbourg, D. Daigle, Inorg. Chem. 14 (1975) 1217.

[51] C.M. M'thiruaine, H.B. Friedrich, E.O. Changamu, M.D. Bala, Acta Cryst. E67 (2011) m924.

[52] L.N. Becka, D.W.J. Cruickshank, Proc. R. Soc(A). 273 (1963) 435.

[53] F. Hanic, V. Šubrtová, Acta Cryst. B25 (1969) 405.

[54] S. Otto, A. Roodt, Inorg. Chem. Commun. 4 (2001) 49

[55] T. Ljungdahl, K. Pettersson, B. Albinson, J. Mantensson, J. Org. Chem. 71 (2006) 1677.

[56] R.J. Sundberg, B. Martin, Chem. Rev. 74 (1974) 471.

[57] M. Powell, R.D. Bailey, C.T. Eagle, G.L. Schimek, T.W. Hanks, W.T. Pennington, Acta Cryst. C53 (1997) 1611.

[58] J.D. Oliver, D.F. Mullica, B.B. Hutchinson, W.O. Milligan, Inorg. Chem. 19 (1980) 165.

[59]   H. Schumann, M. Speis, W.P. Bosman, J.M.M. Smits, P.T. Beurskens, j. Organomet. Chem. 403 (1991) 165.

[60]   J. Li, S.M. Nair, B.C. Noll, C.E. Schulz, W.R. Scheidt, Inorg. Chem. 47 (2008) 3841.

[61]   Y. Zhang, W.A. Hallows, W.J. Ryan, J.G. Jones, G.B. Carpenter, D.A. Sweigart, Inorg. Chem. 33 (1994) 3306.

[62]   Z.N. Zahran, N. Xu, D.R. Powell, G.B. Richter-Addo, Acta Cryst. E65 (2009) m75.

[63]   M. Akita, M. Tarada, M. Tanaka, Y. Morooka, J. Organomet. Chem. 510 (1996) 255.

[64]   Bruker, *APEX2*. Version 2009.1-0. Bruker AXS Inc., Madison, Wisconsin, USA, (2005a).

[65]   Bruker, *SAINT+*. Version 7.60A. (includes *XPREP* and *SADABS*) Bruker AXS Inc., Madison, Wisconsin, USA, (2005b).

[66]   Bruker, *SHELXTL*. Version 5.1. (includes XS, XL, XP, XSHELL) Bruker AXS Inc., Madison, Wisconsin, USA, (1999).

[67]   A.L. Spek, J. Appl. Cryst. 36 (2003) 7.

[68]   L.J. Farrugia, J. Appl. Cryst. 30 (1997) 565.

CHAPTER FIVE

Syntheses, structural elucidation and reactions of allylamino complexes of the type, $[\eta^5\text{-}C_5R_5(CO)_2Fe(NH_2CH_2CH=CH_2)]BF_4$

Cyprian M. M'thiruaine[a], Holger B. Friedrich[a*], Evans O. Changamu[b]

[a] School of Chemistry, University of KwaZulu-Natal, Private Bag X54001, Durban 4000, South Africa [b] Chemistry Department, Kenyatta University, P.O Box 43844, Nairobi, Kenya

* Corresponding author

Abstract

The reaction of 3-aminoprop-1-ene (allylamine) with the etherate complexes $[(\eta^5\text{-}C_5R_5)(CO)_2Fe(E)]BF_4$ (R = H: E= Et$_2$O; R = Me: E = THF) has been investigated and found to give air stable allylamino complexes $[(\eta^5\text{-}C_5R_5)(CO)_2Fe(NH_2CH_2CH=CH_2)]BF_4$ (R = H (**3**) or CH$_3$ (**4**)) with the vinyl functionality pendant on the alkyl chain. These allylamino complexes undergo halogenation reactions on the pendant vinyl group to give high yields of the dihalopropylamino complexes $[Cp(CO)_2Fe\{NH_2CH_2CH(X)CH_2X\}]BF_4$ (Cp = η^5-C$_5$H$_5$; X = Cl (**5**), Br (**6**)) and $[Cp^*(CO)_2Fe\{NH_2CH_2CH(Br)CH_2Br\}]BF_4$ (Cp* = η^5-C$_5$(CH$_3$)$_5$) (**7**), respectively. Complexes **3** and **4** also react with the etherate complexes $[(\eta^5\text{-}C_5R_5)(CO)_2Fe(E)]BF_4$ to yield dinuclear complexes of the type, $[(\eta^5\text{-}C_5R_5)(CO)_2Fe(NH_2CH_2CH=CH_2)Fe(CO)_2(\eta^5\text{-}C_5R'_5)](BF_4)_2$ (R not necessarily equal to R'), in which the two iron moieties are in different electronic environments. The NMR and IR data of the dinuclear complexes show that the allylamine ligand bridges the two metal systems. It is coordinated to the metal on one end *via* the nitrogen of the amine functionality in a η^1-fashion and on the other end *via* the vinylic functionality in a η^2-fashion forming a chiral metallacyclopropane type structure. The reaction of the dinuclear complex $[\{Cp(CO)_2Fe\}_2(NH_2CH_2CH=CH_2)](BF_4)_2$ with NaI in acetone gives $[Cp(CO)_2Fe(NH_2CH_2CH=CH_2)]I$ and $[CpFe(CO)_2I]$ indicating that the iodide displaces the η^2-coordinated metal centre. All these compounds have been fully characterized.

The molecular structures of **3**, **4** and **7** have been determined by single crystal X-ray diffraction.

Keywords: Allylamine; Dihaloallylamino complexes; Halogenations; Chiral complexes.

1. Introduction

The metal allyl and alkenyl complexes $[(\eta^5\text{-}C_5R_5)(CO)_2Fe\{(CH_2)_nCH=CH_2\}]$ (R = H, CH_3; n > 0) have been known for a long time [1]. They are mainly synthesized by displacement of halides from haloalkenes by the anion $[(\eta^5\text{-}C_5R_5)Fe(CO)_2]^-$ [2-7]. They form an important class of organometallic compounds from which other important compounds are prepared. For instance, the alkenyl complexes $[(\eta^5\text{-}(C_5R_5)(CO)_2Fe\{(CH_2)_nCH=CH_2\}]$ (R = H, CH_3; n = 2-5,7) have been shown to undergo an oxidative-hydroboration reaction to yield alkylalcohol complexes [8], while $[Cp(CO)_2Fe\{(CH_2)_nCH=CH_2\}]$ (Cp = $\eta^5\text{-}C_5H_5$, n = 2-4,6) reacts with Ph_3CPF_6 to give $\eta^2\text{-}(\alpha,\omega\text{-diene})$ complexes [9].

The allyl complex $[Cp(CO)_2Fe(CH_2CH=CH_2)]$ has been reported to undergo condensation with the cationic ethylene complex $[Cp(CO)_2Fe(\eta^2\text{-}CH_2=CH_2)]^+$ to give a dinuclear complex $[Cp(CO)_2Fe(CH_2=CHCH_2CH_2CH_2)Fe(CO)_2Cp]^+$ [7], as has the allyl complex with the carbenoid complex $[Cp(CO)_2Fe=CH_2]^+$ to give $[Cp(CO)_2Fe(CH_2=CHCH_2CH_2)Fe(CO)_2Cp]^+$ [10]. The longer chain polymethylene complexes $[Cp(CO)_2Fe\{CH_2=CH(CH_2)_{n-1}CH_2\}Fe(CO)_2Cp]^+$ (n = 4-10) have been prepared by β hydride abstraction of the neutral dinuclear polymethylene complexes $[Cp(CO)_2Fe\{CH_2(CH_2)_nCH_2\}Fe(CO)_2Cp]$ and these studies have clearly shown that the vinyl group is bonded to the metal in a η^2-fashion [11, 12].

The reaction of the metal allyl complex $[Cp(CO)_2Fe(CH_2CH=CH_2)]$ with HCl was reported by Green and Naggy to yield the cationic complex $[Cp(CO)_2Fe(\eta^2\text{-}CH_2=CHCH_2)]Cl$ [3]. However, the reaction of HCl with longer chain alkenyl complexes $[Cp(CO)_2Fe\{(CH_2)_nCH=CH_2\}]$ (n = 2, 3) was reported to yield the chlorido complex $[Cp(CO)_2FeCl]$ as well as their corresponding chloroalkenes [2]. Busetto *et al.* found that the σ-methoxyethyl complex $[Cp(CO)_2Fe(CH_2CH_2OCH_3)]$ reacts with HCl

to give the cationic complex $[Cp(CO)_2Fe(CH_2CH_2)]^+$, rather than $[Cp(CO)_2Fe(CH_2CH_2Cl)]$ [13]. The reaction of $[Cp(CO)_2Fe\{\eta^1\text{-}CH_2N(CH_3)_2\}]$ with CH_3COCl has also been reported to occur *via* a carbon-nitrogen bond cleavage to produce $[Cp(CO)_2Fe(CH_2Cl)]$ [14]. This observation suggests that it is difficult to prepare secondary halide complexes of the type $[Cp(CO)_2Fe\{CH_2)_nCH(X)CH_3\}]$ by hydrohalogenation of metal alkenyl complexes. However, the primary halide complexes of the type $[Cp(CO)_2Fe\{(CH_2)_nCH_2X\}]$ are well known and they are conveniently prepared by the reaction of $Na[CpFe(CO)_2]$ with an equivalent of α,ω-dihaloalkanes [15-17].

Bromination of the allyl complex $[Cp(CO)_2Fe(CH_2CHCH_2)]$, followed by deprotonation provides the complex $[Cp(CO)_2Fe(\eta^2\text{-}CH_2=CHCH_2Br)]PF_6$ [18], which can alternatively be obtained from the reaction of $Na[CpFe(CO)_2]$ with α,ω-dibromopropane followed by *beta* hydride abstraction [19]. Other bromination products reported are $[Cp(CO)_2Fe(\eta^1\text{-}CH_2CH=CHBr)]$ [1], $[Cp(CO)_2Fe\{\eta^2\text{-}CH_2=C(CH_3)CH_2Br\}]BF_4$ [18] and $[Cp(CO)_2Fe(\eta^2\text{-}CH=CHCHBrCH_2CH_2)]PF_6$ [20]. It is also well established that molecular halogens cleave iron-carbon bonds leading to cyclopentadienyl(halo)iron dicarbonyl [21-25]. The dihaloalkyl complexes of the type $[Cp(CO)_2Fe\{(CH_2)_nCH(X)CH_2X\}]$ have not been reported, although the alkenyl complexes $[Cp(CO)_2Fe\{(CH_2)_nCH=CH_2\}]$ are well known [2, 6]. Halogenation is an important chemical transformation, particularly in drug design, because it is known to enhance membrane binding and permeation [26].

Reactions of amines are characterized by high regioselectivity with respect to other electron donor systems such as those with π-bonds. They are good electron donors and therefore they bind strongly to the metal. This implies that aminoalkenes can be tethered to the metal centre leaving the vinyl function free. Thus addition reactions, such as halogenations, could take place on the vinyl functionality without cleaving the metal–nitrogen bond and this would provide a route to a new class of organometallic compounds.

The chromium complexes, $[Cp(NO)Cr(NH_2CH_2CH=CH_2)_2]^+I^-$ and $[Cp(NO)Cr(NH_2CH_2CH=CH_2)I]$ reported by Lezdins *et al.* [27], and the palladium complex $[PdCl_2(NH_2CH_2CH=CH_2)_2]$ reported by Hayes *et al.* [28] are examples of

allylamino complexes that have appeared in literature. There are no reports whatsoever about allylamino complexes of iron and no reports about dihaloalkylamino metal complexes. Herein we report the new allylamino complexes of the type $[(\eta^5\text{-}C_5R_5)(CO)_2Fe(NH_2CH_2CH=CH_2)]BF_4$ (R = H, CH$_3$) and on their reactions with electrophilic reagents.

2. Results and discussion

2.1. Preparation of the complexes $[(\eta^5\text{-}C_5R_5)(CO)_2Fe(NH_2CH_2CH=CH_2)]BF_4$ (R=H, CH$_3$)

The reaction of [Cp(CO)$_2$Fe(OEt$_2$)]BF$_4$, **1**, with an equimolar amount of 3-amino-1-propene at room temperature resulted in the formation of the allylamino complex [Cp(CO)$_2$Fe(NH$_2$CH$_2$CH=CH$_2$)]BF$_4$, **3**, in 98% yield (Scheme 1). The product is partially soluble in dichloromethane, causing it to crystallize out from the solution after 6 h of reaction. It is easily isolated by filtration, contrary to the reported remarkable difficulty encountered in the isolation of neutral alkenyl complexes [4]. Complex **3** was obtained as a yellow microcrystalline solid which was insoluble in hexane and diethyl ether but very soluble in acetone, methanol, water and acetonitrile. It is relatively stable in the solid state and when in nitrogen saturated solutions. However, it undergoes slow photodecomposition when exposed to light to form a brown unidentified substance.

(**1**) R = H; E = Et$_2$O

(**2**) R = CH$_3$; E = THF

(**3**) R = H

(**4**) R = CH$_3$
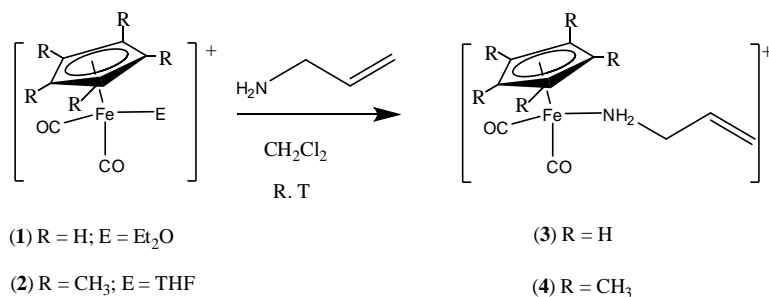
Scheme 1: Reactions of etherate complexes with allylamine.

Similarly, the THF complex [Cp*(CO)$_2$Fe(THF)]BF$_4$ (Cp* = η^5-C$_5$(CH$_3$)$_5$), **2**, reacted with one equivalent of 3-amino-1-propene to give [Cp*(CO)$_2$Fe(NH$_2$CH$_2$CH=CH$_2$)]BF$_4$, **4**, in 78% yield. Unlike complex **3**, compound **4** exhibited high solubility in dichloromethane and stability in the solid state, as well as in solution. This is expected, owing to the presence of the electron releasing pentamethylcyclopentadienyl ligand. No evidence of the coordination occurring at the C=C bond was obtained. When two or more equivalents of the ether complex were used, mixtures of the monuclear complex [(η^5-C$_5$R$_5$)(CO)$_2$Fe(NH$_2$CH$_2$CH=CH$_2$)]BF$_4$ and the dinuclear complex [{(η^5-C$_5$R$_5$)(CO)$_2$Fe}$_2$(NH$_2$CH$_2$CH=CH$_2$)](BF$_4$)$_2$ were formed. It was difficult to isolate the dinuclear complex in its pure form. However, an analytically pure sample of the dinuclear complex can be obtained from the reaction of [(η^5-C$_5$R$_5$)(CO)$_2$Fe(NH$_2$CH$_2$CH=CH$_2$)]BF$_4$ with an equimolar amount of the ether complex [(η^5-C$_5$R$_5$)(CO)$_2$Fe(E)]BF$_4$.

Compounds **3** and **4** resemble the neutral allyl complexes of the type [Cp(CO)$_2$Fe{(CH$_2$)$_n$CH=CH$_2$} reported by various authors [2, 4-6] in the sense that they have a terminal double bond on the alkyl chain. However, they are different in that the allylamino complexes are cationic and contain both amino and terminal double bond functionalities in the same molecule. Therefore, they can be regarded as ligand supported metal-nitrogen moieties in which the metal is sigma-bonded to an aliphatic aminoalkyl group with a reactive pendant vinyl group. The pendant vinylic functionality is accessible to electrophiles through which various novel iron-organometallic complexes can be synthesized. As will be seen in the following sections, allylamino complexes may react by addition of electrophiles across the double bond and by coordination of the C=C bond giving rise to novel chiral complexes. The NMR, IR and elemental analysis characterization data for **3** and **4** are given in the experimental section.

Complex **3** shows IR carbonyl bands at 2051 and 2004 cm^{-1} (*cf.* those of compound **4** observed at 2029 and 1983 cm^{-1}). This is a characteristic region for carbonyl compounds with auxiliary ligands that are strong electron donors such as amines [29-31], thiols [32] or phosphines [33]. Characteristic peaks assignable to N–H asymmetric and symmetric stretching were observed at ca. 3310 and 3279 cm^{-1}, respectively. A peak due to the N–

H bending mode was observed at ca. 1605 cm^{-1}, while a characteristic weak band assignable to uncoordinated C=C stretching was observed at ca. 1640 cm^{-1}. Peaks assignable to =CH out-of-plane bending vibrations were observed at 948 and 682 cm^{-1} [34] in the IR spectrum of compound **3** and at 927 and 663 cm^{-1} in the spectrum of compound **4.** These bands were absent in the infrared spectrum of halogenated and olefin-coordinated compounds (Sections 2.2. and 2.3).

The ^{1}H NMR spectra of both compounds **3** and **4** show well resolved characteristic olefinic proton peaks. A multiplet assignable to the CH= proton was observed at ca. 5.81 ppm and two doublets at 5.28 and 5.23 ppm, each integrating for one proton, assignable to two non equivalent =CH$_2$ protons. These values are within the range reported for alkenyl complexes [2, 5, 35]. The methylene protons alpha to the amine group exhibited a quartet at ca. 2.95 ppm with a coupling constant $^3J_{HH} = 6.51$ Hz. The ^{13}C NMR spectra of both compounds clearly show peaks corresponding to the vinylic carbon in the expected region above 115 ppm. All peaks assignable to allylamino protons slightly shifted upfield upon changing from Cp to Cp*. However, no significant change was noted in the ^{13}C NMR spectra.

2.1.1. The molecular structures of compounds 3 and 4

Single crystal X-ray diffraction data were obtained for complexes **3** and **4**. Compound **3** crystallized as brown blocks in the monoclinic C2/c space group with eight molecular cations and eight counteranions per unit cell, while compound **4** crystallized as brown plates in the triclinic *P-1* space group with two molecular cations and two counteranions per unit cell. Each asymmetric unit of compounds **3** and **4** consists one molecular cation and counteranion as presented in Figs. 1 and 2, respectively. The molecular structures of these compounds show that the iron atom is coordinated in a pseudo-octahedral 3-legged piano stool fashion, with five carbons of the cyclopentadienyl ring occupying the apical positions, while the two CO and allylamine ligands occupy the basal positions. Selected bond lengths and angles for compounds **3** and **4** are listed in Table 1, while the hydrogen bond lengths are summarized in Table 2.

Figs. 3 and 4 show packing of molecules and hydrogen bonding within the crystals of **3** and **4**, respectively. In each crystal, molecules are linked by hydrogen bonds N–H---F,

which fall within the range 2.08 - 2.64 Å. The molecules in **3** are arranged in layers with the allyl chains oriented in the same direction within each layer. This mode of packing is similar to that observed in the complex [Cp(CO)$_2$Fe{NH$_2$(CH$_2$)$_2$CH$_3$}]BF$_4$ [30]. In **4**, the two cations and two anions in the unit cell are centrosymmetrically arranged with the centre of inversion located between two molecules.

The coordination by allylamine occurs *via* the nitrogen atom which forms a σ-bond with the iron atom. The Fe–N bond distances in **3** and **4** are found to be 2.0180(4) Å and 2.0294(14) Å, respectively. As expected, Fe–N in **4** is slightly longer than the equivalent bond in **3**; an observation that can be attributed to the electronic and steric effects of Cp* compared to Cp. The bond lengths are close to the Fe-N bonds observed in other related amino cyclopentadienyliron dicarbonyl complexes [Cp(CO)$_2$Fe{NH$_2$(CH$_2$)$_2$CH$_3$}]BF$_4$, (2.017(8) Å) [30], [Cp(CO)$_2$Fe{NH$_2$(CH$_2$)$_3$CH$_3$}] BF$_4$ (2.013(2) Å, 2.006(2) Å) [30], [{Cp(CO)$_2$Fe}$_2${μ-NH$_2$(CH$_2$)$_2$NH$_2$}](BF$_4$)$_2$ [36] and amino pentamethylcyclopentadienyliron dicarbonyl complexes, [Cp*(CO)$_2$Fe{NH$_2$(CH$_2$)$_2$CH$_3$}]BF$_4$ (2.022(15) Å) [29] and [{Cp*(CO)$_2$Fe}$_2${μ-NH$_2$(CH$_2$)$_2$NH$_2$}](BF$_4$)$_2$ (2.0202(14) Å) [29]. The C9–C10 (1.300(9) Å) and C14–C15 (1.320 (3) Å) bonds in **3** and **4**, respectively, are significantly shorter than the respective bonds, C8–C9(1.496(8) Å) and C13–C14 (1.486(2) Å), indicating double bond character and are in good agreement with the NMR and IR data. The vinyl bond lengths observed are slightly shorter than the theoretical C=C bond length of ca. 1.34 Å [37, 38], but similar to the calculated C=C bond length for terminal alkenes; ethylene (1.315Å), propene (1.316Å) and 2-methylpropene (1.321 Å) [39]. Furthermore, the angles formed by atoms surrounding C9 and C10 in the structure of compound **3**, as well as the angle formed by atoms surrounding C14 and C15 in the structure of compound **4**, are approximately 120 ˚, confirming trigonal planar geometry around each vinylic carbon.
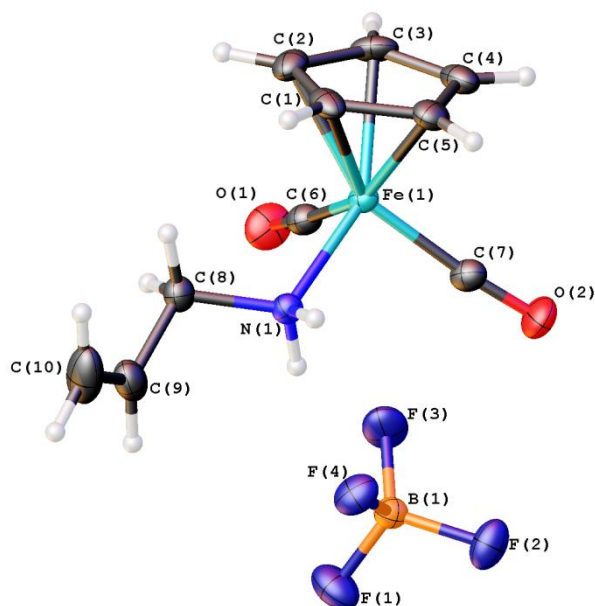
Fig. 1: The molecular structure of compound **3** showing the atom-numbering scheme. Displacement ellipsoids are drawn at 40% probability level and H atoms are shown as small spheres
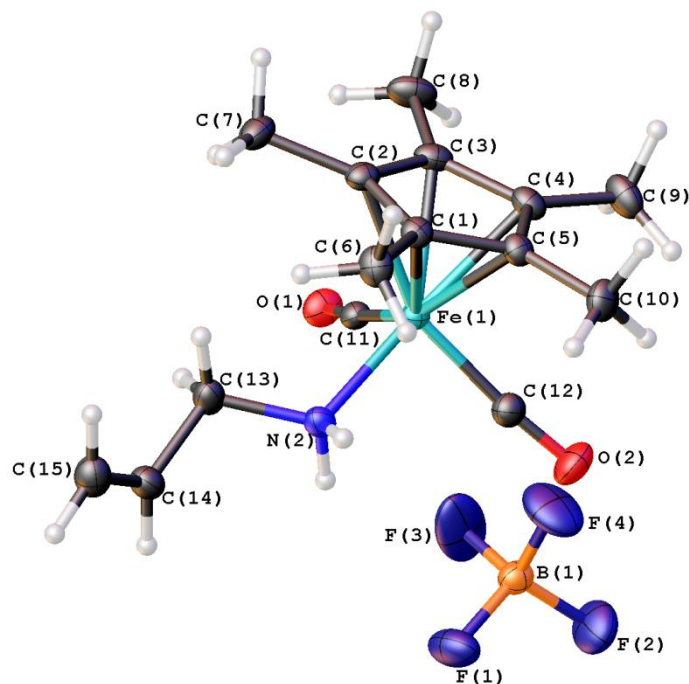
Fig. 2: The molecular structure of compound **4** showing the atom-numbering scheme. Displacement ellipsoids are drawn at 40% probability level and H atoms are shown as small spheres

Table 1. Selected bond lengths and angles for compounds **3** and **4**

Bond length (Å)			Bond angles (°)		
	3	**4**		**3**	**4**
Cent1-Fe1*	1.715		Cent1-Fe1-N1	123.42	
Cent2-Fe1*		1.726	Cent2-Fe1-N2		125.46
Fe1-N1	2.018(4)		Cent1-Fe1-C6	121.91	
Fe1-N2		2.0294(14)	Cent2-Fe1-C11/C1		122.06
N1-C8	1.484(6)		Cent1-Fe1-C7	121.55	
N2-C13		1.491(2)	Cent2-Fe1-C12/C2		120.41
C8-C9	1.496(8)		Fe1-N1-C8	117.0(3)	
C13-C14		1.486(2)	Fe1-N2-C13		118.60(10)
C9-C10	1.300(9)		NI-C8-C9	112.3(4)	
C14-C15		1.320(3)	N2-C13A-C14A		113.06(14)
Fe1-C6	1.780(5)		C8-C9-C10	123.4(7)	
Fe1-C11		1.7843(16)	C13A-C14A-C15A		123.61(18)
Fe1-C7	1.789(5)		C6-Fe1-C7	95.0(2)	
Fe1-C12		1.7926(18)	C11-Fe1-C12		94.89(8)
C6-O1	1.138(6)		N1-Fe1-C6	93.3(2)	
C11-O1		1.136(2)	N2-Fe1-C11		93.94(7)
C7-O2	1.136(6)		N1-Fe1-C7	94.1(2)	
C12-O2		1.133(2)	N2-Fe1-C12		92.06(7)

Cent1 and Cent2 are the centroid of the atoms forming the Cp and Cp rings, (C1, C2, C3, C4 and C5)
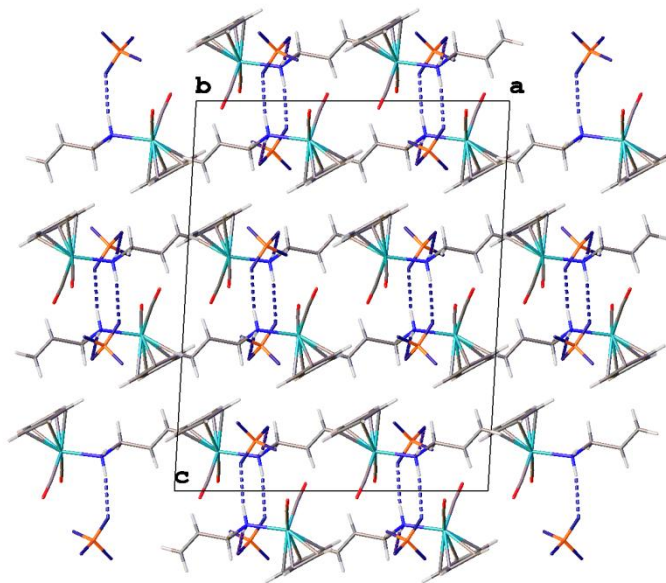
Fig. 3: Crystal packing of compound **3** viewed along the *b*-axis showing hydrogen bonding as indicated by the dotted lines
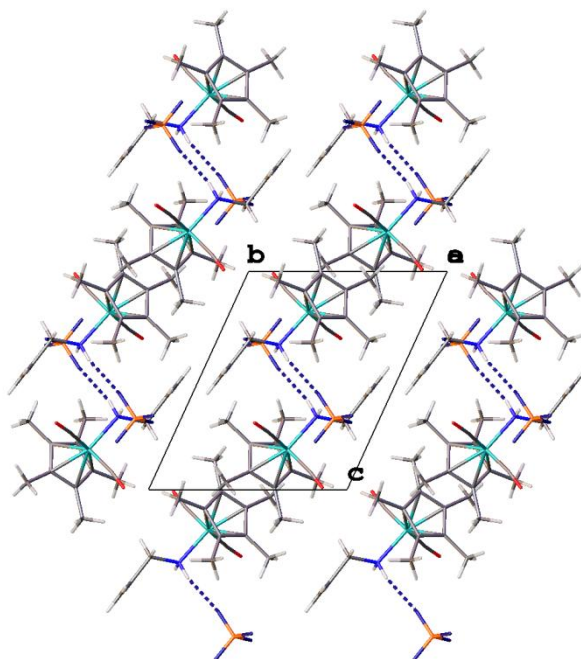
Fig. 4: Crystal packing of compound **4** viewed along the *a*-axis showing hydrogen bonding as indicated by the dotted lines

Table 2. Hydrogen bonds for the compounds **3** and **4** [Å and °]

compound	D-H…A	d(D-H)	d(H…A)	d(D…A)	<(DHA)
3	N(1)-H(1A)...F(4)	0.92	2.13	3.028(5)	165
	N(1)-H(1B)...F(2)#1	0.92	2.08	2.983(5)	166
	N(1)-H(1B)...F(4)#1	0.92	2.64	3.321(5)	132
4	N(2)-H(2A)...F(2)#2	0.92	2.27	3.013(2)	137
	N(2)-H(2B)...F(3)	0.92	2.13	2.891(2)	139

Symmetry transformations used to generate equivalent atoms: #1 -x+1/2,-y+1/2,-z+1; #2 -x,-y+1,-z+1

2.2. Halogenation of compounds *3* and *4*

The cationic allylamino complexes $[(\eta^5\text{-}C_5R_5)(CO)_2Fe(NH_2CH_2CH=CH_2)]BF_4$ (R = H (**3**), CH_3 (**4**)) react readily with Cl_2 and Br_2 in CH_2Cl_2 to give the aminodihalopropane complexes $[(\eta^5\text{-}C_5R_5)(CO)_2Fe\{NH_2CH_2CH(X)CH_2X\}]BF_4$ (R = H; X = Cl (**5**), Br (**6**) and R= CH_3; X = Br (**7**)) as shown in Scheme 2. The compounds **5**, **6** and **7** were obtained as microcrystalline solids. The reaction of compound **4** with chlorine gave a mixture of white and dark green sticky solids which showed no carbonyl bands in the IR spectrum. There was no evidence to suggest the formation of the halide complexes $[(\eta^5\text{-}C_5R_5)Fe(CO)_2X]$ in all these cases.
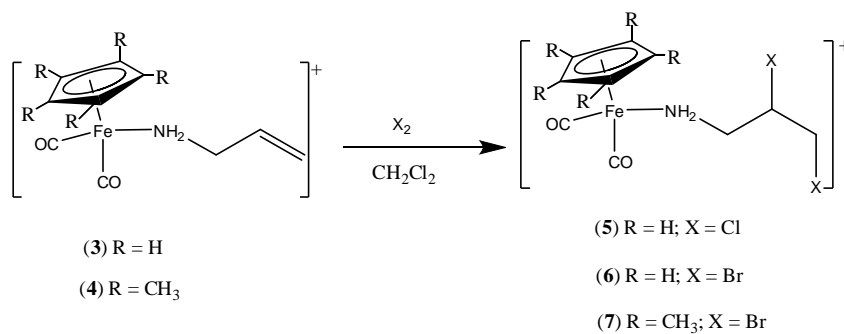
Scheme 2: Halogenation of allylamino complexes

Halogenation is believed to proceed according to the mechanism illustrated in Scheme 3. Initially, the halogen molecule is polarized by pi bond electrons leading to the formation of halonium and halide ions [40]. Then the halide adds to the side opposite the carbon-halogen bond of the halonium ion in order to achieve the maximum overlap of the C–X σ* antibonding molecular orbitals. In this way the two halogens add in an anti-addition fashion resulting in a racemic mixture of (*R*) and (*S*) enantiomers as shown in Scheme 3. This is indeed further corroborated by the single crystal structure of compound **7** (Fig. 3) and the NMR data discussed below.
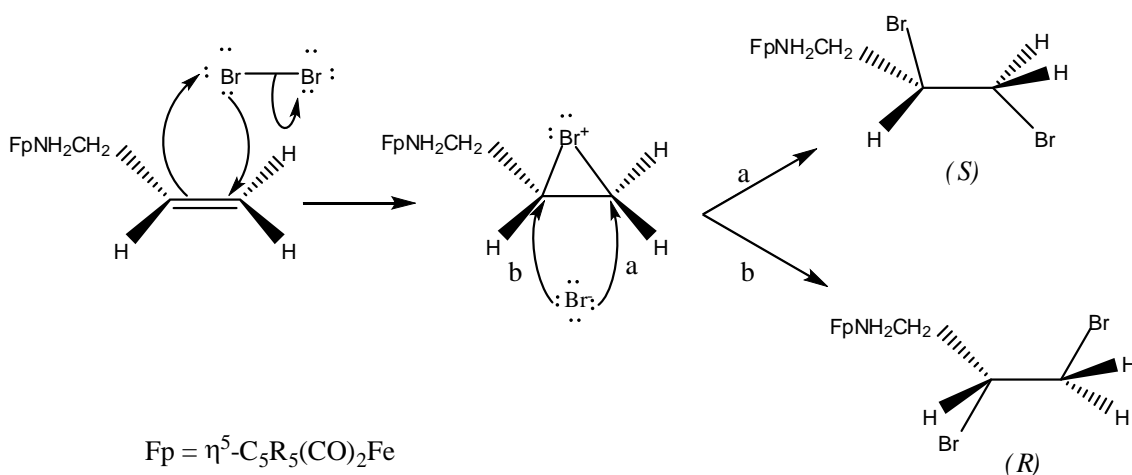
Scheme 3: Proposed mechanism for bromination of compound **3** and **4**

The success of the halogenation reactions of complexes **3** and **4** was marked by the disappearance of the strong IR band between 920 - 950 cm^{-1} and weak IR bands at ca. 1640 cm^{-1} which correspond to =CH out-of-plane bending and C=C stretching vibrations, respectively. The infrared spectrum of compound **5** exhibited a characteristic band assignable to C–Cl at 746 cm^{-1}, while compound **6** showed a vibration band corresponding to C–Br stretching at 652 cm^{-1}, which, as expected, is at a lower wavenumber than that corresponding to C–Cl. A similar peak was observed in the infrared spectrum of compound **7** at 670 cm^{-1}. There was no significant variation in the carbonyl vibration bands upon halogenation, indicating that the halogen atoms were added to the vinyl group which is far from the metal and therefore the electron density on the metal centre was not significantly affected.

As expected for chiral molecules, the protons of the α-CH$_2$ group neighbouring the chiral centre CHX (Scheme 3) are diastereotopic and they show two well separated multiplets at around 3.00 and 2.77 ppm ($\Delta\delta$ ~0.2 ppm), each integrating for one proton. The peaks corresponding to CHX and CH$_2$X were observed at around 4.28 and 3.86 ppm, respectively. This corresponds to an upfield shift of 1.54 and 1.38 ppm relative to the peaks due to CH= and =CH$_2$ of the starting material, respectively, indicating loss of anisotropy upon halogenation. The ^{13}C NMR data for compounds **5**, **6** and **7** were assigned with the help of 2D NMR experiments. As expected, these data show that the position of the peaks due to CO and Cp are independent of the type of halide in the molecule. The ^{13}C NMR spectrum of compound **6** shows a peak assignable to the terminal carbon neighbouring bromine at 31.2 ppm which is 15.1 ppm upfield relative to that of the similar carbon neighbouring chlorine in the ^{13}C NMR spectrum of compound **5**[†], as expected, because chlorine is significantly more electronegative than bromine.

No reaction was noted between the allylamino complexes and formic acid or tetrafluoroacetic acid, even when a large excess of these reagents was used and the mixtures stirred for 24 h at room temperature or at refluxing temperatures. There was also no reaction between the allylamino complexes and hydrogen chloride gas.

[†] The structure of **5** was confirmed by X-ray crystallography though it could not be refined to a publishable level owing to the poor quality of the crystal. This structure is given in Appendix 10.

Interestingly, although amines are weak bases, the allylamino complexes were recovered intact at the end of the period by evaporating the mixture to dryness followed by extraction using dichloromethane and precipitation by diethyl ether. The coordination of the amine functionality probably severely weakens the basic properties of the allylamine, thereby stabilizing the metal-coordinated compounds in acidic medium.

2.2.1. Crystal structure of [Cp*(CO)$_2$Fe{NH$_2$CH$_2$CH(Br)CH$_2$Br}]BF$_4$, 7

Compound **7** is a product of the bromination reaction of the allylamino complex **4.** It was found to crystallize as brown plates in the triclinic *P-1* space group, with two molecular cations and two anions per unit cell. Part of its cationic molecule was found to be disordered over two positions, with C14A, C15A, Br1A and Br2A versus C14B, C15B, Br1B and Br2B each having a site occupancy factor of 0.5. The observed disorder is attributed to the presence of the two enantiomers *R* and *S* in the sample crystal, as is clearly shown in Fig. 5. Depending on the enantioface of the dibromoaminopropane coordinated to the metal, two isomers are possible for this type of compound as depicted in Scheme 3. As seen in Fig. 5, the bromine atoms adopt a gauche type of conformation in the (*R*) enantiomer and an anti conformation in the (*S*) enantiomer, with torsion angles of Br2A–C15A–C14A–Br1A = 69.0(4) ˚ and Br1B–C14B–C15B–Br2B = 178.8(3)˚, respectively. This happens probably in order to allow packing and to reduce steric interaction between the bulky Cp* and Br atoms. The packing in **7** (Fig. 6) is such that molecules are arranged in layers in which the molecules in the alternate layers are oriented in opposite directions. The methyl groups of Cp* fit nicely in the spaces between the *trans* bromine atoms of the neigbouring molecules in a bump-to-hollow fashion. This mode of packing is favoured in order to maximize dispersive interactions, which in turn leads to close-packing of the molecules in the crystal.
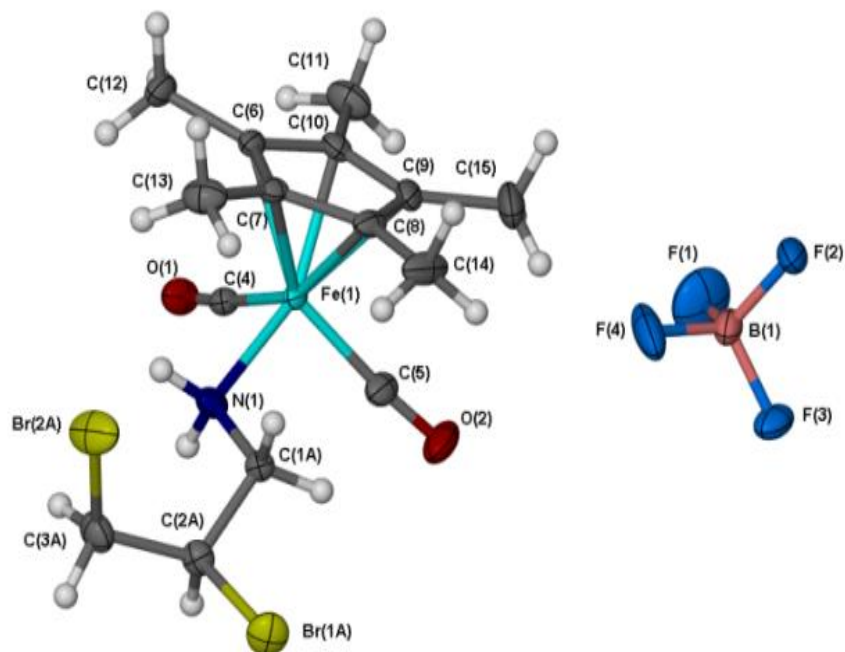
(*R*) enantiomer
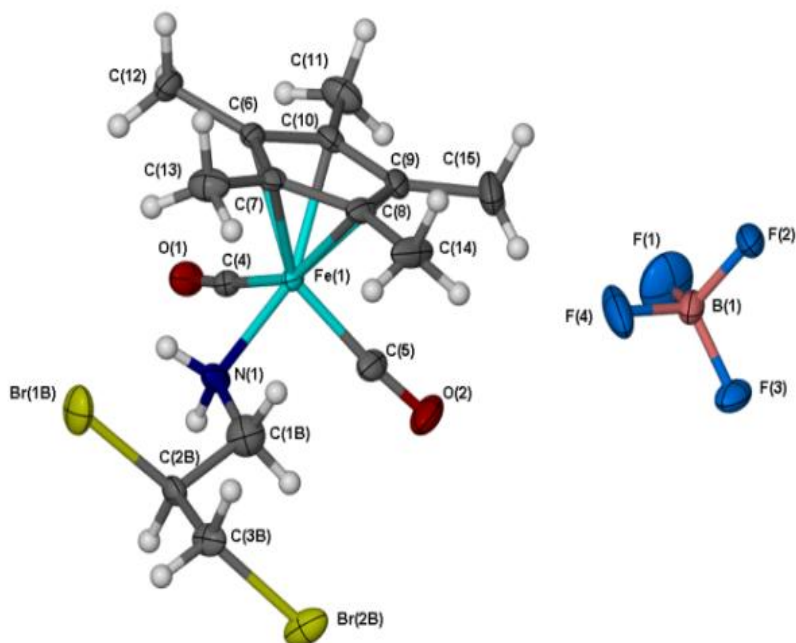
(*S*) enantiomer

Fig. 5: The molecular structures of compound **7** showing the numbering scheme of the atoms in the *R* and *S* enantiomers. Displacement ellipsoids are drawn at 40% probability level and H atoms are shown as small spheres

In the crystal structure, the metal centre is σ-bonded to the nitrogen atom of the dibromoaminopropane ligand with Fe–N bond lengths of 2.036(3), which are slightly longer than those observed in the starting material **4** (2.0294(14) Å), [Cp*(CO)$_2$Fe{NH$_2$(CH$_2$)$_3$CH$_3$}]BF$_4$ (2.022(15) Å) [29] and [{Cp*(CO)$_2$Fe}$_2${μ-NH$_2$(CH$_2$)$_3$NH$_2$}](BF$_4$)$_2$ (2.0182(16), 2.0202(14) Å) [29] . Selected bond lengths and angles are listed in Table 3. The bond C2–C3 is ca. 1.537 Å, which is significantly longer than the corresponding bond C14–C15 in compound **4** by ca. 0. 217 Å. Furthermore, angles C1–C2–C3, C1–C2–Br1, Br1–C2–C3 and C2–C3–Br2 in both the enantiomers of compound **7** are close to 109.5°, which is a characteristic of *sp^3* tetrahedral geometry. This is an unambiguous confirmation that the allylamino complex **4** reacts with bromine to form the saturated dibroaminoalkane complex.

Table 3. Selected bond lengths and angles for compound **7**

Bond length (Å)			Bond angles (°)		
	(*R*)	(*S*)		(*R*)	(*S*)
Cent-Fe1*	1.727	1.727	Cent-Fe1-N1	125.6(5)	125.6(5)
Fe1-C4	1.795(3)	1.795(3)	Cent-Fe1-C4	120.0(1)	120.0(1)
Fe1-C5	1.790(3)	1.790(3)	Cent-Fe1-C5	122.1(8)	122.1(8)
C4-O1	1.133(4)	1.133(4)	Fe1-N1-C1A/B	115.4(3)	121.8(3)
C5-O2	1.137(4)	1.137(4)	NI-C1A/B-C2A/B	111.4(4)	116.4(6)
Fe1-N1	2.036(3)	2.036(3)	C1A/B-C2A/B-C3A/B	115.4(4)	112.5(6)
N1-C1A/B	1.478(6)	1.494(8)	C4-Fe1-C5	96.56(15)	96.56(15)
C1A/B-C2A/B	1.538(7)	1.540(11)	N1-Fe1-C4	91.28(12)	91.28(12)
C2A/B-C3A/B	1.536(8)	1.539(10)	N1-Fe1-C5	93.23(14)	93.23(14)
C2A/B-Br1A/B	1.942(5)	1.956(7)	C1A/B-C2A/B-Br1A/B	107.5(3)	109.0(5)
C3A/B-Br2A/B	1.923(6)	1.967(7)	C2A/B-C3A/B-Br2A/B	113.7(4)	109.5(5)

Cent is the centroid of the atoms forming the Cp rings, (C6, C7, C8, C9 and C10)
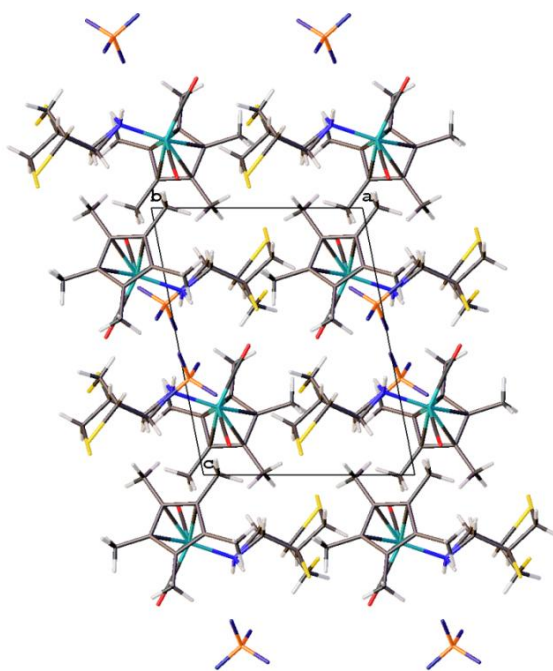
Fig.6: Crystal packing in compound **7** viewed along the *b*-axis

2.3. Metallation of *3* and *4*

Although a wide variety of bridged metal complexes are reported, metal complexes bridged by ligands comprising of two non equivalent binding sites are rare [41]. The reactions of the allylamino complexes **3** and **4** with molar equivalents of the etherate complexes **1** and **2** produced dinuclear complexes (Fig. 7) in which the two iron systems are in different electronic environments. Thus, the reaction of **3** with **1** and **2** in CH_2Cl_2 at room temperature gave the dinuclear complexes **8** and **9**, respectively. Similarly, **4** reacts with **1** and **2** to give the dinuclear complexes **10** and **11**, respectively. Complex **8** is insoluble in dichloromethane, hexane and diethyl ether, but soluble in acetone, methanol, water and acetonitrile. Thus it was easily isolated by filtration and purified by recrystallization from an acetone/diethyl ether mixture (1/3; v/v). Unlike **8**, the other dinuclear complexes are very soluble in dichloromethane and they were precipitated from their solution by addition of diethyl ether. The isolated compounds were characterized by NMR, IR spectroscopy and elemental analysis and the characterization data are given in the Experimental Section.
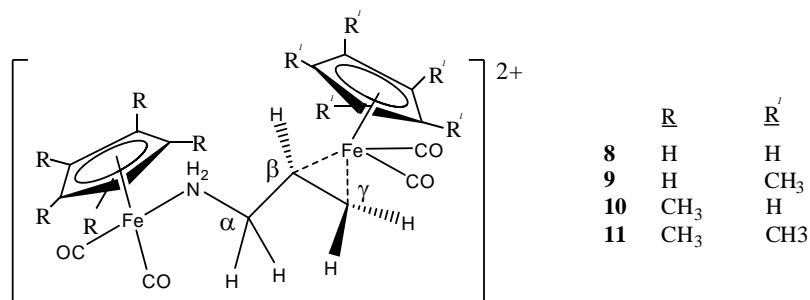
Fig. 7: The dinuclear complexes, $[(\eta^5\text{-}C_5R_5)(CO)_2Fe(NH_2CH_2CH=CH_2)Fe(CO)_2(\eta^5\text{-}C_5R'_5)](BF_4)_2$

As expected, the infrared spectra of compounds **8** and **11** show four absorption bands assignable to the terminal carbonyls. The spectrum of compound **8** shows bands corresponding to the two carbonyls on the $Cp(CO)_2FeCH_2=CH\text{-}$ side of the molecule at 2078 and 2064 cm^{-1} and another two bands assignable to the two terminal carbonyls on the $Cp(CO)_2FeNH_2CH_2\text{-}$ side at 2041 and 2004 cm^{-1}. These data are in close agreement with those of the related olefin complexes with the $Cp(CO)_2FeCH_2=CH\text{-}$ moiety [7, 9, 11, 12, 42-44]. The infrared spectrum of compound **11** shows two peaks assignable to the two terminal carbonyls on the $Cp^*(CO)_2FeCH_2=CH\text{-}$ side at 2050 and 2014 cm^{-1}, which is in agreement with the reported data for related complexes [43, 45]. The other two bands assignable to the two terminal carbonyls on the $Cp^*(CO)_2FeNH_2CH_2\text{-}$ side were observed at 1986 and 1955 cm^{-1}. These values are at considerably lower wavenumbers than the ca. 2023 and 1970 cm^{-1} found for the compound $[Cp^*(CO)_2Fe\{NH_2(CH_2)_3CH_3\}]BF_4$ [29].

The infrared spectrum of compound **9** shows only two bands, while that of **10** shows three bands corresponding to the two sets of terminal carbonyls. The carbonyl bands of compounds **9** and **10** are strong and broad suggesting band overlap. All IR spectra of complexes **8**-**11** show two bands in the N-H stretching region at ca. 3308 and 3268 cm^{-1}, which are assignable to NH asymmetric and symmetric stretching, respectively. The medium band at ca. 1600 cm^{-1} can be assigned to NH bending. The peak at ca.1640 cm^{-1}, as well as the peaks at ca. 938 cm^{-1}, which were assigned to C=C stretching and =CH wagging in the infrared spectra of the parent allylamino complexes, are absent.

The ^{1}H NMR data show that the allylamine molecule links the two metal centres using the amine on one end and the vinyl functionality on the other end. These two

functionalities have different electronic effects and as a result the ^{1}H NMR spectra of compounds **8** and **11** gave two well separated characteristic peaks corresponding to protons of the two cyclopentadienyl ligands and pentamethylcyclopentadienyl ligands in the different electronic environments. In the ^{1}H NMR spectrum of **8**, the two peaks were observed at 5.54 and 5.92 ppm and were assigned to the Cp of the $Cp(CO)_2FeN$ and $Cp(CO)_2FeC$ moieties, respectively. The ^{1}H NMR spectrum of compound **11** exhibited peaks at 1.89 and 2.01 ppm corresponding to Cp* of the $Cp*(CO)_2FeN-$ and $Cp*(CO)_2FeC$ moieties, respectively. The peaks corresponding to the Cp and Cp* ligands attached to the metal on the vinyl end appear downfield relative to those on the amine end. The downfield shift of these peaks upon olefin coordination has been previously attributed to the deshielding effects of the cationic metal centre [9]. However, the influence of π-backdonation of electrons from the metal orbital to the vinylic carbons should not be ignored, since drawing of electrons from the metal increases its electrophilicity, which consequently would lead to deshielding of the Cp or Cp* protons. For this reason, whereas both metal centres are cationic, the Cp or Cp* protons neighbouring the metal on the vinyl end appear at higher chemical shift values than those on the amine side.

The ^{1}H NMR spectra of the mixed ligand compounds **9** and **10**, which are structural isomers, show Cp peaks at 5.20 and 5.90 ppm, while Cp* peaks were observed at 2.01 and 1.90 ppm, respectively. Complexes **8** and **10** show characteristic sharp doublets at ca. 4.14 ppm ($J\sim$ 8.3 Hz) and 3.62 ppm ($J\sim$ 14.24 Hz) assignable to the diastereotopic methylene protons γ to NH_2 which are *cis* and *trans* to βCH. These values are in good agreement with data reported for related cyclopentadienyliron complexes [7, 9, 11, 12, 43, 44]. Similar sharp doublets were observed in the ^{1}H NMR spectra of compounds **9** and **11** at ca. 3.01 ($J\sim$7.76 Hz) and 3.55 ($J\sim$13.84 Hz), also in agreement with data reported for the related pentamethylcyclopentadienyl complexes [43, 45]. The αCH_2 protons are also diastereotopic, hence two separate multiplets assignable to these protons were observed at ca. 2.35 and 3.44 ppm. These observations confirm that compounds **8–11** have a rigid chiral structure which is maintained even in solution. The ^{13}C NMR spectra of compounds **8–11** show peaks assignable to the carbon of the vinyl group coordinated to the metal at chemical shifts below 80 ppm. This is about 59 ppm upfield relative to the pendant vinyl groups in the starting materials (compounds **3** and

4). This is a clear indication that the vinyl group of allylamino ligand links the second metal centre in a η^2-fashion.

2.4. Reaction of [{Cp(CO)$_2$Fe}$_2$(μ-NH$_2$CH$_2$CH=CH$_2$)](BF$_4$)$_2$, 8 with NaI

It is well established that olefin complexes are demetallated when treated with excess NaI to give [CpFe(CO)$_2$I] and the corresponding olefin [12, 44, 46]. Haloalkene displacement when olefin complexes are treated with NaI or Na[CpFe(CO)$_2$] has also been reported [19]. Contrary to these observations, the dinuclear complex **8** reacts with NaI at room temperature in acetone to give the monuclear complex [Cp(CO)$_2$Fe(NH$_2$CH$_2$CH=CH$_2$)]$^+$I$^-$ (**12**) and the known neutral iodo complex [CpFe(CO)$_2$I] [47] according to Eq. 1. There was no evidence of the formation of the dimeric complex [CpFe(CO)$_2$]$_2$ nor of Fe–N bond cleavage, even when the reaction was repeated at 35 ˚C. Complex **12** was obtained as a yellow microcrystalline solid upon treating the dichloromethane extract with diethyl ether. The iodo complex remained in the mother liquor and it was obtained as a grey crystalline solid upon evaporation.

$$[\{Cp(CO)_2Fe\}_2(NH_2CH_2CHCH_2)](BF_4)_2 + 2NaI \longrightarrow [Cp(CO)_2Fe(NH_2CH_2CHCH_2)]I + [CpFe(CO)_2I] + 2NaBF_4$$

$$\textbf{(8)} \qquad\qquad\qquad\qquad\qquad\qquad \textbf{(12)}$$

$$(1)$$
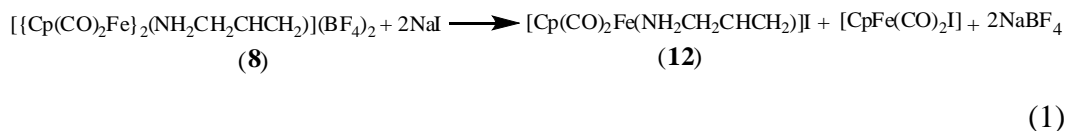
The formation of complex **12** illustrates that the Fe–N bond in the allylamino complex is too strong to be cleaved by the iodide, I$^-$. The complex was characterized by elemental analysis, IR and NMR spectroscopy and the data are listed in Section 4.7. A similar pattern of the IR peaks was observed as for the BF$_4^-$ salt, compound **3,** with the exception of the peaks at 999-1051 cm^{-1} (assigned to BF$_4^-$) and the finger-print region.

3. Conclusion

We have unequivocally shown that the etherate complexes [Cp(CO)$_2$Fe(OEt$_2$)]BF$_4$ and [Cp*Fe(CO)$_2$(THF)]BF$_4$ react with 3-aminoprop-1-ene to give the novel allylamino complexes of the type [(η^5-C$_5$R$_5$)(CO)$_2$Fe(NH$_2$CH$_2$CH=CH$_2$)]BF$_4$, which in turn undergo electrophilic halogenation to form novel chiral complexes of the type [(η^5-

$C_5R_5)(CO)_2Fe\{NH_2CH_2CH(X)CH_2X\}]BF_4$. The crystallographic data of complex $[Cp^*(CO)_2Fe\{NH_2CH_2CH(Br)CH_2Br\}]BF_4$ show that it exists as a mixture of (*R*) and (*S*) enantiomers. The reactions of the etherate complexes with the allylamino complexes is a convenient route to dinuclear complexes of the type $[\{\eta^5\text{-}C_5R_5(CO)_2Fe(NH_2CH_2CH=CH_2)Fe(CO)_2(\eta^5\text{-}C_5R'_5)\}](BF_4)_2$ in which the two metal fragments are bridged by the allylamine *via* the amine on one side and *via* the vinyl group on the other side. Coordination of the vinyl group occurs only after amine coordination, as expected.

4. Experimental

4.1. General

All experimental manipulations of organometallic compounds were carried out under inert atmosphere using standard Schlenk line procedures unless otherwise stated. Reagent grade THF, hexane and Et_2O were distilled from sodium/benzophenone and used immediately; acetone and MeCN were distilled from anhydrous $CaCl_2$ and stored under molecular sieves of porosity size 4; CH_2Cl_2 was distilled from phosphorus(V) oxide and used immediately. Dry chlorine gas was generated according to literature method [48]. The other reagents were used as received from the suppliers without further purification. Melting points were recorded on an Ernst Leitz Wetzlar hot-stage microscope and are uncorrected. Elemental analyses were performed on a LECO CHNS-932 elemental analyzer. Infrared spectra were recorded using an ATR PerkinElmer Spectrum 100 spectrophotometer between 4000–400 cm^{-1}. ^{1}H and ^{13}C NMR spectra were recorded using Bruker 400 MHz and 600 MHz spectrometers and chemical shifts are recorded in ppm. Correlations were confirmed through COSY and HSQC experiments. The deuterated solvents $CDCl_3$ (Aldrich, 99.8%), acetonitrile-d_3 (Merck, 99%), acetone-d_6 (Aldrich, 99.5%) and methanol-d_4 (Aldrich, 99.8%) were used as purchased. The precursors $[Cp(CO)_2Fe(OEt_2)]BF_4$ [30] and $[Cp^*(CO)_2Fe(THF)]BF_4$ [49] were prepared by the literature methods.

4.2. Reaction of allylamine with one equivalent of [Cp(CO)₂Fe(OEt₂)]BF₄ ,**1**

Into a solution of compound **1** (0.86 g, 2.54 mmol) in CH_2Cl_2 (10 ml), allylamine (0.19 ml) was added and the mixture stirred for 6 h under nitrogen at room temperature, after which a yellow precipitate was formed. The mixture was filtered into the pre-weighed Schlenk tube and the residue washed with a minimum amount of dichloromethane (2 ml) followed by diethyl ether (5 ml). A further crop of the compound was recovered from the filtrate by addition of diethyl ether and allowing the mixture to stand at room temperature for 1 h. The mother liquor was syringed off and the residue was washed with diethyl ether to give the yellow microcrystalline solid of [Cp(CO)₂Fe(NH₂CH₂CH=CH₂)]BF₄, **3**. Yield 0.80 g, 98%. Anal. Calc. for $C_{10}H_{12}BF_4FeNO_2$: C, 37.38; H, 3.74; N, 4.36. Found: C, 37.86; H, 3.84; N, 3.99%. ^{1}H NMR (600 MHz, methanol-d_4) 5.36 (s, 5H, Cp), 3.81 (s, 2H, NH₂), 2.95 (q, J_{HH} = 6.60 Hz, 2H, -CH₂), 5.80 (m, 1H, =CH), 5.22 (d, J_{HH} = 10.38 Hz, 1H, =CH *cis*), 5.26 (d, J_{HH} = 17.22 Hz, 1H, =CH *trans*). ^{13}C NMR (600 MHz, methanol-d_4): 85.95 (Cp), 53.88 (-CH₂), 134.99 (CH=), 117.81 (=CH₂), 211.05 (CO). IR (solid state) v_{max}(cm^{-1}): 2051, 2004 (CO); 3307, 3277 (NH₂). Decomposes without melting at temperature > 120 ˚C.

4.3. Reaction of [Cp(CO)₂Fe(NH₂CH₂CH=CH₂)]BF₄, **3** with chlorine

A Schlenk tube equipped with a magnetic bar and charged with a solution of **3** (0.16 g, 0.498 mmol) in CH_2Cl_2 (10 ml) was cooled to -78 ˚C (dry ice/acetone) and then chlorine gas condensed into the mixture. The mixture was stirred and allowed to warm slowly to room temperature for the excess chlorine gas to escape and then it was filtered into a pre-weighed Schlenk tube. Diethyl ether (25 ml) was added and the mixture was allowed to stand overnight, after which a yellow microcrystalline solid was found stuck on the wall of the Shlenk tube. The mother liquor was syringed off and the residue washed with diethyl ether (5 ml) and dried under reduced pressure gave 0.083 g (47%) of compound **5**. Anal. Calc. for $C_{10}H_{12}BCl_2F_4FeNO_2$: C, 30.66; H, 3.09; N, 3.58. Found: C, 30.82; H, 3.46; N, 3.09%. ^{1}H NMR (400 MHz, methanol-d_4) 5.39 (s, 5H, Cp), 4.14 (br, 1H, CHCl), 3.85(br, 2H, NH₂), 3.82 (br, 2H, CH₂Cl), 2.87 (br, 1H, CH₂-N), 2.70 (br, 1H, CH₂-N). ^{13}C NMR (400 MHz, methanol-d_4): 87.63 (Cp), 62.18 (CHCl), 56.71

(CH$_2$-N), 46.87 (CH$_2$Cl), 212.06 (CO). IR (solid-state) ν_{max}(cm^{-1}): 2052, 2001 (CO); 3306, 3274 (NH$_2$). M.p., 63 – 65 ˚C.

4.4. Reaction of compound 3 with bromine

Liquid bromine (0.2 ml, 3.882 mmol) was added to a solution of compound **3** (0.24g, 0.732 mmol) in CH$_2$Cl$_2$ (20 ml) and the mixture stirred under nitrogen for 2 h at room temperature. Excess bromine was removed under vacuum and the mixture evaporated to ca. 7 ml under reduced pressure. Diethyl ether was added until a yellow precipitate was formed and then the mixture was allowed to stand at room temperature for 5 h in the dark. The mother liquor was removed and the yellow residue was washed with diethyl ether (2 x 10 ml). Drying the residue under reduced pressure gave 0.197 g (56% yield) of microcrystalline [Cp(CO)$_2${NH$_2$CH$_2$CH(Br)CH$_2$Br}]BF$_4$, **6**. Anal. Calc. for C$_{10}$H$_{12}$BBr$_2$F$_4$FeNO$_2$: C, 24.99; H, 2.52; N, 2.91. Found: C, 25.06; H, 2.27; N, 2.83%. ^{1}H NMR (400 MHz, methanol-d$_4$) 5.40 (s, 5H, Cp), 4.22 (m, 1H, CHBr), 3.88 (m, 1H, CH$_2$Br), 3.77 (m, 1H, CH$_2$-N), 3.00 (m, 1H, CH$_2$-N), 2.79 (m, 1H, CH$_2$). NH not observed. ^{13}C NMR (400 MHz, methanol-d$_4$): 87.42 (Cp), 57.67 (CH$_2$-N), 52.85 (CHBr), 34.18 (CH$_2$Br), 212.04 (CO). IR (solid state) ν_{max}(cm^{-1}): 2047, 1995 (CO); 3294, 3266 (NH$_2$). M.p., 109 – 110 ˚C.

4.5. Reaction of compound 3 with compound 1

A mixture of compound **1** (0.15 g, 0.440 mmol) in CH$_2$Cl$_2$ (10 ml) and that of compound **3** (0.10 g, 0.31 mmol) in CH$_2$Cl$_2$ (15 ml) was stirred at room temperature for 1 h. An orange solid formed and was allowed to settle for 30 min after which the mother liquor was syringed off. The residue was washed with CH$_2$Cl$_2$ (2 x 5 ml) and dried under reduced pressure. The product was further purified by recrystallizing from acetone/diethyl ether (1/3 v/v) to give a bright yellow microcrystalline solid, [{Cp(CO)$_2$Fe}$_2$(NH$_2$CH$_2$CH=CH$_2$)](BF$_4$)$_2$, **8**. Yield. 0.130 g, 72% Anal. Calc. for C$_{17}$H$_{17}$B$_2$F$_8$FeNO$_2$: C, 34.93; H, 2.93; N, 2.40. Found: C, 34.84; H, 3.40; N, 1.87%. ^{1}H NMR (400 MHz, acetone-d$_6$) 5.92 (s, 5H, Cp), 5.54 (s, 5H, Cp), 4.99 (m, 1H, CH), 4.12 (d, J_{HH} = 8.32 Hz, 1H, *cis* CH), 3.72 (d, J_{HH} = 14.20 Hz,1H, *trans* CH), 3.57 (m, 1H, CH-N), 2.48 (m, 1H, CH-N), 3.76 (s br, 2H, NH$_2$). ^{13}C NMR (400 MHz, acetone-d$_6$): 90.94 (Cp), 87.46 (Cp), 76.96 (CH), 57.42 (CH$_2$-Fe), 56.70 (CH2 -N), 211.81, 211.75,

210.59, 207.87 (CO). IR (solid state) v_{max}(cm^{-1}): 2078, 2064, 2041, 2004 (CO); 3309, 3270 (NH$_2$). Decomposes without melting at temperature > 129 ˚C.

4.6. Reaction of compound *3* with [Cp*Fe(CO)$_2$(THF)]BF$_4$, *2*

To a stirred solution of compound **3** (0.15 g, 0.467 mmol) in CH$_2$Cl$_2$ (10 ml), a solution of **2** (0.19 g; 0.468 mmol) in CH$_2$Cl$_2$ (10 ml) was added within 30 sec. The mixture was stirred for 12 h after which it was filtered into a pre-weighed Schlenk tube and diethyl ether added to the filtrate to give a yellow precipitate. The precipitate was allowed to stand undisturbed for 5 h and then the mother liquor was removed. Washing the residue with diethyl ether (10 ml) and drying it under reduced pressure afforded 0.128 g (42% yield) of the dinuclear mixed ligand complex [Cp(CO)$_2$Fe(NH$_2$CH$_2$CHCH$_2$)Fe(CO)$_2$Cp*](BF$_4$)$_2$, **9**. Anal. Calc. for C$_{22}$H$_{27}$B$_2$F$_8$Fe$_2$NO$_4$: C, 40.36; H, 4.16; N, 2.14. Found: C, 40.46; H, 3.89; N, 2.16%. ^{1}H NMR (400 MHz, acetone-d$_6$) 5.20 (s, 5H, Cp), 3.71 (m, 1H, CH), 3.54 (br, 1H, *cis* CH), 2.85 (br, 1H, *trans* CH), 3.40 (m, 1H, CH-N), 2.35 (m, 1H, CH-N), 2.01 (s, 15H, Cp*) . ^{13}C NMR (400 MHz, acetone-d$_6$): 87.49 (Cp), 77.50 (CH), 60.42 (CH$_2$-Fe), 56.95 (CH$_2$-N), 9.16 (Cp*), 103.85 (C-Cp*), 213.13, 212.38, 211.88, 211.82 (CO). IR (solid state) v_{max}(cm^{-1}): 2053, 2001br (CO); 3304, 3272 (NH). M.p., 40 - 42 ˚C.

4.7. Reaction of [{Cp(CO)$_2$Fe}$_2$(μ-NH$_2$CH$_2$CHCH$_2$)](BF$_4$)$_2$, *8*, with NaI

To an acetone solution (25 ml) of compound **8** (0.33 g, 0.564 mmol) was added NaI (1.02 g, 6.80 mmol). The solution was stirred at 35 ˚C for 12 h, during which the solution turned from yellow to dark brown. The solvent was removed under reduced pressure and the residue extracted with dichloromethane (30 ml). The extract was then concentrated to about one third of the initial volume. Addition of diethyl ether completed the precipitation of the allylamino complex [Cp(CO)$_2$Fe(NH$_2$CH$_2$CH=CH$_2$)]I, **12**, which was filtered off, washed with diethyl ether (2 x 10 ml) and dried under reduced pressure. It was purified further by recrystallization from acetone / diethyl ether 1:4 v/v. to give a bright yellow microcrystalline solid (0.114 g, 56%). Anal. Calc. for C$_{10}$H$_{12}$FeINO$_2$: C, 33.27; H, 3.35; N, 3.88. Found: C, 33.35; H, 3.54; N, 3.76%. ^{1}H NMR (600 MHz, acetonel-d$_6$) 5.62 (s, 5H, Cp), 4.14 (s, 2H, NH$_2$), 3.09 (q, J_{HH} = 6.18 Hz, 2H, -CH$_2$), 6.01 (m, 1H, =CH), 5.15 (d, J_{HH} = 10.02 Hz, 1H,

=CH*cis*), 5.28 (d, J_{HH} = 17.16 Hz, 1H, =CH *trans*). ^{13}C NMR (600 MHz, acetone-d6): 86.54 (Cp), 53.85 (-CH$_2$), 135.77 (CH=), 118.02 (=CH$_2$), 211.73 (CO). IR (solid state) v_{max}(cm[-1]): 2042, 2002 (CO); 3152 br (NH$_2$). M.p., 130-131 ˚C.

The filtrate was evaporated to dryness to give a purple grey microcrystalline solid (0.53 g; 31% yield) which according to IR and NMR was found to be the known [Cp(CO)$_2$FeI] [50]

4.8. Reaction of allylamine with one equivalent of [Cp*Fe(CO)$_2$(THF)]BF$_4$, 2

3-Amino-1-propene (0.039 ml, 0.523 mmol), was added to a solution of compound **2** (0.21 g, 0.517 mmol) in CH$_2$Cl$_2$ (10 ml) and the mixture stirred at room temperature for 12 h. The mixture was filtered into a pre-weighed Schlenk tube and diethyl ether added to the filtrate. The mixture was allowed to stand in the dark at room temperature for 18 h after which yellow-brown crystals stuck on the walls of the Schlenk tube. The mother liquor was syringed off and the crystals washed with diethyl ether (2 x 5 ml) after which it was dried under reduced pressure to give 0.158 g (78%) of compound **4**. Anal. Calc. for C$_{15}$H$_{22}$BF$_4$FeNO$_2$: C, 46.08; H, 5.67; N, 3.58. Found: C, 45.93; H, 6.03; N, 3.39%. ^{1}H NMR (400 MHz, acetone-d$_4$) 1.93 (s, 15H, Cp*), 3.23 (br, 2H, NH$_2$), 3.08 (q, J_{HH} = 6.80 Hz, 2H, -CH$_2$), 5.84 (m, 1H, =CH), 5.21 (d, 1H, J_{HH} = 17.17 Hz, =CH$_2$), 5.15 (d, 1H, J_{HH} = 10.33 Hz, =CH$_2$). ^{13}C NMR (400 MHz, acetone-d$_6$): 9.26 (Cp), 98.71 (C-Cp*), 55.10 (-CH$_2$), 136.57 (CH=), 118.86 (=CH$_2$), 214.42 (CO). IR (solid state) v_{max}(cm[-1]): 2029, 1983 (CO); 3212, 3280 (NH$_2$). M.p., 131-132 ˚C.

4.9. Reaction of [Cp*(CO)$_2$Fe(NH$_2$CH$_2$CH=CH$_2$)]BF$_4$, 4 with bromine

To a solution of compound **4** (0.21 g, 0.537 mmol) in CH$_2$Cl$_2$ (10 ml), bromine (0.05 ml, 1.048 mmol) was added and the mixture stirred for 5 h. The solvent was removed resulting in a yellow solid which was recrystallized from dichloromethane/diethyl ether (1:6 v/v) to give an Orange microcrystalline solid of [Cp*(CO)$_2$Fe{NH$_2$CH$_2$CH(Br)CH$_2$Br}]BF$_4$, **7**. Yield, 0.145 g, 49%. Anal. Calc. for C$_{15}$H$_{22}$BF$_4$Br$_2$FeNO$_2$: C, 32.71; H, 4.03; N, 2.54. Found: C, 32.41; H, 4.06; N, 2.23%. ^{1}H NMR (400 MHz, acetone-d$_6$) 4.47 (m, 1H, CHBr), 3,94 (m, 2H, CH$_2$Br), 3.15 (m, 1H, CH-N), 2.83 (m, 1H, CH-N), 3.34 (br, 2H, NH$_2$), 1.97 (s, 15H, Cp*). ^{13}C NMR

(400 MHz, acetone-d_6): 54.31 (CHBr), 57.07 (CH_2N), 35.16 (CH_2Br), 9.47 (Cp*), 98.83 (C-Cp*), 213.87, 213.70 (CO). IR (solid state) v_{max}(cm^{-1}): 2034, 1978 (CO); 3296, 3268 (NH). M.p., 111-112 ˚C.

4.10. Reaction of compound 4 with compound 1

To a solution of compound **4** (0.12 g, 0.307 mmol) in CH_2Cl_2 (10 ml), a solution of **1** (0.11 g, 0.325 mmol) was added and the mixture stirred overnight. The mixture was filtered and diethyl ether was added into the filtrate to form an orange suspension. The mixture was kept at zero degrees for 8 hours after which it was filtered and the residue washed with diethyl ether (2 x 5 ml) to give an orange–yellow solid. This was dissolved in a minimum of dichloromethane and precipitated using diethyl ether and then filtered. This process was repeated three times to give the pure mixed-ligand compound [Cp*(CO)$_2$Fe(NH$_2$CH$_2$CHCH$_2$)Fe(η^5-C$_5$H$_5$)(CO)$_2$](BF$_4$)$_2$, **10**. Yield 0.091 g, 45%. Anal. Calc. for $C_{22}H_{27}B_2F_8Fe_2NO_4$: C, 40.36; H, 4.16; N, 2.14. Found: C, 40.26; H, 4.19; N, 2.13%. ^{1}H NMR (400 MHz, acetone-d_6) 5.90 (s, 5H, Cp), 5.18 (m, 1H, CH), 4.15(d, J_{HH} = 8.20 Hz, 1H, *cis* CH), 3.58 (d, J_{HH} = 14.28 Hz, 1H, *trans* CH), 3.50 (m, 1H, CH-N), 2.31 (m, 1H, CH-N), 1.90 (s, 15H, Cp*) . ^{13}C NMR (400 MHz, acetone-d_6): 91.03 (Cp), 76.52 (CH), 57.99 (CH$_2$-Fe), 57.02 (CH$_2$-N), 9.18 (Cp*), 98.76 (C-Cp*), 213.90, 213.81, 210.72, 208.31 (CO). IR (solid state) v_{max}(cm^{-1}): 2080, 2027, 1971 (CO); 3311, 3265 (NH). M.p., 33-35 ˚C.

4.11. Reaction of compound 4 with compound 2

To a solution of compound **2** (0.02 g, 0.049 mmol) in CH_2Cl_2 (10 ml), a solution of compound **4** (0.02 g, 0.051mmol) in CH_2Cl_2 (10 ml) was added. The mixture was stirred at room temperature for 16 h after which diethyl ether was added until a yellow precipitate was formed. This was allowed to settle for 20 min and the mother liquor was removed. The residue was washed with diethyl ether and dried under reduced pressure to give 0.018 g of the dinuclear complex [{(Cp*)(CO)$_2$Fe}$_2$(μ-NH$_2$CH$_2$CHCH$_2$)](BF$_4$)$_2$, **11**. Yield. 51%. Anal. Calc. for $C_{27}H_{37}B_2F_8Fe_2NO_4$: C, 44.74; H, 5.14; N, 1.93%. Found: C, 45.12; H, 5.29; N, 1.97%. ^{1}H NMR (400 MHz, acetone-d_6) 4.11 (m, 1H, CH), 3.55 (d, J_{HH} = 13.85 Hz, 1H, *trans* CH), 3.18 (d, J_{HH} = 7.76 Hz, 1H, *cis* CH), 3.28 (m,

1H, CH-N), 2.24 (m, 1H, CH-N), 2.01 (s, Cp*-CH2) 1.89 (s, 15H, Cp*-N) . ^{13}C NMR (400 MHz, acetone-d_6): 78.08 (CH), 60.99 (CH_2-Fe), 57.27 (CH_2-N), 9.19 (Cp*), 9.27 (cp*) 98.74 (C-Cp*), 103.87 (C-Cp*), 213.92, 213.05, (CO). IR (solid state) v_{max}(cm^{-1}): 2050, 2014, 1986, 1955 (CO); 3309, 3259 (NH). Decomposes without melting at temperature > 140 ˚C.

4.12. Single crystal X-ray diffraction

Crystals of compounds **3**, **4** and **7** suitable for single crystal X-ray diffraction were obtained by the liquid diffusion method of crystal growth. A nitrogen-saturated solution of each compound in dichloromethane was layered with diethyl ether and kept in the dark at room temperature for a period of one week. The X-ray diffraction data of **3** and **4** were collected on a Bruker *APEX II CCD* area detector diffractometer with graphite monochromated Mo Kα radiation (50 kV, 30 mA) using the Apex2 [51] data collection software, while that of **7** was collected on *SMART APEX CCD* diffractometer, also using Mo Kα radiation. The structures were solved and refined using *SHELXS-97* and *SHELXL-97* [52] while molecular graphics were generated using *OLEX2* [53]. The crystallographic data and structural refinement information for compounds **3**, **4** and **7** are summarized in Table 4.

Table 4: Crystal data and structure refinement for compound **3**, **4** and **7**

Compound	Compound **3**	Compound **4**	Compound **7**
Empirical formula	$C_{10}H_{12}BF_4$ Fe N O_2	$C_{15}H_{22}BF_4FeNO_2$	$C_{15}H_{22}BBr_2F_4FeNO_2$
Formula weight	320.87	391.00	550.82
Temperature (K)	173(2)	173(2)	100(2)
Wavelength (Å)	0.71073	0.71073	0.71073
Crystal system	monoclinic	Triclinic	Triclinic
Space group	C2/c	P-1	P-1
Unit cell dimension			
a (Å)	15.250(3), $\alpha = 90$	9.5051(2), $\alpha = 64.913(2)$	9.3954(10), $\alpha = 88.6930(10)$
b	8.8443(17), $\beta = 93.209(5)$	9.5487(3) , $\beta = 84.663(2)$	10.5527(11) , $\beta = 79.3410(10)$
c	18.981(4), $\gamma = 90$	11.0937(3), $\gamma = 73.277(2)$	11.0867(12), $\gamma = 66.3740(10)$
Volume (Å^3)	2556.2(8)	872.84(4)	988.09(18)
Z	8	2	2
Density (calculated)(Mg/m^3)	1.668	1.488	1.851
Absorption coefficient (mm^{-1})	1.224	0.910	4.852
F(000)	1296	404	544
Crystal size (mm)	0.39 x 0.29 x 0.13	0.47 x 0.30 x 0.15	0.30 x 0.25 x 0.20
Theta range for data collection	2.15 to 28.00°.	2.03 to 28.00	1.87 – 28.74°.
Index ranges			
h	$-20 \to 20$	$-12 \to 12$	$-12 \to 12$
k	$-11 \to 11$	$-12 \to 12$	$-13 \to 13$
l	$-24 \to 25$	$-14 \to 11$	$-14 \to 14$
Reflections collected	9761	8448	11875
Independent reflections	3083	4204	4698
Internal fit	R(int) = 0.0618	R(int) = 0.0366	R(int) = 0.0206
Absorption correction	integration	integration	Multi-scan
Transmission factor (T_{Min};T_{Max})	0.6469; 0.8571	0.6742; 0.8755	0.3238; 0.4436
Refinement method	Full-matrix least-squares on F^2	Full-matrix least-squares on F^2	Full-matrix least-squares on F^2
parameters	172	222	276
Goodness-of-fit on F^2	1.113	1.029	1.091
Final R indices [I>2sigma(I)]	R1 = 0.0675, wR2 = 0.2098	R1 = 0.0322, wR2 = 0.0802	R1 = 0.0410 wR2 = 0.0909
R indices (all data)	R1 = 0.0840, wR2 = 0.2188	R1 = 0.0422, wR2 = 0.0849	R1 = 0.0475, wR2 = 0.0931
Largest diff. peak and hole(e.Å^{-3})	2.327 and – 0.618	0.508 and – 0.258	1.550 and – 0.905

Acknowledgement

Supplementary material

CCDC 851115, 851116 and 851117 contains the supplementary crystallographic data for compounds **4**, **7** and **3**, respectively. These data can be obtained free of charge *via* http://www.ccdc.cam.ac.uk/conts/retrieving.html, or from the Cambridge Crystallographic Data Centre, 12 Union Road, Cambridge CB2 1EZ, UK; fax: (+44) 1223-336-033; ore-mail: deposit@ccdc.cam.ac.uk. Crystallographic data for compounds 3, 4 and 7 are given in Appendix 9. CD-ROM containing CIF of the crystals and spectroscopic data is given in appendix 12.

References

[1]   M. Rosenblum, Acc. Chem. Res. 7 (1974) 122.

[2]   L. Hermans, S.F. Mapolie, Polyhedron 16 (1997) 869.

[3]   M.L.H. Green, P.L.I. Nagy, J. Chem. Soc. (1963) 189.

[4]   A. Sivaramakrishna, H.S. Clayton, C. Kaschula, J.R. Moss, Coord. Chem. Rev. 251 (2007) 1294.

[5]   M.L.H. Green, M.J. Smith, J. Chem. Soc (A). (1971) 3220.

[6]   G. Joorst, R. Karlie, S.F. Mapolie, S. Afr. J. Chem. 51 (1998) 132.

[7]   P.J. Lennon, A. Rosan, M. Rosenblum, J. Trancrede, P. Waterman, J. Am. Chem. Soc. 102 (1980) 7033.

[8]   G. Joorst, R. Karlie, S.F. Mapolie, Polyhedron 18 (1999) 3377.

[9]   D. Dooling, G. Joorst, S.F. Mapolie, Polyhedron 20 (2001) 467.

[10] T.W. Bodnar, A.R. Cutler, Organometallics 4 (1985) 1558.

[11] E.O. Changamu, H.B. Friedrich, M. Rademeyer, J. Organomet. Chem. 693 (2008) 164.

[12] E.O. Changamu, H.B. Friedrich, J. Organomet. Chem. 692 (2007) 1138.

[13] L. Busetto, A. Palazzi, R. Ros, U. Belluco, J. Organomet. Chem. 25 (1970) 207.

[14] E.K. Barefield, D.J. Sepelak, J. Am. Chem. Soc. 101 (1979) 6542.

[15] H.B. Friedrich, P.A. Makhesha, J.R. Moss, B.K. Williamson, J. Organomet. Chem. 384 (1990) 325.

[16] J.R. Moss, J. Organomet. Chem. 231 (1982) 229.

[17] H.B. Friedrich, K.P. Finch, M.A. Gafoor, J.R. Moss, Inorg. Chim. Acta 206 (1993) 225.

[18] A. Cutler, D. Ehntholt, P. Lennon, K. Nicholas, D.F. Marten, M. Madhavarao, S. Raghu, A. Rosan, M. Rosenblum, J. Am. Chem. Soc. 97 (1975) 3149.

[19] E.O. Changamu, H.B. Friedrich, J. Organomet. Chem. 693 (2008) 3351.

[20] A. Cutler, D. Ehntholt, W.P. Ciering, P. Lennon, S. Raghu, A. Rosan, M. Rosenblum, J. Tancrede, D. Wells, J. Am. Chem. Soc. 98 (1976) 3495.

[21] R.W. Johnson, R.G. Pearso, Chem. Commun. (1970) 986.

[22] P.L. Bock, D.J. Boschetto, J.R. Rasmussen, J.P. Demers, G.M. Whitesides, J. Am. Chem. Soc. 96 (1974) 2814.

[23] F.R. Jensen, V. Madan, D.H. Buchanan, J. Am. Chem. Soc. 93 (1971) 5283.

[24] R.G. Pearson, W.R. Muir, J. Am. Chem. Soc. 92 (1970) 5519.

[25] G.M. Whitesides, D.J. Boschetto, J. Am. Chem. Soc. 93 (1971) 1529.

[26] G. Gerebtzoff, X. Li-Blatter, H. Fischer, A. Frentzel, A. Seeling, Chem. Bio. Chem. 5 (2004) 676.

[27] P. Legzdins, W.S. McNeil, R.J. Batchelor, F.W.B. Einstein, J. Am. Chem. Soc. 117 (1995) 10521.

[28] P.G. Hayes, S.A.M. Stringer, C.M. vogels, S.A. Westcott, Trans. Met. Chem. 26 (2001) 261.

[29] C.M. M'thiruaine, H.B. Friedrich, E.O. Changamu, M.D. Bala, Inorg. Chim. Acta (2011) in press. doi:10.1016/j.ica.2011.1009.1058.

[30] C.M. M'thiruaine, H.B. Friedrich, E.O. Changamu, M.D. Bala, Inorg. Chim. Acta 366 (2011) 105.

[31] M. Akita, S. Kakuta, S. Sugimoto, M. Terada, M. Tanaka, Y. Moro-oka, Organometallics 20 (2001) 2736.

[32] R.B. English, L.R. Nassimbeni, R.J. Haines, J. Chem. Soc. Dalton Trans. (1978) 1379.

[33] P.M. Treichel, R.L. Shubkin, K.W. Barnett, D. Reichard, Inorg. Chem. 5 (1966) 1177.

[34] J. Mohan, Organic Spectroscopy. , 2 ed., Narosa publishing house, New Delhi, 2007.

[35] K. Dralle, N.L. Jaffa, T.l. Roex, J.R. Moss, S. Travis, N.D. Watermeyer, A. Sivaramakrishna, Chem. Commun. (2005) 3865.

[36] C.M. M'thiruaine, H.B. Friedrich, E.O. Changamu, B. Omondi, Acta Cryst. E67 (2011) m485.

[37] R. Hänel, P. Bubenitschek, H. Hopf, P.G. Jones, Acta Cryst. E62 (2006) o1480.

[38] S.S. Batsanov, L.L. Kozhevina, Russ. J. General Chem. 74 (2004) 314.

[39] B.T. Luke, J.R. Collins, G.H. Loew, A.D. McLean, J. Am. Chem. Soc. 112 (1990) 8686.

[40] S.P. McManus, D.W. Ware, R.A. Hames, J. Org. Chem. 43 (1978) 4288.

[41] A. Palazzi, S. Stagni, J. Organomet. Chem. 690 (2005) 2052.

[42] H.B. Friedrich, J.R. Moss, J. Chem. Soc. Dalton Trans. (1993) 2863.

[43] H.S. Clayton, J.R. Moss, M.E. Dry, J. Organomet. Chem. 688 (2003) 181.

[44] D.E. Laycock, J. Hartgerink, M.C. Baird, J. Org. Chem. 45 (1980) 291.

[45] E.O. Changamu, H.B. Friedrich, M. Rademeyer, J. Organomet. Chem. 692 (2007) 2456.

[46] K.M. Nicholas, A.M. Rosan, J. Organomet. Chem. 84 (1975) 351.

[47] B.F. Hallam, P.L. Pauson., J. Chem. Soc. (1956) 3030.

[48] B.S. Furniss, A.J. Hannaford, P.W.G. Smith, A.R. Tatchell, Vogel's, 5th ed., John Wiley and Sons, Inc, New York, 1991.

[49] M. Akita, M. Tarada, M. Tanaka, Y. Morooka, J. Organomet. Chem. 510 (1996) 255.

[50] O.A. Gansow, D.A. Schexnayder, B.Y. Kimura, J. Am. Chem. Soc. 94 (1972) 3406.

[51]   Bruker, *APEX2*. Version 2009.1-0. Bruker AXS Inc., Madison, Wisconsin, USA., (2005).

[52]   G.M. Sheldrick, Acta Cryst. A64 (2008) 112.

[53]   O.V. Dolomanov, L.J. Bourhis, R.J. Gildea, J.A.K. Howard, H. Puschmann, J. Appl. Cryst. 42 (2009) 339

CHAPTER SIX

Regioselective reactions of electrophilic iron dicarbonyl cations, [(η^5-C$_5$R$_5$)(CO)$_2$Fe]$^+$ (R = H, CH$_3$) with heterofunctional amine ligands

Cyprian M. M'thiruaine[a], Holger B. Friedrich[a*], Evans O. Changamu[b]

[a] School of Chemistry, University of KwaZulu-Natal, Private Bag X54001, Durban 4000, South Africa [b] Chemistry Department, Kenyatta University, P.O Box 43844 Nairobi

* Corresponding author

Abstract

The reactions of the ether complexes [(η^5-C$_5$R$_5$)(CO)$_2$Fe(E)]BF$_4$, (R =H, E = Et$_2$O; R = CH$_3$, E = THF) with various ligands possessing two different coordination sites have been investigated. It was established that [(Cp(CO)$_2$Fe(OEt$_2$)]BF$_4$ (Cp = η^5-C$_5$H$_5$), **1**, and [Cp*(CO)$_2$Fe(THF)]BF$_4$ (Cp* = η^5-C$_5$(CH$_3$)$_5$), **2**, react with 1-aminopropanol, 4-methoxybenzylamine and 3-aminopropyltriethoxysilane to give only monuclear complexes of the type [(η^5-C$_5$R$_5$)(CO)$_2$Fe(L)]BF$_4$, irrespective of the reactant ratios. On the other hand, the reaction of **1** with one equivalent of 4-aminobenzonitrile (ABN) furnished both monuclear and dinuclear complexes, [Cp(CO)$_2$Fe(ABN))]BF$_4$ and [{Cp(CO)$_2$Fe}$_2$(µ-ABN)](BF$_4$)$_2$, with the monuclear complex being the major product. The reaction of **1** with 1,4-phenylenedimethanamine (PDA) afforded only the dinuclear complex [{Cp(CO)$_2$Fe}$_2$(µ-PDA)](BF$_4$)$_2$ regardless of the reactant ratios. The reaction of **2** with one equivalent of the monuclear complex [Cp(CO)$_2$Fe(ABN)]BF$_4$ gave the mixed ligand complex [Cp(CO)$_2$Fe(ABN)Fe(CO)$_2$Cp*](BF$_4$)$_2$. The reactions of dipropylamine with [Cp(CO)$_2$Fe(OEt$_2$)]BF$_4$ gave the dipropylamine complex [Cp(CO)$_2$Fe{NH(CH$_2$CH$_2$CH$_3$)$_2$}]BF$_4$. All these compounds are reported for the first time and have been fully characterized by ^{1}H NMR, ^{13}C NMR, IR spectroscopy and elemental analysis. Molecular structures of [Cp(CO)$_2$Fe{NH(CH$_2$CH$_2$CH$_3$)$_2$}]BF$_4$, [Cp*(CO)$_2$Fe{NH$_2$(CH$_2$)$_2$CH$_2$OH}]BF$_4$ and [Cp*(CO)$_2$Fe(NH$_2$C$_6$H$_4$OCH$_3$)]BF$_4$ have been confirmed by single crystal X-ray crystallography.

Keywords: Iron dicarbonyl complexes; Heterofunctional ligands; Regioselectivity

1. Introduction

Despite the great role played by the amine functionality in catalysis [1-5], pharmacology [6-15] and physiology [16-19], the coordination of simple amine ligands to transition metals is an area in chemistry that appears to be relatively ignored. We recently embarked on the study of the reactions of substitutionally unsaturated ether complexes $[(\eta^5\text{-}C_5R_5)(CO)_2Fe(E)]BF_4$ (R = H: E= Et$_2$O; R = Me: E = THF) with various types of amine ligands and we have reported a number of nitrogen-containing complexes [20-23]. We found that these complexes are stable and the majority are soluble in water. Very recently we reported on organometallic complexes of the type $[(\eta^5\text{-}C_5R_5)(CO)_2Fe(NH_2CH_2CH=CH_2)]BF_4$ and showed that the cationic moiety $[(\eta^5\text{-}C_5R_5)(CO)_2Fe]^+$ selectively binds to the amine functionality of the allylamine. It was also found that these compounds can be used as precursors in the syntheses of chiral organometallic compounds, since the pendant vinyl group is capable of undergoing addition reactions such as halogenation or coordination [24]. In this paper we report on amine complexes of iron in which the amine ligand contains a second donor group such as oxygen, cyanide, etc. competing for the metal centre with the amine moiety. The compounds $[(\eta^5\text{-}C_5R_5)(CO)_2Fe\{(CH_2)_3Si(OCH_3)\}]$ (R = H, CH$_3$) [25], $[CpCO)_2Fe\{(CH_2)_3Si(OCH_2CH_3)_3\}]$ [26], $[Cp(CO)_2Fe(C_6H_5OCH_3)]$ [27] and $[(\eta^5\text{-}C_5R_5)(CO)_2Fe\{(CH_2)_nCH_2OH\}](R = H, CH_3)$ [28] resemble, to a degree, some of the compounds reported in this paper.

2. Results and discussion

The reactions of the ether complexes $[(\eta^5\text{-}C_5R_5)(CO)_2Fe(E)]BF_4$ (R = H: E= Et$_2$O (**1**); R = Me: E = THF (**2**)) with heterofunctional amine ligands (1-aminopropanol, 4-methoxybenzylamine, 3-aminopropyltriethoxysilane and 4-aminobenzonitrile) proceed at room temperature with coordination to the amine functionality as shown in Scheme 1. Except for compound **3**, which was obtained as an oil, all other compounds were obtained as yellow moderately air stable solids which are soluble in polar solvents such as water, acetonitrile, methanol and acetone. All of the dinuclear complexes (**12-16**) precipitated out from their reaction mixtures and were easily separated by filtration.

Unlike the dinuclear complexes, all of the monuclear complexes (**3-11**) are also soluble in dichloromethane and they were precipitated from their solution by addition of diethyl ether. The monuclear complexes $[(\eta^5\text{-}C_5R_5)(CO)_2Fe(ABN)]BF_4$ (ABN = 4-aminobenzonitrile; R = H, CH$_3$) are transformed into the dinuclear complexes $[\{(\eta^5\text{-}C_5R_5)(CO)_2Fe\}_2(\mu\text{-}ABN)](BF_4)_2$ by reaction with the appropriate etherate complex. All of these complexes are new and have been fully characterized by IR and NMR spectroscopy and elemental analysis. The molecular structures of **4**, **6** and **8** have been established by single crystal X-ray diffraction. Generally, the melting points or decomposition temperatures of the Cp* complexes are higher than those of their corresponding Cp analogues.

Mononuclear complexes

	R	L
3	H	NH$_2$(CH$_2$)$_2$CH$_2$OH
4	CH$_3$	NH$_2$(CH$_2$)$_2$CH$_2$OH
5	H	*p*-NH$_2$CH$_2$C$_6$H$_4$OCH$_3$
6	CH$_3$	*p*-NH$_2$CH$_2$C$_6$H$_4$OCH$_3$
8	H	NH(CH$_2$CH$_2$CH$_3$)$_2$
9	H	NH$_2$(CH$_2$)$_3$Si(OCH$_2$CH$_3$)$_3$

Ether complexes

	R	E
1	H	Et$_2$O
2	CH$_3$	THF

Mononuclear complexes

	R	L
10	H	NH$_2$C$_6$H$_4$CN
11	CH$_3$	NH$_2$C$_6$H$_4$CN

Binuclear complexes

	R	L
12	H	NH$_2$C$_6$H$_4$CN
13	CH$_3$	NH$_2$C$_6$H$_4$CN
15	H	*p*-(NH$_2$CH$_2$)$_2$C$_6$H$_4$
16	CH$_3$	*p*-(NH$_2$CH$_2$)$_2$C$_6$H$_4$
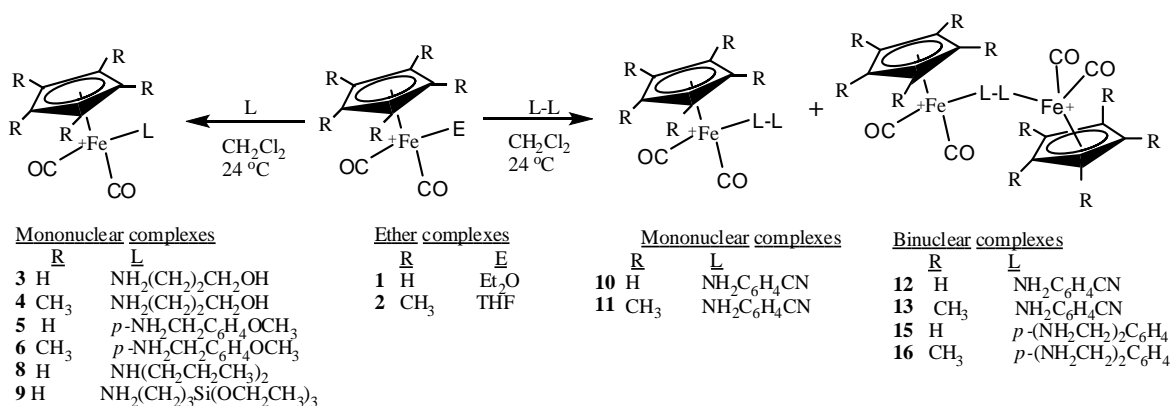
Scheme 1: Reactions of ether complexes with heterofunctional amine ligands

2.1. Synthesis of $[(\eta^5\text{-}C_5R_5)(CO)_2FeL]BF_4$ (**3-9**)

The novel complexes $[(\eta^5\text{-}C_5R_5)(CO)_2FeL]BF_4$ (R = H, CH$_3$; L = NH$_2$(CH$_2$)$_2$CH$_2$OH, NH$_2$CH$_2$C$_6$H$_4$OCH$_3$, NH(CH$_2$CH$_2$CH$_3$)$_2$) and $[Cp(CO)_2Fe\{NH_2(CH_2)_3Si(OCH_2CH_3)_3\}]$ BF$_4$ were obtained in medium to high yields by direct displacement of the ether molecule of the etherate complexes $[(\eta^5\text{-}C_5R_5)(CO)_2Fe(E)]BF_4$ with the appropriate ligands as shown in Scheme 1. Their elemental analysis and infrared spectra data, as well as other physical data, are listed in Table 1. The NMR data is summarized in the experimental section.

In the IR spectra of compounds **3-9**, the v(CO) bands are in the expected range for terminal carbonyl groups of amine-coordinated iron dicarbonyl complexes [20, 22]. The

infrared spectra of the Cp* complexes **4** and **6** show the v(CO) bands at lower frequencies than their Cp counterparts due to the electron releasing ability of the pentamethylcyclopentadienyl ligand which consequently increases the metal→carbon back donation. With the exception of the dipropylamine complex **8**, the infrared spectra of other complexes show two characteristic absorption bands in the range 3315 - 3210 cm^{-1} which correspond to NH_2 symmetrical and asymmetrical stretching. Compound **8** shows one band in this region which is assignable to NH symmetrical stretching.

In the ^{1}H NMR spectra, the regioselective coordination of the metal fragment to NH_2 is unambiguously indicated by downfield shifts of amine protons relative to those of the free ligands. For example, a resonance peak in the ^{1}H NMR spectrum assigned to the amine protons of the coordinated $NH_2CH_2C_6H_4OCH_3$ appeared downfield by ca. 2.18 ppm relative to free ligand, while that of the coordinated $NH_2(CH_2)_2CH_2OH$ shows a downfield shift of ca. 0.64 ppm. Further evidence for amine coordination is a ca. 10.9 ppm downfield shift of the peaks corresponding to the carbon of the methylene group alpha to the amine functionality relative to that of the similar carbon in uncoordinated $NH_2CH_2C_6H_4OCH_3$ and $NH_2(CH_2)_2CH_2OH$, indicating a strong influence of the metal on the amine side. These effects diminish towards the oxygen side, such that the chemical shift of the carbon neighbouring the oxygen does not significantly vary from that of the free ligand. Moreover, the Fe-N bond distances found in the molecular structures of compounds **4**, **6** and **8** (Section 2.1.1) fall within the range 2.020 - 2.058 Å observed for related amine coordinated iron complexes [20-22, 29]. This further confirms that coordination of these ligands occurs *via* the nitrogen atom of the amine group. Although 3-aminopropanol is known to act as a bidentate ligand, whereby N and O are involved in coordination in Ni(NCS)$_2$(C$_3$H$_9$NO)$_2$] [30], in the iron complexes **3** and **4** it acts as a monodentate ligand binding *via* nitrogen only.

The 4-methoxybenzylamine complexes, **5** and **6**, were found to be stable in the aqueous media. For example 75 % of the dissolved compound **5** was recovered from its aqueous solution by extraction using dichloromethane and found to be unchanged after 24 h in aqueous solution as judged by IR, NMR and elemental analysis. The stability of compound **5** in water was further demonstrated by the counter anion exchange reaction with NaBPh$_4$ in deionized water to form [Cp(CO)$_2$Fe(NH$_2$CH$_2$C$_6$H$_4$OCH$_3$)]BPh$_4$ (**7**)

which was also fully characterized. Assignment of ^{1}H NMR and ^{13}C NMR data of compounds **3-9** was done with the help of COSY and HSQC experiments, as well as comparison with the data reported for $[Cp(CO)_2Fe\{CH_2(CH_2)_nCH_2OH\}]$ [28], $[Cp(CO)_2Fe(C_6H_4OCH_3)]$ [31], $[Cp(CO)_2Fe\{CH_2(CH_2)_nCH_3\}]BF_4$ [20] and $[Cp^*(CO)_2Fe\{CH_2(CH_2)_nCH_3\}]BF_4$ [22].

Complex **8**, $[Cp(CO)_2Fe\{NH(CH_2CH_2CH_3)_2\}]BF_4$, was obtained in high yield (73%) by direct displacement of diethyl ether from complex **1** with an equivalent of dipropylamine at room temperature. Similar complexes, $[Cp(CO)_2Fe(NHR_2)]PF_6$ (R = Et, Me, SiMe$_3$) have been obtained in low yield (10 - 35%) from the reaction of $[CpFe(CO)_2Cl]$ with the corresponding amine and NaPF$_6$ [32].

The infrared spectrum of complex **8** shows two strong IR bands in the ν(CO) region at 2061 and 2005 cm^{-1} assignable to two terminal carbonyl ligands and a characteristic single, medium band centred at 3260 cm^{-1} assignable to ν(NH) stretching frequency. The results are in good agreement with the data reported for similar complexes, $[Cp(CO)_2Fe(NHR_2)]PF_6$ (R = Et, Me, SiMe$_3$) [32]. The ^{1}H NMR spectrum of **8** in CDCl$_3$ shows a characteristic triplet, integrating for 6H, at 0.88 ppm (J_{HH} = 7. 28 Hz) corresponding to the two methyl groups. Two poorly resolved multiplets were observed at 1.55 and 2.48 ppm, each integrating for 4H, corresponding to βCH$_2$ and αCH$_2$, respectively, of the two equivalent propyl groups of the coordinated dipropylamine. The characteristic NH proton chemical shift was observed as a broad peak at 4.49 ppm, which was ca. 1.59 ppm downfield relative to those of cyclopentadienyl 1-aminoalkane complexes [20], and ca. 2.19 ppm downfield relative to pentamethylcyclopentadienyl 1-aminoalkane complexes [22]. The ^{13}C NMR spectrum of the complex exhibited a single peak at 86.7 ppm corresponding to the Cp carbons and a single carbonyl peak at 211.1 ppm. As expected, two separate peaks due to the two identical α-carbons and the two identical β-carbons were observed at 60.4 and 20.6 ppm, respectively.

Compound **9** was obtained as a soft yellow solid which decomposed within a month even when stored under nitrogen at 5 ˚C to give an unidentified brown paste. The IR spectrum of **9** showed bands assignable to ν(CO) and ν(NH$_2$) with values that are very close to those observed for other amine coordinated compounds [20]. The ^{1}H NMR spectrum shows that the amine proton shifted downfield by 1.87 ppm relative to that of

uncoordinated 3-aminopropyltriethoxysilane ligand. The shift could be associated with the deshielding effect resulting upon coordination of the amine to the metal.

Table 1: IR, elemental analysis, melting points and percentage yields for monuclear compounds **3-9**

| Compound | Yield (%) | M.p. (˚C) | IR | | Elemental analysis | | |
			ν(CO)	ν(NH)	C: Found (calc)	H: Found (calc)	N: Found (calc)
3	59	oil	2052, 1997	3311, 3273	35.83 (35.40)	4.28(4.13)	3.79 (4.13)
4	62	125	2021, 1969	3300, 3211	43.64 (44.01)	6.08 (5.87)	3.47 (3.42)
5	43	124	2035, 1990	3300, 3273	44.67 (44.89)	4.51 (3.99)	3.94 (3.49)
6	68	170	2021, 1965	3314, 3273	51.41 (50.96)	5.38 (5.52)	3.02 (2.97)
7	59	169	2042, 1990	3299, 3270	74.09 (73.96)	5.47 (5.73)	8.95 (8.82)
8	73	109	2061, 2005	3261	42.32 (42.78)	5.80 (5.52)	3.69 (3.89)
9	47	35	2053, 1998	3308, 3275	39.50 (39.61)	6.02 (5.82)	3.24 2.89)

2.1.1. Single crystal structures of compounds 4, 6 and 8

The molecular structures of compounds **4**, **6** and **8** were established by single crystal X-ray analysis of their tetrafluoroborate salts. Compounds **4** and **6** crystallized in the monoclinic *P2$_1$/c* space group, with one molecular cation and a counterion in each asymmetric unit, while compound **8** crystallized in the tetragonal *P4$_2$/n* space group, with a molecular cation and a counter anion in each asymmetric unit. The molecular structures of **4**, **6** and **8** are shown in Figs. 1a, 2a and 3, respectively.

The overall arrangement around the iron centre corresponds to that of a three-legged piano stool. The iron centre is coordinated to η^5-C$_5$(CH$_3$)$_5$ ligands in compounds **4** and **6** and to a η^5-C$_5$H$_5$ ligand in compound **8**. These ligands occupy three coordination sites to complete an octahedral arrangement around the metal atom with the other sites occupied by two CO ligands and nitrogen of the amine ligand. The distances between the Fe atoms and the centres of the cyclopentadienyl rings are close in all three compounds (1.71 - 1.72 Å) and similar to those in related compounds. Similarly, the Fe–N and Fe–C bond distances exhibited by the molecular structures of **4**, **6** and **8** fall within the range 2.020 - 2.058 and 1.770 - 1.793Å, respectively, observed for related amine coordinated iron complexes; [Cp*(CO)$_2$Fe{NH$_2$(CH$_2$)$_3$CH$_3$}]BF$_4$, 2.022(15)Å and [{Cp*(CO)$_2$Fe}$_2${μ-NH$_2$(CH$_2$)$_3$NH$_2$}](BF$_4$)$_2$, 2.0202 and 2.0182(Å) [22], [{Cp(CO)$_2$Fe}$_2${μ-NH$_2$(CH$_2$)$_2$NH$_2$}](BF$_4$)$_2$, 2.0134(17) and 2.0085(18) Å [21], [Cp(CO)$_2$Fe{NH$_2$(CH$_2$)$_2$CH$_3$}]BF$_4$, 2.017(8)Å, [Cp(CO)$_2$Fe{NH$_2$(CH$_2$)$_3$CH$_3$}]BF$_4$,

2.013(2), 2.006(2) Å [20] and [Cp(CO)$_2$Fe{NH$_2$CH(CH$_3$)$_2$}]BF$_4$, 2.015(4) Å [29].
Selected bond lengths and angles for the compounds **4**, **6** and **8** are listed in Tables 2, 3
and 4, respectively.
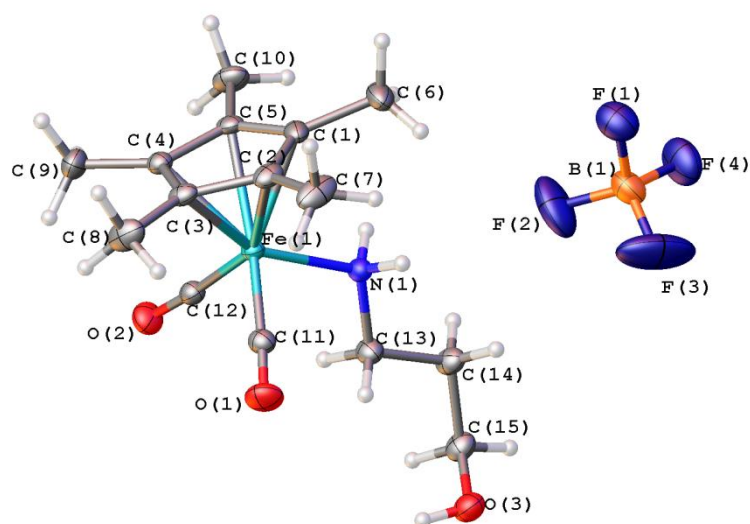
Fig. 1a: Molecular structure of [Cp*(CO)**$_2$**Fe{NH$_2$(CH$_2$)$_2$CH$_2$OH}]BF$_4$, **4**, showing the atomic numbering scheme. Displacement ellipsoids are drawn at 40% probability level and H atoms are shown as small spheres
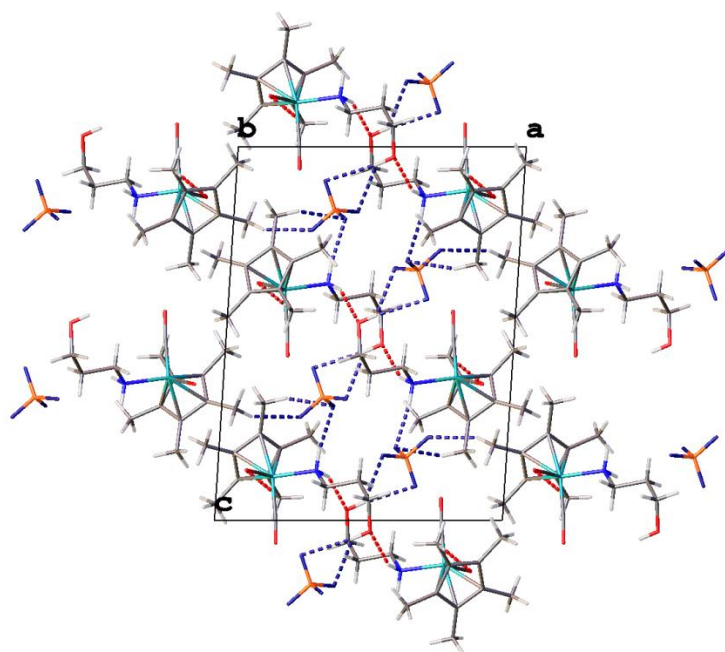
Fig. 1b: Crystal packing of **4** viewed along the *b*-axis showing hydrogen bonding (dotted line).
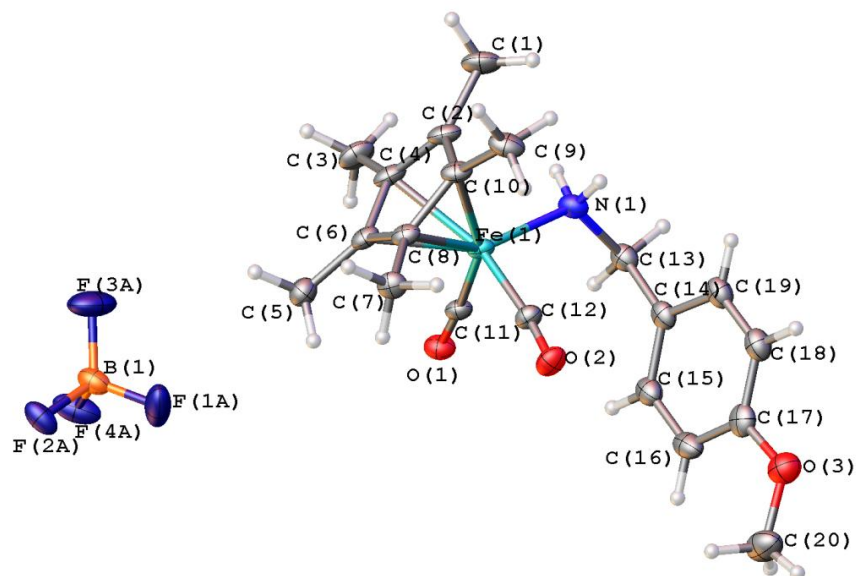
Fig. 2a: Molecular structure of [Cp*(CO)$_2$Fe{NH$_2$CH$_2$C$_6$H$_4$OCH$_3$}]BF$_4$, **6**, showing the atomic numbering scheme with disordered components on the counteranion omitted for clearity. Displacement ellipsoids are drawn at 40% probability level and H atoms are shown as small spheres
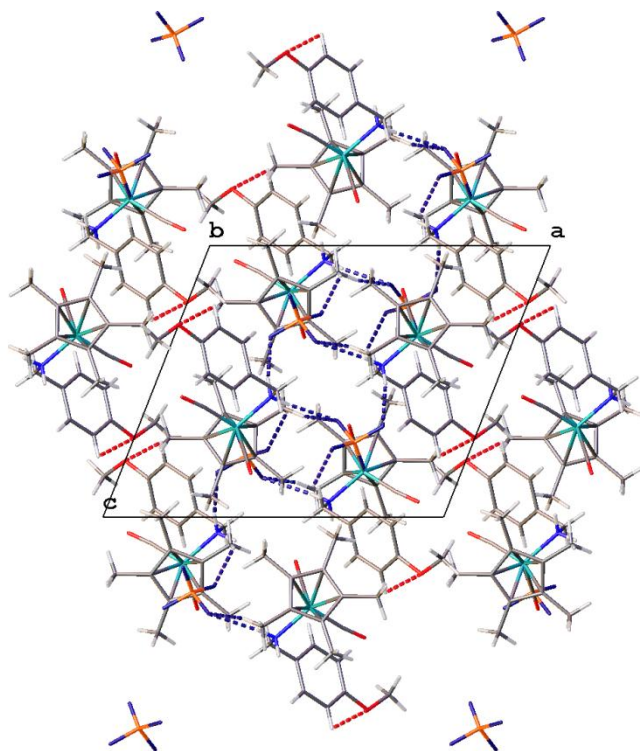
Fig. 2b: Crystal packing of **6** viewed along the *b*-axis showing hydrogen bonding (dotted line)
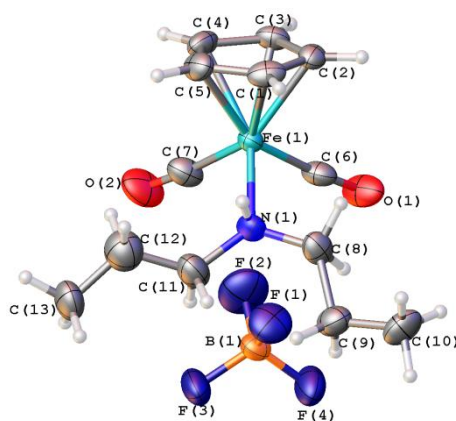
Fig. 3a: Molecular structure of [Cp(CO)$_2$Fe{NH(CH$_2$CH$_3$)$_2$}]BF$_4$, **8**, showing the atomic numbering scheme with the counter anion and disordered components omitted for clarity. Displacement ellipsoids are drawn at 40% probability level and H atoms are shown as small spheres

Table 2. Selected bond lengths and angles for compound **4**

Bond	Length (Å)	Bond	Angle (°)
Cent-Fe1*	1.722	Cent-Fe1-N1	123.61
C11-O1	1.137(3)	Cent-Fe1-C11	121.06
C11-Fe1	1.784(3)	Cent-Fe1-C12	121.39
C12-O2	1.148(3)	O1-C11-Fe1	175.4(2)
C12-Fe1	1.770(3)	O2-C12-Fe1	174.4(2)
C13-N1	1.485(3)	N1-C13-C14	113.6(2)
C13-C14	1.514(3)	C15-C14-C13	112.0(2)
C14-C15	1.513(4)	O3-C15-C14	112.4(2)
C15-O3	1.429(3)	C13-N1-Fe1	116.53(15)
N1-Fe1	2.0209(19)		

Cent is the centroid of the atoms forming the Cp ring, (C1, C2, C3, C4 and C5)

Table 3. Selected bond lengths and angles for compound **6**

Bond	Length (Å)	Bond	Angle (°)
Cent-Fe1*	1.724	Cent-Fe1-N1	122.18
C11-O1	1.145(3)	Cent-Fe1-C11	120.52
C11-Fe1	1.779(2)	Cent-Fe1-C12	120.65
C12-O2	1.142(3)	N1-C13-C14	113.48(19)
C12-Fe1	1.786(2)	C15-C14-C19	118.3(2)
C13-N1	1.497(3)	C15-C14-C13	121.6(2)
C13-C14	1.499(3)	C19-C14-C13	120.0(2)
C14-C15	1.377(4)	C14-C15-C16	121.1(2)
C15-C16	1.409(4)	C17-C16-C15	118.5(2)
C16-C17	1.388(4)	C18-C17-C16	120.9(3)
C17-C18	1.375(4)	C19-C18-C17	120.1(2)
C18-C19	1.367(4)	C18-C19-C14	121.1(3)
C14-C19	1.406(3)	C17-O3-C20	118.3(2)
C17-O3	1.379(3)	C11-Fe1-C12	96.96(10)
C20-O3	1.420(4)	C11-Fe1-N1	92.90(10)
N1-Fe1	2.026(2)	C12-Fe1-N1	97.18(10)
		C13-N1-Fe1	120.30(15)

Cent is the centroid of the atoms forming the Cp ring, (C2, C4, C6, C8 and C10)

Table 4. Selected bond lengths and angles for compound **8**

Bond	Length (Å)	Bond	Angle (°)
Cent-Fe1*	1.715	Cent-Fe1-N1	125.71
C6-O1	1.132(5)	Cent-Fe1-C6	121.76
C6-Fe1	1.793(5)	Cent-Fe1-C7	121.86
C7-O2	1.138(5)	N1-C8-C9	123.2(5)
C7-Fe1	1.774(5)	C8-C9-C10	113.4(5)
C8-N1	1.417(4)	N1-C11-C12	128.2(8)
C8-C9	1.499(5)	C11-C12-C13	120.9(8)
C9-C10	1.507(5)	C11-N1-C8	119.7(5)
C11-N1	1.412(4)	C11-N1-Fe1	124.5(4)
C11-C12	1.419(5)	C8-N1-Fe1	115.5(3)
C12-C13	1.421(6)	C7-Fe1-C6	92.6(2)
N1-Fe1	2.058(4)	C7-Fe1-N1	94.5(3)
		C6-Fe1-N1	91.7(3)

*Cent is the centroid of the atoms forming the Cp ring, (C1, C2, C3, C4 and C5)

In the crystals of compounds **4** and **6** molecules are connected through a series of hydrogen bonds, notably: N–H---F, N–H---O, N–H---F and weak C–H---F intermolecular interactions as shown in Figs. 1b and 2b, to form a three dimensional network structure. The hydrogen bond lengths and angles are given in Table 5.

Table 5. Hydrogen bonds for compounds **4** and **6** [Å and °]

	D-H...A	d(D-H)	d(H...A)	d(D...A)	<(DHA)	Symmetry operators
	C7-H7A…O3	0.98	2.58	3.392(3)	140	1-x, -y, -z
	C7-H7C…O2	0.98	2.49	3.456(3)	167	x, 1+y, z
	C9-H9C…F4	0.98	2.40	3.307(3)	154	1+x, y, z
4	C10-H10C…F1	0.98	2.51	3.362(3)	145	1-x, -½+y, ½-z
	N1-H1A…F1	0.92	2.13	3.033(3)	169	1-x, -½+y, ½-z
	N1-H1B…O3	0.92	2.17	3.020(3)	153	1-x,-y,-z
	O3-H3…F2	0.84	2.33	2.949(3)	131	1-x,-y,-z
	O3-H3…F3	0.84	2.39	3.223(4)	173	1-x,-y,-z
	N1-H1d…F2a	0.87	2.15	3.010(16)	168	1-x, ½+y, ½-z
	N1-H1e…F4a	0.88	2.25	3.113(5)	167	x, ½-y, -½+z
	C1-H1a…F3a	0.98	2.27	3.002(6)	130	1-x, 1-y, 1-z
	C1-H1b…F2a	0.98	2.53	3.456(16)	158	1-x, ½+y, ½-z
6	C1-H1c…F4a	0.98	2.33	3.245(6)	154	x, ½-y, -½+z
	C7-H7b…O2	0.98	2.52	3.478(3)	167	-x, 1-y, -z
	C9-H9b…F2a	0.98	2.53	3.445(16)	156	1-x, ½+y, ½-z
	C20-H20b…F2a	0.98	2.48	3.377(16)	151	-1+x, y, -1+z

2.2. Reactions of *1* and *2* with 4-aminobenzonitrile

4-Aminobenzonitrile (ABN) is a 'push-pull' type of a ligand comprising of NH_2 and CN in *para* positions of the aromatic ring. The NH_2 group is an electron donor, while CN can act as an electron acceptor as well as a weak electron donor. Thus, the reaction of 4-aminobenzonitrile with one equivalent of the ether complex **1** at room temperature gave the monuclear complex $[Cp(CO)_2Fe(ABN)]BF_4$, **10**, and the dinuclear complex $[\{Cp(CO)_2Fe\}_2(\mu\text{-}ABN)](BF_4)_2$, **12**, in 66% and 21% yields, respectively, based on the etherate complex **1**. The dinuclear compound precipitated as soon as the reactants were mixed, but the mixture was stirred for 4 h to ensure complete reaction. The monuclear compound remained in solution and was precipitated as a yellow solid by addition of diethyl ether to the filtrate obtained after separation of the dinuclear complex. The dinuclear complex **12** is a yellow air-stable solid which decomposed without melting at temperatures above 180 °C. It is insoluble in hexane, diethyl ether and chlorinated solvents. However, it is soluble in polar solvents such as acetone, water, acetonitrile and methanol. The monuclear complex, **10**, is moderately stable in the solid state but transformed slowly into the stable dinuclear complex **12** when kept in solution for a long time (> 2 h), even in the absence of complex **1**. The reaction of 4-aminobenzonitrile with two equivalents of the ether complex **1** gave only the dinuclear complex **12**, with the dimer $[CpFe(CO)_2]_2$ being the only by-product isolated from these reactions. Complex **10** reacted with the THF complex, **2**, to form the dinuclear mixed ligand complex $[Cp(CO)_2Fe(\mu\text{-}ABN)Fe(CO)_2Cp^*](BF_4)_2$, **14**, in which the amino end of the ligand is coordinated to the $Cp(CO)_2Fe$ fragment and the cyano end is coordinated to the $Cp^*(CO)_2Fe$ fragment.

4-Aminobenzonitrile (ABN) reacted with one equivalent of **2** to provide both the monuclear and dinuclear complexes $[Cp^*(CO)_2Fe(ABN)]BF_4$, **11,** and $[\{Cp^*(CO)_2Fe\}_2(\mu\text{-}ABN)](BF_4)_2$, **13**. However, due to their high solubility in dichloromethane (the reaction solvent), it was difficult to separate these complexes. A relatively pure sample of the monuclear complex, **11**, was obtained by reacting the THF complex **2** with excess of 4-aminobenzonitrile and precipitating with diethyl ether. The transformation of **11** to the dinuclear complex **13** was faster than the corresponding reaction of compound **10** to give **12**, probably due to the higher affinity that the

Cp*(CO)$_2$Fe group has towards the cyano group, which is a weak donor. Only the dinuclear complex **13** was obtained when the ligand was reacted with two equivalents of the THF complex **2**.

The monuclear complexes **10** and **11** can be easily distinguished from their dinuclear analogues, **12** and **13,** using IR spectroscopy, because ν(CN) increases upon coordination [33-38]. The increase in C≡N stretching frequency as been attributed to increased C≡N bond polarity as the electronegativity of the nitrogen atom of the nitrile group increases on nitrogen-metal bond formation [39]. Complexes **10** and **11** exhibited a weak absorption band at ca. 2239 cm^{-1} corresponding to an uncoordinated cyano group, while the dinuclear complexes **12** and **14** show a peak corresponding to the coordinated cyano group at ca. 2269 cm^{-1}. In addition, the IR spectra of the dinuclear complexes exhibited two bands in the C–O stretching region within the range 2032 – 2081 cm^{-1}, which are assignable to the terminal carbonyls on the cyano side, because nitriles are weakly bound to the metal. These values are in agreement with reported data for related nitrile coordinated cyclopentadienyliron dicarbonyl complexes [33, 36, 37]. The two other expected bands corresponding to terminal carbonyls on the amine side were found to lie within the range 1987- 2040 cm^{-1}, which is also in good agreement with data reported for the related alkylamine complexes [20, 22, 29]. Complex **12** shows a broad strong band at 2040 cm^{-1} suggesting a band overlap. The infrared spectra for the monuclear complexes **10** and **11** show two strong ν(CO) bands assignable to the two terminal carbonyls in the range 1975 – 2056 cm^{-1}. Complex **10** exhibited the ν(CO) bands at 2056 and 2002 cm^{-1}, which, as expected, are at higher wavenumber relative to those of **11**.

The foregoing observations indicate that the metal fragments have a preference for the amino group over the cyano group such that coordination to the cyano group occurs only after the amine group is coordinated. Both monuclear and dinuclear complexes exhibited peaks in their infrared spectra corresponding to NH$_2$ symmetric and asymmetric stretching frequencies at ca. 3374 and 3267 cm^{-1}, respectively. The spectra also show a peak due to the NH bending mode at ca 1605 cm^{-1}. The NH$_2$ stretching frequencies are higher relative to those observed in aliphatic amine complexes. This is probably due to the inductive effect by the aromatic ring neighbouring the amine group.

152
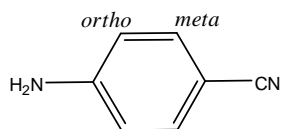
Fig. 4: The labelling scheme for 4-aminobenzonitrile

The ^{1}H NMR spectrum of the monuclear complex, **10**, shows a singlet assignable to the five protons of the cyclopentadienyl ligand at 5.37 ppm and two doublets corresponding to the two identical protons at each of the *ortho* and *meta* positions (Fig.4) of the phenyl ring at 7.22 and 7.74 ppm, respectively. Its ^{13}C NMR spectrum shows a peak corresponding to two *ortho* carbons at 121.0 ppm which is 5.5 ppm down-field relative to that of the similar carbon in the free ligand.

The ^{1}H NMR spectra of the dinuclear complexes **12**, **13** and **14** clearly show that the 4-aminobenzonitrile group bridged the two metal fragments. The ^{1}H NMR spectrum of complex **12** shows two distinct singlets corresponding to the Cp group attached to Fe on the cyano side and the Fe on the amine side, respectively. Similarly, the ^{1}H NMR spectrum of **13** exhibited two distinct peaks corresponding to two non-equivalent Cp* groups, while the mixed ligand complex shows a peak corresponding to the Cp attached to the Fe on the amine side and a peak corresponding to Cp* attached to the Fe on the cyano side. The peaks due to the Cp or Cp* protons on the cyano side are deshielded due to the weak donating ability of the cyano group as compared to the amine which is a strong electron donor. This results in weak metal-carbon backdonation to CO, which causes the IR stretching bands of the terminal carbonyls attached to the metal on the cyano side to appear at higher stretching frequencies relative to their counterparts on the amine side. Furthermore, the ^{13}C NMR data of the dinuclear complexes **12**, **13** and **14** show four peaks in the carbonyl region, which can be assigned to the two sets of terminal carbonyl groups. Generally, the ^{13}C NMR data of the dinuclear complexes show that the electrophilic effect of the metal is more felt on the amine side than on the cyano side. For example, the peak due to the carbons at the *ortho* position shifted downfield relative to those of the free ligand by ca 7.4 ppm, compared to a 1.7 ppm downfield shift of the peaks due to the *meta* carbon upon coordination.

2.3. Reactions of 1 and 2 with 1,4-phenylenedimethanamine (PDA)

The reaction of the etherate complexes, **1** and **2**, with one or two equivalents of 1,4-phenylenedimethanamine (ABM) at room temperature results in immediate formation of the dinuclear complexes [{(η^5-C$_5$R$_5$)(CO)$_2$Fe}$_2$(μ-PDA)](BF$_4$)$_2$ (R = H (**15**), R = CH$_3$ (**16**)) as the only isolable amine complexes. The dimers [(η^5-C$_5$R$_5$)Fe(CO)$_2$]$_2$ (R = H, CH$_3$) were the only by-products isolated from the mother liquors. Dinuclear complexes **15** and **16** were obtained as yellow powders that are insoluble in hexane, diethyl ether and dichloromethane. They show two strong ν(CO) bands assignable to the four terminal carbonyls in the range 1970 - 2054 cm^{-1}, with those of compound **15** appearing at higher frequency than those of **16** by ca. 28 cm^{-1}. The ^{1}H NMR spectrum of compound **15** in acetone shows four characteristic singlets at 5.58, 3.89, 3.68 and 7.34 ppm corresponding to 10H (Cp), 4H (NH$_2$), 4H (CH$_2$) and 4H (C$_6$H$_4$), respectively. The peak corresponding to the amine protons appeared downfield relative to the 2.83 ppm observed for the free ligand. This can be ascribed to deshielding of the amine protons as nitrogen donates its lone pair of electrons to the metal. A similar pattern was observed in complex **16**, whose NMR data were collected in acetonitrile. The ^{13}C NMR spectra of complexes **15** and **16** show a peak assignable to two identical methylene carbons at 56.5 ppm and 54.5 ppm, respectively, further confirming that the amine ligand symmetrically links the two metals *via* the nitrogens.

The complex **15** undergoes counteranion exchange with sodium tetraphenyl borate in deionized water to give the analytically pure complex [{Cp(CO)$_2$Fe}$_2$(μ-PDA)](BPh$_4$)$_2$, **17**, in 63% yield. Complex **17** was obtained as a yellow microcrystalline solid which is insoluble in water, dichloromethane and hexane, but soluble in acetone, acetonitrile and methanol.

3. Conclusion

The reactions of the ether complexes [(η^5-C$_5$R$_5$)(CO)$_2$Fe(E)]BF$_4$ (R = H: E= Et$_2$O; R = Me: E = THF) with heterofunctional amine ligands have shown that the cation [(η^5-C$_5$R$_5$)(CO)$_2$Fe]$^+$ selectively binds to the amine functionality to form monuclear complexes. The homofunctional 1,4-phenylenedimethanamine gave only dinuclear

complexes in all stoichiometric ratios. The molecular structures of [Cp*(CO)$_2$Fe{NH$_2$(CH$_2$)$_2$CH$_2$OH}]BF$_4$, [Cp*(CO)$_2$Fe{NH$_2$CH$_2$C$_6$H$_4$OCH$_3$}]BF$_4$ and [Cp(CO)$_2$Fe{NH(CH$_2$CH$_2$CH$_3$)$_2$}]BF$_4$ have been confirmed by single crystal x-ray crystallography.

4. Experimental

4.1. General

All experimental manipulations were carried out under inert atmosphere using standard Schlenk procedures unless otherwise stated. Reagent grade THF, hexane and Et$_2$O were distilled from sodium/benzophenone and used immediately; acetone and MeCN were distilled from anhydrous CaCl$_2$ and stored under molecular sieves of porosity size 4; CH$_2$Cl$_2$ was distilled from phosphorus(v) oxide and used immediately. The other chemical reagents were used as received from the suppliers without further purification. Melting points were recorded on an Ernst Leitz Wetzlar hot-stage microscope and are uncorrected. Elemental analyses were performed on a LECO CHNS-932 elemental analyzer. Infrared spectra were recorded using an ATR Perkin Elmer Spectrum 100 spectrophotometer between 4000–400 cm^{-1}. ^{1}H and ^{13}C NMR spectra were recorded using Bruker topspin 400 MHz and 600 MHz spectrometers and chemical shifts are recorded in ppm. Correlations were confirmed through COSY and HSQC experiments. The precursors [Cp(CO)$_2$Fe(OEt$_2$)]BF$_4$ [20] and [Cp*(CO)$_2$Fe(THF)]BF$_4$ [40] were prepared by literature methods.

4.2. Reactions of *1* with NH$_2$(CH$_2$)$_2$CH$_2$OH

3-Aminopropan-1-ol (0.12 ml, 1.57 mmol) was added to a solution of complex **1** (0.627 g, 1.86 mmol) in CH$_2$Cl$_2$ (10 ml). The mixture was stirred at room temperature for 6 h after which golden yellow oil droplets were seen stuck to the walls of the Schlenk tube. The mother liquor was carefully syringed off. The residue oil was washed with two portions of 5 ml CH$_2$Cl$_2$ and dried under reduced pressure to give 0.314 g of **3** as a golden yellow oil. ^{1}H NMR (400 MHz, CD$_3$CN): δ 5.28 (s, 5H, Cp), 2.75 (s, 2H, NH$_2$), 2.43 (m, 2H, αCH$_2$), 1.58 (m, 2H, βCH$_2$), 3.53 (t, J_{HH} = 5.84 Hz, 2H, γCH$_2$), 1.77 (s,

1H, OH).^{13}C NMR (400 MHz, CD$_3$CN): 85.94 (Cp), 50.64 (αCH$_2$), 34.20 (βCH$_2$), 59.10 (γCH$_2$), 210.89.

4.3. Reaction of *2* with NH$_2$(CH$_2$)$_2$CH$_2$OH

To a solution of compound **2** (0.284 g, 0.70 mmol) in CH$_2$Cl$_2$ (10 ml), 3-aminopropanol (0.05 ml, 0.67 mmol) was added. The mixture was stirred under nitrogen for 20 h at room temperature after which the mixture was filtered into a preweighed Schlenk tube and diethyl ether (30 ml) added. The mixture was then allowed to stand for 16 h in the dark at room temperature after which the grey–yellow solid settled at the bottom of the Schlenk tube. The mother liquor was syringed off, the residue washed with 5 ml diethyl ether and dried under reduced pressure to give a yellow solid with a grey tint. This solid was purified further by recrystallization from CH$_2$Cl$_2$/Et$_2$O and dried under reduced pressure to give 0.170 g of **4** as a bright yellow microcrystalline solid. ^{1}H NMR (600 MHz, CDCl$_3$) 1.83 (s, 15H, C$_5$(CH$_3$)$_5$), 2.92 (s, 2H, NH$_2$), 2.54 (m, 2H, αCH$_2$), 1.78 (m, 2H, βCH$_2$), 3.78 (t, J_{HH} = 4.89 Hz, 2H, γCH$_2$), 1.55 (s, 1H, OH). ^{13}C NMR (400 MHz, CDCl$_3$): 9.17 (C$_5$(CH$_3$)$_5$), 97.57 (C$_5$(CH$_3$)$_5$), 53.63 (αCH$_2$), 33.13 (βCH$_2$), 62.99 (γCH$_2$), 212.56 (CO).

4.4. Reaction of *1* with NH$_2$CH$_2$C$_6$H$_4$OCH$_3$

A Schlenk tube was charged with a solution of complex **1** (1.110 g, 3.28 mmol) in CH$_2$Cl$_2$ (10 ml) and 4-methoxybenzylamine (0.45 ml; 3.45 mmol) was added dropwise while stirring the mixture. The stirring was continued for 10 h after which the mixture was filtered into a pre-weighed Schlenk tube. The residue was washed with several portions of 5 ml CH$_2$Cl$_2$ to give 0.280 g of a white microcrystalline solid. To the filtrate, diethyl ether was added until the yellow precipitate of [Cp(CO)$_2$Fe{NH$_2$CH$_2$C$_6$H$_4$OCH$_3$}]BF$_4$, 5, formed and then the mother liquor syringed off. The yellow residue was washed with 5 x 5 ml CH$_2$Cl$_2$ to give 0.566 g of **5** as a yellow microcrystalline solid. ^{1}H NMR (400 MHz, acetone-d$_6$): δ 5.58 (s, 5H, Cp), 3.89 (s, 4H, NH$_2$), 3.63 (t, J_{HH} = 7.04 Hz,,2H, NCH$_2$), 6.89 (d, J_{HH} = 8.64 Hz, 2H *ortho*, C$_6$H$_4$), 7.28 (d, J_{HH} = 8.60 Hz, 2H *meta*, C$_6$H$_4$), 3.78 (s, 3H, CH$_3$). ^{13}C NMR (400 MHz, acetone-d$_6$): δ 87.50 (Cp), 56.25 (CH$_2$), 132.06 (C-CH$_2$), 114.90 (C$_{ortho}$), 130.77 (C$_{meta}$), 55.62 (CH$_3$), 212.31 (CO).

4.5. Reaction of *2* with NH$_2$CH$_2$C$_6$H$_4$OCH$_3$

A Schlenk tube equipped with a magnetic bar was charged with a solution of **2** (0.297 g, 0.73 mmol) in CH$_2$Cl$_2$ (10 ml) and 4-methoxybenzylamine (0.1 ml, 0.77 mmol) added. The mixture was stirred at room temperature for 18 h resulting in a brown-yellow solution. Diethyl ether was added until a yellow precipitate formed. The mixture was allowed to stand for 30 min, after which the precipitate was filtered and the residue washed with two portions of 10 ml diethyl ether. The residue was dried under reduced pressure resulting in a yellow microcrystalline solid of **6** (0.234 g). ^{1}H NMR (400 MHz, acetone-d$_6$): δ 1.95 (s, 15H, C$_5$(CH$_3$)$_5$), 3.40 (s, 2H, NH$_2$), 3.58 (t, J_{HH} = 6.60 Hz, 2H, CH$_2$), 6.90 (d, J_{HH} = 8.64 Hz , 2H, *o*-CH), 7.25 (d, J_{HH} = 8.48 Hz, 2H, *m*-CH), 3.78 (s, 3H, CH$_3$). ^{13}C NMR (600 MHz, acetone-d$_6$) 8.41 (C$_5$(<u>C</u>H$_3$)$_5$), 54.88(CH$_2$), 131.00 (C-CH$_2$), 113.98 (*o*-CH), 129.78 (*m*-CH), 160.00 (<u>C</u>-OCH$_3$), 54.73(CH$_3$), 213.34 (CO).

4.6. Reactions of *1* with dipropylamine

To a solution of **1** (0.36 g, 1.065 mmol) in CH$_2$Cl$_2$ (15 ml), dipropylamine (0.16 ml, 1.169 mmol) was added dropwise and the reaction mixture stirred for 4 h, after which time the solution colour changed to brown from deep red. Diethyl ether was then added until a yellow precipitate formed. The precipitate was filtered under nitrogen resulting in a yellow solid which was washed with 2 x 10 ml diethyl ether and dried under reduced pressure to afford 0.285 g of **8** as a yellow microcrystalline solid. ^{1}H NMR (400 MHz, CDCl$_3$): δ 5.32 (s, 5H, Cp), 4.52 (s, 1H, -NH), 2.48 (b, 4H, αCH$_2$), 1.53 (m, 4H, βCH$_2$), 0.88 (t, J_{HH} = 7.08 Hz, 6H, CH$_3$). ^{13}C NMR (400 MHz, CDCl$_3$): δ 86.71 (Cp), 60.45 (α C), 20.56 (β C), 11.06 (CH$_3$), 211.13 (CO).

4.7. Reaction of *1* with NH$_2$(CH$_2$)$_3$Si(OCH$_2$CH$_3$)$_3$

A pre-weighed Schlenk tube was charged with a solution of complex **1** (1.97 g, 5.83 mmol) in CH$_2$C1$_2$ (30 ml). While stirring, 3-aminopropyltriethoxysilane (1.30 ml, 5.56 mmol) was added dropwise to the solution and the progress of the reaction periodically monitored by IR. The reaction was judged complete after 1 h 30 min when two carbonyl absorption bands had appeared at 2053 and 1998 cm^{-1} and bands at 2064 and 2010 cm^{-1} had dissapeared. The solution mixture was reduced to about *ca.* 10 ml by evaporation under reduced pressure and diethyl ether was added until an orange suspension was

formed. Then the mixture was kept at -78 ˚C for 15 min, after which an orange solid separated out and settled at the bottom of the Schlenk tube. While maintaining the mixture at -78 ˚C, the mother liquor was syringed off and the residue washed with 3 portions of 5 ml diethyl ether after which it was dried under reduced pressure to give a brown oil. The oil was purified by column chromatography on silica and eluted using tetrahydrofuran. An orange band was eluted first, followed by the red-purple band of the iron dimer. Removal of the solvent from the orange fraction under reduced pressure gave 1.270 g of an analytically pure yellow soft solid of $[Cp(CO)_2Fe\{NH_2(CH_2)_3Si(OCH_2CH_3)_3\}]BF_4$, **9**. ^1H NMR (400 MHz, $CDCl_3$): δ 5.28 (s, 5H, Cp), 2.94 (br, 2H, NH_2), 2.29 (br, 2H, αCH_2), 1.62 (br, 2H, βCH_2), 0.56 (br, 2H, γCH_2), 3.77 (br, 6H, $O-CH_2$), 1.18 (br, 9H, CH_3). ^{13}C NMR (400 MHz, $CDCl_3$): δ 86.10 (Cp), 55.54 (αC), 25.68 (βC), 7.05 (γC), 58.50 (O-C), 18.25 (CH_3), 210.59 (CO).

4.8. Recovery of 5 from its aqueous solution

Compound **5** (0.122 g, 0.30 mmol) was dissolved in deionized water (20 ml) and the resulting solution allowed to stand in dark for 24 h after which it was extracted with CH_2Cl_2 (5 x 10 ml). The extract was concentrated to *ca*. 7 ml under reduced pressure and then diethyl ether was added until a yellow precipitate formed. The mixture was allowed to stand for 30 min after which the mother liquor was removed by filtration and the residue dried under reduced pressure for 4 h to give 0.092 g (75 %) of $[Cp(CO)_2Fe(NH_2C_6H_4OCH_3)]BF_4$. The NMR and IR data were found to be identical to those given in Section 4.4 above.

4.9. Reaction of 5 with sodium tetraphenylborate in water

To an aqueous solution (10 ml) of compound **5** (0.152 g, 0.38 mmol), a solution of $NaBPh_4$ (0.30 g, 0.88 mmol) in deionized water (10 ml) was added. A yellow precipitate formed immediately and the mixture was filtered under gravity after stirring for 10 min and the residue washed with a minimum amount of ice-cooled methanol (2 ml), followed by diethyl ether (10 ml). Then it was dried under reduced pressure to give 0.329 g (59%) of $[Cp(CO)_2Fe(NH_2C_6H_4OCH_3)]BPh_4$, **7**. ^1H NMR (600 MHz, CD_3CN): 5.28 (s, 5H, Cp), 2.90 (s, 2H, NH_2), 3.36 (t, J_{HH} = 6.67 Hz, 2H, CH_2), 6.91 (d, J_{HH} = 8.22, 2H *ortho*, C_6H_4), 7.20 (d, J_{HH} = 8.22, 2H, $m-CH_2$), 3.77 (s, 3H, CH_3), 6.84 (t, J_{HH}

= 6.90 Hz , 4H *para,* C_6H_5), 6.99 (t, J_{HH} = 7.17 Hz, 8H *meta,* C_6H_5), 7.27 (br, 8H *ortho,* C_6H_5). ^{13}C NMR (600 MHz, CD_3CN); 86.23 (Cp), 55.08 (CH_2), 135.73 (C-para, C_6H_4), 114.04 (C-*ortho,* C_6H_4), 129.84 (C*meta,* C_6H_4), 55.04 (CH_3), 211.02 (CO).

4.10. Reaction of 4-aminobenzonitrile (ABN) with one equivalents of *1*

A Schlenk tube equipped with a magnetic bar was charged with a mixture of compound **1** (1.170 g, 3.46 mmol) in CH_2Cl_2 (10 ml) and 4-aminobenzonitrile (0.544 g, 4.61 mmol) in CH_2Cl_2 (10 ml). The mixture was stirred for 4 h resulting in a yellow precipitate which was filtered into a pre-weighed Schlenk tube. The residue was washed with five portions of CH_2Cl_2 (10 ml) and dried under reduced pressure to give **12** as a yellow solid. Yield: 0.23 g, 21%. Anal. Calc. for $C_{21}H_{16}B_2F_8Fe_2N_2O_4$: C, 39.06; H, 2.50; N, 4.34. Found: C, 39.19; H, 2.28; N, 4.24%. ^{1}H NMR (methanol-d_4) 5.61 (s, 5H, Cp-CN), 5.36 (s, 5H, Cp-NH), NO (NH_2), 7.24 (d, J_{HH} = 8.40Hz, 2H, *o*-CH), 7.86 (d, J_{HH} = 8.24Hz, 2H, *m*-CH). ^{13}C NMR (methanol-d_4): 88.22 (Cp-CN), 87.48 (Cp-NH), 108.44 (C-NH), 122.48 (*o*-CH), 136.66 (*m*-CH), 136.04 (C-CN), 154.28 (CN), 211.47, 209.32 (CO). IR (solid state) v_{max}(cm^{-1}): 2081, 2040, 2003 (CO); 3351, 3268 (NH_2); 2263. Decomposes without melting at temperature > 181 ˚C.

To the filtrate, diethyl ether was added until an orange precipitate formed. The precipitate was allowed to settle for 1 h after which the mother liquor was syringed off and the precipitate washed with four portions of diethyl ether and dried under reduced pressure to give **10** an orange microcrystalline solid. Yield: 0.87 g, 66%. Anal. Calc. for $C_{14}H_{11}BF_4FeN_2O_2$: C, 44.03; H, 2.90; N, 7.34. Found: C, 44.12; H, 2.87; N, 6.90. ^{1}H NMR (400 MHz, methanol-d_4): δ 5.37 (s, 5H, Cp), NO (NH_2), 7.22 (d, J_{HH} = 8.40 Hz, 2H, *o*-CH), 7. 74 (d, J_{HH} = 8.22 Hz, 2H, *m*-CH). ^{13}C NMR (methanol-d_4): δ 86.56 (Cp), 109.00 (C-NH_2), 121.04 (*o*-CH), 133.85 (*m*-CH), 117.58 (C-CN), 151.08 (CN), 210.16 (CO). IR (solid state) v_{max}(cm^{-1}): 2056, 2002 (CO); 3391, 3267 (NH_2); 2231 (CN). M.p., 52-54 ˚C.

4.11. Reaction of ABN with two equivalents of *1*

The procedure was executed as explained in Section 4.10. Complex **1** (1.36 g, 4.02 mmol) was reacted with ABN (0.240 g, 2.03 mmol) to give only the dinuclear complex

[{Cp(CO)$_2$Fe}$_2$μ-(ABN)](BF$_4$)$_2$, **12** as a yellow solid. Yield: 1.15 g, 89%. NMR, IR and other physical data were found to be identical to those of the dinuclear compound in Section 4.10 above.

4.12. Reaction of ABN with one equivalent of compound 2

To a solution of compound **2** (0.176 g, 0.43 mmol) in CH$_2$Cl$_2$ (10 ml), in a Schlenk tube equipped with a magnetic bar, a solution of ABN (0.050 g, 0.42 mmol) in CH$_2$Cl$_2$ (5 ml) was added. The mixture was stirred at room temperature, while monitoring the progress of the reaction using IR, and was stopped after 4 h when judged complete. The mixture was filtered into a pre-weighed Schlenk tube and diethyl ether added until a yellow precipitate formed. The mother liquor was removed and the residue washed with diethyl ether (2 x 5 ml) and dried under reduced pressure to give **11** as a yellow solid. Yield: 0.085 g, 53%. Anal. Calc. for C$_{19}$H$_{21}$BF$_4$FeN$_2$O$_2$: C, 50.48; H, 4.68; N, 6.20. Found: C, 49.52; H, 4.54; N, 6.83%. ^{1}H NMR (CD$_3$CN); 1.85 (d, J_{HH} = 9.00Hz, 15H, C$_5$(CH$_3$)$_5$), 4.76 (NH$_2$), 7.20 (d, J_{HH} = 8.44Hz, 2H, o-CH), 7.74 (d, J_{HH} = 8.52Hz, 2H, m-CH). ^{13}C NMR (CD$_3$CN); 8.28 (C$_5$(C̲H$_3$)$_5$), 97.84 (C̲$_5$(CH$_3$)$_5$), 106.91 (C-NH), 120.85 (C$_O$), 134.46 (C$_m$), 131.91 (C-CN), 151.58 (CN), 211.73 (CO). IR (solid state) v_{max}(cm^{-1}): 2043, 1975 (CO); 3380, 3261 (NH$_2$); 2246 (CN).

4.13. Reaction of ABN with two equivalents of compound 2

A solution of ABN (0.033 g, 0.28 mmol) in CH$_2$Cl$_2$ (5 ml) was added to a solution of compound **2** (0.23 g, 0.57 mmol) in CH$_2$Cl$_2$ (10 ml) in a Schlenk tube equipped with a magnetic bar. The mixture was stirred at room temperature overnight resulting in a brown solution which was filtered into a pre-weighed Schlenk tube. Diethyl ether was added to the filtrate until a yellow precipitate formed. The mother liquor was syringed off and the precipitate washed with 5 ml of diethyl ether and dried under reduced pressure to give **13** as a yellow solid. Yield: 0.190 g, 86%. Anal. Calc. for C$_{31}$H$_{36}$B$_2$F$_8$Fe$_2$N$_2$O$_4$: C, 47.37; H, 4.62; N, 3.56. Found: C, 47.67; H, 4.15; N, 3.73%. ^{1}H NMR (400 MHz, CD$_3$CN): 1.86 (s, 15H, C$_5$(CH$_3$)$_5$-CN), 1.84 (s, 15H, C$_5$(CH$_3$)$_5$-NH), 4.78 (s, br, 2H, NH$_2$), 7.73 (d, J_{HH} = 8.56 Hz, 2H, m-CH), 7.19 (d, J_{HH} = 8.56 Hz, 2H, o-CH). ^{13}C NMR (400 MHz, CD$_3$CN): 8.46 (C$_5$(CH$_3$)$_5$-CN), 8.39 (C$_5$(CH$_3$)$_5$-NH), 97.90 (C$_5$(CH$_3$)$_5$), 97.84 (C$_5$(CH$_3$)$_5$), 120.84 (o-CH), 134.65 (m-CH), 151.59 (CN), NO (C-

CN), NO (C-NH), 211.73, 210.17 (CO). IR (solid state) v_{max}(cm^{-1}): 2050, 2032, 2017, 1987 (CO); 3270 (NH$_2$), 2274 (CN). M.p., 176-177 ˚C.

4.14. Reaction of [Cp(CO)$_2$Fe(ABN)]BF$_4$, 10 with 2

A solution of compound **10** (0.800 g, 2.09 mmol) in CH$_2$Cl$_2$ (20 ml) was added to solution of compound **2** (0.868 g, 2.14 mmol) and then the mixture was stirred at room temperature for 6 h after which a yellow precipitate formed. The mixture was allowed to settle for 30 min and then the mother liquor was removed and the residue was washed with CH$_2$Cl$_2$ (5 x 10 ml). The residue was dried under reduced pressure to give **14** a yellow solid. Yield: 0.703 g, 47%. Anal. Calc. for C$_{26}$H$_{26}$B$_2$F$_8$Fe$_2$N$_4$O$_4$: C, 43.63; H, 3.66; N, 3.91. Found: C, 43.68; H, 3.85; N, 3.64%. ^{1}H NMR (400 MHz, MeOD): δ 7.75 (d, J_{HH} = 8.20 Hz, H, C$_6$H$_4$), 7.23 (d, J_{HH} = 8.08 Hz , H, C$_6$H$_4$), 5.31 (s, 5H, Cp),NO (4H, NH$_2$), 1.89 (s, 15H, Cp*), ^{13}C NMR (400 MHz, MeOD): δ 134.76 (C, C$_6$H$_4$), 121.14 (C, C$_6$H$_4$), 85.88 (Cp), 8.56 (Cp*), 99.54 (Cp*), 106.99 (C-NH), 132 (C-CN), 152.06 (CN) 210.39, 210.02 (CO). IR (solid state): ν(CO) 2051, 2004 cm^{-1}. Decomposes without melting at temperature > 170 ˚C.

4.15. Reaction of 1,4-phenylenedimethanamine (PDA) with one equivalents of 1

A Schlenk tube equipped with a magnetic bar was charged with a solution of complex **1** (0.521 g, 1.54 mmol) in CH$_2$Cl$_2$ (20 ml) and a solution of PDA (0.209 g, 1.54 mmol) in CH$_2$Cl$_2$ (10 ml) added. The mixture was stirred for 5 h and allowed to stand under nitrogen at room temperature overnight after which a yellow precipitate settled at the bottom of the Schlenk tube. The mother liquor was syringed off, the residue washed with 4 portions of CH$_2$Cl$_2$ (4 x10 ml) and dried under reduced pressure to give **15** as a yellow solid. Yield: 0.317 g, 62%. Anal. Calc. for C$_{22}$H$_{22}$B$_2$F$_8$Fe$_2$N$_2$O$_4$: C, 39.81; H, 3.34; N, 4.22. Found: C, 39.68; H, 3.26; N, 4.18%. ^{1}H NMR (400 MHz, acetone-d$_6$): δ 5.58 (s, 10H, Cp), 3.89 (s, 2H, NH$_2$), 3.68 (br, 4H, CH$_2$), 7.34 (s, 4H, =CH). ^{13}C NMR (400 MHz, acetone-d$_6$): δ 87.56 (Cp), 56.54 (CH$_2$), 129.63 (=CH), 139.95 (C-CH$_2$), 212.28 (CO). IR (solid state) v_{max}(cm^{-1}): 2054, 1999 (CO); 3319, 3284 (NH$_2$). Decomposes without melting at temperature > 160 ˚C.

4.16. Reaction of PDA with two equivalents of 1

The reaction was executed in a manner similar as described in Section 4.15 above, by reacting **1** (0.867 g, 2.57 mmol) with PDA (0.175 g, 1.29 mmol). Yield: 0.694 g, 81%. IR and NMR data were identical to those given in Section 4.15 above.

4.17. Reaction of 2 with PDA

The reaction was executed as explained in Section 4.15, by reacting **2** (0.837 g, 2.06 mmol) with PDA (0.301 g, 2.21 mmol). Yield: 0.580 g, 70%. Anal. Calc. for $C_{32}H_{42}B_2F_8Fe_2N_2O_4$: C, 47.80; H, 5.27; N, 3.48. Found: C, 47.45; H, 5.67; N, 3.74%. ^{1}H NMR (400 MHz, CD$_3$CN): δ 1.86 (s, 30 H, C$_5$(CH$_3$)$_5$), 2.55 (s, br, 4H, NH$_2$), 3.44 (t, J_{HH} = 7.46 Hz, 4H, CH$_2$), 7.30 (s, 4H, C$_6$H$_4$). ^{13}C NMR (400 MHz, CD$_3$CN): δ 8.22 (C$_5$(CH$_3$)$_5$), 97.43 (C$_5$(CH$_3$)$_5$), 54.45 (CH$_2$), 128.35 (C$_6$H$_4$), NO (C-CH$_2$) 212.76 (CO). IR (solid state) v_{max}(cm^{-1}): 2027, 1970 (CO); 3304, 3268 (NH$_2$). M.p., 167-169 ˚C.

4.18. Reaction of [{Cp(CO)$_2$Fe}$_2$(µ-PDA)](BF$_4$)$_2$, 16, with sodium tetraphenylborate

To a solution of compound **16** (0.483 g, 0.728 mmol) in deionized water (10 ml) in a 100 ml-beaker, a solution of NaBPh$_4$ (0.584 g, 1.706 mmol) in deionized water (15 ml) was added. The rest of the procedure was carried out in similar fashion as in the reaction of **5** with sodium tetraphenylborate described in Section 4.9. Yield: 0.517 g, 63%. Anal. Calc. for $C_{70}H_{62}B_2F_8Fe_2N_2O_4$: C, 74.50; H, 5.54; N, 2.48. Found: C, 74.16; H, 5.77; N, 2.92%. ^{1}H NMR (400 MHz, acetone-d$_6$): δ 5.54 (s, 10H, Cp), 3.88 (s, 4H, NH$_2$), 3.66 (br, 4H, CH$_2$), 7.33 (br, 20H, C$_6$H$_4$ and =CH o-Ph), 6.92 (t, J_{HH}= 7.36Hz, 16H, =CH-*met*-Ph), 6.77 (t, J_{HH}=7.12, 8H, =CH-*par*-Ph). ^{13}C NMR (400 MHz, acetone-d6): δ 87.50 (Cp), 56.50 (CH$_2$), 139.94 (CH$_2$-C), 129 (C$_6$H$_4$), 137.05 (=CH o-Ph), 126.01 (=CH-*met*-Ph), 122.24 (=CH-*par*-Ph), 212.25 (CO). IR (solid state) v_{max}(cm^{-1}): 2048, 1994 (CO); 3280, 3226 (NH$_2$). Decomposes without melting at temperature > 190 ˚C.

4.19. X-ray crystallographic study

Crystals of compounds **4**, **6** and **8** suitable for single crystal X-ray diffraction study were obtain by the slow liquid diffusion method of crystal growth. Compounds **4** and **6** were

grown in dichloromethane/diethyl ether, while compound **8** was grown in a chloroform/hexane solvent system over a period of 4 - 5 days. Their crystal data were collected on a Bruker *APEX II CCD* area detector diffractometer [41] and the crystal structures solved by direct methods using *SHELXS-97* [42] while molecular graphics were generated using *OLEX2* [43].. Non-hydrogen atoms were first refined isotropically, followed by anisotropic refinement by full matrix least-squares calculations based on F^2 using *SHELXTL-97* [42]. Hydrogen atoms were first located in the difference map, then positioned geometrically and allowed to ride on their respective parent atoms. In **8**, the dipropylamine group was found to be disordered and was refined over two positions using *ISOR*, *SADI*, *DELU*, *SIMU* and *EADP* restraints. The crystal structure and refinement information are given in Table 6.

Table 6: Crystal data and structure refinement information for compounds **4**, **6** and **8**

Compound	4	6	8
Empirical formula	$C_{15}H_{24}BF_4FeNO_3$	$C_{20}H_{26}BF_4FeNO_3$	$C_{13}H_{20}BF_4FeNO_2$
Formula weight	409.01	471.08	364.96
Temperature (K)	173(2)	100(2) K	173(2)
Wavelength (Å)	0.71073	0.71073	0.71073
Crystal system	monoclinic	monoclinic	Tetragonal
Space group	$P2_1/c$	$P2_1/c$	$P4_2/n$
Unit cell dimension			
a (Å)	12.6672(6), $\alpha = 90$	14.4746(17), $\alpha = 90$	18.0975(11), $\alpha = 90$
b	8.6666(5), $\beta = 93.656(2)$	12.8314(15), $\beta = 111.460(3)$	18.0975(11), $\beta = 90$
c	16.5010(10), $\gamma = 90$	12.4154(15), $\gamma = 90$	10.2085(7), $\gamma = 90$
Volume (Å^3)	1807.82(17)	2146.0(4)	3343.5(4)
Z	4	4	8
Density (calculated)(Mg/m^3)	1.503	1.458	1.450
Absorption coefficient (mm^{-1})	0.887	0.758	0.945
F(000)	848	976	1504
Crystal size (mm)	0.44 x 0.30 x 0.08	0.20 x 0.17 x 0.04	0.52 x 0.14 x 0.12
Theta range for data collection	1.61 – 28.00	2.19 – 28.97°.	1.59 - 25.98°.
Index ranges			
h	-16 → 10	-19→ 19	-22 → 19
k	-10 → 11	-16 → 17	-22→ 19
l	-21 → 21	-16 → 16	-12 → 12
Reflections collected	11570	65733	12432
Independent reflections	4358	5559	3292
Internal fit	R(int) = 0.0561	R(int) = 0.0764	R(int) = 0.0795
Absorption correction	Integration	Semi-empirical	Integration
Transmission factor ($T_{Min};T_{Max}$)	0.6964; 0.9325	0.8634; 0.9704	0.6393; 0.8950
Refinement method parameters	Full-matrix least-squares on F^2 232	Full-matrix least-squares on F^2 322	Full-matrix least-squares on F^2 230
Goodness-of-fit on F^2	0.915	1.030	0.904
Final R indices [I>2sigma(I)]	R1 = 0.0452, wR2 = 0.0932	R1 = 0.0399, wR2 = 0.0869	R1 = 0.0506, wR2 = 0.1202
R indices (all data)	R1 = 0.0753, wR2 = 0.1026	R1 = 0.0751, wR2 = 0.1046	R1 = 0.1077, wR2 = 0.1433
Largest diff. peak and hole(e.Å^{-3})	0.855 and -0.678	0.514 and -0.592	0.563 and -0.389

Acknowledgement

Supplementary Material

CCDC 848026, 848027 and 848028 contains the supplementary crystallographic data for compound **4**, **6** and **8**. These data can be obtained free of charge from The Cambridge Crystallographic Data Centre *via* www.ccdc.cam.ac.uk/data_request/cif. Crystallographic data for compounds **4**, **6** and **8** are given in Appendix 11. CD-ROM containg CIF of the crystals and spectroscopic data is given in appendix 12.

References

[1]   L.-W. Xu, J. Luo, Y. Lu, Chem. Commun. (2009) 1807.

[2]   P. Daka, Z. Xu, A. Alexa, H. Wang, Chem. Commun. 47 (2011) 224.

[3]   L.-W. Xu, Y. Lu, Org. Biomol. Chem. 6 (2008) 2047.

[4]   C. Liu, Q. Zhu, K.-W. Huang, Y. Lu, Org. Lett. 13 (2011) 2638.

[5]   S. Hu, J. Li, J. Xiang, J. Pan, S. Luo, J.-P. Cheng, J. Am. Chem. Soc. 132 (2010) 7216.

[6]   I.B. Eisdorfer, R.J. Warren, J.E. Zarembo, J. Pharm. Sci. 57 (1968) 195.

[7]   B. Kersten, Chromatographia 34 (1992) 607.

[8]   J. Bowman, L. Tang, C.E. Silverman, J. Pharm. Biomed. Anal. 23 (2000) 663.

[9]   S.M. Celuch, A.V. Juorio, Naunyn-Schmiedeberg's Arch. Pharmacol. 336 (1987) 391.

[10] F. Buffoni, Trends Pharmacol. Sci. 4 (1983) 313.

[11] S.K. Srivastava, P.M.S. Chauhan, A.P. Bhaduri, P.K. Murthy, R.K. Chatterjee, Bioorg. Med. Chem. Lett. 10 (2000) 313.

[12] O.K. Onajole, Y. Coovadia, T. Govender, H.G. Kruger, G.E.M. Maguire, D. Naidu, N. Singh, P. Govender, Chem. Bio. Drug Des. 77 (2011) 295.

[13] F.M.F. Vergara, M.d.G.M.O. Henriques, A.L.P. Candea, J.L. Wardell, M.V.N.D. Souza, Bioorg. Med. Chem. Lett. 19 (2009) 4937.

[14] A.M. Kaufmann, J.P. Krise, J. Pharm. Sci. 96 (2007) 729.

[15] E.W. Neuse, A.G. Perlwitz, Amine-Functionalized, Water-Soluble Polyamides as Drug Carriers, Water-Soluble Polymers, vol. 467, American Chemical Society, 1991, pp. 394.

[16] E. Agostinelli, Amino Acids 27 (2004) 345.

[17] J. Karovičova, Z. Kohajdova, Chem. Pap. 59 (2005) 70.

[18] C. Naccari, M.T. Galceran, E. Moyano, M. Cristani, L. Siracusa, D. Trombetta, Food Chem. Toxicol. 47 (2009) 321.

[19] B. Tadolini, J. Biochem. 249 (1988) 33.

[20] C.M. M'thiruaine, H.B. Friedrich, E.O. Changamu, M.D. Bala, Inorg. Chim. Acta 366 (2011) 105.

[21] C.M. M'thiruaine, H.B. Friedrich, E.O. Changamu, B. Omondi, Acta Cryst. E67 (2011) m485.

[22] C.M. M'thiruaine, H.B. Friedrich, E.O. Changamu, M.D. Bala, Inorg. Chim. Acta (2011) in press. doi:10.1016/j.ica.2011.1009.1058.

[23] C.M. M'thiruaine, H.B. Friedrich, E.O. Changamu, M.D. Bala, (2011) submitted to Inorg. Chim. Acta.

[24] C.M. M'thiruaine, H.B. Friedrich, E.O. Changamu, B. Omondi, (2011) Submitted to Poyhedron.

[25] M. Moran, C. Pascual, I. Cuadrado, J.R. Masaguer, J. Losada, J. Organomet. Chem. 363 (1989) 157.

[26] P. Braunstein, D. Cauzzi, G. Predieri, A. Tiripicchio, J. Chem. Soc., Chem. Commun. (1995) 229.

[27] J.D. Cotton, G.A. Morris, J. Organomet. Chem. 145 (1978) 245.

[28] G. Joorst, R. Karlie, S. Mapolie, Polyhedron 18 (1999) 3377.

[29] M. Akita, S. Kakuta, S. Sugimoto, M. Terada, M. Tanaka, Y. Moro-oka, Organometallics 20 (2001) 2736.

[30] S.B. Sanni, A.T.H. Lenstra, Acta Cryst. C41 (1985) 199.

[31]   S. Yasuda, H. Yorimitsu, K. Oshima, Organometallics 27 (2008) 4025.

[32]   E. Roman, D. Catheline, D. Astruc, J. Organomet. Chem. 236 (1982) 229.

[33]   H. Schumann, M. Speis, W.P. Bosman, J.M.M. Smits, P.T. Beurskens, J. Organomet. Chem. 403 (1991) 165.

[34]   B. Callan, A.R. Manning, F.S. Stephens, J. Organomet. Chem. 331 (1987) 357.

[35]   C.M. M'thiruaine, H.B. Friedrich, E.O. Changamu, M.D. Bala, Acta Cryst. E67 (2011) m924.

[36]   A. Palazzi, S. Stagni, S. Bordoni, M. Monari, S. Selva, Organometallics 21 (2002) 3774.

[37]   M.H. Garcia, M.P. Robalo, A.P.S. Teixeira, A.R. Dias, M.F.M. Piedade, M.T. Duarte, J. Organomet. Chem. 632 (2001) 145.

[38]   H. Schumann, S. Martin, J. Organomet. Chem. 403 (1991) 165.

[39]   H.J. Coerver, C. Curran, J. Am. Chem. Soc. 80 (1958) 3522.

[40]   M. Akita, M. Tarada, M. Tanaka, Y. Morooka, J. Organomet. Chem. 510 (1996) 255.

[41]   Bruker, *APEX2*. Version 2009.1-0. Bruker AXS Inc., Madison, Wisconsin, USA., (2005).

[42]   G.M. Sheldrick, Acta Cryst. A64 (2008) 112.

[43]   O.V. Dolomanov, L.J. Bourhis, R.J. Gildea, J.A.K. Howard, H. Puschmann, J. Appl. Cryst. 42 (2009) 339.

CHAPTER SEVEN

Conclusions

The novel substitutionally labile etherate complex $[Cp(CO)_2Fe(OEt_2)]BF_4$ has been prepared, isolated and characterized. Three alternative methods for the synthesis of the complex were investigated, among which the protonation of the methyl complex $[Cp(CO)_2FeCH_3]$ with $HBF_4.Et_2O$, followed by addition of a large excess of diethyl ether proved to be superior. The complex reacts with aliphatic, *N*-heterocyclic and aromatic amines to provide a wide range of new amine complexes. These reactions proceed smoothly by displacement of the ether molecules of the etherate complex by the appropriate amine ligand in dichloromethane at room temperature. Thus, the alkylamino complexes $[Cp(CO)_2Fe\{NH_2(CH_2)_nCH_3\}]BF_4$ (n = 2-6) and α,ω-diaminoalkane complexes $[\{Cp(CO)_2Fe\}_2\{NH_2(CH_2)_nNH_2\}](BF_4)_2$ (n = 2-4,6) have been synthesized and fully characterized. The electrospray mass spectra of the alkylamino complexes show a fragmentation pattern that begins with loss of the counter anion, followed by successive loss of the carbonyl groups. The α,ω-diaminoalkane complexes on the other hand show a complex fragmentation pattern due to the influence of the two metal centres. The molecular structures of $[Cp(CO)_2Fe\{NH_2(CH_2)_nCH_3\}]BF_4$ (n = 2,3) and $[\{Cp(CO)_2Fe\}_2\{NH_2(CH_2)_2NH_2\}](BF_4)_2$ have been determined by X-ray crystallography and show that the packing of the molecules is assisted by hydrogen bonding in addition to other intermolecular attractions. The hydrogen bonding occurs mainly between the fluoride of the counter anion BF_4^- and the amine hydrogen.

Novel pentamethylcyclopentadienyl complexes $[Cp^*(CO)_2Fe\{NH_2(CH_2)_nCH_3\}]BF_4$ (n = 2-6) and $[\{Cp^*(CO)_2Fe\}_2\{NH_2(CH_2)_3NH_2\}](BF_4)_2$ have been synthesized from the reaction between $[Cp^*(CO)_2Fe(THF)]BF_4$ and the appropriate amine ligand. These complexes are also fully characterized and, furthermore, the molecular structures of $[Cp^*(CO)_2Fe\{NH_2(CH_2)_3CH_3\}]BF_4$ and $[\{Cp^*(CO)_2Fe\}_2\{NH_2(CH_2)_3NH_2\}](BF_4)_2$ have been determined. The fragmentation patterns of the $[Cp^*(CO)_2Fe\{NH_2(CH_2)_nCH_3\}]BF_4$ series have also been determined by mass spectrometry. Their water-solubility and stability has been demonstrated by a counteranion exchange reaction between an aqueous solution of $[Cp^*(CO)_2Fe\{NH_2(CH_2)_5CH_3\}]BF_4$ and $NaBPh_4$ which leads to the BPh_4^- salt.

N-heterocyclic complexes of the type $[(\eta^5\text{-}C_5R_5)(CO)_2FeL]BF_4$ (R = H, CH$_3$; L = hexamethylenetetramine (HMTA), 1,4-diazabicyclo[2.2.2]octane (DABCO), 1-methylimidazole (1-meIm)), $[\{(\eta^5\text{-}C_5R_5)(CO)_2Fe\}_2(\mu\text{-}HMTA)](BF_4)_2$ (R = H, CH$_3$) and $[\{(\eta^5\text{-}C_5H_5)(CO)_2Fe\}_2(\mu\text{-}DABCO)](BF_4)_2$ have been synthesized by the reaction of the *N*-heterocyclic ligand with the appropriate etherate complex. The molecular structures of $[\{Cp(CO)_2Fe\}_2(\mu\text{-}HMTA)](BF_4)_2$, $[(\eta^5\text{-}C_5R_5)(CO)_2Fe(1\text{-}meIm)]BF_4$ (R = H and CH$_3$) have been confirmed by X-ray crystallography.

The novel allylamino complexes $[(\eta^5\text{-}C_5R_5)(CO)_2Fe(NH_2CH_2CH=CH_2)]BF_4$ (R = H, CH$_3$) have been prepared from the reaction of the etherate complexes $[Cp(CO)_2Fe(OEt_2)]BF_4$ and $[Cp^*(CO)_2Fe(THF)]BF_4$ and have been shown to undergo halogenation reactions on the vinyl group to form the new chiral aminohalopropane complexes $[(\eta^5\text{-}C_5R_5)(CO)_2Fe\{NH_2CH_2CH(X)CH_2X\}]BF_4$ (R = H; X = Cl, Br; R = CH$_3$; X = Br). These complexes have been fully characterized and the molecular structures of $[(\eta^5\text{-}C_5R_5)(CO)_2Fe(NH_2CH_2CH=CH_2)]BF_4$ (R = H, CH$_3$) and $[Cp^*(CO)_2Fe\{NH_2CH_2CH(Br)CH_2Br\}]BF_4$ have been determined by single crystal X-ray crystallography, of which the structure of $Cp^*(CO)_2Fe\{NH_2CH_2CH(Br)CH_2Br\}]BF_4$ confirms the existence of the *R* and *S* enantiomers of the compound. The allylamino complexes also have been shown to react with the etherate complexes to form the hitherto unknown chiral dinuclear complexes $[\{(\eta^5\text{-}C_5R_5)(CO)_2Fe\}_2(NH_2\text{-}CH_2CH=CH_2)](BF_4)_2$ (R = H, CH$_3$), $[(Cp(CO)_2Fe(NH_2CH_2CH=CH_2)Fe(CO)_2Cp^*](BF_4)_2$ and $[(Cp^*(CO)_2Fe(NH_2CH_2\text{-}CH=CH_2)Fe(CO)_2Cp](BF_4)_2$, which have also been fully characterized. Their NMR and IR data show that the allylamine ligand coordinated to the metal on one end *via* the nitrogen of the amine functionality in a monohapto fashion and on the other end *via* the vinylic functionality in dihapto fashion resulting in metallacyclopropane-type structures. The reaction of $[\{Cp(CO)_2Fe\}_2(NH_2CH_2CH=CH_2)](BF_4)_2$ with NaI in acetone was found to proceed by cleavage of the dihapto coordinated metal centre accompanied by displacement of the BF$_4^-$ anions by iodide to form $[Cp(CO)_2Fe(NH_2CH_2CH=CH_2)]I$ and $[Cp(CO)_2FeI]$.

The reactions of the etherate complexes $[Cp(CO)_2Fe(OEt_2)]BF_4$ and $[Cp^*(CO)_2Fe(THF)]BF_4$ with heterofunctional ligands such as

$NH_2(CH_2)_3Si(OCH_2CH_3)_3$, $NH_2CH_2CH_2CH_2OH$ and p-$NH_2CH_2C_6H_4OCH_3$ have been investigated, and the results show that the ligands bonded to the $(\eta^5$-$C_5R_5)(CO)_2Fe$ moieties through the amine functionality leading to the new complexes $[(Cp(CO)_2Fe\{(NH_2(CH_2)_3Si(OCH_2CH_3)_3\}]BF_4$ and $[(\eta^5$-$C_5R_5)(CO)_2FeL]BF_4$ (R = H, CH_3; L = $NH_2CH_2CH_2CH_2OH$, p-$NH_2CH_2C_6H_4OCH_3$). The molecular structures of $[Cp^*(CO)_2Fe(p$-$NH_2CH_2C_6H_4OCH_3)]BF_4$ and $[Cp^*(CO)_2Fe(NH_2CH_2CH_2CH_2OH)]BF_4$ have been determined by X-ray crystallography and confirm that the coordination of these ligands is *via* the amine group. Further, the NMR and IR data of the new mononuclear complexes $[(\eta^5$-$C_5R_5)(CO)_2Fe(NH_2C_6H_4CN)]BF_4$ (R = H, CH_3) also indicates that the metal fragments have a preference for the amino group over the cyano group. However, these mononuclear complexes transform to the more stable dinuclear complexes $[\{(\eta^5$-$C_5R_5)(CO)_2Fe\}_2(NH_2C_6H_4CN)](BF_4)_2$, in which the ligand bridges the two metal fragments *via* the amine on one side and the cyano on the other end.

The reaction of $[Cp(CO)_2Fe(NH_2C_6H_4CN)]BF_4$ with $[Cp^*(CO)_2Fe(THF)]BF_4$ led to the mixed ligand complex $[Cp(CO)_2Fe(NH_2C_6H_4CN)Fe(CO)_2Cp^*](BF_4)_2$ in which the $(\eta^5$-$C_5H_5)(CO)_2Fe$ group bonds to the amine side owing to its electrophilic nature as compared to the $(\eta^5$-$C_5(CH_3)_5)(CO)_2Fe$ moiety.

The reaction of 1,4-phenylenedimethanamine and the etherate complexes gives only dinuclear complexes $[\{(\eta^5$-$C_5R_5)(CO)_2Fe\}_2(NH_2CH_2C_6H_4CH_2NH_2)](BF_4)_2$ (R = H, CH_3) in all stoichiometric ratios. These complexes in turn undergo counter anion exchange reaction with $NaBPh_4$ in aqueous medium to form the BPh_4^- salt complexes $[\{(\eta^5$-$C_5R_5)(CO)_2Fe\}_2(NH_2CH_2C_6H_4CH_2NH_2)](BPh_4)_2$.

The molecular structures of the known acetonitrile complex $[Cp^*(CO)_2Fe(NCCH_3)]BF_4$[‡] and formato complex $[\{Cp(CO)_2Fe\}_2\{\mu$-$OC(H)O\}]BF_4$[§] have also been determined by X-ray crystallography.

In conclusion, a total of 54 novel compounds have been synthesized and fully characterized. Molecular structures of 16 compounds have been determined. The Fe–N bond lengths fall in the range 2.006 – 2.058 Å in aliphatic amine complexes, while in

---

[‡] See: M'thiruaine et al. Acta Cryst. E67(2011) m924. (Appendix 2)
[§] See: M'thiruaine et al. Acta Cryst. E67(2011) m1252. (Appendix 3)

hexamethylenetetramine and 1-methylimidazole the Fe–N bond lengths fall in the ranges 2.082 – 2.082 Å and 1.973 – 1.980 Å, respectively. Generally, the Fe–N bond lengths of cyclopentadienyl complexes are shorter than those of the corresponding pentadienylcyclopentadienyl complexes. Similarly, the distance from the metal centre to the centroid of cyclopentadienyl in the cyclopentadienyl complexes is shorter than the distance from the metal centre to the centroid of the pentamethylcyclopentadienyl ligand in the corresponding pentamethylcyclopentadienyl complexes, reflecting the electron releasing ability of the pentamethylcyclopentadienyl ligand. In all the crystals of amine-containing complexes with the BF_4^- counteranion, molecules are connected by hydrogen bonding in addition to other intermolecular attractions. The hydrogen bonding occurs mainly between the amine hydrogen and fluorine of the tetrafluoroborate. The iron atoms in these complexes adopt a three-legged piano-stool geometry, with the cyclopentadienyl or pentamethylcyclopentadienyl rings occupying the apical positions and the two carbonyls and the amine nitrogen occupying the basal positions.

It is clear that a wide range of new compounds were conveniently prepared from the etherate complexes $[Cp(CO)_2Fe(Et_2O)]BF_4$ and $[Cp^*(CO)_2Fe(THF)]BF_4$. Many of them are water soluble and exhibited interesting chemistry. Of particular interest in the future is the investigation of their catalysis and biological uses.

APPENDICES

APPENDIX 1

(μ-Ethane-1,2-diamine-$\kappa^2 N$:N')bis[dicarbonyl(η^5-cyclopentadienyl)iron(II)] bis(tetrafluoridoborate)

Cyprian M. M'thiruaine[a], Holger B. Friedrich[a*], Evans O. Changamu[b], Bernard Omondi[c*]

[a] School of Chemistry, University of KwaZulu-Natal, Private Bag X54001, Durban 4000, South Africa [b] Chemistry Department, Kenyatta University, P.O Box 43844 Nairobi, Kenya [c]Department of Chemistry, University of Johannesburg P.O Box 524 Auckland Pack Johannesburg, 2006

* Corresponding author

Key indicators: single-crystal X-ray study; T = 100 K; Mean σ(C-C) = 0.003Å; R factor = 0.033; wR factor = 0.084; data-to-parameter ratio = 18.0.

Abstract

The asymmetric unit of the title compound, $Fe_2(C_5H_5)_2(C_2H_8N_2)(CO)_4](BF_4)_2$, **1**, contains two half-cations, each located on a centre of symmetry, and two tetrafluoridoborate anions. The iron atoms adopt a three-legged piano-stool geometry. All amine H atoms are involved in N–H⋯F hydrogen bonds, which consolidate the crystal packing along with weak C–H⋯O and C–H⋯F interactions.

Related literature

For the synthesis of the title compound and our previous work in this area, see: M'thiruaine *et al*. [1]. For related dinuclear structures, see references: [2-6].

(**1**)
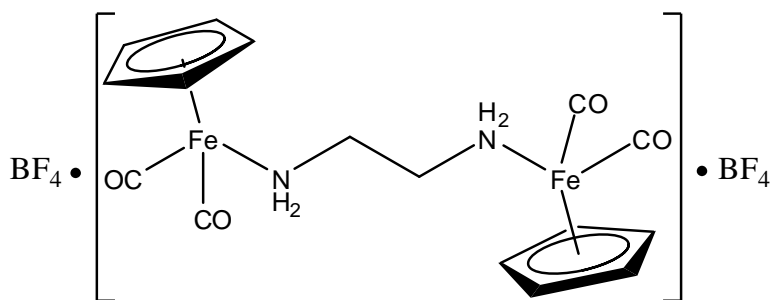
Experimental

Crystal data

$Fe_2(N_2(CH_2)_2(C_5H_5)_2(CO)_4(BF_4)_2$	$V = 2214.2(2)Å^3$
$M_r = 587.64$	$Z = 4$
Monoclinic, $P2_1/c$	Mo Kα radiation
$a = 11.5593(7)$ Å	$\theta = 1.77 - 28.31°$
$b = 15.5194(9)$ Å	$\mu = 1.40$ mm^{-1}
$c = 12.4056$ (8) Å	$T = 100$ K
$\beta = 95.7740(10)°$	0.22 X 0.10 X 0.03

Data Collection

Bruker X8 APEX 11 4K Kappa CCD defractometer	50802 measured reflections
	5222 independent reflections
Absorption correction: multi-scan	4550 reflections with $I > 2\sigma(I)$
SADABS	$R_{int} = 0.0501$
$T_{min} = 0.7476$ $T_{max} = 0.9591$	

Refinement

$R[F^2>2\sigma(F^2)] = 0.033$	4 restraints
$wR(F^2) = 0.084$	H-atoms parameters constrained.
$S = 1.14$	$\Delta\rho_{max} = 0.520$ e Å^{-3}
5520 reflections	$\Delta\rho_{min} = 0.352$ e Å^{-3}
307 parameters	

Table1: Hydrogen-bond geometry (Å, °)

D-H⋯A	D-H	H⋯A	D⋯A	D-H⋯A
N1-H1A⋯F8[i]	0.92	2.11	2.994 (2)	160
N1-H1B⋯F4[ii]	0.92	2.06	2.890 (2)	149
N2-H2B⋯F7[iii]	0.92	1.99	2.886 (2)	164
C3-H3⋯F1[iv]	1	2.36	3.326 (3)	163
C5-H5⋯F5[v]	1	2.39	3.216 (3)	139
C10-H10⋯O2[vi]	1	2.56	3.397 (3)	141
C10-H10⋯O3[vi]	1	2.57	3.326 (3)	132
C12-H12⋯F2[ii]	1	2.37	3.200 (3)	140

Symmetry code: (i) x+1, y, z (ii) x,y, z+1; (iii) x, -y+½, z-½; (iv) −x + 2, -y,-z+1; (v) x+1, -y+½, z-½; (vi)-x+1, y+½, -z+³/₂

Data collection: APEX2 [7]; cell refinement: SAINT-plus [7]; data reduction: SAINT-plus and XPREP [7]; program(s) used to solve structure: SHELXS97 [8]; Program(s) used to refine structures: SHELXS97 [8]; Molecular graphics: ORTEP-3 [9]; Software used to prepare material for publication: WinGX [10].

Comment

The title compound is a water soluble organometallic compound which was prepared as part of our ongoing study on functionalized alkyl transition metal complexes [1-6]. The asymmetric unit (Fig. 1) has two half-cations, each located on a centre of symmetry, and two tetrafluoroborate counteranions. The Fe metals are coordinated in three-legged piano-stool fashion with the cyclopentadienyl rings occupying the apical positions and two carbonyl ligands and one ethylenediamine nitrogen occupying the basal positions. The cyclopentadienyl ligands are trans to each other and the ethylenediamine ligands display a trans conformation. The Fe–Cg distance are 1.7123 (3) and 1.7103 (3) Å for atoms Fe1 and Fe2, respectively (Cg is the centroid of the cyclopentadienyl rings). In the crystal structure, the amine hydrogen atoms and the fluorine atoms of the tetrafluoroborate anions are engaged in three N–H···F intermolecular interactions (Table 1). Three H atoms of the cyclopentadienyl rings are also involved in C–H···F intermolecular interactions. Three C–H···O hydrogen bonds then complete the stabilization of the crystal lattice (Fig. 2).
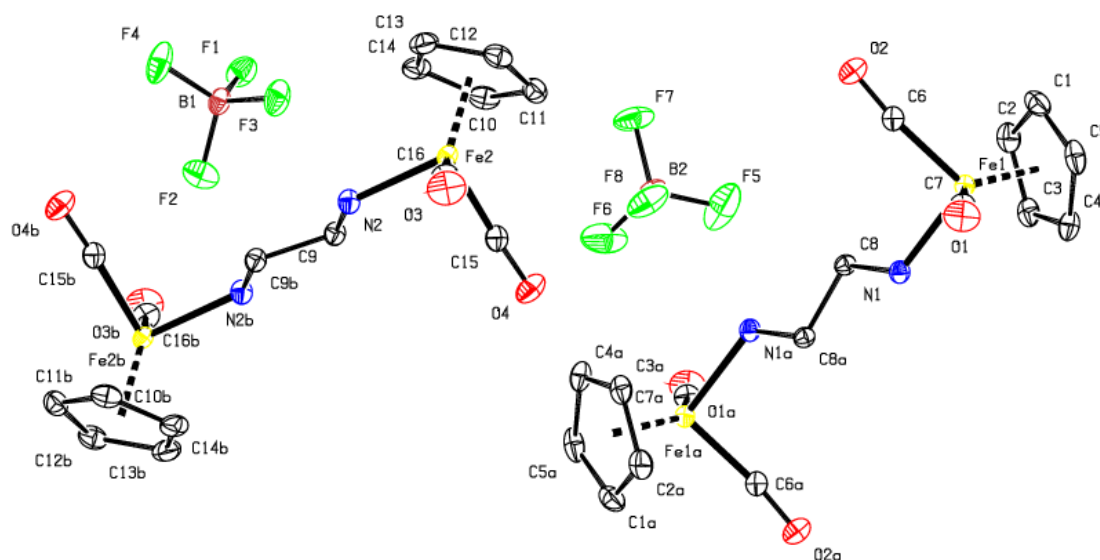
Fig. 1. The asymmetric unit of $[Fe_2(C_5H_5)_2(C_2H_8N_2)(CO)_4](BF_4)_2$ with displacement ellipsoids drawn at the 50% probability level. Hydrogen atoms are omitted for clarity. Symmetry codes: (a) 2-x, -y, 2-z (b) 1-x, 1-y, 1-z
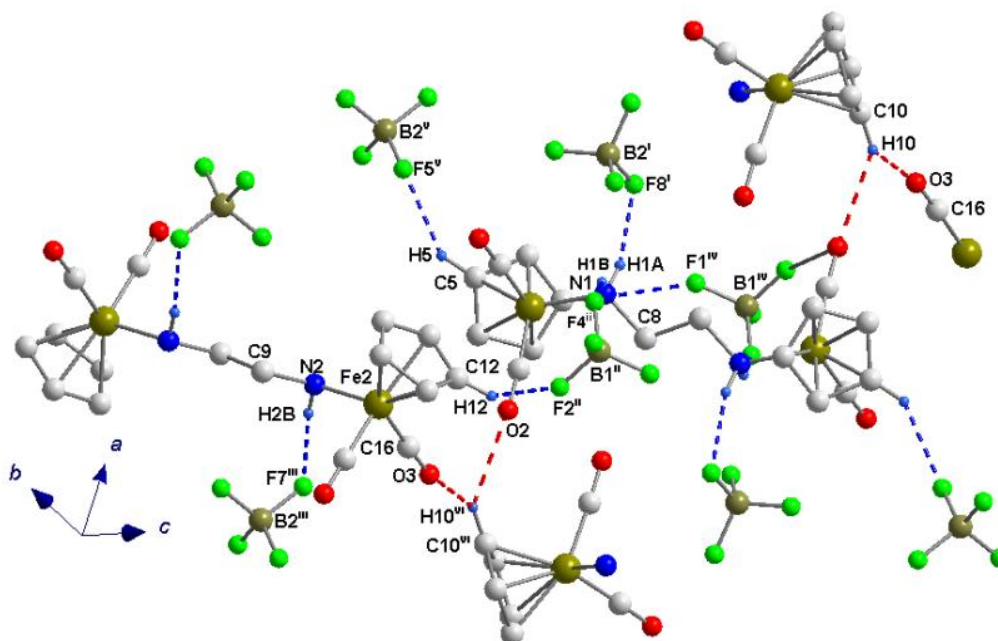
Fig. 2: The partial crystal packing of [Fe$_2$(C$_5$H$_5$)$_2$(C$_2$H$_8$N$_2$)(CO)$_4$](BF$_4$)$_2$ showing N-H---F, C-H---O and C-H---F interactions (dashed lines). Symmetry code (i) x+1, y, z; (ii) x, y, z+1; (iii) x, -y+½, z-½; (iv) −x + 2, -y, -z+1 (v) x+1, -y+½, z-½ (vi) −x + 1, y + ½, -z + ⅔

Experimental

The compound was synthesized by reacting ethylenediamine with two equivalents of [CpFe(CO)$_2$(OEt$_2$)]BF$_4$, according to the literature procedures [1]. Yield: 0.339 g, 78%; of the yellow crystals of [{CpFe(CO)$_2$}$_2$μ-NH$_2$(CH$_2$)$_2$NH$_2$](BF$_4$)$_2$; M.P: dec > 120 ˚C; spectroscopic analysis: ^{1}H NMR (400 MHz, acetone-d$_6$): δ 5.48 (s, 10H, Cp), 3.33 (s, 4H, NH$_2$), 2.58 (s, 4H, CH$_2$). ^{13}C NMR (400 MHz, acetone-d$_6$): δ 87.43 (Cp), 54.50 (CH$_2$), 211.92 (CO). Ms: m/z 500.8 [[{CpFe(CO)$_2$}$_2$NH$_2$CH$_2$CH$_2$NH$_2$]BF$_4$]$^+$; 236.7 [CpFe(CO)$_2$NH$_2$CH$_2$CH$_2$NH$_2$]$^+$ 220.9   [CpFe(CO)$_2$NH$_2$CH$_2$CH$_2$]$^+$;   206.6 [CpFe(CO)$_2$NH$_2$CH$_2$]$^+$;   194.6   [CpFe(CO)$_2$NH$_2$+2H]$^+$;   176.6   [CpFe(CO)$_2$]$^+$; elemental analysis: calculated for C$_{16}$H$_{18}$B$_2$F$_8$Fe$_2$N$_2$O$_4$: C, 32.65; H, 3.06; N, 4.76. Found: C, 32.96; H, 3.28; N, 5.02%.   IR (solid state): ν(CO) 2054, 2001 cm^{-1}; ν(NH) 3315, 3276 cm^{-1}.

Refinement

All H atoms were placed in geometrically idealized positions and constrained to ride on their parent atoms, with C-H = 0.99-1.00Å. N-H = 0.92 Å, and with U$_{iso}$(H) =

$1.2U_{eq}(C,N)$. In the final refinement cycles restraints were applied to the anisotropic displacement parameters of atoms Fe1 and C7 (SIMU and DELU instructions in SHELXL97, [8]. Two reflections (-822,526) were identified as outliers and removed from the refinement.

Acknowledgement

Supplementary Material

Supplementary data and figures for this paper are available from the IUCr electronic archives (Reference: RZ2564). A full version of this paper is available from journals.iucr.org. doi:10.1107/S1600536811010154

References

[1]   C.M. M'thiruaine, H.B. Friedrich, E.O. Changamu, M.D. Bala, Inorg. Chim. Acta 366 (2011) 105.

[2]   E.O. Changamu, H.B. Friedrich, M. Rademeyer, J. Organomet. Chem. 693 (2008) 164.

[3]   E.O. Changamu, H.B. Friedrich, M.A. Fernandes, Inorg. Chim. Acta 362 (2009) 2947.

[4]   H.B. Friedrich, M.O. Onani, M. Rademeyer, Acta Cryst. E61 (2005) m144.

[5]   E.O. Changamu, H.B. Friedrich, M. Rademeyer, J. Organomet. Chem. 692 (2007) 2456.

[6]   E.O. Changamu, H.B. Friedrich, R.A. Howie, M. Rademeyer, J. Organomet. Chem. 692 (2007) 5091.

[7]   Bruker, *APEX2*. SAINT-plus, SADABS and XPREP. Bruker AXS Inc., Madison, Wisconsin, USA. (2007).

[8]   G.M. Sheldrick, Acta Cryst. A64 (2008) 112.

[9]   L.J. Farrugia, J. Appl. Cryst. 30 (1997) 565.

[10]   L.J. Farrugia, J. Appl. Cryst. 32 (1999) 837.

APPENDIX 2

Acetonitriledicarbonyl(η⁵-pentamethylcyclopentadienyl)iron(II) tetrafluoridoborate

Cyprian M. M'thiruaine[a], Holger B. Friedrich[a*], Evans O. Changamu[b], Muhammad D. Bala[a*]

[a] School of Chemistry, University of KwaZulu-Natal, Private Bag X54001, Durban 4000, South Africa [b] Chemistry Department, Kenyatta University, P.O Box 43844 Nairobi, Kenya

* Corresponding author

Key indicators: single-crystal X-ray study; T = 173 K; Mean σ(C-C) = 0.006Å; R factor = 0.044; wR factor = 0.120; data-to-parameter ratio = 16.3.

Abstract

In the structure of the title compound, $[Fe\{\eta^5-C_5(CH_3)_5\}(NCCH_3)(CO)_2]BF_4$, **1** the arrangement of ligands around the Fe atom is in a Pseudo-octahedral three-legged piano stool fashion in which the pentamethylcyclopentadienyl (Cp*) ligand occupies three apical coordination sites, while the two carbonyl and one acetonitrile ligand form the basal axes of the coordination. The Fe–N bond length is 1.924(3) Å and the Fe-Cp* centroid distance is 1.722Å.

Related literature

For the synthetic route to the title compound, see reference: [1]; For the structure of related analogue based on the Cp moeity, see reference:[2]; For acetonitrile coordination *via* carbon see reference [3]; For our previous work in this area, see: [4, 5].

(**1**)
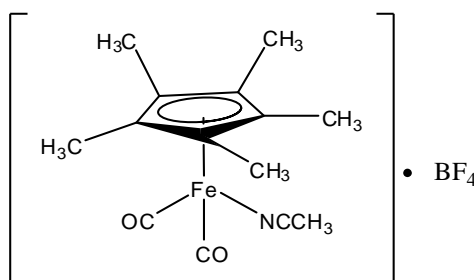
Experimental

Crystal data

$C_{14}H_{18}FeNO_2.BF_4$ $V = 1673.5(3) Å^3$
$M_r = 374.95$ $Z = 4$
Orthorhombic, $Pna2_1$ Mo Kα radiation
$a = 17.6211(17)$ Å $\mu = 0.946$ mm^{-1}
$b = 6.5141(7)$ Å $T = 173(2)$K
$c = 14.5794(13)$ Å   0.54 mm X 0.34 mm X 0.12mm

Data Collection

Bruker APEX - 11 CCD difractometer   9060 measured reflections
Absorption correction: integration   3496 independent reflections
XPREP   2941 reflections with $I > 2\sigma(I)$
$T_{min} = 0.6290, T_{max} = 0.8949$ $R_{int} = 0.0440$

Refinement

$R[F^2 > 2\sigma(F^2)] = 0.044$ H-atoms parameters constrained.
$wR(F^2) = 0.120$ $\Delta\rho_{max} = 0.760$ e Å^{-3}
3496 reflections $\Delta\rho_{min} = -0.394$ e Å^{-3}
214 parameters   Absolute structure: Flack (1983)
1 restraints   13942 Friedel pairs
                                             Flack Parameter: -0.02(3)

Data collection: APEX2 [6]; Cell refinement: *SAINT-plus*[6]; Data reduction: *SAINT-plus*; programs used to solve structure: *SHELXTL* [7]; Program used to refine structures: *SHELXTL* ; Molecular graphics: *ORTEP-3* [8]; Software used to prepare materials for publication: *SHELXTL*.

Comment

The title compound **1** was obtained as a side product in our ongoing investigation of the reactions of substitutionally unsaturated metal complexes with nitrogen donor ligands [4, 5]. The compound has been previously reported as the product of oxidative cleavage of the Fe–Fe bond in $[\eta^5\text{-}C_5(CH_3)_5Fe(CO)_2]_2$ in acetonitrile and also as a product of the reaction between $[\eta^5\text{-}C_5(CH_3)_5Fe(CO)_2(THF)]BF_4$ and acetonitrile [1], but its crystal structure has not been reported.

Compound **1** crystallizes in orthorhombic Pna2₁/c space group, with four discrete molecular cations and four counteranion in the unit cell. The arrangement of ligand around Fe is in pseudo-octahedral 3-legged piano stool fashion in which the the pentamethylcyclopentadienyl moiety occupies three coordination sites while the two carbonyl ligands and acetonitrile nitrogen complete the coordination. The Fe–N bond length of 1.924(3) Å, is close to 1.91(1) Å reported for [CpFe(CO)$_2$(NCCH$_3$)]BF$_4$ [3] but shorter than the Fe–N bond found in the pyrrol complex, [CpFe(CO)$_2$(C$_4$H$_4$N)] (1.962(3) Å), and aminoalkane complexes, [CpFe(CO)$_2$(NH$_2$(CH$_2$)$_n$CH$_3$)]BF$_4$ (n=2,3) (2.017(8), 2.013(3) and 2.006(2) Å) [4] and [{CpFe(CO)$_2$}$_2$(μ-(NH$_2$CH$_2$CH$_2$NH$_2$)](BF$_4$)$_2$ (2.0134(17) and 2.0085(18) Å) [5]. It is also interesting to note tha Fe–C [2] and Fe–N [3] coordination of acetonitrile (NCCH$_3$) molecule to Fe has been reported for Cp based complexes.
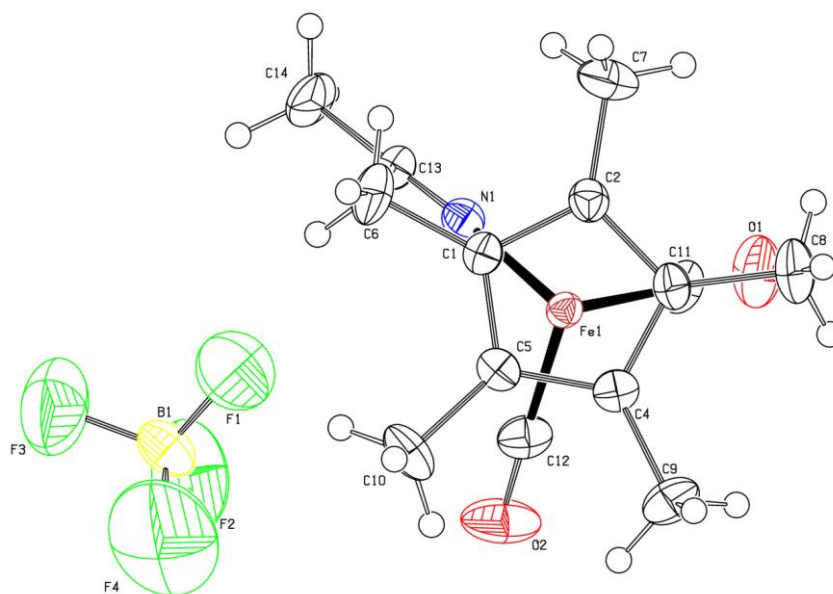
Fig. 1: Molecular structure of the title complex with the atom numbering scheme. Displacement ellipsoids are drawn at 50% probability level. H atoms are presented as small spheres of arbitrary radius.

Experimental

The title compound **1** was synthesized following the method of Catheline and Astruc [1]. Compound 1 was obtained as a yellow microcrystalline solid in an isolated yield of 92%.

Anal. Calc. for $C_{14}H_{18}BF_4FeNO_2$: C, 44.80; H, 4.80; N, 3.73. Found: C, 44.95; H, 4.13; N, 3.76%. ^1H NMR (400 MHz, $CDCl_3$): δ 2.48 (s, 3H, $NCCH_3$), 1.85 (s, 15H, $C_5(CH_3)_5$). ^{13}C NMR (400 MHz, $CDCl_3$): δ 4.68 (NC$\underline{C}H_3$) 9.54 ($C_5(\underline{C}H_3)_5$), 99.19 ($\underline{C}_5(CH_3)_5$), 210.08 (CO). IR (solid state): v(CO) 2044, 1992 cm^{-1}, v(CN) 2299 cm^{-1}. M.p = 158-160 ˚C.

Refinement

All H-atoms were refined using a riding model, with C–H = 0.98Å and U_{ISO} (H) = 1.5 U_{eq} (C) for CH_3.

Acknowledgement

Supplementary Material

Supplementary data and figures for this paper are available from the IUCr electronic archives (Reference: HG5040). A full version of this paper is available from journals.iucr.org. doi:10.1107/S1600536811021350.

References

[1]   D. Catheline, D. Astruc, J. Organomet. Chem. 266 (1984) C11 - C14.

[2]   B. Callan, A.R. Manning, F.S. Stephens, J. Organomet. Chem. 331 (1987) 357-377.

[3]   S. Fadel, K. Weidenheimer, M.L. Ziegler, Z. Anorg. Allg. Chem. 453 (1979) 98. .

[4]   C.M. M'thiruaine, H.B. Friedrich, E.O. Changamu, M.D. Bala, Inorg. Chim. Acta 366 (2011) 105.

[5]   C.M. M'thiruaine, H.B. Friedrich, E.O. Changamu, B. Omondi, Acta Cryst. E67 (2011) m485.

[6]   Bruker, *APEX2*. Version 2009.1-0. Bruker AXS Inc., Madison, Wisconsin, USA., (2005).

[7]   G.M. Sheldrick, Acta Cryst. A64 (2008) 112.

[8]   L.J. Farrugia, J. Appl. Cryst. 30 (1997) 565.

APPENDIX 3

(μ-Formato-$\kappa^2 O$:O')bis[dicarbonyl(η^5-cyclopentadienyl)iron(II)] tetrafluoridoborate

Cyprian M. M'thiruaine[a], Holger B. Friedrich[a*], Evans O. Changamu[b], Bernard Omondi[a*]

[a] **School of Chemistry, University of KwaZulu-Natal, Private Bag X54001, Durban 4000, South Africa** [b] **Chemistry Department, Kenyatta University, P.O Box 43844 Nairobi, Kenya**

* Corresponding author

Key indicators: single-crystal X-ray study; T = 100 K; Mean σ(C-C) = 0.003Å; R factor = 0.028; wR factor = 0.069; data-to-parameter ratio = 17.2

Abstract

In the structure of the title compound $[Fe_2(C_5H_5)_2(CHO_2)(CO)_4]BF_4$, **1** each Fe^{II} atom is coordinated in a pseudo-octahedron three piano-stool fashion. The cyclopentadienyl ligand occupies three *fac* coordination sites while the two carbonyl ligands and formate O atom occupy the remaining three sites.

Related literature

For synthesis of the title and other analogous compounds, see reference [1]; For monuclear formate complex $[Fe(\kappa^1\text{-}OCHO)(\eta^5\text{-}C_5H_5)(CO)_2]$, see [2, 3] For related compounds see: [4-6].

(**1**)
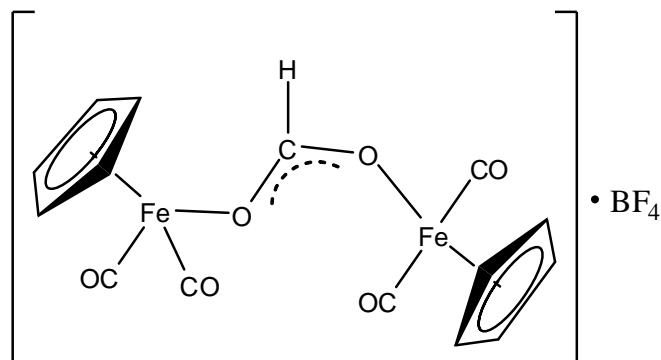
Experimental

Crystal data

$[Fe_2(C_5H_5)_2(CHO_2)(CO)_4]BF_4$
$M_r = 485.75$
Monoclinic, $P2_1/c$
$a = 7.4964(5)$ Å
$b = 17.8845(14)$ Å
$c = 14.1931(9)$ Å
$\beta = 115.144(3)°$

$V = 1722.5(2)$ Å^3
$Z = 4$
Mo Kα radiation
$\mu = 1.757$ mm^{-1}
$T = 100(2)$K
0.24 x 0.11 x 0.1

Data Collection

Bruker X8 APEXII 4K Kappa CCD
diffractometer
Absorption correction:
multi-scan (SADABS; Bruker, 2007)
$T_{min} = 0.6768, T_{max} = 0.8439$

41366 measured reflections
4341 independent reflections
3784 reflections with $I > 2\sigma(I)$
$R_{int} = 0.048$

Refinement

$R[F^2 > 2\sigma(F^2)] = 0.028$
$wR(F^2) = 0.069$
$S = 1.02$
4341 reflections
253 parameters

11 restraints
H-atoms parameters constrained.
$\Delta\rho_{max} = 1.38$ e Å^{-3}
$\Delta\rho_{min} = -0.92$ e Å^{-3}

Data collection: *APEX2* [7]; cell refinement: *SAINT-plus* [7]; data reduction: *SAINT-plus* and *XPREP* [7]; program(s) used to solve structure: *SHELXS97* [8]; program(s) used to refine structure: *SHELXL97* [8]; molecular graphics: *ORTEP-3* [9]; software used to prepare material for publication: *WinGX* [10].

Comment

There has been a considerable interest in metalloformates and metallocarboxylates due to their potential application in catalysis of water-gas shift reactions [2, 3] and catalytic reduction of CO_2 [1, 11, 12]. In connection to this the neutral monuclear formate complex $[(\eta^5-C_5H_5)Fe(CO)_2(\eta^1-OC(H)O)]$ has been prepared using different routes [1, 3, 13] and its molecular structure is well known [2, 3]. The cationic dinuclear complex $[\{(\eta^5-C_5H_5)Fe(CO)_2\}_2(\mu-OC(H)O)]PF_6$ has been reported as the product of the reaction between the neutral monuclear complex $[(\eta^5-C_5H_5)Fe(CO)_2(\eta^1-OC(H)O)]$ and $[(\eta^5-C_5H_5)Fe(CO)_2(THF)]PF_6$, and has been assumed to exist as a syn-syn isomer based on

the spectroscopic data [1]. The same authors have reported various formate bridged heterodinuclear complexes [11] but none of their crystal structures are known.

The title compound **1** was obtained in high yields from the reaction of formic acid with two equivalents of diethyl ether complex $[(\eta^5-C_5H_5)Fe(CO)_2(O(CH_2CH_3)_2)]BF_4$. This is a part of our study on the reactions of the diethyl ether complex with electron pair donor ligands [4, 5].

The title compound **1** crystallizes in monoclinic P2$_1$/c space group, with one discrete molecular cations and one counter anion in the asymmetric unit. Each Fe is coordinated in a pseudo-octahedral three-legged piano stool fashion in which the iron metal capped with cyclopentadienyl occupies three coordination sites while the two carbonyl ligands and formate oxygen occupy the the other three coordination sites (Fig. 1). The Fe–O bond length of 1.9844(13) and 1.9686(13) Å are close to 1.957(2)Å reported for the neutral monuclear complex $[(\eta^5-C_5H_5)Fe(CO)_2(\eta^1-OC(H)O)]$ [3]. The two O–C bonds of the formate group (-OC(H)O-) are identical, with the bond distance being equal to 1,256(2) and 1.258 (2) Å, which is close to 1.277(3)Å and 1.208(4) found for coordinated and uncoordinated O–C of formate moiety in the complex $[(\eta^5-C_5H_5)Fe(CO)_2(\eta^1-OC(H)O)]$, respectively. The identical bond lengths of the two C–O bonds of bridging formate indicate electron delocalization between the two oxygen atoms of formate moiety. Thus the structure in shown in Fig. 1 is an overall structure of two resonance structures: [Fp-O=C(H)O-Fp]$^+$ and [Fp-O-(H)C=O-Fp]$^+$. This greatly contributes to the stability of the title compounds in both solution and solid state. The Fp moieties are oriented in the solid state so as to adopt syn-anti isomer structure contrary to the assumption made by Tso and Cutler [1].
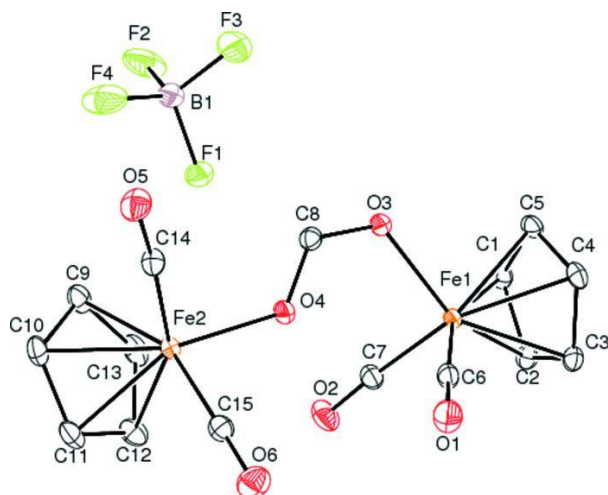
Fig. 1: View of **1** (50% probability displacement ellipsoids) with H atoms omitted for clarity.

Experimental

The compound was synthesized as described below and its spectroscopic data is in good agreement with data reported for PF_6^- salt.

To a solution of $[(\eta^5\text{-}C_5H_5)Fe(CO)_2(O(CH_2CH_3)_2)]BF_4$ (0.560 g, 1.66 mmol) in CH_2Cl_2 (10 ml), 98% formic acid (0.030ml, 0.796 mmol) was added and the mixture stirred at room temperature for 5 hours after which diethyl ether was added to precipitate the formate compound as a light red solid. The mixture was allowed to stand for 30 min and then the mother liquor was syringed off and the residue was washed with (2 x 5 ml) diethyl to give 0.70 g (87 % yield) of light red solid. Anal. Calc. for $C_{15}H_{11}BF_4Fe_2O_6$: C, 37.09; H, 2.28% Found: C, 36.53; H, 2.57%. ^1H NMR (400 MHz, acetone-d_6): δ 5.46 (s, 10H, Cp), 7.18 (s, 1H, OCHO). ^{13}C NMR (400 MHz, acetone-d_6): δ 86.88 (Cp) 212.23 (CO). IR (solid state): ν(CO) 2057, 2039, 1985 cm^{-1}, ν(OCO) 1562cm^{-1}. M.p 109 – 110 ºC.

Refinement

All H atoms were placed in geometrically idealized positions and constrained to ride on their parent atoms, with C–H = 0.95-1.00Å and with $U_{iso}(H) = 1.2U_{eq}(C)$.

Supplementary Material

Supplementary data and figures for this paper are available from the IUCr electronic archives (Reference: NG5211).   A full version of this paper is available from journals.iucr.org. doi:10.1107/S1600536811032764

References

[1]   C.C. Tso, A.R. Cutler, Organometallics 4 (1985) 1242.

[2]   D.J. Darensbourg, M.B. Fischer, J. Raymond E. Schmidt, B.J. Baldwin, J. Am. Chem. Soc. 103 (1981) 1297.

[3]   D.J. Darensbourg, C.S. Day, M.B. Fischer, Inorg. Chem. 20 (1981) 3511-3519.

[4]   C.M. M'thiruaine, H.B. Friedrich, E.O. Changamu, M.D. Bala, Inorg. Chim. Acta 366 (2011) 105.

[5]   C.M. M'thiruaine, H.B. Friedrich, E.O. Changamu, B. Omondi, Acta Cryst. E67 (2011) m485.

[6]   J.R. Pinkes, C.J. Masi, R. Chiulli, B.D. Steffey, A.R. Cutler, Inorg. Chem. 36 (1997) 70.

[7]   Bruker, *APEX2*, *SAINT*-plus, *SADABS* and *XPREP*. Bruker AXS Inc., Madison, Wisconsin, USA., (2007).

[8]   G.M. Sheldrick, Acta Cryst. A64 (2008) 112.

[9]   L.J. Farrugia, J. Appl. Cryst. 30 (1997) 565.

[10]   L.J. Farrugia, J. Appl. Cryst. 32 (1999) 837.

[11]   C.C. Tso, A.R. Cutler, Inorg. Chem. 29 (1990) 471.

[12]   J.R. Pinkes, C.J. Masi, R. Chiulli, B.D. Steffey, A.R. cutler, Inorg. Chem. 36 (1997) 70 -79.

[13]   B.D. Dombek, R.J. Angelici, Inorg. Chem. 7 (1973) 345.

APPENDIX 4

X-ray Crystallographic Data Pertaining to Chapter Two

Table 1A. Bond lengths [Å] for [CpFe(CO)$_2$NH$_2$(CH$_2$)$_2$CH$_3$]BF$_4$.

Bond	Length	Bond	Length
C(1)-C(5)	1.408(3)	C(6)-Fe(1)	1.776(2)
C(1)-C(2)	1.424(3)	C(7)-O(2)	1.142(3)
C(1)-Fe(1)	2.1250(19)	C(7)-Fe(1)	1.793(2)
C(2)-C(3)	1.428(3)	C(8)-N(1)	1.489(2)
C(2)-Fe(1)	2.1075(19)	C(8)-C(9)	1.527(3)
C(3)-C(4)	1.407(3)	C(9)-C(10)	1.524(3)
C(3)-Fe(1)	2.0949(19)	N(1)-Fe(1)	2.0178(16)
C(4)-C(5)	1.444(3)	B(1)-F(4)	1.372(3)
C(4)-Fe(1)	2.0847(19)	B(1)-F(3)	1.380(3)
C(5)-Fe(1)	2.109(2)	B(1)-F(1)	1.385(3)
C(6)-O(1)	1.139(3)	B(1)-F(2)	1.403(3)

Table 2A. Bond angles [°] for [CpFe(CO)$_2$NH$_2$(CH$_2$)$_2$CH$_3$]BF$_4$.

Bonds	Angle	Bonds	Angle
C(5)-C(1)-C(2)	108.74(17)	C(7)-Fe(1)-C(3)	124.51(9)
C(5)-C(1)-Fe(1)	69.96(11)	N(1)-Fe(1)-C(3)	141.88(8)
C(2)-C(1)-Fe(1)	69.67(11)	C(4)-Fe(1)-C(3)	39.35(9)
C(1)-C(2)-C(3)	107.24(18)	C(6)-Fe(1)-C(2)	101.77(9)
C(1)-C(2)-Fe(1)	71.00(11)	C(7)-Fe(1)-C(2)	157.00(9)
C(3)-C(2)-Fe(1)	69.67(11)	N(1)-Fe(1)-C(2)	102.82(7)
C(4)-C(3)-C(2)	108.76(18)	C(4)-Fe(1)-C(2)	66.69(8)
C(4)-C(3)-Fe(1)	69.93(11)	C(3)-Fe(1)-C(2)	39.72(8)
C(2)-C(3)-Fe(1)	70.61(11)	C(6)-Fe(1)-C(5)	153.92(8)
C(3)-C(4)-C(5)	107.56(18)	C(7)-Fe(1)-C(5)	92.81(10)
C(3)-C(4)-Fe(1)	70.72(11)	N(1)-Fe(1)-C(5)	110.98(7)
C(5)-C(4)-Fe(1)	70.77(11)	C(4)-Fe(1)-C(5)	40.27(8)
C(1)-C(5)-C(4)	107.68(18)	C(3)-Fe(1)-C(5)	66.34(8)
C(1)-C(5)-Fe(1)	71.19(11)	C(2)-Fe(1)-C(5)	66.19(8)
C(4)-C(5)-Fe(1)	68.96(11)	C(6)-Fe(1)-C(1)	139.86(9)
O(1)-C(6)-Fe(1)	175.42(19)	C(7)-Fe(1)-C(1)	126.56(10)
O(2)-C(7)-Fe(1)	175.5(2)	N(1)-Fe(1)-C(1)	88.35(7)
N(1)-C(8)-C(9)	111.37(16)	C(4)-Fe(1)-C(1)	66.32(8)
C(10)-C(9)-C(8)	111.30(18)	C(3)-Fe(1)-C(1)	65.92(8)
C(8)-N(1)-Fe(1)	117.99(11)	C(2)-Fe(1)-C(1)	39.33(8)
C(6)-Fe(1)-C(7)	93.36(10)	C(5)-Fe(1)-C(1)	38.85(8)
C(6)-Fe(1)-N(1)	93.94(8)	F(4)-B(1)-F(3)	109.86(19)
C(7)-Fe(1)-N(1)	93.21(8)	F(4)-B(1)-F(1)	111.1(2)
C(6)-Fe(1)-C(4)	114.24(9)	F(3)-B(1)-F(1)	109.58(19)
C(7)-Fe(1)-C(4)	91.37(9)	F(4)-B(1)-F(2)	109.30(17)
N(1)-Fe(1)-C(4)	151.13(8)	F(3)-B(1)-F(2)	108.81(18)
C(6)-Fe(1)-C(3)	89.44(9)	F(1)-B(1)-F(2)	108.20(18)

Table 3A. Bond lengths [Å] for [CpFe(CO)$_2$NH$_2$(CH$_2$)$_3$CH$_3$]BF$_4$

Bond	Length	Bond	Length
C(1)-C(5)	1.400(4)	C(13)-Fe(2)	2.089(2)
C(1)-C(2)	1.411(3)	C(14)-C(15)	1.409(4)
C(1)-Fe(1)	2.117(2)	C(14)-Fe(2)	2.077(3)
C(2)-C(3)	1.428(4)	C(15)-C(16)	1.417(4)
C(2)-Fe(1)	2.099(2)	C(15)-Fe(2)	2.085(3)
C(3)-C(4)	1.407(4)	C(16)-Fe(2)	2.100(2)
C(3)-Fe(1)	2.083(3)	C(17)-O(3)	1.138(3)
C(4)-C(5)	1.420(4)	C(17)-Fe(2)	1.790(2)
C(4)-Fe(1)	2.083(3)	C(18)-O(4)	1.133(3)
C(5)-Fe(1)	2.100(2)	C(18)-Fe(2)	1.789(3)
C(6)-O(1)	1.132(3)	C(19)-N(2)	1.479(3)
C(6)-Fe(1)	1.795(2)	C(19)-C(20)	1.527(4)
C(7)-O(2)	1.134(3)	C(20)-C(21)	1.510(4)
C(7)-Fe(1)	1.791(3)	C(21)-C(22)	1.517(4)
C(8)-N(1)	1.492(3)	N(2)-Fe(2)	2.006(2)
C(8)-C(9)	1.514(3)	B(1)-F(3)	1.371(4)
C(9)-C(10)	1.527(4)	B(1)-F(2)	1.373(4)
C(10)-C(11)	1.521(4)	B(1)-F(1)	1.384(4)
N(1)-Fe(1)	2.013(2)	B(1)-F(4)	1.393(4)
C(12)-C(13)	1.403(4)	B(2)-F(7)	1.369(4)
C(12)-C(16)	1.404(4)	B(2)-F(5)	1.379(4)
C(12)-Fe(2)	2.111(3)	B(2)-F(8)	1.391(4)
C(13)-C(14)	1.421(4)	B(2)-F(6)	1.405(4)

Table 4A. Bond angles [°] for [CpFe(CO)$_2$NH$_2$(CH$_2$)$_3$CH$_3$]BF$_4$

Bonds	Angle	Bonds	Angle
C(5)-C(1)-C(2)	108.8(2)	C(15)-C(14)-C(13)	108.0(2)
C(5)-C(1)-Fe(1)	69.93(14)	C(15)-C(14)-Fe(2)	70.53(15)
C(2)-C(1)-Fe(1)	69.75(13)	C(13)-C(14)-Fe(2)	70.52(14)
C(1)-C(2)-C(3)	107.4(2)	C(14)-C(15)-C(16)	107.7(2)
C(1)-C(2)-Fe(1)	71.14(13)	C(14)-C(15)-Fe(2)	69.89(15)
C(3)-C(2)-Fe(1)	69.45(14)	C(16)-C(15)-Fe(2)	70.77(15)
C(4)-C(3)-C(2)	107.8(2)	C(12)-C(16)-C(15)	108.1(2)
C(4)-C(3)-Fe(1)	70.23(15)	C(12)-C(16)-Fe(2)	70.94(15)
C(2)-C(3)-Fe(1)	70.62(14)	C(15)-C(16)-Fe(2)	69.65(14)
C(3)-C(4)-C(5)	108.1(3)	O(3)-C(17)-Fe(2)	175.7(2)
C(3)-C(4)-Fe(1)	70.28(16)	O(4)-C(18)-Fe(2)	176.1(2)
C(5)-C(4)-Fe(1)	70.79(16)	N(2)-C(19)-C(20)	110.3(2)
C(1)-C(5)-C(4)	107.9(2)	C(21)-C(20)-C(19)	113.6(2)
C(1)-C(5)-Fe(1)	71.29(14)	C(20)-C(21)-C(22)	112.3(2)
C(4)-C(5)-Fe(1)	69.53(15)	C(19)-N(2)-Fe(2)	120.36(17)
O(1)-C(6)-Fe(1)	176.6(2)	C(18)-Fe(2)-C(17)	95.77(11)
O(2)-C(7)-Fe(1)	176.3(2)	C(18)-Fe(2)-N(2)	91.42(10)
N(1)-C(8)-C(9)	112.1(2)	C(17)-Fe(2)-N(2)	94.10(10)
C(8)-C(9)-C(10)	112.1(2)	C(18)-Fe(2)-C(14)	123.86(12)
C(11)-C(10)-C(9)	112.1(2)	C(17)-Fe(2)-C(14)	89.37(11)
C(8)-N(1)-Fe(1)	117.37(15)	N(2)-Fe(2)-C(14)	144.04(10)
C(7)-Fe(1)-C(6)	96.20(11)	C(18)-Fe(2)-C(15)	90.70(11)
C(7)-Fe(1)-N(1)	92.21(10)	C(17)-Fe(2)-C(15)	115.96(11)
C(6)-Fe(1)-N(1)	93.03(11)	N(2)-Fe(2)-C(15)	149.49(10)
C(7)-Fe(1)-C(4)	91.97(12)	C(14)-Fe(2)-C(15)	39.57(10)
C(6)-Fe(1)-C(4)	115.74(12)	C(18)-Fe(2)-C(13)	156.17(11)
N(1)-Fe(1)-C(4)	150.26(10)	C(17)-Fe(2)-C(13)	100.50(10)
C(7)-Fe(1)-C(3)	125.05(12)	N(2)-Fe(2)-C(13)	104.56(10)
C(6)-Fe(1)-C(3)	88.85(11)	C(14)-Fe(2)-C(13)	39.90(10)
N(1)-Fe(1)-C(3)	142.29(10)	C(15)-Fe(2)-C(13)	66.55(10)
C(4)-Fe(1)-C(3)	39.49(10)	C(18)-Fe(2)-C(16)	92.24(11)

C(7)-Fe(1)-C(2)	157.19(11)	C(17)-Fe(2)-C(16)	154.48(11)
C(6)-Fe(1)-C(2)	99.82(10)	N(2)-Fe(2)-C(16)	109.91(10)
N(1)-Fe(1)-C(2)	102.99(10)	C(14)-Fe(2)-C(16)	66.21(11)
C(4)-Fe(1)-C(2)	66.45(11)	C(15)-Fe(2)-C(16)	39.58(10)
C(3)-Fe(1)-C(2)	39.93(10)	C(13)-Fe(2)-C(16)	65.91(10)
C(7)-Fe(1)-C(5)	92.92(11)	C(18)-Fe(2)-C(12)	126.18(11)
C(6)-Fe(1)-C(5)	154.23(11)	C(17)-Fe(2)-C(12)	137.91(11)
N(1)-Fe(1)-C(5)	110.68(9)	N(2)-Fe(2)-C(12)	88.62(11)
C(4)-Fe(1)-C(5)	39.68(10)	C(14)-Fe(2)-C(12)	65.96(11)
C(3)-Fe(1)-C(5)	66.32(11)	C(15)-Fe(2)-C(12)	65.92(11)
C(2)-Fe(1)-C(5)	65.95(10)	C(13)-Fe(2)-C(12)	39.01(10)
C(7)-Fe(1)-C(1)	126.36(11)	C(16)-Fe(2)-C(12)	38.95(10)
C(6)-Fe(1)-C(1)	137.36(11)	F(3)-B(1)-F(2)	110.0(2)
N(1)-Fe(1)-C(1)	88.32(9)	F(3)-B(1)-F(1)	109.5(3)
C(4)-Fe(1)-C(1)	65.77(10)	F(2)-B(1)-F(1)	112.3(3)
C(3)-Fe(1)-C(1)	65.99(10)	F(3)-B(1)-F(4)	109.5(3)
C(2)-Fe(1)-C(1)	39.10(9)	F(2)-B(1)-F(4)	107.7(3)
C(5)-Fe(1)-C(1)	38.78(10)	F(1)-B(1)-F(4)	107.7(2)
C(13)-C(12)-C(16)	108.6(3)	F(7)-B(2)-F(5)	110.3(3)
C(13)-C(12)-Fe(2)	69.66(14)	F(7)-B(2)-F(8)	110.1(3)
C(16)-C(12)-Fe(2)	70.11(15)	F(5)-B(2)-F(8)	109.3(3)
C(12)-C(13)-C(14)	107.6(2)	F(7)-B(2)-F(6)	110.3(3)
C(12)-C(13)-Fe(2)	71.32(15)	F(5)-B(2)-F(6)	107.9(2)
C(14)-C(13)-Fe(2)	69.58(14)	F(8)-B(2)-F(6)	108.9(3)

APPENDIX 5

Mass spectra of the 1-aminoalkane complexes
$[Cp(CO)Fe\{NH_2(CH_2)_nCH_3\}]BF_4$ (n = 2-6)
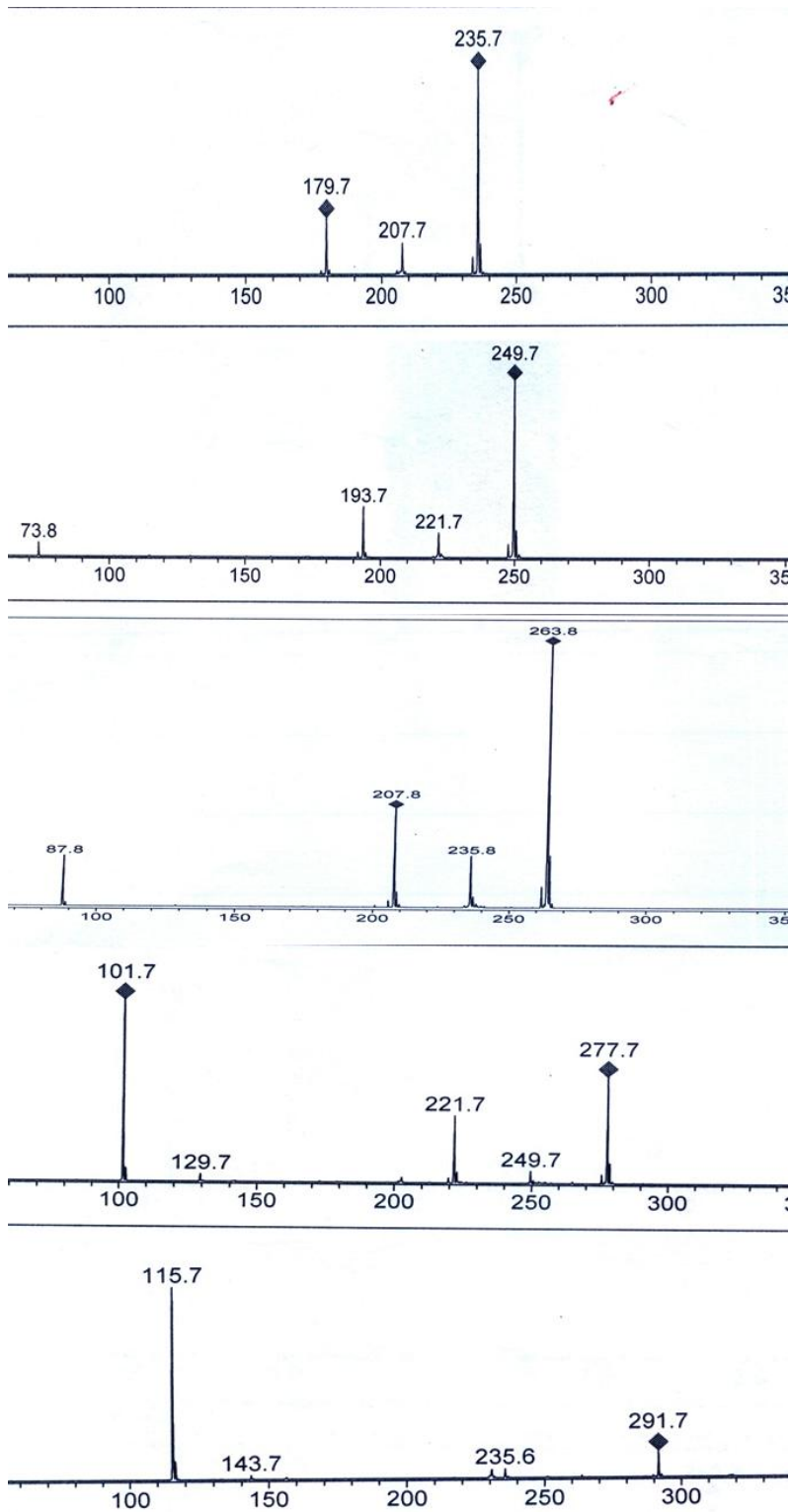
APPENDIX 6

X-ray Crystallographic Data Pertaining to Chapter Three

Table 5A.   Bond lengths [Å] and angles [°] for [Cp*Fe(CO)$_2$NH$_2$(CH$_2$)$_3$CH$_3$]BF$_4$

Bond	Length	Bond	Length
C(1)-C(2)	1.425(3)	C(5)-Fe(1)	2.097(2)
C(1)-C(5)	1.439(3)	C(11)-O(1)	1.137(3)
C(1)-C(6)	1.505(3)	C(11)-Fe(1)	1.787(2)
C(1)-Fe(1)	2.105(2)	C(12)-O(2)	1.143(3)
C(2)-C(3)	1.423(3)	C(12)-Fe(1)	1.777(2)
C(2)-C(7)	1.499(3)	C(13)-N(1)	1.482(3)
C(2)-Fe(1)	2.132(2)	C(13)-C(14)	1.517(2)
C(3)-C(4)	1.436(3)	C(14)-C(15)	1.507(3)
C(3)-C(8)	1.500(3)	C(15)-C(16)	1.516(3)
C(3)-Fe(1)	2.120(2)	N(1)-Fe(1)	2.0220(15)
C(4)-C(5)	1.419(3)	B(1)-F(4)	1.351(3)
C(4)-C(9)	1.510(3)	B(1)-F(3)	1.372(3)
C(4)-Fe(1)	2.0949(19)	B(1)-F(2)	1.383(3)
C(5)-C(10)	1.497(3)	B(1)-F(1)	1.385(3)

Table 6A. Bond angles [°] for [Cp*Fe(CO)$_2$NH$_2$(CH$_2$)$_3$CH$_3$]BF$_4$

Bond	Angle	Bond	Angle
C(2)-C(1)-C(5)	107.43(18)	C(13)-N(1)-Fe(1)	119.16(12)
C(2)-C(1)-C(6)	127.2(2)	C(12)-Fe(1)-C(11)	95.79(11)
C(5)-C(1)-C(6)	124.95(19)	C(12)-Fe(1)-N(1)	93.17(8)
C(2)-C(1)-Fe(1)	71.34(13)	C(11)-Fe(1)-N(1)	94.82(8)
C(5)-C(1)-Fe(1)	69.65(13)	C(12)-Fe(1)-C(4)	115.43(9)
C(6)-C(1)-Fe(1)	129.89(16)	C(11)-Fe(1)-C(4)	89.04(9)
C(3)-C(2)-C(1)	108.62(18)	N(1)-Fe(1)-C(4)	150.63(8)
C(3)-C(2)-C(7)	124.4(2)	C(12)-Fe(1)-C(5)	88.51(10)
C(1)-C(2)-C(7)	126.9(2)	C(11)-Fe(1)-C(5)	121.65(9)
C(3)-C(2)-Fe(1)	70.02(12)	N(1)-Fe(1)-C(5)	143.15(8)
C(1)-C(2)-Fe(1)	69.36(13)	C(4)-Fe(1)-C(5)	39.56(8)
C(7)-C(2)-Fe(1)	127.59(16)	C(12)-Fe(1)-C(1)	99.25(10)
C(2)-C(3)-C(4)	107.68(18)	C(11)-Fe(1)-C(1)	155.34(9)
C(2)-C(3)-C(8)	125.7(2)	N(1)-Fe(1)-C(1)	103.69(7)
C(4)-C(3)-C(8)	126.3(2)	C(4)-Fe(1)-C(1)	66.87(8)
C(2)-C(3)-Fe(1)	70.87(12)	C(5)-Fe(1)-C(1)	40.05(8)
C(4)-C(3)-Fe(1)	69.13(11)	C(12)-Fe(1)-C(3)	154.02(9)
C(8)-C(3)-Fe(1)	130.48(16)	C(11)-Fe(1)-C(3)	92.00(9)
C(5)-C(4)-C(3)	108.08(17)	N(1)-Fe(1)-C(3)	110.85(7)
C(5)-C(4)-C(9)	126.02(18)	C(4)-Fe(1)-C(3)	39.83(8)
C(3)-C(4)-C(9)	125.65(19)	C(5)-Fe(1)-C(3)	66.44(9)
C(5)-C(4)-Fe(1)	70.29(11)	C(1)-Fe(1)-C(3)	66.37(8)
C(3)-C(4)-Fe(1)	71.04(11)	C(12)-Fe(1)-C(2)	136.97(11)
C(9)-C(4)-Fe(1)	128.68(16)	C(11)-Fe(1)-C(2)	126.91(9)
C(4)-C(5)-C(1)	108.17(17)	N(1)-Fe(1)-C(2)	88.69(7)
C(4)-C(5)-C(10)	126.53(18)	C(4)-Fe(1)-C(2)	66.20(8)
C(1)-C(5)-C(10)	125.1(2)	C(5)-Fe(1)-C(2)	66.17(8)
C(4)-C(5)-Fe(1)	70.15(12)	C(1)-Fe(1)-C(2)	39.29(9)
C(1)-C(5)-Fe(1)	70.30(12)	C(3)-Fe(1)-C(2)	39.11(8)
C(10)-C(5)-Fe(1)	129.10(17)	F(4)-B(1)-F(3)	109.9(2)
O(1)-C(11)-Fe(1)	173.89(19)	F(4)-B(1)-F(2)	108.0(3)
O(2)-C(12)-Fe(1)	175.69(19)	F(3)-B(1)-F(2)	109.6(2)
N(1)-C(13)-C(14)	112.61(17)	F(4)-B(1)-F(1)	109.3(2)
C(15)-C(14)-C(13)	112.09(17)	F(3)-B(1)-F(1)	111.2(2)
C(14)-C(15)-C(16)	113.78(19)	F(2)-B(1)-F(1)	108.8(2)

Table 7A. Bond length (Å) for [{Cp*Fe(CO)$_2$}$_2$ μ-{NH$_2$(CH$_2$)$_3$NH$_2$}](BF$_4$)$_2$

Bond	Length	Bond	Length
C(1A)-C(5A)	1.424(7)	C(13)-N(1)	1.489(2)
C(1A)-C(2A)	1.445(14)	C(13)-C(14)	1.521(2)
C(1A)-C(6A)	1.488(9)	C(14)-C(15)	1.527(2)
C(1A)-Fe(1)	2.102(9)	C(15)-N(2)	1.490(2)
C(2A)-C(3A)	1.417(9)	C(16)-C(17)	1.492(2)
C(2A)-C(7A)	1.497(10)	C(17)-C(26)	1.419(2)
C(2A)-Fe(1)	2.050(10)	C(17)-C(19)	1.423(2)
C(3A)-C(4A)	1.429(6)	C(17)-Fe(2)	2.1350(17)
C(3A)-C(8A)	1.495(6)	C(18)-C(19)	1.497(3)
C(3A)-Fe(1)	2.077(4)	C(19)-C(22)	1.437(2)
C(4A)-C(5A)	1.419(5)	C(19)-Fe(2)	2.1134(18)
C(4A)-C(9A)	1.499(5)	C(20)-C(22)	1.495(3)
C(4A)-Fe(1)	2.128(4)	C(22)-C(24)	1.419(3)
C(5A)-C(10A)	1.508(6)	C(22)-Fe(2)	2.0862(17)
C(5A)-Fe(1)	2.160(4)	C(23)-C(24)	1.498(3)
C(4B)-C(5B)	1.402(12)	C(24)-C(26)	1.445(2)
C(4B)-C(3B)	1.419(10)	C(24)-Fe(2)	2.0799(17)
C(4B)-C(9B)	1.514(10)	C(25)-C(26)	1.495(2)
C(4B)-Fe(1)	2.092(7)	C(26)-Fe(2)	2.1075(17)
C(3B)-C(2B)	1.439(13)	C(27)-O(4)	1.137(2)
C(3B)-C(8B)	1.509(11)	C(27)-Fe(2)	1.7864(19)
C(3B)-Fe(1)	2.126(8)	C(28)-O(3)	1.136(2)
C(5B)-C(1B)	1.402(15)	C(28)-Fe(2)	1.7932(19)
C(5B)-C(10B)	1.494(11)	B(1)-F(3)	1.373(3)
C(5B)-Fe(1)	2.075(8)	B(1)-F(1)	1.386(3)
C(2B)-C(1B)	1.44(3)	B(1)-F(2)	1.391(3)
C(2B)-C(7B)	1.50(2)	B(1)-F(4)	1.397(2)
C(2B)-Fe(1)	2.16(2)	B(2)-F(8)	1.364(3)
C(1B)-C(6B)	1.505(18)	B(2)-F(6)	1.368(3)
C(1B)-Fe(1)	2.081(16)	B(2)-F(7)	1.379(3)
C(11)-O(2)	1.136(2)	B(2)-F(5)	1.391(2)
C(11)-Fe(1)	1.7839(19)	N(1)-Fe(1)	2.0182(16)
C(12)-O(1)	1.137(2)	N(2)-Fe(2)	2.0202(14)
C(12)-Fe(1)	1.7893(19)		

Table 8A. Bond angles (°) for [{Cp*Fe(CO)$_2$}$_2$ μ-{NH$_2$(CH$_2$)$_3$NH$_2$}](BF$_4$)$_2$

Bonds	Angle	Bonds	Angle
C(5A)-C(1A)-C(2A)	106.4(6)	F(8)-B(2)-F(6)	107.8(2)
C(5A)-C(1A)-C(6A)	125.3(7)	F(8)-B(2)-F(7)	111.4(2)
C(2A)-C(1A)-C(6A)	128.2(6)	F(6)-B(2)-F(7)	110.45(19)
C(5A)-C(1A)-Fe(1)	72.7(4)	F(8)-B(2)-F(5)	109.43(18)
C(2A)-C(1A)-Fe(1)	67.7(5)	F(6)-B(2)-F(5)	108.4(2)
C(6A)-C(1A)-Fe(1)	127.6(5)	F(7)-B(2)-F(5)	109.31(19)
C(3A)-C(2A)-C(1A)	108.7(7)	C(13)-N(1)-Fe(1)	117.68(11)
C(3A)-C(2A)-C(7A)	126.7(7)	C(15)-N(2)-Fe(2)	117.61(11)
C(1A)-C(2A)-C(7A)	124.4(6)	C(11)-Fe(1)-C(12)	95.41(9)
C(3A)-C(2A)-Fe(1)	70.9(4)	C(11)-Fe(1)-N(1)	93.32(8)
C(1A)-C(2A)-Fe(1)	71.6(5)	C(12)-Fe(1)-N(1)	94.91(8)
C(7A)-C(2A)-Fe(1)	127.6(6)	C(11)-Fe(1)-C(2A)	91.4(3)
C(2A)-C(3A)-C(4A)	107.9(5)	C(12)-Fe(1)-C(2A)	116.2(2)
C(2A)-C(3A)-C(8A)	125.5(6)	N(1)-Fe(1)-C(2A)	147.9(2)
C(4A)-C(3A)-C(8A)	126.5(5)	C(11)-Fe(1)-C(5B)	142.6(3)
C(2A)-C(3A)-Fe(1)	68.9(5)	C(12)-Fe(1)-C(5B)	120.6(4)
C(4A)-C(3A)-Fe(1)	72.1(2)	N(1)-Fe(1)-C(5B)	93.1(3)
C(8A)-C(3A)-Fe(1)	127.8(3)	C(2A)-Fe(1)-C(5B)	65.2(4)
C(5A)-C(4A)-C(3A)	107.7(4)	C(11)-Fe(1)-C(3A)	124.5(2)

C(5A)-C(4A)-C(9A)	125.7(5)	C(12)-Fe(1)-C(3A)	88.61(13)
C(3A)-C(4A)-C(9A)	126.3(5)	N(1)-Fe(1)-C(3A)	141.58(19)
C(5A)-C(4A)-Fe(1)	71.9(2)	C(2A)-Fe(1)-C(3A)	40.1(3)
C(3A)-C(4A)-Fe(1)	68.2(2)	C(5B)-Fe(1)-C(3A)	53.5(3)
C(9A)-C(4A)-Fe(1)	130.1(3)	C(11)-Fe(1)-C(1B)	103.4(4)
C(4A)-C(5A)-C(1A)	109.3(6)	C(12)-Fe(1)-C(1B)	152.8(4)
C(4A)-C(5A)-C(10A)	125.6(5)	N(1)-Fe(1)-C(1B)	103.4(4)
C(1A)-C(5A)-C(10A)	125.1(5)	C(2A)-Fe(1)-C(1B)	44.8(4)
C(4A)-C(5A)-Fe(1)	69.5(2)	C(5B)-Fe(1)-C(1B)	39.4(4)
C(1A)-C(5A)-Fe(1)	68.3(4)	C(3A)-Fe(1)-C(1B)	64.5(4)
C(10A)-C(5A)-Fe(1)	128.8(3)	C(11)-Fe(1)-C(4B)	147.0(3)
C(5B)-C(4B)-C(3B)	108.8(8)	C(12)-Fe(1)-C(4B)	87.7(3)
C(5B)-C(4B)-C(9B)	123.5(11)	N(1)-Fe(1)-C(4B)	119.2(4)
C(3B)-C(4B)-C(9B)	127.6(11)	C(2A)-Fe(1)-C(4B)	58.4(3)
C(5B)-C(4B)-Fe(1)	69.7(5)	C(5B)-Fe(1)-C(4B)	39.3(4)
C(3B)-C(4B)-Fe(1)	71.6(5)	C(3A)-Fe(1)-C(4B)	22.6(3)
C(9B)-C(4B)-Fe(1)	127.2(5)	C(1B)-Fe(1)-C(4B)	65.8(5)
C(4B)-C(3B)-C(2B)	108.1(12)	C(11)-Fe(1)-C(1A)	93.57(19)
C(4B)-C(3B)-C(8B)	126.1(10)	C(12)-Fe(1)-C(1A)	155.5(3)
C(2B)-C(3B)-C(8B)	125.6(12)	N(1)-Fe(1)-C(1A)	107.3(3)
C(4B)-C(3B)-Fe(1)	69.1(5)	C(2A)-Fe(1)-C(1A)	40.7(4)
C(2B)-C(3B)-Fe(1)	71.7(9)	C(5B)-Fe(1)-C(1A)	49.5(3)
C(8B)-C(3B)-Fe(1)	129.0(5)	C(3A)-Fe(1)-C(1A)	67.6(3)
C(4B)-C(5B)-C(1B)	108.0(9)	C(1B)-Fe(1)-C(1A)	10.3(4)
C(4B)-C(5B)-C(10B)	129.7(11)	C(4B)-Fe(1)-C(1A)	72.6(3)
C(1B)-C(5B)-C(10B)	122.3(12)	C(11)-Fe(1)-C(3B)	107.8(2)
C(4B)-C(5B)-Fe(1)	71.0(4)	C(12)-Fe(1)-C(3B)	89.7(3)
C(1B)-C(5B)-Fe(1)	70.5(7)	N(1)-Fe(1)-C(3B)	157.9(2)
C(10B)-C(5B)-Fe(1)	126.1(6)	C(2A)-Fe(1)-C(3B)	29.5(3)
C(1B)-C(2B)-C(3B)	105.6(14)	C(5B)-Fe(1)-C(3B)	66.2(3)
C(1B)-C(2B)-C(7B)	130.7(13)	C(3A)-Fe(1)-C(3B)	16.71(16)
C(3B)-C(2B)-C(7B)	123.7(16)	C(1B)-Fe(1)-C(3B)	66.0(5)
C(1B)-C(2B)-Fe(1)	67.2(10)	C(4B)-Fe(1)-C(3B)	39.3(3)
C(3B)-C(2B)-Fe(1)	69.1(8)	C(1A)-Fe(1)-C(3B)	65.8(4)
C(7B)-C(2B)-Fe(1)	128.8(13)	C(11)-Fe(1)-C(4A)	157.51(12)
C(5B)-C(1B)-C(2B)	109.5(13)	C(12)-Fe(1)-C(4A)	99.27(16)
C(5B)-C(1B)-C(6B)	128.5(12)	N(1)-Fe(1)-C(4A)	102.24(15)
C(2B)-C(1B)-C(6B)	121.7(11)	C(2A)-Fe(1)-C(4A)	66.8(3)
C(5B)-C(1B)-Fe(1)	70.0(7)	C(5B)-Fe(1)-C(4A)	22.2(3)
C(2B)-C(1B)-Fe(1)	73.2(10)	C(3A)-Fe(1)-C(4A)	39.71(17)
C(6B)-C(1B)-Fe(1)	128.1(10)	C(1B)-Fe(1)-C(4A)	57.4(4)
O(2)-C(11)-Fe(1)	175.42(17)	C(4B)-Fe(1)-C(4A)	19.5(3)
O(1)-C(12)-Fe(1)	173.76(18)	C(1A)-Fe(1)-C(4A)	66.5(2)
N(1)-C(13)-C(14)	110.71(14)	C(3B)-Fe(1)-C(4A)	55.6(2)
C(13)-C(14)-C(15)	114.47(14)	C(11)-Fe(1)-C(2B)	85.9(5)
N(2)-C(15)-C(14)	113.02(14)	C(12)-Fe(1)-C(2B)	124.7(5)
C(26)-C(17)-C(19)	109.38(15)	N(1)-Fe(1)-C(2B)	140.4(5)
C(26)-C(17)-C(16)	125.68(16)	C(2A)-Fe(1)-C(2B)	9.7(5)
C(19)-C(17)-C(16)	124.94(16)	C(5B)-Fe(1)-C(2B)	66.3(6)
C(26)-C(17)-Fe(2)	69.42(10)	C(3A)-Fe(1)-C(2B)	49.2(4)
C(19)-C(17)-Fe(2)	69.62(10)	C(1B)-Fe(1)-C(2B)	39.5(7)
C(16)-C(17)-Fe(2)	127.46(12)	C(4B)-Fe(1)-C(2B)	65.9(5)
C(17)-C(19)-C(22)	107.02(15)	C(1A)-Fe(1)-C(2B)	33.6(6)
C(17)-C(19)-C(18)	126.11(17)	C(3B)-Fe(1)-C(2B)	39.2(4)
C(22)-C(19)-C(18)	126.53(16)	C(4A)-Fe(1)-C(2B)	71.8(6)
C(17)-C(19)-Fe(2)	71.26(10)	C(27)-Fe(2)-C(28)	97.00(9)
C(22)-C(19)-Fe(2)	68.98(10)	C(27)-Fe(2)-N(2)	94.14(8)
C(18)-C(19)-Fe(2)	129.99(13)	C(28)-Fe(2)-N(2)	94.16(7)
C(24)-C(22)-C(19)	108.51(15)	C(27)-Fe(2)-C(24)	116.98(8)
C(24)-C(22)-C(20)	126.02(17)	C(28)-Fe(2)-C(24)	87.28(8)
C(19)-C(22)-C(20)	125.29(17)	N(2)-Fe(2)-C(24)	148.47(7)
C(24)-C(22)-Fe(2)	69.86(10)	C(27)-Fe(2)-C(22)	88.70(8)
C(19)-C(22)-Fe(2)	71.01(10)	C(28)-Fe(2)-C(22)	119.54(8)
C(20)-C(22)-Fe(2)	128.85(14)	N(2)-Fe(2)-C(22)	145.61(7)

C(22)-C(24)-C(26)	107.91(15)	C(24)-Fe(2)-C(22)	39.81(7)
C(22)-C(24)-C(23)	125.97(17)	C(27)-Fe(2)-C(26)	155.36(8)
C(26)-C(24)-C(23)	125.94(17)	C(28)-Fe(2)-C(26)	91.86(8)
C(22)-C(24)-Fe(2)	70.33(10)	N(2)-Fe(2)-C(26)	108.14(7)
C(26)-C(24)-Fe(2)	70.85(10)	C(24)-Fe(2)-C(26)	40.35(7)
C(23)-C(24)-Fe(2)	128.12(14)	C(22)-Fe(2)-C(26)	67.01(7)
C(17)-C(26)-C(24)	107.14(15)	C(27)-Fe(2)-C(19)	97.73(8)
C(17)-C(26)-C(25)	126.58(16)	C(28)-Fe(2)-C(19)	154.15(8)
C(24)-C(26)-C(25)	126.15(16)	N(2)-Fe(2)-C(19)	105.82(7)
C(17)-C(26)-Fe(2)	71.51(10)	C(24)-Fe(2)-C(19)	67.10(7)
C(24)-C(26)-Fe(2)	68.79(10)	C(22)-Fe(2)-C(19)	40.01(7)
C(25)-C(26)-Fe(2)	127.93(13)	C(26)-Fe(2)-C(19)	66.65(7)
O(4)-C(27)-Fe(2)	174.33(17)	C(27)-Fe(2)-C(17)	134.84(8)
O(3)-C(28)-Fe(2)	172.23(17)	C(28)-Fe(2)-C(17)	127.78(8)
F(3)-B(1)-F(1)	110.26(19)	N(2)-Fe(2)-C(17)	88.71(6)
F(3)-B(1)-F(2)	110.54(18)	C(24)-Fe(2)-C(17)	66.26(7)
F(1)-B(1)-F(2)	107.99(17)	C(22)-Fe(2)-C(17)	65.99(7)
F(3)-B(1)-F(4)	110.81(17)	C(26)-Fe(2)-C(17)	39.07(7)
F(1)-B(1)-F(4)	108.37(17)	C(19)-Fe(2)-C(17)	39.13(7)
F(2)-B(1)-F(4)	108.79(18)		

APPENDIX 7

Mass spectra of the 1-aminoalkane complexes

$[Cp^*(CO)Fe\{NH_2(CH_2)_nCH_3\}]BF_4$ (n = 2-6)
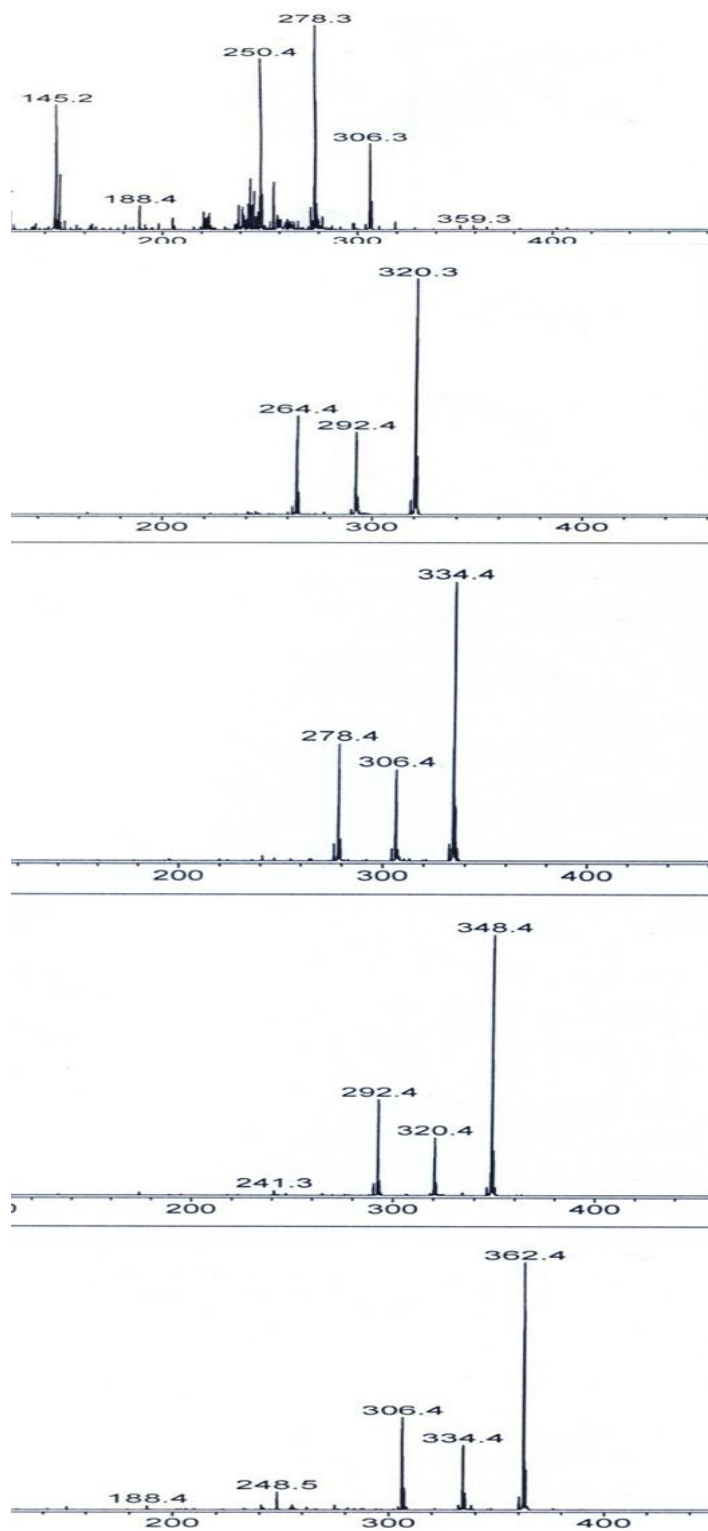
APPENDIX 8

X-ray Crystallographic Data Pertaining to Chapter Four

Table 9A.   Bond lengths [Å] and angles [°] for [Cp*Fe(CO)$_2$NH$_2$(CH$_2$)$_3$CH$_3$]BF$_4$

Bond	Length	Bond	Length
C(1)-C(2)	1.425(3)	C(5)-Fe(1)	2.097(2)
C(1)-C(5)	1.439(3)	C(11)-O(1)	1.137(3)
C(1)-C(6)	1.505(3)	C(11)-Fe(1)	1.787(2)
C(1)-Fe(1)	2.105(2)	C(12)-O(2)	1.143(3)
C(2)-C(3)	1.423(3)	C(12)-Fe(1)	1.777(2)
C(2)-C(7)	1.499(3)	C(13)-N(1)	1.482(3)
C(2)-Fe(1)	2.132(2)	C(13)-C(14)	1.517(2)
C(3)-C(4)	1.436(3)	C(14)-C(15)	1.507(3)
C(3)-C(8)	1.500(3)	C(15)-C(16)	1.516(3)
C(3)-Fe(1)	2.120(2)	N(1)-Fe(1)	2.0220(15)
C(4)-C(5)	1.419(3)	B(1)-F(4)	1.351(3)
C(4)-C(9)	1.510(3)	B(1)-F(3)	1.372(3)
C(4)-Fe(1)	2.0949(19)	B(1)-F(2)	1.383(3)
C(5)-C(10)	1.497(3)	B(1)-F(1)	1.385(3)

Table 10A. Bond angles [°] for [Cp*Fe(CO)$_2$NH$_2$(CH$_2$)$_3$CH$_3$]BF$_4$

Bond	Angle	Bond	Angle
C(2)-C(1)-C(5)	107.43(18)	C(13)-N(1)-Fe(1)	119.16(12)
C(2)-C(1)-C(6)	127.2(2)	C(12)-Fe(1)-C(11)	95.79(11)
C(5)-C(1)-C(6)	124.95(19)	C(12)-Fe(1)-N(1)	93.17(8)
C(2)-C(1)-Fe(1)	71.34(13)	C(11)-Fe(1)-N(1)	94.82(8)
C(5)-C(1)-Fe(1)	69.65(13)	C(12)-Fe(1)-C(4)	115.43(9)
C(6)-C(1)-Fe(1)	129.89(16)	C(11)-Fe(1)-C(4)	89.04(9)
C(3)-C(2)-C(1)	108.62(18)	N(1)-Fe(1)-C(4)	150.63(8)
C(3)-C(2)-C(7)	124.4(2)	C(12)-Fe(1)-C(5)	88.51(10)
C(1)-C(2)-C(7)	126.9(2)	C(11)-Fe(1)-C(5)	121.65(9)
C(3)-C(2)-Fe(1)	70.02(12)	N(1)-Fe(1)-C(5)	143.15(8)
C(1)-C(2)-Fe(1)	69.36(13)	C(4)-Fe(1)-C(5)	39.56(8)
C(7)-C(2)-Fe(1)	127.59(16)	C(12)-Fe(1)-C(1)	99.25(10)
C(2)-C(3)-C(4)	107.68(18)	C(11)-Fe(1)-C(1)	155.34(9)
C(2)-C(3)-C(8)	125.7(2)	N(1)-Fe(1)-C(1)	103.69(7)
C(4)-C(3)-C(8)	126.3(2)	C(4)-Fe(1)-C(1)	66.87(8)
C(2)-C(3)-Fe(1)	70.87(12)	C(5)-Fe(1)-C(1)	40.05(8)
C(4)-C(3)-Fe(1)	69.13(11)	C(12)-Fe(1)-C(3)	154.02(9)
C(8)-C(3)-Fe(1)	130.48(16)	C(11)-Fe(1)-C(3)	92.00(9)
C(5)-C(4)-C(3)	108.08(17)	N(1)-Fe(1)-C(3)	110.85(7)
C(5)-C(4)-C(9)	126.02(18)	C(4)-Fe(1)-C(3)	39.83(8)
C(3)-C(4)-C(9)	125.65(19)	C(5)-Fe(1)-C(3)	66.44(9)
C(5)-C(4)-Fe(1)	70.29(11)	C(1)-Fe(1)-C(3)	66.37(8)
C(3)-C(4)-Fe(1)	71.04(11)	C(12)-Fe(1)-C(2)	136.97(11)
C(9)-C(4)-Fe(1)	128.68(16)	C(11)-Fe(1)-C(2)	126.91(9)
C(4)-C(5)-C(1)	108.17(17)	N(1)-Fe(1)-C(2)	88.69(7)
C(4)-C(5)-C(10)	126.53(18)	C(4)-Fe(1)-C(2)	66.20(8)
C(1)-C(5)-C(10)	125.1(2)	C(5)-Fe(1)-C(2)	66.17(8)
C(4)-C(5)-Fe(1)	70.15(12)	C(1)-Fe(1)-C(2)	39.29(9)
C(1)-C(5)-Fe(1)	70.30(12)	C(3)-Fe(1)-C(2)	39.11(8)
C(10)-C(5)-Fe(1)	129.10(17)	F(4)-B(1)-F(3)	109.9(2)
O(1)-C(11)-Fe(1)	173.89(19)	F(4)-B(1)-F(2)	108.0(3)
O(2)-C(12)-Fe(1)	175.69(19)	F(3)-B(1)-F(2)	109.6(2)
N(1)-C(13)-C(14)	112.61(17)	F(4)-B(1)-F(1)	109.3(2)
C(15)-C(14)-C(13)	112.09(17)	F(3)-B(1)-F(1)	111.2(2)
C(14)-C(15)-C(16)	113.78(19)	F(2)-B(1)-F(1)	108.8(2)

Table 11A. Bond Lengths (Å) for [{Cp*}Fe(CO)₂(1-meIm)]BF₄

Bond	Length	Bond	Length
C(1)-C(2)	1.411(4)	C(11)-O(1)	1.142(3)
C(1)-C(5)	1.423(4)	C(11)-Fe(1)	1.778(3)
C(1)-C(6)	1.501(4)	C(12)-O(2)	1.133(3)
C(1)-Fe(1)	2.154(3)	C(12)-Fe(1)	1.787(3)
C(2)-C(3)	1.431(3)	C(13)-N(1)	1.330(3)
C(2)-C(7)	1.502(3)	C(13)-N(2)	1.347(3)
C(2)-Fe(1)	2.105(2)	C(14)-C(15)	1.362(3)
C(3)-C(4)	1.418(3)	C(14)-N(1)	1.385(3)
C(3)-C(8)	1.503(3)	C(15)-N(2)	1.362(3)
C(3)-Fe(1)	2.080(2)	C(16)-N(2)	1.467(3)
C(4)-C(5)	1.431(3)	N(1)-Fe(1)	1.9781(18)
C(4)-C(9)	1.500(3)	F(1)-B(1)	1.383(4)
C(4)-Fe(1)	2.082(2)	F(2)-B(1)	1.337(4)
C(5)-C(10)	1.503(3)	F(3)-B(1)	1.348(4)
C(5)-Fe(1)	2.126(2)	F(4)-B(1)	1.342(4)

Table 12A. Bond Angles (Å) for [{Cp*}Fe(CO)₂(1-meIm)]BF₄

Bonds	Angle	Bonds	Angle
C(2)-C(1)-C(5)	108.8(2)	C(13)-N(2)-C(15)	107.88(19)
C(2)-C(1)-C(6)	125.5(2)	C(13)-N(2)-C(16)	125.3(2)
C(5)-C(1)-C(6)	125.6(2)	C(15)-N(2)-C(16)	126.8(2)
C(2)-C(1)-Fe(1)	68.79(15)	C(11)-Fe(1)-C(12)	93.55(13)
C(5)-C(1)-Fe(1)	69.52(14)	C(11)-Fe(1)-N(1)	94.72(10)
C(6)-C(1)-Fe(1)	127.53(19)	C(12)-Fe(1)-N(1)	93.04(10)
C(1)-C(2)-C(3)	107.4(2)	C(11)-Fe(1)-C(3)	88.29(11)
C(1)-C(2)-C(7)	125.4(2)	C(12)-Fe(1)-C(3)	123.16(11)
C(3)-C(2)-C(7)	126.7(3)	N(1)-Fe(1)-C(3)	143.47(9)
C(1)-C(2)-Fe(1)	72.54(14)	C(11)-Fe(1)-C(4)	114.91(11)
C(3)-C(2)-Fe(1)	69.07(13)	C(12)-Fe(1)-C(4)	90.78(11)
C(7)-C(2)-Fe(1)	129.44(19)	N(1)-Fe(1)-C(4)	149.83(9)
C(4)-C(3)-C(2)	108.4(2)	C(3)-Fe(1)-C(4)	39.85(9)
C(4)-C(3)-C(8)	126.3(2)	C(11)-Fe(1)-C(2)	99.74(11)
C(2)-C(3)-C(8)	125.1(2)	C(12)-Fe(1)-C(2)	157.35(12)
C(4)-C(3)-Fe(1)	70.13(13)	N(1)-Fe(1)-C(2)	103.96(9)
C(2)-C(3)-Fe(1)	70.95(13)	C(3)-Fe(1)-C(2)	39.98(10)
C(8)-C(3)-Fe(1)	127.92(19)	C(4)-Fe(1)-C(2)	67.02(9)
C(3)-C(4)-C(5)	107.6(2)	C(11)-Fe(1)-C(5)	153.48(11)
C(3)-C(4)-C(9)	125.9(2)	C(12)-Fe(1)-C(5)	94.31(12)
C(5)-C(4)-C(9)	126.3(2)	N(1)-Fe(1)-C(5)	110.10(9)
C(3)-C(4)-Fe(1)	70.02(13)	C(3)-Fe(1)-C(5)	66.28(9)
C(5)-C(4)-Fe(1)	71.81(13)	C(4)-Fe(1)-C(5)	39.74(9)
C(9)-C(4)-Fe(1)	127.18(19)	C(2)-Fe(1)-C(5)	66.01(9)
C(1)-C(5)-C(4)	107.6(2)	C(11)-Fe(1)-C(1)	137.15(11)
C(1)-C(5)-C(10)	126.5(2)	C(12)-Fe(1)-C(1)	128.94(12)
C(4)-C(5)-C(10)	125.6(2)	N(1)-Fe(1)-C(1)	88.93(9)
C(1)-C(5)-Fe(1)	71.65(14)	C(3)-Fe(1)-C(1)	65.48(10)
C(4)-C(5)-Fe(1)	68.45(13)	C(4)-Fe(1)-C(1)	65.84(9)
C(10)-C(5)-Fe(1)	130.22(19)	C(2)-Fe(1)-C(1)	38.67(10)
O(1)-C(11)-Fe(1)	176.1(3)	C(5)-Fe(1)-C(1)	38.84(10)
O(2)-C(12)-Fe(1)	177.0(2)	F(2)-B(1)-F(4)	108.3(3)
N(1)-C(13)-N(2)	110.6(2)	F(2)-B(1)-F(3)	110.3(3)
C(15)-C(14)-N(1)	108.9(2)	F(4)-B(1)-F(3)	110.9(3)
C(14)-C(15)-N(2)	106.71(19)	F(2)-B(1)-F(1)	108.9(3)
CC(13)-N(1)-C(14)	105.91(19)	F(4)-B(1)-F(1)	108.6(3)
C(13)-N(1)-Fe(1)	125.94(16)	F(3)-B(1)-F(1)	109.8(3)
C(14)-N(1)-Fe(1)	127.99(15)		

Table 13A. Bond lengths (Å) for [CpFe(CO)$_2$(1-meIm)]BF$_4$

Bond	Length	Bond	Length
C(1)-C(2)	1.370(8)	C(21)-N(3)	1.318(4)
C(1)-C(5)	1.373(9)	C(21)-N(4)	1.336(4)
C(1)-Fe(1)	2.091(4)	C(22)-N(4)	1.469(5)
C(2)-C(3)	1.377(7)	N(3)-Fe(2)	1.977(3)
C(2)-Fe(1)	2.083(4)	C(23)-C(24)	1.397(6)
C(3)-C(4)	1.370(8)	C(23)-C(27)	1.406(6)
C(3)-Fe(1)	2.076(4)	C(23)-Fe(3)	2.108(4)
C(4)-C(5)	1.380(9)	C(24)-C(25)	1.418(6)
C(4)-Fe(1)	2.072(4)	C(24)-Fe(3)	2.091(4)
C(5)-Fe(1)	2.074(5)	C(25)-C(26)	1.405(6)
C(6)-O(1)	1.136(4)	C(25)-Fe(3)	2.076(4)
C(6)-Fe(1)	1.787(4)	C(26)-C(27)	1.404(6)
C(7)-O(2)	1.136(5)	C(26)-Fe(3)	2.083(3)
C(7)-Fe(1)	1.789(4)	C(27)-Fe(3)	2.096(4)
C(8)-C(9)	1.357(5)	C(28)-O(5)	1.136(5)
C(8)-N(1)	1.385(5)	C(28)-Fe(3)	1.788(4)
C(9)-N(2)	1.372(5)	C(29)-O(6)	1.133(4)
C(10)-N(1)	1.326(4)	C(29)-Fe(3)	1.789(4)
C(10)-N(2)	1.339(4)	C(30)-C(31)	1.354(5)
C(11)-N(2)	1.462(5)	C(30)-N(5)	1.380(4)
N(1)-Fe(1)	1.973(3)	C(31)-N(6)	1.367(5)
C(12)-C(16)	1.399(7)	C(32)-N(5)	1.328(4)
C(12)-C(13)	1.407(7)	C(32)-N(6)	1.341(4)
C(12)-Fe(2)	2.118(4)	C(33)-N(6)	1.467(5)
C(13)-C(14)	1.406(6)	N(5)-Fe(3)	1.980(3)
C(13)-Fe(2)	2.099(4)	F(1)-B(1)	1.360(6)
C(14)-C(15)	1.406(6)	F(2)-B(1)	1.382(5)
C(14)-Fe(2)	2.079(4)	F(3)-B(1)	1.391(6)
C(15)-C(16)	1.415(6)	F(4)-B(1)	1.395(6)
C(15)-Fe(2)	2.078(4)	F(5)-B(5)	1.379(5)
C(16)-Fe(2)	2.099(4)	F(6)-B(5)	1.308(6)
C(17)-O(3)	1.129(5)	F(7)-B(5)	1.359(5)
C(17)-Fe(2)	1.787(4)	F(8)-B(3)	1.352(6)
C(18)-O(4)	1.139(5)	B(3)-F(12)	1.314(6)
C(18)-Fe(2)	1.788(4)	B(3)-F(9)	1.335(6)
C(19)-C(20)	1.352(6)	B(3)-F(11)	1.340(6)
C(19)-N(3)	1.376(5)	F(10)-B(5)	1.381(6)
C(20)-N(4)	1.365(5)		

Table 14A. Bond angles (°) for [CpFe(CO)$_2$(1-meIm)]BF$_4$

Bonds	Angle	Bonds	Angle
C(2)-C(1)-C(5)	108.3(5)	C(17)-Fe(2)-C(13)	97.20(18)
C(2)-C(1)-Fe(1)	70.5(3)	C(18)-Fe(2)-C(13)	154.47(18)
C(5)-C(1)-Fe(1)	70.1(3)	N(3)-Fe(2)-C(13)	107.12(15)
C(1)-C(2)-C(3)	108.3(5)	C(15)-Fe(2)-C(13)	66.01(18)
C(1)-C(2)-Fe(1)	71.2(3)	C(14)-Fe(2)-C(13)	39.32(16)
C(3)-C(2)-Fe(1)	70.4(3)	C(17)-Fe(2)-C(16)	157.63(18)
C(4)-C(3)-C(2)	107.5(5)	C(18)-Fe(2)-C(16)	98.0(2)
C(4)-C(3)-Fe(1)	70.6(3)	N(3)-Fe(2)-C(16)	105.45(15)
C(2)-C(3)-Fe(1)	70.9(3)	C(15)-Fe(2)-C(16)	39.59(17)
C(3)-C(4)-C(5)	108.6(5)	C(14)-Fe(2)-C(16)	66.23(17)
C(3)-C(4)-Fe(1)	70.9(3)	C(13)-Fe(2)-C(16)	65.75(19)
C(5)-C(4)-Fe(1)	70.6(3)	C(17)-Fe(2)-C(12)	132.70(19)
C(1)-C(5)-C(4)	107.3(5)	C(18)-Fe(2)-C(12)	134.7(2)
C(1)-C(5)-Fe(1)	71.4(3)	N(3)-Fe(2)-C(12)	87.48(15)
C(4)-C(5)-Fe(1)	70.5(3)	C(15)-Fe(2)-C(12)	65.52(18)
O(1)-C(6)-Fe(1)	176.8(3)	C(14)-Fe(2)-C(12)	65.57(17)
O(2)-C(7)-Fe(1)	176.6(3)	C(13)-Fe(2)-C(12)	38.99(18)

C(9)-C(8)-N(1)	108.8(3)	C(16)-Fe(2)-C(12)	38.76(19)
C(8)-C(9)-N(2)	106.6(3)	C(24)-C(23)-C(27)	108.8(4)
N(1)-C(10)-N(2)	111.0(3)	C(24)-C(23)-Fe(3)	69.9(2)
C(10)-N(1)-C(8)	106.0(3)	C(27)-C(23)-Fe(3)	70.0(2)
C(10)-N(1)-Fe(1)	126.5(2)	C(23)-C(24)-C(25)	107.5(4)
C(8)-N(1)-Fe(1)	127.5(2)	C(23)-C(24)-Fe(3)	71.3(2)
C(10)-N(2)-C(9)	107.6(3)	C(25)-C(24)-Fe(3)	69.6(2)
C(10)-N(2)-C(11)	125.6(3)	C(26)-C(25)-C(24)	107.7(4)
C(9)-N(2)-C(11)	126.8(3)	C(26)-C(25)-Fe(3)	70.5(2)
C(6)-Fe(1)-C(7)	93.00(17)	C(24)-C(25)-Fe(3)	70.7(2)
C(6)-Fe(1)-N(1)	93.27(14)	C(27)-C(26)-C(25)	108.4(4)
C(7)-Fe(1)-N(1)	93.73(14)	C(27)-C(26)-Fe(3)	70.9(2)
C(6)-Fe(1)-C(4)	123.0(2)	C(25)-C(26)-Fe(3)	70.0(2)
C(7)-Fe(1)-C(4)	89.69(19)	C(26)-C(27)-C(23)	107.5(4)
N(1)-Fe(1)-C(4)	143.3(2)	C(26)-C(27)-Fe(3)	69.9(2)
C(6)-Fe(1)-C(5)	157.9(2)	C(23)-C(27)-Fe(3)	70.9(2)
C(7)-Fe(1)-C(5)	98.5(2)	O(5)-C(28)-Fe(3)	177.7(4)
N(1)-Fe(1)-C(5)	104.7(2)	O(6)-C(29)-Fe(3)	176.2(4)
C(4)-Fe(1)-C(5)	38.9(3)	C(31)-C(30)-N(5)	108.3(3)
C(6)-Fe(1)-C(3)	92.90(18)	C(30)-C(31)-N(6)	107.0(3)
C(7)-Fe(1)-C(3)	117.0(2)	N(5)-C(32)-N(6)	110.2(3)
N(1)-Fe(1)-C(3)	148.22(18)	C(32)-N(5)-C(30)	106.7(3)
C(4)-Fe(1)-C(3)	38.6(2)	C(32)-N(5)-Fe(3)	126.4(2)
C(5)-Fe(1)-C(3)	65.1(2)	C(30)-N(5)-Fe(3)	126.6(2)
C(6)-Fe(1)-C(2)	97.48(18)	C(32)-N(6)-C(31)	107.7(3)
C(7)-Fe(1)-C(2)	153.73(18)	C(32)-N(6)-C(33)	125.0(3)
N(1)-Fe(1)-C(2)	109.57(17)	C(31)-N(6)-C(33)	127.2(3)
C(4)-Fe(1)-C(2)	64.4(2)	C(28)-Fe(3)-C(29)	95.72(18)
C(5)-Fe(1)-C(2)	64.7(2)	C(28)-Fe(3)-N(5)	91.11(14)
C(3)-Fe(1)-C(2)	38.7(2)	C(29)-Fe(3)-N(5)	92.79(14)
C(6)-Fe(1)-C(1)	131.7(2)	C(28)-Fe(3)-C(25)	91.18(17)
C(7)-Fe(1)-C(1)	135.0(2)	C(29)-Fe(3)-C(25)	119.14(18)
N(1)-Fe(1)-C(1)	88.49(15)	N(5)-Fe(3)-C(25)	147.56(16)
C(4)-Fe(1)-C(1)	64.4(2)	C(28)-Fe(3)-C(26)	121.45(17)
C(5)-Fe(1)-C(1)	38.5(3)	C(29)-Fe(3)-C(26)	89.22(16)
C(3)-Fe(1)-C(1)	64.56(19)	N(5)-Fe(3)-C(26)	147.02(15)
C(2)-Fe(1)-C(1)	38.3(2)	C(25)-Fe(3)-C(26)	39.49(17)
C(16)-C(12)-C(13)	108.6(4)	C(28)-Fe(3)-C(24)	96.95(18)
C(16)-C(12)-Fe(2)	69.9(2)	C(29)-Fe(3)-C(24)	155.46(17)
C(13)-C(12)-Fe(2)	69.8(2)	N(5)-Fe(3)-C(24)	107.86(16)
C(14)-C(13)-C(12)	107.8(4)	C(25)-Fe(3)-C(24)	39.80(18)
C(14)-C(13)-Fe(2)	69.6(2)	C(26)-Fe(3)-C(24)	66.24(16)
C(12)-C(13)-Fe(2)	71.2(2)	C(28)-Fe(3)-C(27)	157.37(17)
C(13)-C(14)-C(15)	108.0(4)	C(29)-Fe(3)-C(27)	95.56(17)
C(13)-C(14)-Fe(2)	71.1(2)	N(5)-Fe(3)-C(27)	107.86(14)
C(15)-C(14)-Fe(2)	70.2(2)	C(25)-Fe(3)-C(27)	66.19(16)
C(14)-C(15)-C(16)	108.0(4)	C(26)-Fe(3)-C(27)	39.27(16)
C(14)-C(15)-Fe(2)	70.3(2)	C(24)-Fe(3)-C(27)	65.98(16)
C(16)-C(15)-Fe(2)	71.0(2)	C(28)-Fe(3)-C(23)	132.45(18)
C(12)-C(16)-C(15)	107.6(4)	C(29)-Fe(3)-C(23)	131.75(18)
C(12)-C(16)-Fe(2)	71.3(2)	N(5)-Fe(3)-C(23)	89.42(14)
C(15)-C(16)-Fe(2)	69.4(2)	C(25)-Fe(3)-C(23)	65.72(17)
O(3)-C(17)-Fe(2)	177.2(4)	C(26)-Fe(3)-C(23)	65.47(16)
O(4)-C(18)-Fe(2)	175.2(4)	C(24)-Fe(3)-C(23)	38.86(18)
C(20)-C(19)-N(3)	108.6(4)	C(27)-Fe(3)-C(23)	39.07(16)
C(19)-C(20)-N(4)	106.7(3)	F(1)-B(1)-F(2)	109.7(4)
N(3)-C(21)-N(4)	110.7(3)	F(1)-B(1)-F(3)	110.1(4)
C(21)-N(3)-C(19)	106.3(3)	F(2)-B(1)-F(3)	109.8(4)
C(21)-N(3)-Fe(2)	127.2(2)	F(1)-B(1)-F(4)	110.1(4)
C(19)-N(3)-Fe(2)	126.3(3)	F(2)-B(1)-F(4)	108.4(4)
C(21)-N(4)-C(20)	107.6(3)	F(3)-B(1)-F(4)	108.6(4)
C(21)-N(4)-C(22)	125.4(3)	F(12)-B(3)-F(9)	109.5(5)
C(20)-N(4)-C(22)	127.0(3)	F(12)-B(3)-F(11)	110.0(5)
C(17)-Fe(2)-C(18)	92.31(18)	F(9)-B(3)-F(11)	105.8(5)

C(17)-Fe(2)-N(3)	93.09(14)	F(12)-B(3)-F(8)	107.4(4)
C(18)-Fe(2)-N(3)	95.92(15)	F(9)-B(3)-F(8)	110.2(5)
C(17)-Fe(2)-C(15)	121.48(17)	F(11)-B(3)-F(8)	113.9(5)
C(18)-Fe(2)-C(15)	88.82(18)	F(6)-B(5)-F(7)	111.0(4)
N(3)-Fe(2)-C(15)	144.95(15)	F(6)-B(5)-F(5)	109.9(4)
C(17)-Fe(2)-C(14)	91.40(16)	F(7)-B(5)-F(5)	112.5(4)
C(18)-Fe(2)-C(14)	117.13(17)	F(6)-B(5)-F(10)	107.8(5)
N(3)-Fe(2)-C(14)	146.43(14)	F(7)-B(5)-F(10)	105.8(4)
C(15)-Fe(2)-C(14)	39.54(17)	F(5)-B(5)-F(10)	109.7(4)

APPENDIX 9

X-ray Crystallographic Data Pertaining to Chapter Five

Table 15A. Bond lengths (Å) for [Cp*Fe(CO)$_2$(NH$_2$CH$_2$CHCH$_2$)]BF$_4$

Bond	Length	Bond	Length
C(1)-C(5)	1.417(2)	C(5)-Fe(1)	2.1179(16)
C(1)-C(2)	1.434(2)	C(11)-O(1)	1.136(2)
C(1)-C(6)	1.499(2)	C(11)-Fe(1)	1.7843(16)
C(1)-Fe(1)	2.1366(15)	C(12)-O(2)	1.133(2)
C(2)-C(3)	1.435(2)	C(12)-Fe(1)	1.7926(18)
C(2)-C(7)	1.498(2)	C(13)-C(14)	1.486(2)
C(2)-Fe(1)	2.1202(16)	C(13)-N(2)	1.491(2)
C(3)-C(4)	1.422(3)	C(14)-C(15)	1.320(3)
C(3)-C(8)	1.506(2)	N(2)-Fe(1)	2.0294(14)
C(3)-Fe(1)	2.0963(17)	B(1)-F(4)	1.357(2)
C(4)-C(5)	1.443(2)	B(1)-F(3)	1.363(2)
C(4)-C(9)	1.498(2)	B(1)-F(1)	1.371(2)
C(4)-Fe(1)	2.0884(17)	B(1)-F(2)	1.379(2)
C(5)-C(10)	1.499(2)		

Table 16A. Bond angles (°) for [Cp*Fe(CO)$_2$(NH$_2$CH$_2$CHCH$_2$)]BF$_4$

Bonds	Angle	Bonds	Angle
C(5)-C(1)-C(2)	108.96(14)	C(14)-C(13)-N(2)	113.06(14)
C(5)-C(1)-C(6)	124.54(15)	C(15)-C(14)-C(13)	123.61(18)
C(2)-C(1)-C(6)	126.49(15)	C(13)-N(2)-Fe(1)	118.60(10)
C(5)-C(1)-Fe(1)	69.84(9)	C(11)-Fe(1)-C(12)	94.89(8)
C(2)-C(1)-Fe(1)	69.70(9)	C(11)-Fe(1)-N(2)	93.94(7)
C(6)-C(1)-Fe(1)	127.42(12)	C(12)-Fe(1)-N(2)	92.06(7)
C(1)-C(2)-C(3)	106.78(15)	C(11)-Fe(1)-C(4)	110.66(7)
C(1)-C(2)-C(7)	127.65(16)	C(12)-Fe(1)-C(4)	90.78(8)
C(3)-C(2)-C(7)	125.13(16)	N(2)-Fe(1)-C(4)	154.90(6)
C(1)-C(2)-Fe(1)	70.93(9)	C(11)-Fe(1)-C(3)	87.19(7)
C(3)-C(2)-Fe(1)	69.21(9)	C(12)-Fe(1)-C(3)	125.47(8)
C(7)-C(2)-Fe(1)	130.72(12)	N(2)-Fe(1)-C(3)	142.27(7)
C(4)-C(3)-C(2)	108.97(15)	C(4)-Fe(1)-C(3)	39.72(7)
C(4)-C(3)-C(8)	125.92(17)	C(11)-Fe(1)-C(5)	150.50(7)
C(2)-C(3)-C(8)	124.94(17)	C(12)-Fe(1)-C(5)	90.36(7)
C(4)-C(3)-Fe(1)	69.84(9)	N(2)-Fe(1)-C(5)	114.90(6)
C(2)-C(3)-Fe(1)	71.00(9)	C(4)-Fe(1)-C(5)	40.13(6)
C(8)-C(3)-Fe(1)	128.90(12)	C(3)-Fe(1)-C(5)	66.44(7)
C(3)-C(4)-C(5)	107.41(15)	C(11)-Fe(1)-C(2)	102.10(7)
C(3)-C(4)-C(9)	125.91(16)	C(12)-Fe(1)-C(2)	155.69(8)
C(5)-C(4)-C(9)	126.49(17)	N(2)-Fe(1)-C(2)	103.85(6)
C(3)-C(4)-Fe(1)	70.44(10)	C(4)-Fe(1)-C(2)	67.08(7)
C(5)-C(4)-Fe(1)	71.04(9)	C(3)-Fe(1)-C(2)	39.80(7)
C(9)-C(4)-Fe(1)	127.74(12)	C(5)-Fe(1)-C(2)	66.39(7)
C(1)-C(5)-C(4)	107.86(15)	C(11)-Fe(1)-C(1)	140.96(7)
C(1)-C(5)-C(10)	126.95(15)	C(12)-Fe(1)-C(1)	123.52(7)
C(4)-C(5)-C(10)	125.05(16)	N(2)-Fe(1)-C(1)	91.58(6)
C(1)-C(5)-Fe(1)	71.26(9)	C(4)-Fe(1)-C(1)	66.33(6)
C(4)-C(5)-Fe(1)	68.84(9)	C(3)-Fe(1)-C(1)	65.91(6)
C(10)-C(5)-Fe(1)	128.65(12)	C(5)-Fe(1)-C(1)	38.90(6)
F(4)-B(1)-F(2)	110.12(18)	C(2)-Fe(1)-C(1)	39.37(6)
F(3)-B(1)-F(2)	107.96(18)	F(4)-B(1)-F(3)	109.89(19)
F(1)-B(1)-F(2)	109.42(16)	F(4)-B(1)-F(1)	110.52(17)
O(1)-C(11)-Fe(1)	173.59(15)	F(3)-B(1)-F(1)	108.88(18)
O(2)-C(12)-Fe(1)	174.37(17)		

Table 17A. Bond lengths (Å) for [CpFe(CO)$_2$(NH$_2$CH$_2$CHCH$_2$)]BF$_4$

Bond	Length	Bond	Length
C(1)-C(2)	1.386(8)	C(6)-Fe(1)	1.780(5)
C(1)-C(5)	1.405(7)	C(7)-O(2)	1.136(6)
C(1)-Fe(1)	2.107(5)	C(7)-Fe(1)	1.789(5)
C(2)-C(3)	1.444(8)	C(8)-N(1)	1.484(6)
C(2)-Fe(1)	2.097(5)	C(8)-C(9)	1.496(8)
C(3)-C(4)	1.405(9)	C(9)-C(10)	1.300(9)
C(3)-Fe(1)	2.081(5)	B(1)-F(3)	1.376(7)
C(4)-C(5)	1.430(8)	B(1)-F(1)	1.384(7)
C(4)-Fe(1)	2.087(5)	B(1)-F(2)	1.395(6)
C(5)-Fe(1)	2.102(5)	B(1)-F(4)	1.396(6)
C(6)-O(1)	1.138(6)	N(1)-Fe(1)	2.018(4)

Table 18A. Bond angles (°) for [CpFe(CO)$_2$(NH$_2$CH$_2$CHCH$_2$)]BF$_4$

Bonds	Angle	Bonds	Angle
C(2)-C(1)-C(5)	110.8(5)	C(6)-Fe(1)-N(1)	93.3(2)
C(2)-C(1)-Fe(1)	70.4(3)	C(7)-Fe(1)-N(1)	94.1(2)
C(5)-C(1)-Fe(1)	70.3(3)	C(6)-Fe(1)-C(3)	89.4(2)
C(1)-C(2)-C(3)	106.7(5)	C(7)-Fe(1)-C(3)	117.4(2)
C(1)-C(2)-Fe(1)	71.1(3)	N(1)-Fe(1)-C(3)	148.0(2)
C(3)-C(2)-Fe(1)	69.2(3)	C(6)-Fe(1)-C(4)	119.8(2)
C(4)-C(3)-C(2)	107.8(5)	C(7)-Fe(1)-C(4)	88.5(2)
C(4)-C(3)-Fe(1)	70.5(3)	N(1)-Fe(1)-C(4)	146.5(2)
C(2)-C(3)-Fe(1)	70.4(3)	C(3)-Fe(1)-C(4)	39.4(3)
C(3)-C(4)-C(5)	108.3(5)	C(6)-Fe(1)-C(2)	95.6(2)
C(3)-C(4)-Fe(1)	70.0(3)	C(7)-Fe(1)-C(2)	155.2(2)
C(5)-C(4)-Fe(1)	70.6(3)	N(1)-Fe(1)-C(2)	107.6(2)
C(1)-C(5)-C(4)	106.4(5)	C(3)-Fe(1)-C(2)	40.4(2)
C(1)-C(5)-Fe(1)	70.7(3)	C(4)-Fe(1)-C(2)	66.8(2)
C(4)-C(5)-Fe(1)	69.5(3)	C(6)-Fe(1)-C(5)	156.1(2)
O(1)-C(6)-Fe(1)	175.6(5)	C(7)-Fe(1)-C(5)	96.4(2)
O(2)-C(7)-Fe(1)	174.9(5)	N(1)-Fe(1)-C(5)	106.70(19)
N(1)-C(8)-C(9)	112.3(4)	C(3)-Fe(1)-C(5)	66.7(2)
C(10)-C(9)-C(8)	123.4(7)	C(4)-Fe(1)-C(5)	39.9(2)
F(3)-B(1)-F(1)	110.0(4)	C(2)-Fe(1)-C(5)	66.3(2)
F(3)-B(1)-F(2)	110.2(5)	C(6)-Fe(1)-C(1)	131.3(2)
F(1)-B(1)-F(2)	109.0(5)	C(7)-Fe(1)-C(1)	133.3(2)
F(3)-B(1)-F(4)	109.4(4)	N(1)-Fe(1)-C(1)	89.36(19)
F(1)-B(1)-F(4)	109.9(5)	C(3)-Fe(1)-C(1)	65.6(2)
F(2)-B(1)-F(4)	108.2(4)	C(4)-Fe(1)-C(1)	65.5(2)
C(8)-N(1)-Fe(1)	117.0(3)	C(2)-Fe(1)-C(1)	38.5(2)
C(6)-Fe(1)-C(7)	95.0(2)	C(5)-Fe(1)-C(1)	39.0(2)

Table 19A. Bond lengths (Å) for [Cp*Fe(CO)$_2$(NH$_2$CH$_2$CH(Br)CH$_2$Br]BF$_4$

Bond	Length	Bond	Length
Fe1-N1	2.036(2)	C7-C13	1.494(4)
Fe1-C4	1.794(3)	C7-C8	1.432(4)
Fe1-C5	1.790(3)	C10-C6	1.437(4)
Fe1-C7	2.138(3)	C10-C9	1.421(4)
Fe1-C10	2.091(3)	C10-C11	1.500(4)
Fe1-C6	2.122(3)	C6-C12	1.501(4)
Fe1-C9	2.096(3)	F1-B1	1.361(5)
Fe1-C8	2.107(3)	C9-C8	1.430(5)
Br1A-C2A	1.942(5)	C9-C15	1.497(4)
N1-C1A	1.478(6)	C8-C14	1.498(4)
N1-C1B	1.494(8)	C1A-C2A	1.537(2)
F2-B1	1.392(4)	C2A-C3A	1.537(2)
F3-B1	1.394(4)	Br2A-C3A	1.923(6)
C4-O1	1.133(4)	Br1B-C2B	1.956(8)
C5-O2	1.137(4)	Br2B-C3B	1.967(7)
F4-B1	1.374(4)	C3B-C2B	1.539(2)
C7-C6	1.418(4)	C2B-C1B	1.539(2)

Table 20A. Bond angles (°) for [Cp*Fe(CO)$_2$(NH$_2$CH$_2$CH(Br)CH$_2$Br]BF$_4$

Bond	Angle	Bond	angle
N1-Fe1-C7	91.47(11)	C6-C10-C11	126.1(3)
N1-Fe1-C10	153.85(11)	C9-C10-Fe1	70.36(17)
N1-Fe1-C6	114.00(11)	C9-C10-C6	107.7(3)
N1-Fe1-C9	143.68(12)	C9-C10-C11	126.1(3)
N1-Fe1-C8	105.01(11)	C11-C10-Fe1	127.9(2)
C4-Fe1-N1	91.29(11)	C7-C6-Fe1	71.14(15)
C4-Fe1-C7	123.68(12)	C7-C6-C10	108.0(2)
C4-Fe1-C10	90.34(12)	C7-C6-C12	125.5(3)
C4-Fe1-C6	90.36(11)	C10-C6-Fe1	68.91(16)
C4-Fe1-C9	124.73(13)	C10-C6-C12	126.2(3)
C4-Fe1-C8	155.32(12)	C12-C6-Fe1	130.11(19)
C5-Fe1-N1	93.23(13)	C10-C9-Fe1	69.98(16)
C5-Fe1-C4	96.56(13)	C10-C9-C8	108.5(3)
C5-Fe1-C7	139.35(12)	C10-C9-C15	125.3(3)
C5-Fe1-C10	112.50(13)	C8-C9-Fe1	70.51(16)
C5-Fe1-C6	151.78(13)	C8-C9-C15	126.1(3)
C5-Fe1-C9	87.54(13)	C15-C9-Fe1	129.2(2)
C5-Fe1-C8	100.81(12)	C7-C8-Fe1	71.45(16)
C10-Fe1-C7	66.22(11)	C7-C8-C14	127.0(3)
C10-Fe1-C6	39.88(11)	C9-C8-Fe1	69.71(16)
C10-Fe1-C9	39.66(12)	C9-C8-C7	107.5(3)
C10-Fe1-C8	66.87(12)	C9-C8-C14	125.1(3)
C6-Fe1-C7	38.89(11)	C14-C8-Fe1	130.3(2)
C9-Fe1-C7	66.03(12)	F2-B1-F3	108.1(3)
C9-Fe1-C6	66.31(11)	F4-B1-F2	109.6(3)
C9-Fe1-C8	39.78(13)	F4-B1-F3	110.3(3)
C8-Fe1-C7	39.41(11)	F1-B1-F2	111.2(3)
C8-Fe1-C6	66.24(10)	F1-B1-F3	108.8(3)
C1A-N1-Fe1	115.4(2)	F1-B1-F4	108.9(3)
C1B-N1-Fe1	121.8(3)	N1-C1A-C2A	111.4(4)
O1-C4-Fe1	174.5(3)	C1A-C2A-Br1A	107.6(3)
O2-C5-Fe1	174.8(3)	C3A-C2A-Br1A	110.7(3)
C6-C7-Fe1	69.96(16)	C3A-C2A-C1A	115.4(5)
C6-C7-C13	124.8(3)	C2A-C3A-Br2A	113.7(4)
C6-C7-C8	108.3(3)	C2B-C3B-Br2B	109.5(5)
C13-C7-Fe1	129.0(2)	C3B-C2B-Br1B	103.7(5)
C8-C7-Fe1	69.13(16)	C1B-C2B-Br1B	109.0(5)
C8-C7-C13	126.8(3	C1B-C2B-C3	112.5(6)
C6-C10-Fe1	71.21(16)	N1-C1B-C2B	116.4(5)

APPENDIX 10

Representative structures of [Cp(CO)$_2$Fe{NH$_2$CH$_2$CH(Cl)CH$_2$Cl]BF$_4$
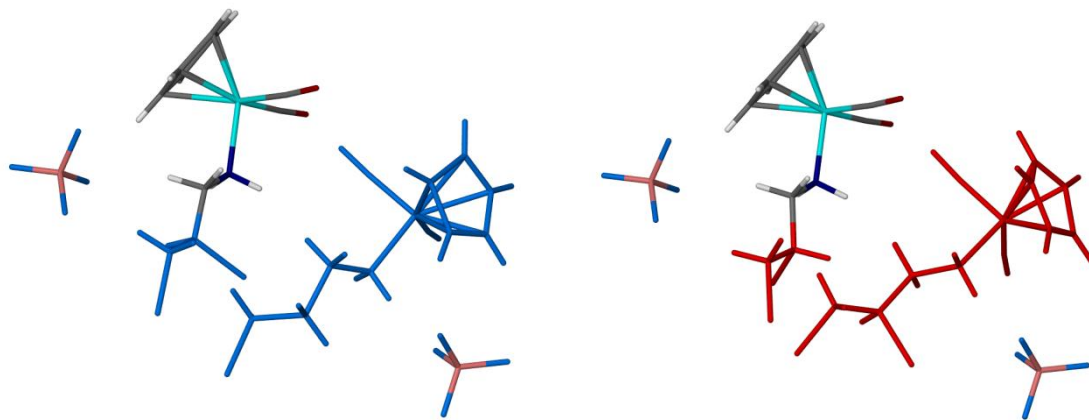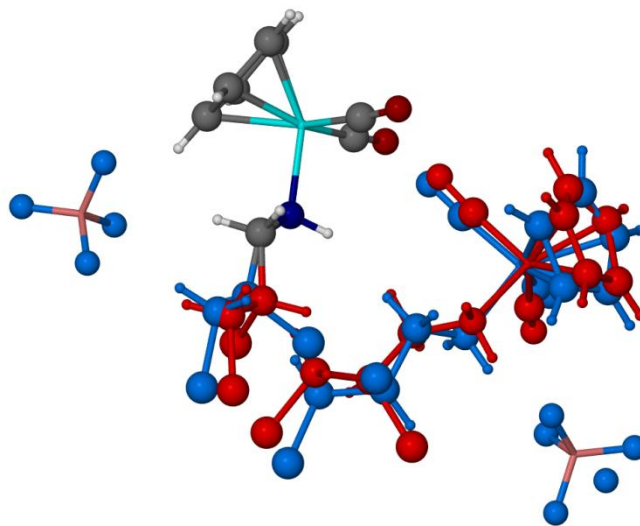
APPENDIX 11

X-ray Crystallographic Data Pertaining to Chapter Six

Table 21A. Bond Lengths (Å) for $[\{\eta^5\text{-}C_5(CH_3)_5\}Fe(CO)_2(NH_2CH_2CH_2CH_2OH)]BF_4$

Bond	Length	Bond	Length
C(1)-C(2)	1.413(4)	C(5)-Fe(1)	2.106(2)
C(1)-C(5)	1.436(4)	C(11)-O(1)	1.137(3)
C(1)-C(6)	1.497(4)	C(11)-Fe(1)	1.784(3)
C(1)-Fe(1)	2.133(3)	C(12)-O(2)	1.148(3)
C(2)-C(3)	1.436(4)	C(12)-Fe(1)	1.770(3)
C(2)-C(7)	1.509(4)	C(13)-N(1)	1.485(3)
C(2)-Fe(1)	2.112(3)	C(13)-C(14)	1.514(3)
C(3)-C(4)	1.416(3)	C(14)-C(15)	1.513(4)
C(3)-C(8)	1.503(4)	C(15)-O(3)	1.429(3)
C(3)-Fe(1)	2.090(2)	N(1)-Fe(1)	2.0209(19)
C(4)-C(5)	1.437(3)	B(1)-F(3)	1.345(5)
C(4)-C(9)	1.501(3)	B(1)-F(4)	1.361(4)
C(4)-Fe(1)	2.095(2)	B(1)-F(2)	1.365(4)
C(5)-C(10)	1.496(4)	B(1)-F(1)	1.399(4)

Table 22A. Bond Angles (°) for $[\{\eta^5\text{-}C_5(CH_3)_5\}Fe(CO)_2(NH_2CH_2CH_2CH_2OH)]BF_4$

Bond	Angle	Bond	Angle
C(2)-C(1)-C(5)	108.6(2)	C(13)-N(1)-Fe(1)	116.53(15)
C(2)-C(1)-C(6)	126.4(3)	C(12)-Fe(1)-C(11)	96.45(12)
C(5)-C(1)-C(6)	125.0(3)	C(12)-Fe(1)-N(1)	94.02(10)
C(2)-C(1)-Fe(1)	69.79(15)	C(11)-Fe(1)-N(1)	93.04(10)
C(5)-C(1)-Fe(1)	69.18(14)	C(12)-Fe(1)-C(3)	112.99(11)
C(6)-C(1)-Fe(1)	128.00(18)	C(11)-Fe(1)-C(3)	90.84(11)
C(1)-C(2)-C(3)	107.9(2)	N(1)-Fe(1)-C(3)	152.09(10)
C(1)-C(2)-C(7)	126.0(3)	C(12)-Fe(1)-C(4)	86.91(11)
C(3)-C(2)-C(7)	125.9(3)	C(11)-Fe(1)-C(4)	124.29(11)
C(1)-C(2)-Fe(1)	71.32(15)	N(1)-Fe(1)-C(4)	142.37(10)
C(3)-C(2)-Fe(1)	69.17(15)	C(3)-Fe(1)-C(4)	39.56(10)
C(7)-C(2)-Fe(1)	129.09(18)	C(12)-Fe(1)-C(5)	99.19(11)
C(4)-C(3)-C(2)	108.1(2)	C(11)-Fe(1)-C(5)	156.48(11)
C(4)-C(3)-C(8)	125.1(2)	N(1)-Fe(1)-C(5)	103.22(9)
C(2)-C(3)-C(8)	126.6(3)	C(3)-Fe(1)-C(5)	66.90(10)
C(4)-C(3)-Fe(1)	70.42(14)	C(4)-Fe(1)-C(5)	40.01(9)
C(2)-C(3)-Fe(1)	70.86(14)	C(12)-Fe(1)-C(2)	152.04(11)
C(8)-C(3)-Fe(1)	128.01(19)	C(11)-Fe(1)-C(2)	91.74(12)
C(3)-C(4)-C(5)	108.3(2)	N(1)-Fe(1)-C(2)	112.24(9)
C(3)-C(4)-C(9)	125.5(2)	C(3)-Fe(1)-C(2)	39.97(10)
C(5)-C(4)-C(9)	126.1(2)	C(4)-Fe(1)-C(2)	66.57(10)
C(3)-C(4)-Fe(1)	70.02(14)	C(5)-Fe(1)-C(2)	66.53(10)
C(5)-C(4)-Fe(1)	70.38(13)	C(12)-Fe(1)-C(1)	137.79(11)
C(9)-C(4)-Fe(1)	128.38(19)	C(11)-Fe(1)-C(1)	125.41(12)
C(1)-C(5)-C(4)	107.1(2)	N(1)-Fe(1)-C(1)	89.42(9)
C(1)-C(5)-C(10)	127.0(2)	C(3)-Fe(1)-C(1)	66.12(10)
C(4)-C(5)-C(10)	125.7(2)	C(4)-Fe(1)-C(1)	66.26(10)
C(1)-C(5)-Fe(1)	71.21(14)	C(5)-Fe(1)-C(1)	39.61(10)
C(4)-C(5)-Fe(1)	69.61(14)	C(2)-Fe(1)-C(1)	38.88(10)
C(10)-C(5)-Fe(1)	128.86(19)	F(3)-B(1)-F(4)	113.8(3)
O(1)-C(11)-Fe(1)	175.4(2)	F(3)-B(1)-F(2)	109.6(3)
O(2)-C(12)-Fe(1)	174.4(2)	F(4)-B(1)-F(2)	109.6(3)
N(1)-C(13)-C(14)	113.6(2)	F(3)-B(1)-F(1)	108.1(3)
C(15)-C(14)-C(13)	112.0(2)	F(4)-B(1)-F(1)	106.3(3)
O(3)-C(15)-C(14)	112.4(2)	F(2)-B(1)-F(1)	109.4(3)

Table 23A. Bond lengths (Å) for [{η⁵-C₅(CH₃)₅}Fe(CO)₂(NH₂CH₂C₆H₄OCH₃)]BF₄

Bond	Length	Bond	Length
C(1)-C(2)	1.497(3)	C(13)-N(1)	1.497(3)
C(2)-C(4)	1.415(4)	C(13)-C(14)	1.499(3)
C(2)-C(10)	1.432(3)	C(14)-C(15)	1.377(4)
C(2)-Fe(1)	2.141(2)	C(14)-C(19)	1.406(3)
C(3)-C(4)	1.499(3)	C(15)-C(16)	1.409(4)
C(4)-C(6)	1.438(3)	C(16)-C(17)	1.388(4)
C(4)-Fe(1)	2.108(2)	C(17)-C(18)	1.375(4)
C(5)-C(6)	1.493(3)	C(17)-O(3)	1.379(3)
C(6)-C(8)	1.419(3)	C(18)-C(19)	1.367(4)
C(6)-Fe(1)	2.092(2)	C(20)-O(3)	1.420(4)
C(7)-C(8)	1.496(3)	B(1)-F(3B)	1.274(7)
C(8)-C(10)	1.435(3)	B(1)-F(1A)	1.286(4)
C(8)-Fe(1)	2.097(2)	B(1)-F(2B)	1.36(3)
C(9)-C(10)	1.499(3)	B(1)-F(3A)	1.379(5)
C(10)-Fe(1)	2.107(2)	B(1)-F(2A)	1.411(16)
C(11)-O(1)	1.145(3)	B(1)-F(4B)	1.421(6)
C(11)-Fe(1)	1.779(2)	B(1)-F(4A)	1.437(4)
C(12)-O(2)	1.142(3)	B(1)-F(1B)	1.467(5)
C(12)-Fe(1)	1.786(2)	Fe(1)-N(1)	2.026(2)

Table 24A. Bond angles (°) for [{η⁵-C₅(CH₃)₅}Fe(CO)₂(NH₂CH₂C₆H₄OCH₃)]BF₄

Bond	Angle	Bond	Angle
C(4)-C(2)-C(10)	108.7(2)	F(2B)-B(1)-F(2A)	15.6(14)
C(4)-C(2)-C(1)	125.7(2)	F(3A)-B(1)-F(2A)	120.4(7)
C(10)-C(2)-C(1)	125.6(2)	F(3B)-B(1)-F(4B)	115.0(5)
C(4)-C(2)-Fe(1)	69.29(13)	F(1A)-B(1)-F(4B)	65.8(4)
C(10)-C(2)-Fe(1)	69.01(12)	F(2B)-B(1)-F(4B)	119.7(9)
C(1)-C(2)-Fe(1)	128.52(19)	F(3A)-B(1)-F(4B)	131.3(4)
C(2)-C(4)-C(6)	107.88(19)	F(2A)-B(1)-F(4B)	105.9(6)
C(2)-C(4)-C(3)	127.3(2)	F(3B)-B(1)-F(4A)	73.9(4)
C(6)-C(4)-C(3)	124.6(2)	F(1A)-B(1)-F(4A)	112.7(4)
C(2)-C(4)-Fe(1)	71.82(14)	F(2B)-B(1)-F(4A)	107.1(11)
C(6)-C(4)-Fe(1)	69.37(13)	F(3A)-B(1)-F(4A)	103.1(3)
C(3)-C(4)-Fe(1)	129.06(17)	F(2A)-B(1)-F(4A)	103.8(6)
C(8)-C(6)-C(4)	107.8(2)	F(4B)-B(1)-F(4A)	47.9(3)
C(8)-C(6)-C(5)	125.7(2)	F(3B)-B(1)-F(1B)	110.3(4)
C(4)-C(6)-C(5)	126.3(2)	F(1A)-B(1)-F(1B)	39.9(2)
C(8)-C(6)-Fe(1)	70.38(13)	F(2B)-B(1)-F(1B)	107.9(11)
C(4)-C(6)-Fe(1)	70.58(14)	F(3A)-B(1)-F(1B)	78.6(3)
C(5)-C(6)-Fe(1)	128.50(17)	F(2A)-B(1)-F(1B)	106.7(7)
C(6)-C(8)-C(10)	108.42(19)	F(4B)-B(1)-F(1B)	103.2(4)
C(6)-C(8)-C(7)	125.0(2)	F(4A)-B(1)-F(1B)	143.1(3)
C(10)-C(8)-C(7)	126.3(2)	C(17)-O(3)-C(20)	118.3(2)
C(6)-C(8)-Fe(1)	70.02(12)	C(11)-Fe(1)-C(12)	96.96(10)
C(10)-C(8)-Fe(1)	70.42(13)	C(11)-Fe(1)-N(1)	92.90(10)
C(7)-C(8)-Fe(1)	129.62(16)	C(12)-Fe(1)-N(1)	97.18(10)
C(2)-C(10)-C(8)	107.1(2)	C(11)-Fe(1)-C(6)	88.89(10)
C(2)-C(10)-C(9)	126.3(2)	C(12)-Fe(1)-C(6)	114.91(9)
C(8)-C(10)-C(9)	126.2(2)	N(1)-Fe(1)-C(6)	147.41(9)
C(2)-C(10)-Fe(1)	71.60(13)	C(11)-Fe(1)-C(8)	121.02(10)
C(8)-C(10)-Fe(1)	69.65(13)	C(12)-Fe(1)-C(8)	86.91(9)
C(9)-C(10)-Fe(1)	129.19(18)	N(1)-Fe(1)-C(8)	145.19(9)
O(1)-C(11)-Fe(1)	175.2(2)	C(6)-Fe(1)-C(8)	39.61(9)
O(2)-C(12)-Fe(1)	171.7(2)	C(11)-Fe(1)-C(10)	155.54(10)
N(1)-C(13)-C(14)	113.48(19)	C(12)-Fe(1)-C(10)	96.71(10)
C(15)-C(14)-C(19)	118.3(2)	N(1)-Fe(1)-C(10)	105.39(9)
C(15)-C(14)-C(13)	121.6(2)	C(6)-Fe(1)-C(10)	66.93(9)
C(19)-C(14)-C(13)	120.0(2)	C(8)-Fe(1)-C(10)	39.93(9)
C(14)-C(15)-C(16)	121.1(2)	C(11)-Fe(1)-C(4)	92.80(10)
C(17)-C(16)-C(15)	118.5(2)	C(12)-Fe(1)-C(4)	153.05(10)
C(18)-C(17)-O(3)	115.7(2)	N(1)-Fe(1)-C(4)	107.37(9)
C(18)-C(17)-C(16)	120.9(3)	C(6)-Fe(1)-C(4)	40.05(9)
O(3)-C(17)-C(16)	123.3(3)	C(8)-Fe(1)-C(4)	66.61(9)
C(19)-C(18)-C(17)	120.1(2)	C(10)-Fe(1)-C(4)	66.55(9)
C(18)-C(19)-C(14)	121.1(3)	C(11)-Fe(1)-C(2)	127.99(10)
F(3B)-B(1)-F(1A)	138.7(4)	C(12)-Fe(1)-C(2)	134.56(10)
F(3B)-B(1)-F(2B)	100.6(10)	N(1)-Fe(1)-C(2)	87.82(9)
F(1A)-B(1)-F(2B)	114.7(10)	C(6)-Fe(1)-C(2)	66.02(9)
F(3B)-B(1)-F(3A)	32.4(3)	C(8)-Fe(1)-C(2)	65.95(9)
F(1A)-B(1)-F(3A)	113.3(4)	C(10)-Fe(1)-C(2)	39.38(8)
F(2B)-B(1)-F(3A)	105.0(9)	C(4)-Fe(1)-C(2)	38.89(10)
F(3B)-B(1)-F(2A)	114.8(7)	C(13)-N(1)-Fe(1)	120.30(15)
F(1A)-B(1)-F(2A)	103.3(7)		

Table 25A. Bond lengths [Å] and angles [°] for [CpFe(CO)₂NH(CH₂CH₂CH₃)₂]BF₄

Bond	length	Bond	Length
C(1)-C(2)	1.381(6)	C(7)-Fe(1)	1.774(5)
C(1)-C(5)	1.395(6)	C(8)-N(1)	1.417(4)
C(1)-Fe(1)	2.103(4)	C(8)-C(9)	1.499(5)
C(2)-C(3)	1.415(6)	C(9)-C(10)	1.507(5)
C(2)-Fe(1)	2.097(4)	C(11)-N(1)	1.412(4)
C(3)-C(4)	1.399(6)	C(11)-C(12)	1.419(5)
C(3)-Fe(1)	2.070(4)	C(12)-C(13)	1.421(6)
C(4)-C(5)	1.393(6)	N(1)-Fe(1)	2.058(4)
C(4)-Fe(1)	2.073(4)	B(1)-F(4)	1.365(6)
C(5)-Fe(1)	2.090(4)	B(1)-F(2)	1.366(6)
C(6)-O(1)	1.132(5)	B(1)-F(1)	1.375(6)
C(6)-Fe(1)	1.793(5)	B(1)-F(3)	1.383(6)
C(7)-O(2)	1.138(5)		

Table 26A. Bond angles [°] for [CpFe(CO)₂NH(CH₂CH₂CH₃)₂]BF₄

Bond	Angle	Bond	Angle
C(2)-C(1)-C(5)	109.1(4)	F(1)-B(1)-F(3)	109.7(4)
C(2)-C(1)-Fe(1)	70.6(2)	C(7)-Fe(1)-C(6)	92.6(2)
C(5)-C(1)-Fe(1)	70.1(3)	C(7)-Fe(1)-N(1)	94.5(3)
C(1)-C(2)-C(3)	107.6(4)	C(6)-Fe(1)-N(1)	91.7(3)
C(1)-C(2)-Fe(1)	71.0(3)	C(7)-Fe(1)-C(3)	108.9(2)
C(3)-C(2)-Fe(1)	69.1(2)	C(6)-Fe(1)-C(3)	92.89(19)
C(4)-C(3)-C(2)	107.3(4)	N(1)-Fe(1)-C(3)	155.9(3)
C(4)-C(3)-Fe(1)	70.4(2)	C(7)-Fe(1)-C(4)	87.1(2)
C(2)-C(3)-Fe(1)	71.2(2)	C(6)-Fe(1)-C(4)	127.5(2)
C(5)-C(4)-C(3)	108.5(4)	N(1)-Fe(1)-C(4)	140.7(3)
C(5)-C(4)-Fe(1)	71.1(3)	C(3)-Fe(1)-C(4)	39.46(16)
C(3)-C(4)-Fe(1)	70.2(2)	C(7)-Fe(1)-C(5)	103.9(2)
C(4)-C(5)-C(1)	107.5(4)	C(6)-Fe(1)-C(5)	156.4(2)
C(4)-C(5)-Fe(1)	69.8(3)	N(1)-Fe(1)-C(5)	103.5(4)
C(1)-C(5)-Fe(1)	71.1(3)	C(3)-Fe(1)-C(5)	66.00(18)
O(1)-C(6)-Fe(1)	175.8(4)	C(4)-Fe(1)-C(5)	39.08(17)
O(2)-C(7)-Fe(1)	175.3(5)	C(7)-Fe(1)-C(2)	148.5(2)
N(1)-C(8)-C(9)	123.2(5)	C(6)-Fe(1)-C(2)	91.75(19)
C(8)-C(9)-C(10)	113.4(5)	N(1)-Fe(1)-C(2)	116.5(3)
N(1)-C(11)-C(12)	128.2(8)	C(3)-Fe(1)-C(2)	39.70(16)
C(11)-C(12)-C(13)	120.9(8)	C(4)-Fe(1)-C(2)	65.82(17)
C(11)-N(1)-C(8)	119.7(5)	C(5)-Fe(1)-C(2)	65.38(18)
C(11)-N(1)-Fe(1)	124.5(4)	C(7)-Fe(1)-C(1)	142.6(2)
C(8)-N(1)-Fe(1)	115.5(3)	C(6)-Fe(1)-C(1)	123.9(2)
F(4)-B(1)-F(2)	111.3(5)	N(1)-Fe(1)-C(1)	92.5(4)
F(4)-B(1)-F(1)	109.1(4)	C(3)-Fe(1)-C(1)	65.48(18)
F(2)-B(1)-F(1)	109.0(4)	C(4)-Fe(1)-C(1)	65.15(18)
F(4)-B(1)-F(3)	109.9(4)	C(5)-Fe(1)-C(1)	38.88(17)
F(2)-B(1)-F(3)	107.8(5)	C(2)-Fe(1)-C(1)	38.40(16)

APPENDIX 12

Compact disk

Spectroscopic data and CIF files of compounds contained in chapters 2-6

Softwares required to access files contained in the compact disk

PDF- Adobe PDF reader or any other appropriate software
CIF- Mercury, OLex 2 or any other appropriate software